NITROGEN UTILIZATION DURING SPRING PHYTOPLANKTON BLOOM DEVELOPMENT IN THE SOUTHEAST BERING SEA

RECOMMENDED:

Chairman, Advisory Committee

Head, Marine Science Program

Director, Division of Marine Sciences

APPROVED:

Director of Graduate Programs

20 December 1983

Date

NITROGEN UTILIZATION DURING SPRING PHYTOPLANKTON BLOOM DEVELOPMENT IN THE SOUTHEAST BERING SEA

A

THESIS

Presented to the Faculty of the University of Alaska

in Partial Fulfillment of the Requirements

for the Degree of

DOCTOR OF PHILOSOPHY

by

Raymond Nicholas Sambrotto, B.A., M.S.

Fairbanks, Alaska

December, 1983

ABSTRACT

Interactions between a high latitude, continental shelf, spring phytoplankton bloom and water column physics and chemistry were studied using ^{15}N measured rates of nitrogen uptake. Peak bloom conditions commenced when the mixed layer shallowed and minimized respirational losses. Integrative light - mixing growth models were accurate during early bloom stages. An advection - diffusion model associated peak bloom nitrate uptake with pycnocline mixing rates of 2.1 m d^{-1} in an 18 m mixed layer. The accumulation of surface buoyancy was a reliable index of peak bloom temporal and spatial "patchiness" since mixing rates influenced both respirational losses and nutrient supply.

Maximum nitrogen specific uptake rates ($hr.^{-1}$), unlike those of carbon, coincided with peak bloom conditions. Although species compositions among peak bloom periods were similar, particulate C/N ratios were not. Apparently, both intercellular factors and prevailing mixing conditions influence specific uptake rates and cell composition. A large proportion of new (nitrate) to total productivity was associated with the dominance of the early bloom forming diatoms in the mixed layer. In the absence of these net plankton the residual nanoplankton dominated community exhibited a greater dependence on regenerated nitrogen.

Nitrate uptake averaged 700 mg-at m^{-2} during the spring bloom and 1 g-at m^{-2} $year^{-1}$. The yearly f factor was 0.40. Nitrogen uptake based

carbon productivity was 188 g C m^{-2} $year^{-1}$. A mass balance of the inorganic carbon system indicates that nitrate uptake alone cannot account for all the carbon leaving the surface layer. The correspondence between $^{15}NO_3^-$ uptake measurements and nitrate decreases suggests the diffusion of slope water into the middle shelf is slow.

Large scale meteorological patterns may be responsible for the interannual variability observed in production. Frequent May storm activity prolonged peak bloom periods, while calm conditions promoted extensive Chl *a* layers. The passage of atmospheric low pressure systems was also associated with the cross shelf "pumping" of water masses.

TABLE OF CONTENTS

LIST OF FIGURES

LIST OF TABLES

ACKNOWLEDGEMENTS

I would like to acknowledge the generous contributions of time and energy given me by the members of my graduate committee. It has been a pleasure to work with Drs. Ted Cooney, Joe Niebauer, Bill Reeburgh, and Paul Reichardt who never seemed too busy to invest some time in the supplications of a pestering graduate student. Dr. John Goering, as my major advisor, provided a number of contributions to whatever accomplishments result from this work. These include a stimulating work environment which was more enjoyable than I believed possible before my acquaintance with him. Also, working with John taught me that a modern scientist can bring a wide range of human attributes to the job in addition to expertise in hypotheses testing. Many other individuals from the faculty and personnel of the Institute of Marine Science and the University of Alaska have also contributed to making my graduate studies very rewarding.

This work was supported by a grant from the National Science Foundation (#DPP76:23340) through its sponsorship of the PROBES project. It was an interesting and exciting oceanographic research project and I thoroughly enjoyed my "apprenticeship" in it. The impact of many of the PROBES scientists and personnel are reflected in this dissertation. Such contributions as reliable nutrient analysis by Brookhaven National Lab were indispensable. The help and guidance of such people as Drs. Don Hood and Larry Coachman may not be as obvious however, and was especially appreciated.

In the last but not least department, I acknowledge the unmatched contributions of my wife Beverly to my graduate studies. Her tangible help such as additions to cash flow and homemade bread were important. These pale however, beside her major contributions, which were sticking with me and giving me a center around which to organize my various and sundry undertakings. Thanks Bev. I would also like to acknowledge the support of my parents and family, as well as Colby and Lia, who were always fun and that is an important contribution. Also, people I never met from outside the scientific community contributed to my work (or at least the motivations behind it).

> When Brahma, or the God of Gods, said the Shaster, resolved to recreate the world after one of its periodical dissolutions, he gave birth to Vishnoo, to preside over the work; but the Vedas, or mystical books, whose perusal would seem to have been indispensable to Vishnoo before beginning the creation, and which therefore must have contained something in the shape of practical hints to young architects, these Vedas were lying at the bottom of the waters;...
>
> Herman Melville, Moby Dick

CHAPTER 1

INTRODUCTION

1.1 The Oceanographic Context of the Present Work

Chemical measurements are the basis for the present quantitative understanding of environmental organization. The problems inherent in the analysis of very large scale (i.e. planetary) processes has fostered the development of the interdisciplinary study of biogeochemistry (Odum, 1971), and in oceanography the systems approach has been advocated as an organizing concept for field studies (Walsh, 1972). Biogeochemistry provides a framework which ameliorates many of the difficulties faced in integrating the results of diverse, reductional studies into general theory, a recognized obstacle in ecological work (Becht, 1974).

The present study focuses on the interaction of spring phytoplankton growth with nitrogen cycling. The study site is a temperate continental shelf during the period in which the biological system develops from essentially abiotic end of winter conditions to the very productive spring

bloom and beyond. The elemental cycles most extensively documented throughout the biosphere have been the major constituents of organic material (eg. carbon, nitrogen, and phosphorous). The formation of living material is a critical stage in the cycle of many elements (Ehrlich et al., 1977), and in the ocean the list of bioactive elements continues to grow (Quinby - Hunt and Turekian, 1983).

A basic assumption made during this study was that information on nutrient cycling would contribute to "ecosystem analysis" by providing a common analytical framework based on measurements of elemental cycling among the biotic and abiotic components of the system (Pomeroy, 1970). Such an analysis is useful in several respects. Climatic factors can produce temporal variations in food chains of interest to man (Bakun, et al., 1982). The ability to predict such variation depends in part on a quantitative understanding of the mechanisms regulating the intensity and patterns of primary production. This ability is particularly important in productive fishing areas such as the southeast Bering Sea. Additionally, anthropogenic influences on components of the major nutrient cycles such as CO_2 and N_2O may have far reaching environmental consequences (Hansen et al., 1981, Crutzen, 1974). Predictive models for these atmospheric constituents will require detailed knowledge of carbon and nitrogen cycling in a variety of environments, among which continental shelves may be of particular importance (Walsh et al., 1981a).

1.2 Phytoplankton Growth on Temperate Continental Shelves

The ecology and growth of phytoplankton on continental shelves has been studied for over half a century (Table 1). The list in Table 1 is by no means complete. It is intended to reflect the extent and diversity of effort devoted to measuring biological productivity on shelf regimes which cover approximately 2.9×10^7 km^2 of the earth's surface (Sverdrup, et al., 1942). In these studies, a variety of techniques were employed; from nutrient mass balance (Atkins, 1922) to the use of carbon and nitrogen tracers (Eppley, et al., 1979). The study areas cover a wide range of temperate and polar latitude from the relatively unproductive polar areas (Vedernikov and Solov'yeva, 1972) to more seasonally productive waters (McRoy and Goering, 1976). The scope of these studies varies from comprehensive descriptions including hydrography and general oceanography of seasonal signals (e.g. Gran and Braarud, 1935) to those which focused on short time scale, diel biological response (Prezlin and Ley, 1980).

Much of the yearly phytoplankton production on high latitude shelves is associated with brief but intense periods of growth during the spring diatom bloom. Marked seasonal and spatial variations in phytoplankton stocks have been reported in waters of several temperate and high latitude shelves (Riley, 1956, Holligan and Harbour, 1977). The identification and quantification of the environmental variables controlling the observed patterns of phytoplankton growth in the sea has been an area of active research for several decades.

Table 1

Studies of Phytoplankton Production on Continental Shelves

Investigator	Area
Atkins, 1923	English Channel
Cooper, 1933	English Channel
Gran and Braarud, 1935	Gulf of Maine
Riley, 1956	Long Island Sound
Semina, 1960	Northwest Bering Sea
Steeman - Nielsen, 1958	West Greenland
Pratt, 1965	Narragansett Bay
Mandelli et al., 1970	Coastal Long Island
Vedernikov and Solov'yeva, 1972	Barents Sea
Platt, 1972	Gulf of St. Laurence
McRoy et al., 1972	Eastern Bering Sea
Smayda, 1973	Narragansett Bay
Petersen and Miller, 1975	Oregon Shelf
El Sayed and Turner, 1977	Antarctic Shelf
Holligan and Harbor, 1977	English Channel
Kaiser and Schultz, 1978	Baltic Sea
Pingree, et al., 1978	North Sea
Eppley et al., 1978	Southern California Bight
Iverson et al., 1979a	Southeast Bering
Prezelin and Ley, 1980	Southern California Bight
Sharp and Church, 1981	Mid Atlantic Bight
Legendre et al., 1981	Hudson Bay
Malone et al., 1983	New York Bight

The general process of plant growth involves the synthesis of organic matter from C, H, N, O, P, S, K, (in some cases Si) and an assortment of micronutrients. Organic matter synthesis is dependent on the availability of an energy source, in this case (light) and raw materials (nutrients). Figure 1 is a reproduction of an early mass balance approach to phytoplankton growth during the spring "bloom" or "growth outburst" in the English Channel (Cooper, 1933), and serves to illustrate the seasonal reduction in ambient nutrient levels associated with such growth. By mathematically converting nutrients to plant biomass, Cooper found that the estimates of production based on the disappearance of most of these nutrients agreed quite well.

The accuracy of current isotopic field methodologies for measuring marine phytoplankton growth is itself in a healthy state of reexamination (Gieskes et al., 1979, Goldman et al., 1979). Biochemical studies have accumulated a growing body of information on the intercellular flow of both carbon (Morris et al., 1981) and nitrogen (Syrett, 1981) and further progress in understanding the dynamics of marine phytoplankton growth call for what Yentsch (1980), has termed, a "coalescence of disciplines".

1.3 The Marine Nitrogen Cycle

A schematic representation of the biological pathways in the marine nitrogen cycle is shown in Figure 2, which was adapted from Liu (1979), to emphasize the importance of organic nitrogen (org N) in the various

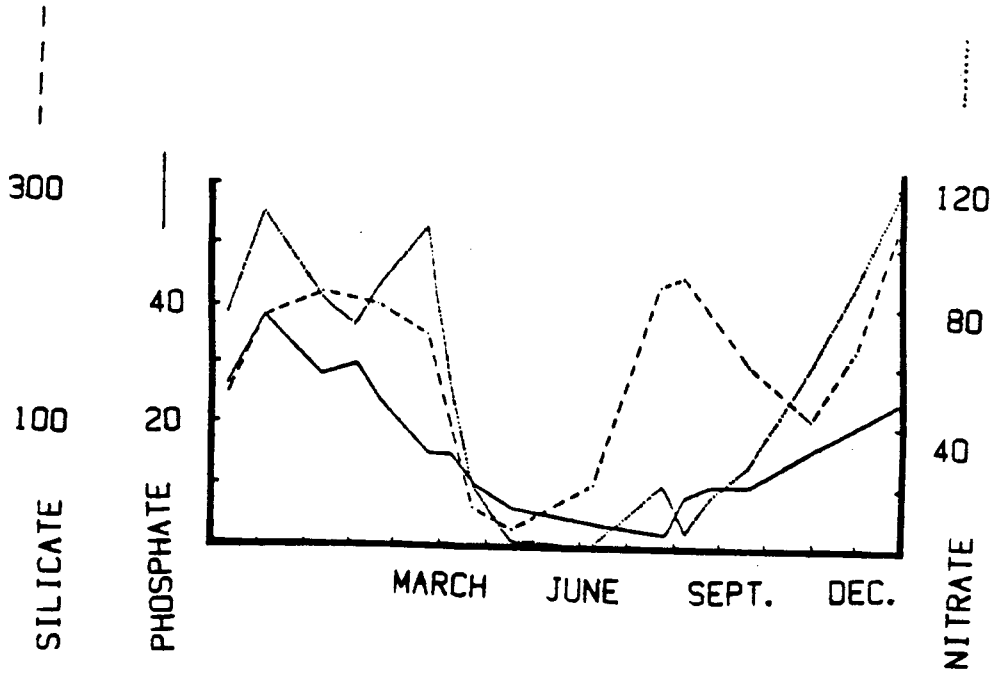

Figure 1.

Changes in nutrient chemistry during the spring bloom in the English Channel (from Cooper, 1933).

transformations. Nitrogen exhibits one of the most complex and interesting cycles among the macronutritive substances since it can exist in a variety of oxidation states. Although the major pathways have been known for some time (Cooper, 1937), there remain large discrepancies among budgets due to the paucity of data for most steps and analytical problems for certain nitrogen species. The overall rate of N_2O production (or consumption) by the ocean for example, while currently unknown, is of importance due to the role N_2O plays in regulating atmospheric ozone (Crutzen, 1971).

In denitrification, NO_3^- is used as an electron acceptor by heterotrophic bacteria. Although many genera of bacteria have this capability, it has been suggested that the term only be applied when gaseous products (N_2 or N_2O) are produced (Delwiche and Bryan, 1976). Nitrate reduction or immobilization also occurs in denitrifying environments, although it is considered of less importance than denitrification (Goering and Dugdale, 1966, Dugdale et al., 1977). Denitrification is a sequential process with NO_2^- as an intermediate (Goering et al., 1973). Also, the amount of N_2O produced during denitrification appears to be inversely proportional to the growth conditions of the denitrifiers, such as substrate and oxygen concentrations.

Delwiche and Bryan (1976), found that any N_2O formed is efficiently reabsorbed and converted to N_2. Only below pH 7.0 (an unusually low pH for water column sea water) was a substantial amount of N_2O produced. Likewise, Cohen and Gorden (1978), observed the disappearance of N_2O from the denitrifying zone which they attributed to consumption during denitrification. Also, large areas of the eastern tropical north Pacific appear to be very active areas of denitrification (Codispoti and Richards,

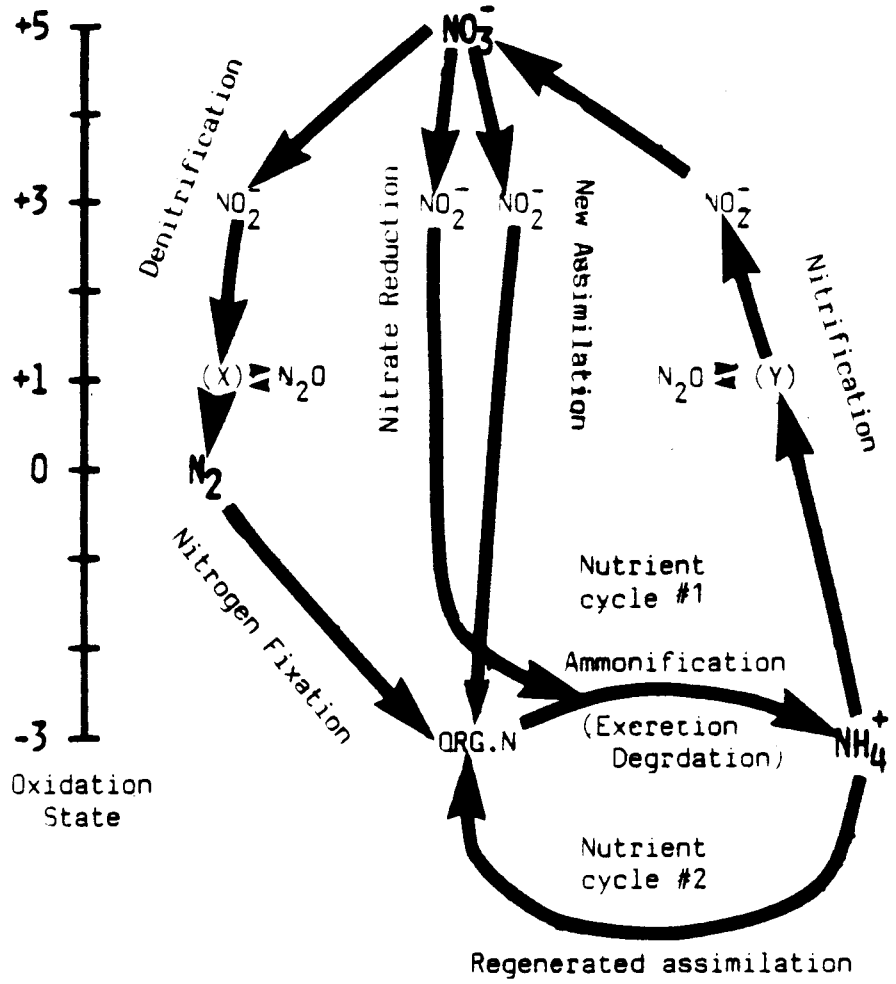

Figure 2.

The major biological pathways of the marine nitrogen cycle. X and Y are two unknown intermediates.

1976). Continental shelves and coastal areas, however, are probably the most important sites of marine denitrification (Goering, 1978).

During nitrification, NH_4^+ is oxidized to NO_3^- also in a two step process with NO_2^- as an intermediate. Two different types of chemoautotrophic bacteria carry out the oxidation of ammonium to nitrite and nitrite to nitrate, namely Nitrosomonas and Nitrobacter respectively. These genera appear very similar to soil nitrifying organisms (Lehninger, 1970). Nitrification is oxygen sensitive and rates are higher at low oxygen levels (Carlucci and McNally, 1969). The process is found in a variety of marine environments (McElroy et al., 1978, Ward et al., 1982), and evidence is accumulating that there is a net production of N_2O under these circumstances (Goreau, et al., 1980, Broecker and Peng, 1982).

Abiotic factors affect components of the nitrogen cycle in addition to the biological reactions outlined in Figure 2. An inventory and a budget which considers some of these factors relative to phytoplankton utilization is presented in Table 2 based on extensive reviews by Rosswall (1981), and Liu (1979). The estimate intervals on the input and output processes are large. For example, uncertainties of factors of four or more exist regarding marine denitrification. Also, changes from earlier studies are evident. Marine nitrogen fixation, for example, was considered by Vaccaro (1965) to be negligible. More recently it has been suggested to be a substantial source for combined nitrogen (Bolin, 1979), due to the ubiquity of cyanobacteria in the marine environment (Johnson and Sieburth, 1979, Martinez, et al., 1983). Importantly, from budgets of the planet nitrogen cycle, it appears that anthropogenic inputs from such activities as fertilizer production are beginning to have measurable effects on aspects of

Table 2.

Inventory and Budget of Marine Nitrogen Cycle.

	Inventory (in 10^{12}g) (1)
N_2	2.2×10^7
N_2O	2.0×10^2
NO_3^-	5.7×10^5
NO_2^-	5.0×10^2
NH_4^+	7.0×10^3
DON	5.3×10^5
PON	$0.2\text{-}2.4 \times 10^5$

	Budget (in 10^{12}g yr^{-1})	
Total N use by phytoplankton	$3.2\text{-}7.2 \times 10^3$ (2)	
NO_3^- use by phytoplankton	$0.6\text{-}1.4 \times 10^3$ (3)	
Allochthonous inputs	50 - 250 (4)	≃ Outputs
- N fixation		- Burial
- Rain and Fallout		- Denitrification
- Runoff		- N_2O evasion
		- NH_4^+ and organic volatilization

(1) - Soederland and Svensson, 1976.
(2) - Based on range of marine surface production by De Vooys (1979), and an assumed C/N utilization ratio of 5.66 (w/w).
(3) - Based on 19% new production (Eppley and Peterson, 1979).
(4) - Based on range of estimates summarized by Rosswall (1981).

the nitrogen cycle (Bolin and Arrehnius, 1977).

Many approaches have been taken in addressing the mechanisms which control the observed properties of sea water. These include geochemical balance, (Mackenzie and Garrels, 1966), kinetic models, (Broecker, 1971), advection - diffusion models, (Craig, 1969), and a variety of models describing more specific oceanic properties. Sillen (1967), suggested that over long time scales, seawater is in thermodynamic equilibrium with various minerals. In the analysis of biologically active sea water constituents on shorter time scales, however, it must be recognized that chemical properties of the ocean reflect the dynamics of an interactive system. Predictive ability therefore, depends on understanding the kinetic controls on aspects such as nutrient cycles (Wollast, 1981).

Since the nitrogen cycle is so closely associated with the production and degradation of organic matter, measurements of biological rates of nitrogen transformations are crucial in such a kinetic approach. On an areal basis, the ocean is less productive than land, although due to its greater area accounts for ca. 33% of the total global carbon fixed by photosynthesis (Bunt, 1972). Oceanic productivity is geographically and temporally heterogeneous, however. Wide areas of the low latitude ocean are extremely oligotrophic while shelf and upwelling areas in which favorable light and nutrient conditions exist are much more productive (Koblentz - Mishke, Volkovinski and Kobanova, 1970, Ryther, 1963).

Eutrophic ocean areas are associated with a relatively greater dependence on nitrate as a nitrogen source (Eppley and Peterson, 1979).

Importantly, these latter areas contribute most of the higher trophic level productivity of the world oceans used by man (Ryther, 1969). Eppley and Peterson (1979) estimate the overall proportion of new : total production in the world ocean at 18 - 20%. This ratio was used to estimate the proportion of marine productivity exported from the surface water. The 18 -20 % figure is almost twice that derived from earlier geochemical box models. The actual percentage which new productivity comprises of total productivity varies from low values in oligotrophic oceanic waters to 60% or more in coastal or upwelling areas. Large rates of nitrate uptake are associated with high carbon productivity.

The data in Table 2 indicate that the oceanic NH_4^+ pool turns over due to phytoplankton utilization approximately once a year, while the turnover rate of the NO_3^- pool is less than 1% $year^{-1}$. Harrison (1980), altered the concept of regenerated production to include all utilization not supported by extraoceanic input. This approach however, disregards the large disparity in time scales between NH_4^+ regeneration and nitrification in the two nutrient cycles in Figure 2. Also, the distinction drawn by Dugdale and Goering (1967), between new and regenerated productivity has implications beyond phytoplankton ecology in view of the differential oxidation changes associated with the two assimilation processes.

The nutrient cycle formed by nitrification and photoassimilative nitrate reduction and ammonification implies that nitrification and its associated N_2O production are largely dependent on, and limited by, the photoassimilative reduction of nitrate by phytoplankton. A similar conclusion was reached by Pierotti and Rasmussen (1980), who found N_2O supersaturations associated with productive regions in the eastern tropical

Pacific. Apart from allochthonous nitrogen from continental runoff, new production is generally associated with an oxidative change in nitrogen. This oxidative change necessitates the consideration of phytoplankton nitrate utilization data in more general studies of the marine nitrogen cycle. The original implicit restriction of regenerated production to short time scale, in situ processes, therefore, is useful even apart from its application to trophic studies.

Nitrate uptake and its subsequent assimilation is dependent on a deep (e.g. subsurface) supply of nitrate to the trophogenic zone. This supply in turn, depends on the baroclinic nature of the water column (Yentsch, 1974). The assimilation of regenerated nitrogen however, depends on excretion and/or degradation in the water column. Detrital organic material settling on the sea floor can release dissolved inorganic nutrients back into the water column upon decomposition, and relatively high fluxes of NH_4^+ from anoxic sediments into the water column have been measured (Rowe, et al., 1977). If the bottom lies within the surface mixed layer this process can be a direct source of regenerated nitrogen for phytoplankton growth.

Predominantly, however, regenerated nitrogen used by phytoplankton is supplied by in situ metabolic activities of small size class microheterotrophs (Harrison, 1978). The C/N ratio of amino acid substrates available to these organisms averages ca. 3.85. The C/N composition of bacteria, however, is 12. Due to this discrepancy in composition, during the process of converting substrates to microheterotrophic biomass, organic nitrogen is made available to plants as ammonium (Wright, 1974).

Generally, the rate of nitrogen excretion by larger heterotrophs decreases with increasing size similar to the trend observed for phosphorous

(Johannes, 1964). In most zooplankton studied the dominant form of excreted nitrogen was ammonium and was temperature dependent (Corner and Davies, 1971). Under certain conditions such as those of the Peru upwelling area where huge stocks of anchovies are found, the excretion of nekton can be a major source of regenerated nitrogen (Whitledge, 1978).

In a spatial analysis of the importance of excreted nitrogen to phytoplankton, Jawed (1973), found that in near shore waters off the coast of Washington, regenerated nitrogen was relatively unimportant but increased in importance with distance offshore. While regenerated nitrogen is always an important source of nitrogen for phytoplankton growth, this is especially true in oligotrophic oceanic water. For example, in a study of the unproductive central north Pacific, Eppley, et al., (1973) compared nitrogen excretion to assimilation and concluded that the coupling between these two processes in this area may approach 100%.

1.4 ^{15}N Studies of the Marine Nitrogen Cycle

Neess et al. (1962) were the first investigators to measure rates of nitrogen transformations in the aquatic environment with ^{15}N. This stable isotope had previously been used in agricultural and biochemical studies. The use of ^{15}N in productivity studies has not been as extensive as the more easily measured radioisotope ^{14}C however, since the technique involves mass spectrometry or emission band spectroscopy to measure a change in ^{15}N atom % abundance. The radioisotope of nitrogen (^{13}N) has too short a half life to be practical in extensive field applications (Gersberg et al., 1976). Methodology based on ^{15}N has been adapted to measure rates in virtually every

biological pathway of the nitrogen cycle (Hauck, 1973). For example, ^{15}N nitrogen fixation rates in the ocean were carried out (Dugdale et al., 1964), as have aquatic denitrification rates (Goering and Dugdale, 1966; Brezonik and Lee, 1968).

Phytoplankton uptake of nitrogen is measured by the incorporation of ^{15}N into particulate material during an incubation. Conversely, the dilution of the isotopic composition of the dissolved pool by selected processes can also be measured (Alexander, 1970). Research work based on this methodology continues to proliferate, and it has been used in several elegant approaches such as the simultaneous measurement of nitrification and nitrate reduction (Koike and Hattori, 1977). An isotope dilution method has been used to measure NH_4^+ regeneration in water column samples that had been fractionated by size (Harrison, 1978, Caperon, et al., 1979), and in anoxic sediments (Blackburn, 1979).

The methodology in each of the studies is quite similar in their use of the change in the ambient $^{15}N/(^{15}N+^{14}N)$ ratio to measure regeneration. The results of all three water column studies suggest the importance of the microzooplankton and nanoplankton in regenerating nitrogen in the environments sampled. The isotope dilution technique has not been applied directly to measurements of macrozooplankton excretion but should also prove to be a useful tool for this measurement.

In all the ^{15}N methodologies, the preparation of a sample, which is tractable by the available gasification procedures for delivery to the mass spectrometer inlet system is crucial. Schell (1978) developed the chemical methodology to immobilize nitrous acid as a diazo compound which could then be combusted, and this method has found application in studies of nitrification

(Wofsy, 1981).

By far the most widespread application of the ^{15}N technique in marine systems has been the measurement of surface water biological uptake rates of dissolved inorganic nitrogen (Dugdale and Goering, 1967). Although measurements of carbon productivity are more commonly used in the study of marine production, nitrogen productivity is a useful parameter in several respects. As Dugdale and Goering (1967) point out, nitrate uptake represents new productivity and indicates the plant production available for export from or consumption in the upper water under steady state conditions.

Recent microbiological studies indicate that most of the nitrogen in marine microorganisms is in protein, (Cuhel et al., 1981). Also, in phytoplankton, protein production appears to be conserved under a variety of growth conditions (Morris et al., 1979). Measurements of nitrate utilization by spring bloom phytoplankton, therefore, largely represent "primary protein production". Such protein production may be a more conservative and reliable indicator of food availability than carbon production, due to the more ubiquitous role of carbon in cellular chemistry.

When the utilization of major dissolved nutrients by phytoplankton is compared to the availability of these nutrients in sea water (on the basis of atomic ratios), most elements are available in excess quantities. Notable exceptions are nitrogen, phosphorus, and in some cases silicon (Redfield, Ketchum and Richards, 1963). The availability of these nutrients, in the appropriate situations, can be thought of as "limiting" the synthesis of organic matter and the productivity of a food chain. Nitrogen, however, is generally the element in shortest supply in most marine pelagic systems (Ryther and Dunston, 1971) and in some lakes (Murphy, 1980). The simplifying

assumption of single nutrient limitation originated from early agricultural concepts (Liebig, 1840) and has been used in the theoretical development of nutrient limited phytoplankton growth models (Dugdale, 1967). Actual nitrogen limitation is not an essential assumption in the present study, however, since at higher organizational levels, constraints on ecosystems usually involve consideration of the interaction among several elements (Lichens, 1981).

High rates of nitrate uptake are associated with eutrophic ocean regions (Dugdale and Goering, 1970). In further field applications, MacIsaac and Dugdale (1972) reported a differential light dependence of nitrate and ammonium uptake and the inhibition of nitrate uptake by ammonium. The substrate "kinetics" of nitrogen uptake by both natural and laboratory phytoplankton has been studied by the ^{15}N technique. The half saturation value for nitrate and ammonium uptake varies and is related to typical ambient concentrations (Eppley et al., 1969, Eppley and Thomas, 1969, MacIssac and Dugdale, 1969). Further work suggested patterns of nitrogen utilization were dependent on the trophic status of the water column (Thomas, 1970).

An enzymatic method of measuring nitrate reductase activity was developed (Packard, et al., 1971), and a comparison among methods for nitrogen assimilation studies has been made (McCarthy and Eppley, 1972). Recently an interesting refinement in ^{14}C methodology was developed to measure protein synthesis directly. This method indicates protein synthesis can account for 85% of assimilated nitrogen (Ditullio and Laws, 1983).

Phytoplankton can utilize nitrogen from organic compounds and ^{15}N labeled urea has been used to demonstrate this capacity (McCarthy, 1972). Urea hydrolyzing bacteria may play a role in this pathway (Zobel and Feltham, 1935). McCarthy (1972) found that urea accounted for 28% of total nitrogen

uptake in coastal waters during his study period. In the north Pacific, urea uptake was ca. 50% of that for ammonium (Eppley, et al., 1977). Phytoplankton are capable of utilizing nitrogen from dissolved amino acids to a limited extent, although the uptake rates are only a few percent of either nitrate or ammonium (Schell, 1974).

Ammonium is the nitrogen source most readily used by phytoplankton (Walsh and Dugdale, 1971; McCarthy et al., 1977). Studies have followed in which the relative uptake of nitrate and ammonium have been related to the ambient ammonium concentration (Olson, 1980). It is not clear, however, that the relationship is due solely to inhibition of nitrate uptake by ammonium uptake as has been shown in laboratory studies on the green alga Chlorella (Syrett and Morris, 1963).

Caveats pertaining to the ^{15}N technique recognized in the earlier studies have received quantitative reexamination (Glibert, et al., 1982). In oligotrophic waters of low ambient ammonium concentration and high regenerative potential, the standard mathematical model of Shepard (1963) may underestimate ammonium uptake. Shepard's (1963) model assumes constant external pool enrichment throughout the incubation, which may not be the case in certain situations. This changing external pool enrichment is, in fact, the basis of dilution techniques. More detailed approaches to ^{15}N measurements are needed to test the hypothesis that in oligotrophic waters phytoplankton exploit micropatches of ammonium with elevated uptake rates sustained for short periods of time (McCarthy and Goldman, 1979).

1.5 The Laboratory: The Southeast Bering Sea

The Bering Sea until recently, had been one of the lesser studied ocean areas scientifically. Following the exploratory studies by Vitus Bering (1725 - 1741) and James Cook (1778 - 1779), extensive exploitation of the Bering Sea's marine mammal and fisheries resources by technologically advanced countries took place. Additionally, the area has long been the source of a subsistence living for the native peoples of the area. Only a synopsis of the oceanographic features important to the present work will be given here. More general descriptions are available in Hood (1983) and the volumes edited by Hood and Calder (1981).

From 1978 to 1982 the National Science Foundation sponsored PROBES (Processes and Resources of the Bering Sea Shelf) project collected oceanographic data in the Southeast Bering Sea (Figure 3). These data documented the development of intense diatom-dominated spring blooms on this subarctic shelf (Iverson et al., 1979a). Most of the important environmental influences on spring bloom development have been evaluated during the PROBES project. Therefore, the southeast Bering Sea shelf presents an unusually good "laboratory" in which to attempt an improved quantitative analysis of bloom development along recognized environmental gradients.

Classic studies of high latitude phytoplankton growth long ago established the dependence of the light conditions which phytoplankton experience on the mixing characteristics of the upper water column (Gran and Braarud, 1935, Riley, 1942, Riley et al., 1949). Since then, the application

Figure 3.

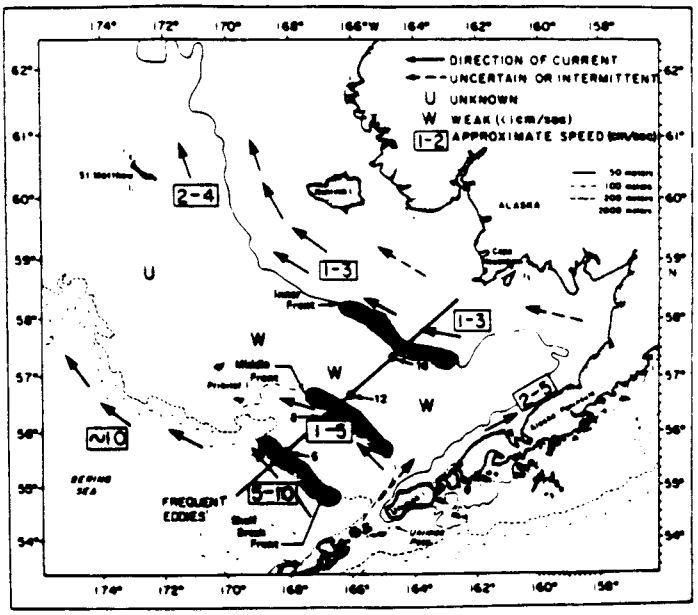

Figure 4.

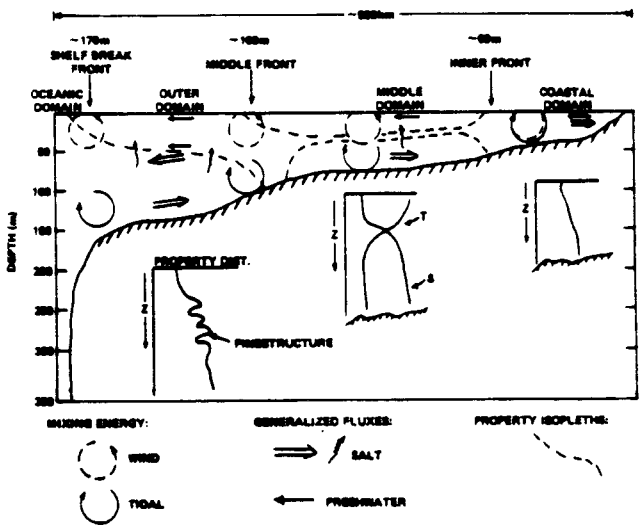

Figure 3.

Estimated mean circulation, approximate location of fronts and main cross shelf PROBES line on the southeast Bering Sea shelf (modified from Kinder and Schumacher, 1981).

Figure 4.

Schematic summarization of vertical property distributions and fluxes on the southeastern Bering Sea shelf (from Coachman, et al., 1980).

of tracer techniques has prompted a more detailed analysis of such influences as light inhibition, (Steele, 1962) and nutrient concentration (Dugdale, 1967), and allowed phytoplankton growth to be treated in systematic analyses (Winter et al., 1975). There is a continuing effort to reconcile photosynthetic rate measurements with surface water physics since earlier parameterizations cannot account for phytoplankton growth dynamics on a mechanistic basis (Marra, 1978).

Other purely physical factors such as temperature affect growth (Mandelli, et al., 1970, Eppley, 1972). Also, horizontal advection acts against the spatial integrity of phytoplankton patches by what can be parameterized as a diffusive action (Okubo, 1974). Such a diffusive effect greatly complicates developmental studies in the open ocean. Additionally, biological factors such as grazing affect the size and structure of phytoplankton communities (Walsh, 1976).

1.5.1 Physics

Iverson et al. (1979a) reported observations supporting the hypothesis that major food webs leading to large stocks of pelagic and benthic fauna on the eastern Bering Sea shelf are separated in space by their relationships to a complex physical system of oceanic/shelf fronts separated by interfront regions (Figure 3). The fronts arise from changes in the mixing energy balance between tides (shearing up from bottom) and winds (mixing down from surface)(Coachman and Walsh, 1981). In the coastal domain the two mixing energies overlap leading to vertically homogeneous water. At the depths

in the middle shelf domain the two mixing energy sources are separated and under conditions of sufficient surface buoyant energy input, a separate, lighter surface layer develops (Figure 4). The transition from this two layered water column to the vertically mixed coastal water has been identified as a structural front caused by the changing balance between buoyant energy content and tidal mixing (Schumacher, et al. 1979).

This cross-shelf physical structure results in each domain exhibiting distinct temperature, salinity and stratification properties as well as different circulation features (Coachman et al., 1980). The shelf break front is within $\pm$ 50 km of the shelf break (ca. 170 m isobath), about 500 km from shore; the middle front lies over the 80-100 m isobaths, 350-400 km from shore; and the inner front is centered over the 50 m isobath, 80-150 km from shore. Proceeding landward from the shelf break front, the hydrographic domains which these fronts define, are called outer, middle and coastal.

Long term mean currents on the shelf are small (ca. 1-2 cm/sec drift to the Northwest, Figure 3). The distributions of properties are governed largely by a diffusion defined to include the tidal scales (Coachman and Charnell, 1979). This diffusion results in a cross-shelf flux of properties between the two adjacent water masses (Bering Sea - slope water and middle shelf water) which is perpendicular to both the isobaths and the northwest drift. Current records from the middle shelf indicate that subtidal flow exhibited almost no net flow (Coachman, 1982).

The circulation on the southeastern Bering Sea shelf is tidally dominated. Extensive moored current meter and satellite drifter observations indicate scalar mean tidal speeds of ca. 20 to 25 cm sec^{-1}, increasing shoreward. Tidal excursions can be as great as 6 km., and most of the

horizontal kinetic energy is at tidal frequencies. Tidal kinetic energy varies from 60% over the outer shelf to >90% in the coastal domain. Subtidal flow is weak (1 to 5 cm sec^{-1}) and parallel to the fronts in the vicinity of the shelf break and inner fronts, while flow in the middle domain is insignificant (Figure 3).

No evidence exists for mass or momentum exchange between this shelf and adjacent oceanic waters by eddies or current rings. Because some freshwater is continually added by land runoff while the long term cross shelf salinity field is essentially constant, on-off shelf fluxes of freshwater and salt are continuous and primarily tidally driven. A hypothesis explaining the Bering Sea shelf fronts based on the conservation of salt is discussed by Coachman et al. (1980).

During the spring bloom on the southeastern Bering Sea middle shelf, phytoplankton growth rates are large relative to horizontal diffusive forces. In the analysis of bloom developmental patterns, therefore, horizontal advection is a tractable influence. Due to the lack of other mixing forces besides the predictable influence of tides over large areas of this shelf, wind mixing can periodically contribute most of the water column mixing energy (Schumacher and Kinder, 1983).

1.5.2 Shelf Nutrient Supply

Data are scarce on the nutrient load of Alaskan rivers (Hood and Reeburgh, 1974). Most of the nutrient supply to the shelf is thought to come from an on shore flux — a mechanism important for nutrient supply

to temperate shelves generally (Riley, 1967). On the broad, high latitude southeast Bering Sea shelf, coastal upwelling is not an important factor supplying surface nutrients for plant growth. The estimated average vertical velocity is significantly lower than upwelling areas and even other shelf areas such as Georges Bank (Walsh, 1983). Nutrients move horizontally onto shallower shelf areas as a diffusive flux from offshore Bering Sea-Slope water and are then dependent on vertical wind mixing to reach surface waters (Coachman and Walsh, 1982).

The spatial variability or "patchiness" of chlorophyll distribution has been shown repeatedly to coincide with physical hydrographic features in the coastal environment (e.g., Seeliger et al., 1978). In the Bering Sea this is also true in places where the frontal systems may act as conduits of nutrients to the surface and are areas of active phytoplankton growth throughout the summer (Iverson et al., 1979b). The dependence of surface water nutrient supply on specific combinations of physical conditions has been observed in a variety of coastal environments (Winter et al., 1975, Sinclair, 1978). Important similarities to the present study area exist, such as the covariability Sinclair (1978) found in the St. Lawrence estuary between neap-spring tidal mixing and nutrient supply to the mixed layer.

Also similar to the present study area are the frontal regions of the northwest European shelf (Pingree et al., 1978). The spatial distributions of Chl _a_ on the European shelf were shown to correspond to what PROBES calls the inner front (Figure 3). The position of this tidally mixed front depended on the dissipation rate of tidal mixing energy in the water column, which in turn is a function of water column height and tidal current velocity. The northern European shelf work also relates the observed spatial pattern of production to

specific mixing properties of the water column. Summer surface Chl a distributions were correlated with the seaward transition to stratified shelf waters and declined offshore as deeper water allowed for a more intense, deeper, pycnocline. The data they present indicate the baroclinic nature of the fronts and suggest the isopycnal mixing of surface and deeper water in these frontal areas.

1.5.3 Climate and Shelf Hydrography

Historically, storm tracks pass over the middle shelf domain of the southeastern Bering Sea from February through April (Brower et al., 1977). During an average year, about 14 storms pass over the region during these months with 25-36% of the associated wind velocities greater than 22 knots. The lack of temperature and salinity structure in the water during winter allow these early spring winds to easily mix the water column to the bottom on the middle shelf. Usually, by May, storm tracks move out of the eastern Bering Sea and mean wind speeds drop to 13-14 knots. Storms occasionally pass through the region after May, however (Brower et al., 1977).

The mean position of the maximum upper air winds (which tend to guide or "steer" the surface lows) is approximately parallel to the 40^{o} latitude, some 1600 km south of the eastern Bering Sea shelf. Niebauer (1980, 1983) has suggested the winter atmospheric circulation is the driving force behind large year to year temperature variations in this area. The region has been under the influence of a general warming trend since 1976, and 1979 and 1981 were especially warm years. Monthly mean sea surface temperatures for a

300 km square centered on the Pribilof Islands for May 1979-1981 were 4.66°C, 2.89°C, and 4.13°C respectively, or 2.41°C, 0.64°C and 1.88°C above normal. Inspection of monthly mean 700 mb (approximately 3000 m above sea level) flow patterns of "steering winds" indicate that the mean late winter and spring air flow was from the south leading to the above normal temperatures in 1979-1981 (Niebauer, 1983). Conversely, predominantly northerly winds produce colder middle shelf water temperatures (McLain and Favorite, 1976).

Such short term climatic fluctuations play a large role in conditioning the water of the middle shelf domain (Niebauer, 1980). In cold years this region is ice covered (e.g., 1976), in warm years it is not (e.g., 1978-1982). The spring bottom water temperature distribution reflects the severity of the previous winter. As evidence of the paucity of cross shelf exchange occurring in this region, in any one year, bottom temperature varies little from spring to fall (Coachman and Charnell, 1979). The bottom temperature range is approximately -1 to 4° depending on the previous winter (Coachman and Charnell, 1979). The formation of a stable upper layer in spring may first be initiated by ice melt in cold years, whereas in warm years changes in salinity seem to play a small role in controlling density. Seasonally, surface temperatures vary from below freezing in winter, to 10° C in summer.

1.5.4 Shelf Biology

The eastern Bering Sea has long been a biologically productive region to man. This shelf covers only 0.33% of world's ocean area yet provides approximately 5% of the total world fishery catch (Goering and McRoy, 1981).

An intense multinational fishing effort is applied annually to the Bering sea. In 1978 for example, almost 1 MT of walleye pollock (Theragra chalcogramma) having a dockside value of $92.4 million was harvested in the southeastern portion alone. This, together with the catch from other pollock fishing grounds, made pollock the largest single species food fishery in the world during that year (Smith, 1981). The area also supports a significant crab and yellow fin sole fishery (Otto, 1981 and Bakkala, 1981).

The catch per unit area is comparable to the shelves off Nova Scotia and in the northern North Sea, (Coachman and Walsh, 1981). This suggests that the larger fish yields may be the result of the extensive shelf area. Attempts at building a mechanistic model capable of accurately predicting variations in the "maximum sustainable yield" of these resources has already begun (Laevastu and Favorite, 1977). Such work is significant since apparent pollock densities over the past 20 years have varied by up to 50% (Smith, 1981).

Grazing studies suggest that copepod feeding activities have a significantly greater impact on outer shelf and oceanic areas than on the middle shelf (Cooney and Coyle, 1982, Figure 3). Shoreward of the middle front, most of the spring bloom production is not consumed by the pelagic fauna. Much of this phytoplankton biomass reaches the bottom intact and supports a large benthic standing stock on the eastern Bering shelf (Stoker, 1981). The bypassing of the pelagic food web occurs in the middle shelf domain because the phytoplankton community is geographically isolated from the large and effective grazers of the outer shelf region (Dagg et al., 1982).

Grazing can significantly influence the observed pattern and intensity of phytoplankton growth. Grazing effects have been incorporated into mathematical models of production for some time (Riley, Stommel, and Bumpus,

1953). The control of phytoplankton community structure by higher trophic levels has been suggested as an important factor influencing the exchange of energy between trophic levels (Steele and Frost, 1977). In the southeast Bering Sea maximum spring Chl a values were about four times greater at middle shelf stations than at those near the heavily grazed shelf break (Goering and Iverson, 1979).

Discernable differences in community taxonomic composition also exist between the two domains. Diatoms dominate the phytoplankton community in the middle shelf domain, while smaller non-diatom plants are prevalent on the outer shelf (Kocur, 1982). These cross-shelf differences in community composition appear to be related to the differences in grazing activity. The observed middle shelf diatom blooms therefore, develop under relatively little grazing pressure.

1.5.5 - Time and Space Scales of Oceanographic Sampling

The scale of oceanographic phenomena which can be addressed in a given study is determined by the resolution of the time / space sampling grid (Stommel, 1963). This is also a useful way to segregate biological field studies. In the analysis of Steele (1978), the resolution of a given oceanic biological signal depends largely on the "platform" used and the time scales of sampling. A characteristic phytoplankton growth response can be observed throughout an entire spectrum of stabilization - destabilization periods (Legendre, 1980), from the relatively unvarying conditions of oligotrophic tropical waters to the high frequency changes in stability

wrought by the M_2 tide and upwelling.

The ability to accurately resolve a signal of a given period depends on the sampling frequency (Neumann and Pierson, 1966). Time series considered in this study, for example, are based on a station occupation frequency of approximately every 5 days. Observations at unequal intervals hamper a strictly statistical approach to bloom development (Chatfield, 1980). The sampling frequency however, was more than sufficient to resolve the yearly phytoplankton bloom signal which becomes more intense at high latitude due to the lagged response of grazing in colder waters (Cushing, 1975). It was also sufficient to resolve events of higher frequency such as the periodic M_f (spring - neap) tidal cycle (period ca. 14 days) and certain aperiodic wind events.

1.6 Study Objectives

Generally, the goals were to:

1) construct time series of phytoplankton nitrogen utilization during the bloom period.
2) examine the influence seasonal changes in vertical mixing exert on nitrogen productivity and the nature of this interaction.
3) examine the applicability of current nutrient uptake and growth models to the nonsteady state spring bloom period.
4) compare nitrogen productivity measurements to other methods of estimating productivity from PROBES data.
5) evaluate the importance of grazing in cross shelf nitrogen utilization patterns.
6) look for interannual variability in nitrogen production and attempt to identify underlying mechanisms.
7) relate the new : total production occurring on this shelf to other marine areas and make preliminary estimates of the impact this photoassimilative reduction of combined inorganic nitrogen has on other aspects of the marine nitrogen cycle.

Chapter 2

Methods

2.1 Field methods

2.1.1 General Field Methods

Indicated on the main PROBES station line in Figure 3 are the locations of stations 5, 8, 12 and 16. At station 12 particularly, extensive time series productivity rate measurements and nutrients were obtained. Productivity data were collected across the shelf on the indicated station line and along others north and south of it as well. The standard station numbering begins at the shelf break with station number 1 and proceeds inshore at 23 km. intervals. At each station a Plessey 9040 series CTD (conductivity, temperature, and depth) cast was made, which included the collection of water samples with a rosette of 1.7 l Niskin bottles. The CTD data were averaged over 1 m intervals and field calibrated with in situ water samples.

Seawater density derived from the CTD data were used to calculate the Brunt Vaisala frequency, a measure of the vertical stability of the water column. This parameter can be thought of as the frequency with which a parcel of water will oscillate in the vertical when displaced a small distance from its equilibrium position, or alternately, as the theoretical maximum frequency for interval waves before mixing occurs. In shallow water, the Brunt Vaisala frequency (N) is defined as:

$$N = [(g/\rho \times d\sigma_t/dz) \times 10^{-3}]^{1/2} \qquad (1)$$

where g = acceleration due to gravity, ρ = water density, σ_t = sigma t and z = depth. For this study, Brunt Vaisala periods (BVP) were calculated as $2\pi \times N^{-1}$ over depth intervals of 2 m.

A mixed layer depth was defined as the shallowest depth of occurrence of a 0.02 σ_t change from the average σ_t value of the top 3 meters. Surface pressure weather charts were obtained from the National Weather Service, Anchorage, Alaska through the University of Alaska Arctic Environmental Information and Data Center by J. Niebauer. Geostrophic wind speeds were calculated from surface pressure maps for a 3^{o} square centered at 57^{o} N, 163.3^{o} W (Bakun, 1973) and supplied by Dr. L. Coachman.

Bottle samples were taken throughout the water column, but were more closely spaced near the surface than in deeper water . The bottle samples were analyzed for nutrient content (NO_3^-, NO_2^-, NH_4^+, $Si(OH)_4$, PO_3^{3-}, and urea, onboard ship using conventional autoanalyzer II techniques (Whitledge, et al. 1981). Discrete Chl a measurements were also made using the acetone extracted fluorescence method (Strickland and Parsons 1972).

Productivity stations were routinely occupied each day at 0800 hrs. local time. Water samples at these stations were collected with 30 liter acid-washed Niskin bottles held on a General Oceanics Rosette sampler. The productivity sampling depths were the depths to which 100, 50, 30, 15, 5, 1 and 0.1 percent of surface photosynthetically active radiation penetrated. Photosynthetically active radiation (PAR) is defined as the light energy between the wavelengths of 400 and 700 nm on the electromagnetic spectrum and measured in units of quanta (Einsteins). PAR penetration was measured with a LI-COR, Inc. underwater quanta sensor at the beginning of the productivity cast at each station. The bulk extinction coefficient, k, was estimated from these casts. Daily integrated surface PAR measurements were obtained with a deck mounted sensor and integrator.

Particulate carbon samples were analyzed on a Carla Erba elemental analyzer under the supervision of Dr. Richard Iverson. Triplicate 200 ml samples were filtered through precombusted glass pads and analyzed on return to the laboratory. Total particle volume and size distribution were obtained using a Coulter Counter Model TA II on the ship. The instrument was calibrated with latex spheres of known diameter and either 100 or 400 μm aperture tubes were used, depending on the size range of interest. Such tubes have an accuracy range of 4 - 40% of aperture diameter.

Total carbon dioxide (ΣCO_2) was determined by Dr. L. Codispoti and the techniques are described in Codispoti et al., (1981). They consisted of stripping acidified freshly collected sea water samples with nitrogen gas and measuring the CO_2 content with a Beckman 215B IR Analyzer standardized with sodium carbonate. Measurements of pCO_2 referred to in this study were made by Dr. D. Hood by the methods described in Hood (1981). The partial

pressure of CO_2 gas in surface water pumped continuously from the ship's sea chest was measured in an equilibrated gas stream by a Beckman model 215 IR infrared gas analyzer. Standardization was made against gases of known concentration based on the primary standards of C. D. Keeling of Scripps Institution of Oceanography, LaJolla, California for the 1976-80 data and the Bureau of Standards for the 1981 data.

2.1.2 Instantaneous Rate Measurements

Water from each Niskin bottle, or from several Niskin bottles tripped at the same depth, was placed in 20 l Nalgene carboys. The carboy contents were mixed during subsampling for nutrients and phytoplankton standing crop measurements and rate incubations. For the 24 hour ^{15}N incubations the bottles were subsampled into 1.7 l plastic bottles covered with neutral density nickel screen (Perforated Products) to simulate in situ light levels. The incubations were done in seawater cooled on deck incubators. These incubators kept the bottle contents within several degrees of the three meter seawater temperature.

Standard nitrogen productivity incubations lasted 24 hrs.. This method avoided the need to scale shorter rate measurements to daily rates based on an assumed diel signal in productivity rates. Also, the 1.7 l incubation bottles are less sensitive to bottle effects which can be severe in small volume, extended incubations (Venrick et al., 1977). In the 24 hour incubation bottles, the final concentration of added label was 23.1 mg-at m^{-3} $^{15}NO_3^-$, 11.6 mg-at m^{-3} $^{15}NH_4^+$, or 11.6 mg-at m^{-3} ^{15}N urea, depending on

the specific uptake rate sought.

The relatively large ^{15}N concentrations employed minimized two potential sources of error. Nitrogen uptake rates are concentration dependent and often display a hyperbolic (Michaelis - Menton) response to external pool concentrations (MacIssac and Dugdale, 1972). Uptake during the incubation did not change the external pool concentrations significantly, and thereby avoided concentration dependent changes in uptake rates Secondly, especially in the case of NH_4^+ and other regeneration products, the ^{15}N enrichment of the external pool can be diluted during the incubation, also producing an underestimate of uptake rates (Glibert, et al., 1982a). The ^{15}N additions used in the 24 hour incubations were generally insensitive to large changes in enrichment. The large nitrogen addition used however, was far greater than a trace amount (i.e. > 10% of ambient). The rates from such an experimental design therefore must be considered maximum rates under the given light conditions.

Short term incubations to measure the maximum light and nutrient saturated specific uptake rates for NO_3^-, NH_4^+ and urea (V_{max}) were also carried out. Water from the 50% light depth was subsampled into 1-liter glass incubation bottles. The V_{max} data were obtained from one of two types of experiments. During a light kinetic experiment, saturating levels of substrate were added to bottles covered with one of a range (0.1%-100) of neutral density light screens. A substrate kinetic experiment involved incubating all subsamples at the same (50%) light level but with different concentrations of added label. These kinetic experiments were designed to also yield estimates of the community half saturation value for uptake as a function of light (k_{light}) and ambient substrate concentration (k_s)

The substrate kinetic experiments require low NO_3^- levels in order to measure NO_3^- specific uptake rates at low ambient concentrations. When necessary, samples were held on deck in stirred 20 l carboys in a specially built, sea water cooled incubator. Light conditions corresponding to approximately the 40% light depth were present in the holdover experimental containers. The results of a typical NO_3^- kinetic experiment are shown in Figure 5. A hyperbola of the form $v = (S \times V_{max})/(K_s + S)$ where S = the substrate concentration, was fit to the data by the method of Cleland (1967). This approach uses an iterative technique with a least squares end point to estimate the parameters V_{max} and K_s and their respective confidence intervals and produced more consistent, unbiased results than straight line transformations of the hyperbolic equation, (Nimmo and Atkins, 1979).

From these kinetic experiments V_{max} for NO_3^- uptake was taken as the rate reached under simultaneously saturating light and NO_3^- conditions. In most cases saturation of the substrate uptake processes occurred in light of less than 1 ein. m^{-2} hr^{-1} and at approximately 10 times the Michaelis "constant" (k_s) for substrate uptake. The NO_3^- and NH_4^+ levels at saturation, however, displayed more variability than did the saturating light levels.

Incubation times for the V_{max} experiments were kept as short as possible, yet long enough to insure a sufficient enrichment in the final sample (1.5-4 hrs.). Incubations were done at the same time period each day (from 10:00-14:00 hrs., local time) to control for diel periodicity in uptake rates. Such periodicity was inferred from daily cycles in inorganic nutrients in oligotrophic tropical and subtropical regimes (Goering et al. 1964), and is evident in a variety of phytoplankton properties (Smayda,

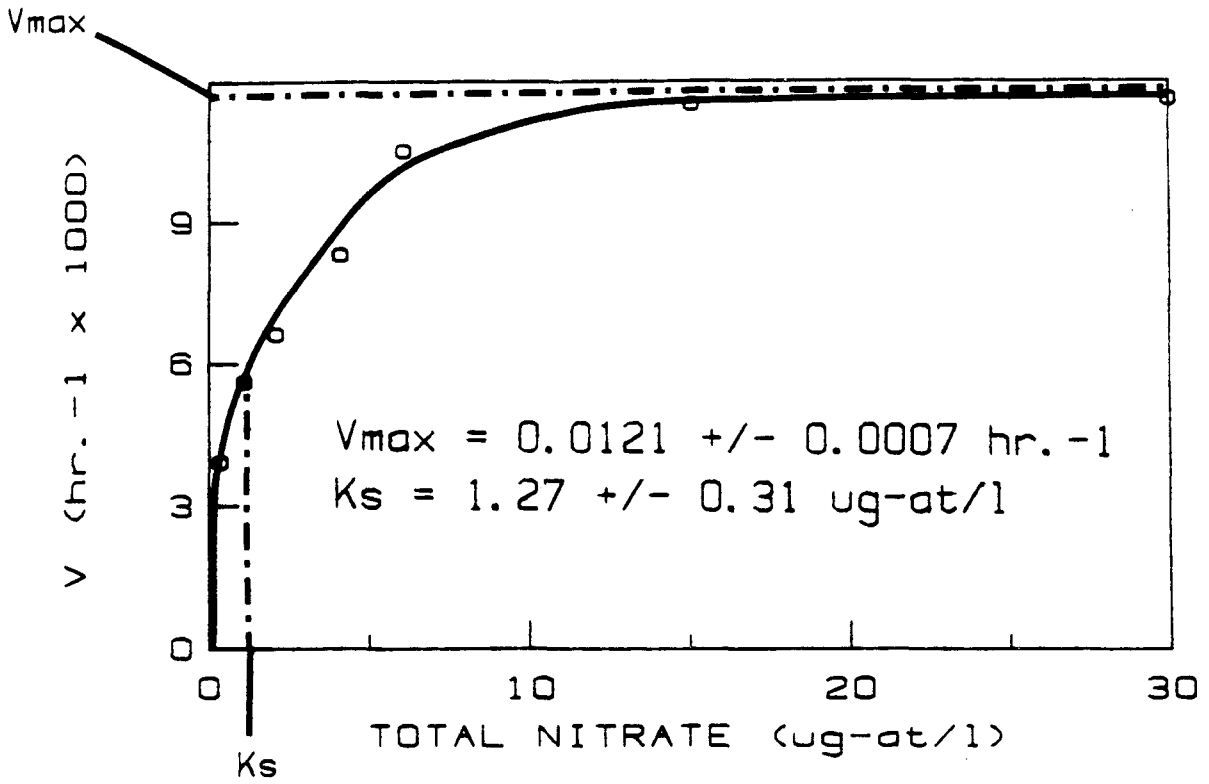

Figure 5.

Results of a typical nitrate kinetic experiment in which the parameters $V_{(max)}$ and K_s are indicated.

1975).

The particulate material was filtered from the incubation bottles at the termination of the incubations onto Gelman glass fiber filters type A/E which have a nominal retention capability of 0.8 μm. Zero time blanks were taken periodically. The filters were usually frozen when still wet and lyopholized on return to the laboratory. In 1981, however, the filters were dried immediately in an onboard drying oven at 50^{o}C after it was determined that there was no measurable loss of volatile nitrogen.

Carbon productivity was measured by R. Iverson. Briefly, the method used was as follows. One dark and two light milk dilution bottles of 160 ml capacity were filled from each light depth carboy. Ten microcuries of $NaH^{14}CO3$ were added to each bottle with an Oxford pipette. Sodium carbonate only was used to buffer the deionized water to avoid metal contamination effects described by Fitzwater et al. (1982). The ^{14}C solution was standardized by the method of Iverson et al (1976).

The ^{14}C productivity samples were incubated between 6 and 10 hours. The same simulated in situ light levels were used as for nitrogen productivity, save for the 0.1% light depth which was not usually sampled for ^{14}C measurements. Samples were taken from the incubator, placed in a dark box, and immediately filtered in subdued light through Whatman GF/C filters which were washed with filtered seawater at the end of filtration. Each filter was placed in a Nalgene Filmware tube to which 3 ml of Scintiverse liquid scintillation cocktail was added. The tubes were heat-sealed and allowed to stand for several hours until the GF/C filters became clear. Carbon-14 activity was measured with a Beckman LS 100C liquid scintillation spectrometer on board the R/V T. G. Thompson. External

standard / channels ratio standardization was used.

Carbonate alkalinity was determined with the method described in Strickland and Parson (1972). Daily carbon productivity was estimated by first subtracting the dark bottle carbon fixation estimate from the mean of the two light bottle carbon fixation estimates. The incubation period did not include several hours of light post-dawn and before dusk. Linearity of carbon fixation with light energy was assumed for these periods. It was further assumed that the ratio of productivity to light energy was the same during these periods as during the incubation periods. The productivity estimate for the incubation period was multiplied by the ratio of PAR during the daylight day to PAR during the incubation period to provide an estimate of daily productivity. The second assumption is weak although the mean ratio of daily PAR to incubation period PAR was 1.25 (s = 0.17, n = 64) for 1981. This suggests the calculation was not particularly sensitive to the violation of that assumption.

2.2 Laboratory Nitrogen Analysis Methods

2.2.1 Sample Preparation

The conversions of the sample nitrogen to N_2 gas for analysis was accomplished using an automated micro-Dumas procedure on a Coleman nitrogen analyzer. The basic conversion methodology used here differed little from that described by Barsdate and Dugdale (1965) except for the inclusion of

Silver Vanadate in the post heater tube to remove halogenated compounds from the sample stream. An inlet system was constructed using 1/8 inch stainless steel tubing and swagelok connections (Figure 5).

Metal to glass connections were also employed on the glass liquid nitrogen cold trap which removed the ultra pure CO_2 gas from the sample stream as it entered the inlet system from the Coleman. This proceedure followed the original methodology of Barsdate and Dugdale (1965). It is important to remove the CO_2 since it decomposes under the influence of the high frequency discharge in the emission spectroscope to form CO. This gas has a spectral band near that of $^{14}N^{15}N$ and therefore the at% (atom %) ^{15}N based on this peak will be erroneously high (Fiedler and Proksch, 1975). Partly because of this, molecular sieve (#5A) was incorporated into the inlet system (Figure 5).

After passing through the initial N_2 cold trap, the sample gas was absorbed onto the N_2 cooled sieve. The sample was released from the sieve by heating with Nichrome wire and the valve from the sieve closed when a pressure of 3 torr in the inlet system was achieved. At least 1 torr pressure was needed in the discharge tube to produce a steady emission. Lower pressures can be increased with a noble gas but due to the relatively large volumes filtered and the eutrophic nature of the area this was not necessary.

The molecular sieve step further purified the sample since the sieve has a much lower affinity for N_2 gas than the contaminating CO_2 which was selectively retained on the molecular sieve. Other gasses, such as water vapor and oxygen, can disturb the discharge. Water vapor is easily removed by the initial N_2 cold trap and residual oxygen is consumed by the oxidation

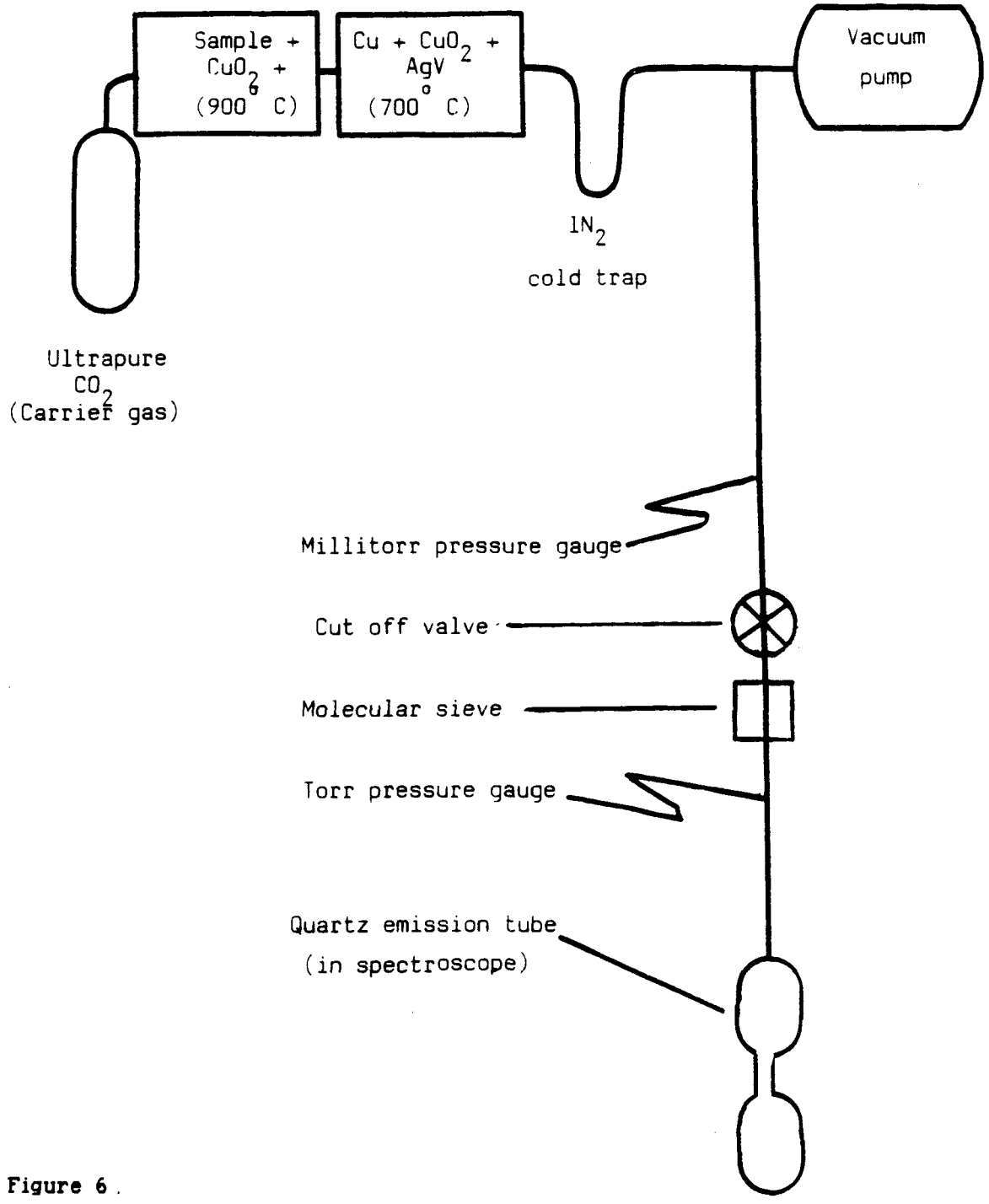

Figure 6.

Schematic of inlet system used for emission band spectroscopy of N_2 gas.

The reduction in volume of the inlet system in conjunction with the superior vacuum characteristics of the metal system over the previous glass configuration made it possible to dispense with the use of a diffusion pump. A large volume mechanical "roughing" pump and the liquid nitrogen cold trap were sufficient to attain millitorr pressure levels in the inlet system if care was taken to avoid the atmospheric contact with the interior walls of the system and allow for degassing for a sufficient time ()1 day) prior to use.

2.2.2 Measurement of Atom % ^{15}N

Sample atom % ^{15}N was measured by emission band spectroscopy using a Jasco model NIA-1 instrument (Japan Spectroscopic Co. Ltd., Ishikawa-cha, Hachioji City, Tokyo, Japan). A similar instrument has been used for phytoplankton ^{15}N uptake measurements by Murphy (1980). A metal to glass connection was necessary at the electrodeless quartz discharge tube, which is essentially a blind appendage off the inlet system, permanently installed between the antennae of the high frequency generator in the spectroscope. A frequency of 13 MHz at 50 W was used to produce an emitting plasma in the low pressure (1-4 torr) N_2 gas sample.

The mass differences among the N_2 molecules of various isotopic composition manifest themselves mainly in vibrational and rotational energies and produce a spectrum of wavelengths in the emitted light. The grating monochrometer used in the Jasco instrument had a reciprocal dispersion of 30 Å/mm. The emitting plasma was scanned at a rate of 20

Å/min. over the range of 2973 Å to 2993 Å. This part of the electromagnetic spectrum included the wavelengths of the band heads of the three isotopic molecules of nitrogen gas, (2977 Å - $^{14}N_2$, 2983 Å - $^{15}N^{14}N$ and 2989 Å - $^{15}N_2$)

2.2.3 Particulate Nitrogen Measurements

Initial Particulate nitrogen (PN) measurements (i.e. - pre-1980) were made on the same Coleman instrument used to combust the enrichment samples by the original manufacturer's suggested method. For samples collected after 1980, sample nitrogen was measured by the pressure generated in the calibrated Jasco inlet system. Two thermocouple gauge tubes (Veeco Instruments, Inc., model TG.70 & TG 270, Terminal Dr., Plainview, N.Y.) were incorporated into the inlet system (Figure 5). One provided measurement of gas pressures in the range of 1-1000 millitorr and the other from 0-27 torr. Each tube could be monitored by an appropriate gauge control calibrated according to the manufacturer's specifications. Assuming nitrogen behaves as an ideal gas and given the constant volume and temperature of the inlet system, the pressure generated by a sample will be proportional to the number of moles present.

The pressure reading for the sample nitrogen measurement was taken just before the sample was absorbed onto the molecular sieve. After this point the sample is restricted to the emission tube area by a cut off valve. This avoids the "dead space" caused by the LN_2 cold trap and provides greater pressure in the emission tube which becomes important in samples of low

total nitrogen.

A problem arose in getting visual pressure readings of sufficient precision from the gauge controls due to the exponential response of the meter. This was overcome by reading the millivolt output from the gauges on a 3 1/2 digit multimeter (Hewlett/Packard Co.). A manual switch was used to select the source of the incoming analog signal to the multimeter. Readings from the extremes of the control gauges (i.e. <2mv or >8mv) were avoided due to the poor response of the gauges outside their midranges.

2.2.4 Calibration of ^{15}N - PN System

The combined enrichment - sample nitrogen measurement system was calibrated using a series of phthalimide standards of known enrichment made from appropriate solution mixtures of ^{15}N phthalimide and normal at% abundance phthalimide. The enriched phthalimide, as well as all other ^{15}N labeled compounds used in this study were obtained from Prochem Isotopes, Summit, N. J.. Phthalimide (C_6H_4-CONHCO) worked well for several reasons. It is a relatively inexpensive organic compound that is tractable via the Dumas method and has approximately the same C/N ratio as the organic material in the samples. It is also easily recrystallized in any enrichment by adding carefully weighed amounts of the labeled and unlabeled chemical into very hot water. After dissolution needle shaped crystals form upon cooling. In this way standard enrichments of 1, 4, 7, 10, 15 and 25 at% were made.

These standards were used to calibrate both the total nitrogen and atom % enrichment measurement systems on the same standard runs. The phthalimide standards were weighed in aluminum combustion boats on an electrobalance (Cahn Model 4700, Cerritos, CA). Standards as small as 0.3 μg-at N could be weighed out in this manner.

Barsdate and Dugdale (1965) noted that samples of known enrichment were underestimated when the sample particulate nitrogen was low. They attributed this underestimate to the dilution effect of the blank nitrogen in the system. In the present modified system, the simultaneous measurement of sample particulate nitrogen and atom % ^{15}N enrichment made it possible to quantify the nitrogen blank by measuring the relationship between sample nitrogen content and atom % enrichment underestimate (Figure 7).

Atom % enrichment is defined as the percent of all N atoms which are ^{15}N, and when no blank N is present:

$$at\%_t = 100 \times ({}^{15}N_s / PN_s) \qquad (2)$$

Where ${}^{15}N_s = {}^{15}N$ in sample and PN_s = total nitrogen in the sample, and $at\%_t$ = the true atom % enrichment of the sample. When nitrogen is present in the emission tube from a contamination source (here assumed to be atmospheric nitrogen) an apparent atom % (at $\%_a$) is actually measured:

$$at\%_a = 100 \times [{}^{15}N_s + (.00366 \times PN_b)]/(PN_s + PN_b) \qquad (3)$$

Where PN_b is the blank nitrogen in the system. The value for atmospheric atom % ^{15}N was assumed to be 0.366 (Junk and Svek, 1958). Rearranging

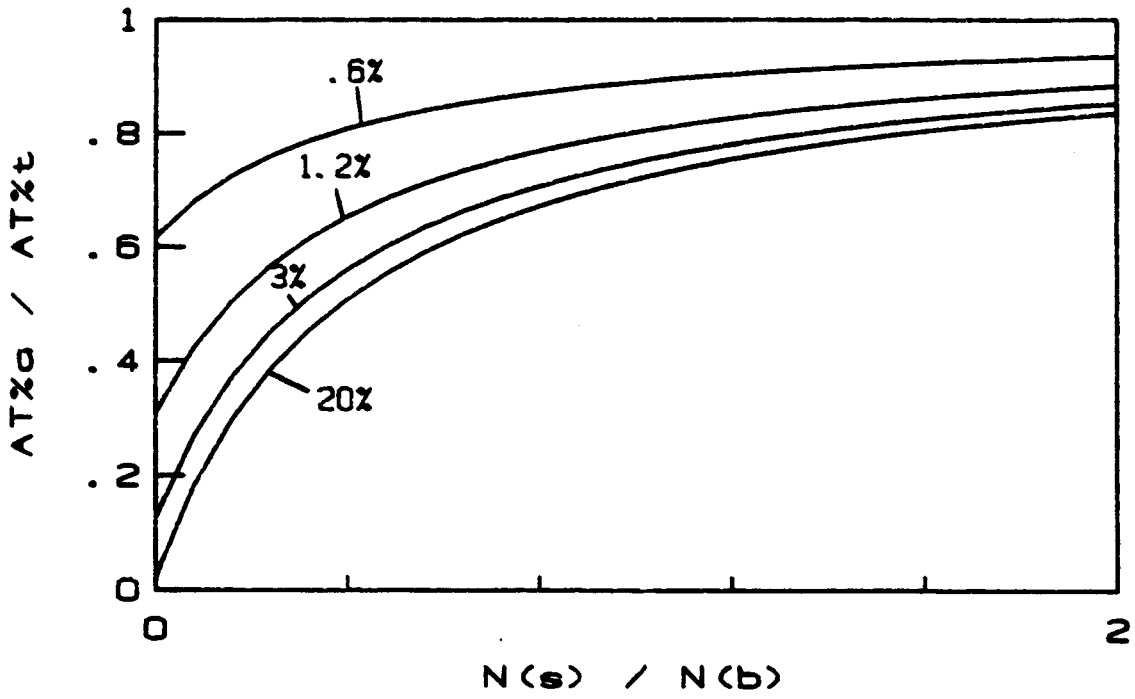

Figure 7.

Effect of blank N_2 in emission tube (N_b) on apparent sample enrichment ($at\%_a$).

equation 2 yields:

$$100 \times {}^{15}N_s = at\%_t \times PN_s \quad (4)$$

substituting equation 4 into equation 3:

$$at\%_a = [(at\%_t \times PN_s) + (0.366 \times PN_b)]/(PN_s + PN_b) \quad (5)$$

rearranging:

$$PN_s \times (at\%_t - at\%_a) = PN_b \times (at\%_a - 0.366) \quad (6)$$

After analyzing each preweighed ^{15}N Phthalimide standard all of the variables in equation 6 were known with the exception of the blank nitrogen (PN_b). Equation 6 was then treated as a straight line equation of the type y=mx and linear regression statistics can be used to find the blank nitrogen value (the slope of the line) and its 95% confidence interval (Figure 8). System blank nitrogen values measured in this way varied from 0.25 to 0.60 μg-at N depending on the Coleman instrument used to combust the samples.

As indicated in Figure 7, the actual sample atom % enrichment can be significantly underestimated when the blank nitrogen is a significant proportion of the total nitrogen present in the inlet system especially at high sample enrichments. Figure 9 indicates the ratio of sample nitrogen to blank nitrogen that is necessary to insure less than a 5% dilution caused underestimate at various sample enrichments.

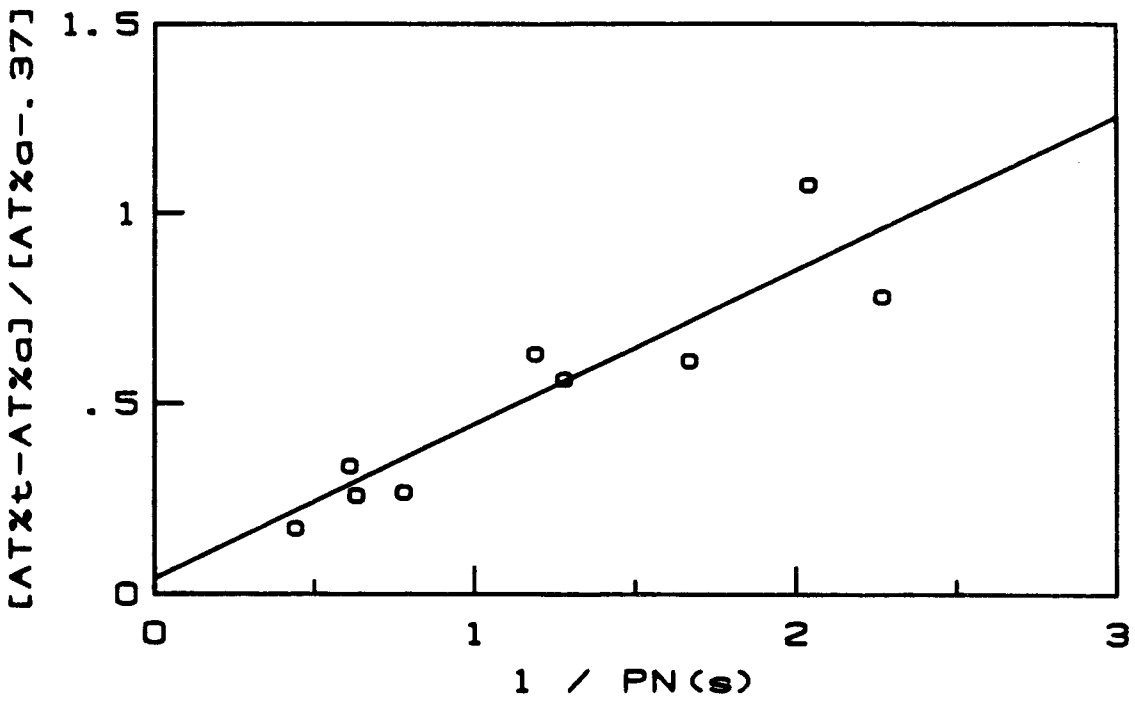

Figure 8.

Method used to estimate blank nitrogen (PN_b) in sample runs.

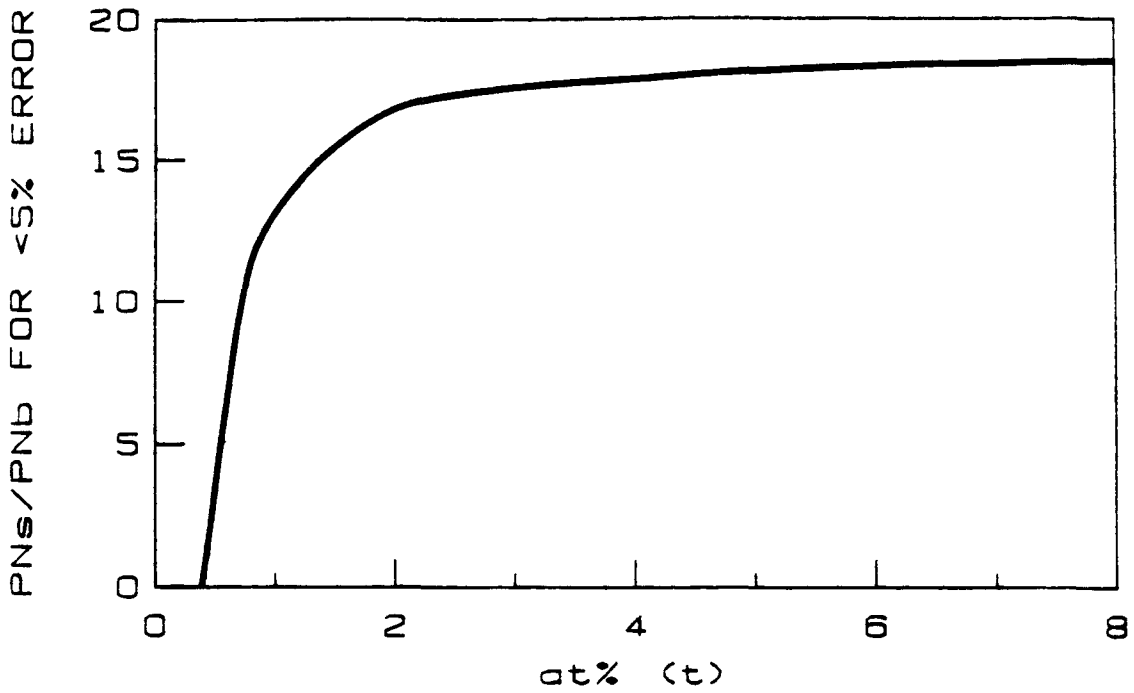

Figure 9.

PN_s / PN_b ratio necessary to avoid more than a 5% underestimate of $at\%_t$.

When constructing the standard curve for atom % abundance measurements from the spectroscope, therefore, only measured atom % abundances from samples with a very favorable PN_S/PN_B ratio (i.e. >20) were used. In this way the standard curve for measured enrichments (Figure 10) reflects the response of the JASCO instrument itself and is essentially free of the effects of blank dilution.

The 95% confidence interval for the slope of the standard curve in Figure 7 indicated that the system had an accuracy of $\pm$ 4% of the actual atom % enrichment value over the entire range of standards (0.37 - 24 atom %). In practice the standard curve for atom % enrichment was used as 2 subunits, one regression line for enrichments over 5 atom % and one for those below (Figure 10 a and b). This corrected for the "flatter" response of the JASCO at low enrichments and improved the accuracy of the standard curves to $\pm$ 3%. Replicate measurements of the same ^{15}N phthalimide standard indicated the precision of the system (standard deviation of replicates / $\bar{x}$) is $\pm$ 5% which does not change noticeably over the range of standards employed.

The sample nitrogen measurement system was calibrated on the same standards used for enrichment and typical calibration curves for the two vacuum gauges are shown in Figure 11 a and b. The accuracy of this method of determining sample nitrogen varied with the nitrogen content of the sample as shown in Figure 12. The 1.73 l incubation bottles which were used usually collected more than 2 μg-at of particulate nitrogen. The blank nitrogen value was subtracted from the total nitrogen in the inlet system to get the sample nitrogen content. The relative error of the atom % and sample nitrogen measurements can be used to estimate the relative error

A.

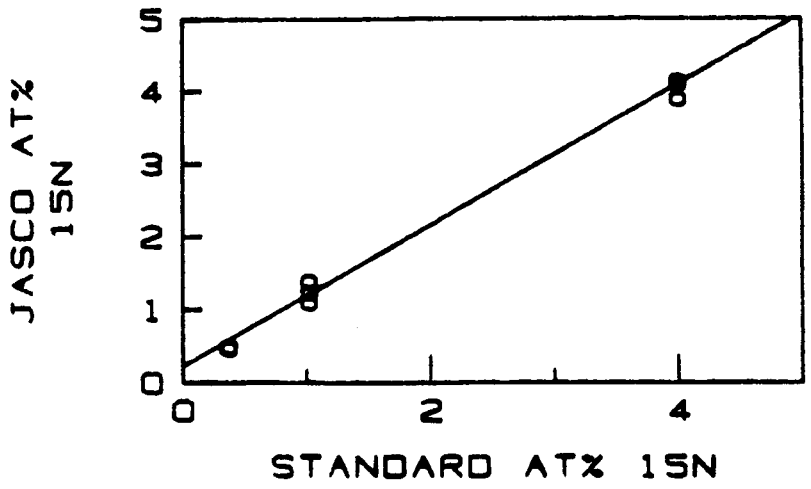

B.

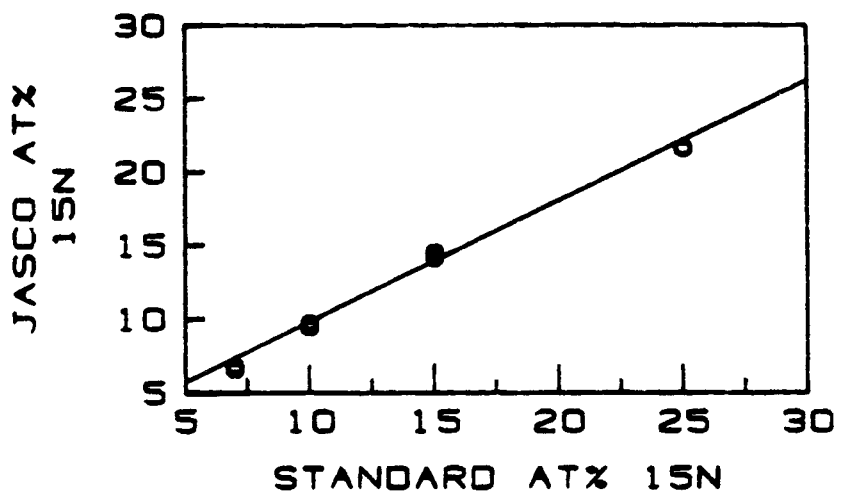

Figure 10

Standard curve for at% ^{15}N measured on Jasco spectroscope; a) standards less than 5%, b) standards more than 5%.

A.

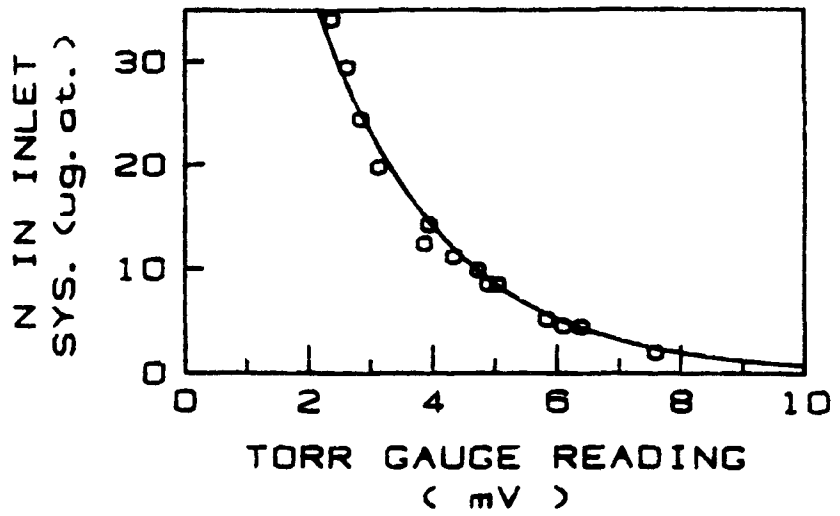

B.

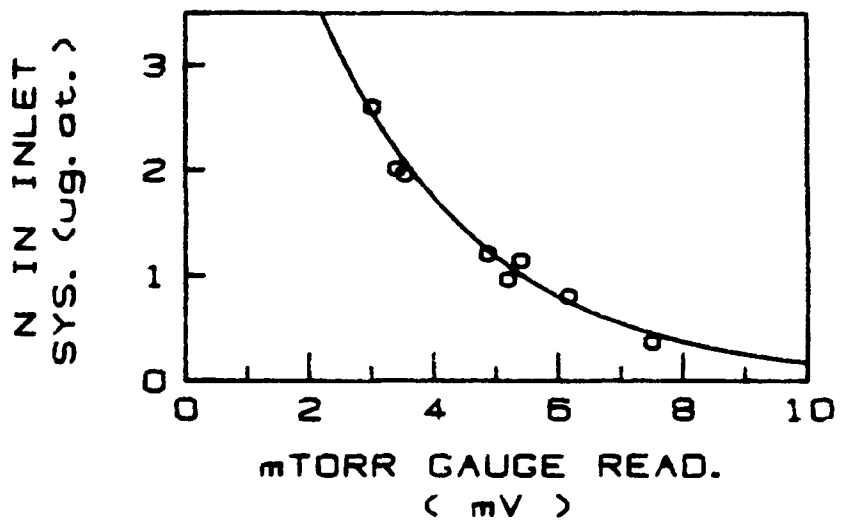

Figure 11.

Standard curves for PN measurements from pressure generated in inlet system on; a) torr gauge, and b) mtorr gauge.

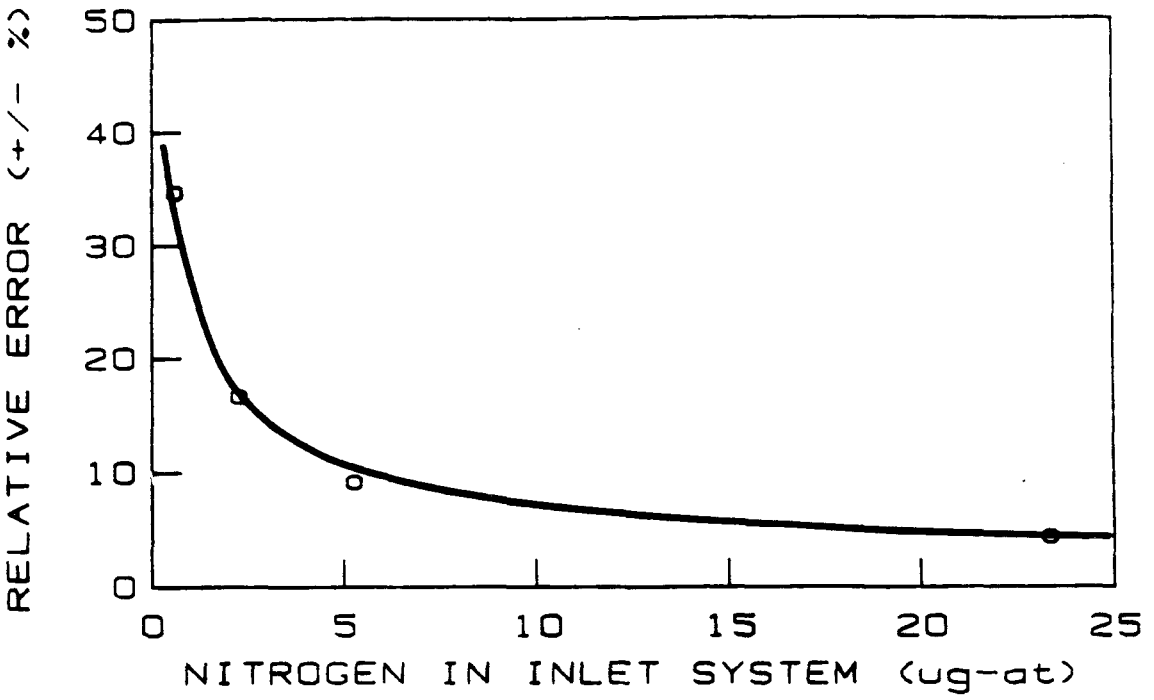

Figure 12.

Relative error of PN determinations at given sample size.

of a computed product such as Σ (v x PN) (Laitinen and Harris, 1975).

2.2.5 Analysis System Data Collection

Assuming Equilibrium in the following equation:

$$^{14}N_2 + {}^{15}N_2 = 2[{}^{14}N{}^{15}N] \qquad (7)$$

The law of mass action derived from equation 7 can be substituted into the definition of atom % ^{15}N to yield:

$$\text{at \% } {}^{15}N = ({}^{15}N_2 + 0.5 \text{ x } {}^{15}N{}^{14}N)/({}^{15}N_2 + {}^{14}N{}^{15}N + {}^{14}N_2) \qquad (8)$$

from which the following formula can be derived (Fiedler & Proksch, 1975):

$$\text{at \% } {}^{15}N = 100/(2R+1); \text{ where } R = {}^{14}N{}^{14}N \; / \; {}^{15}N{}^{14}N \qquad (9)$$

In calculating the atom % ^{15}N abundance from the emission spectrum, the peak heights of the $^{15}N^{14}N$ peak and the $^{14}N_2$ peak were measured, and their ratio taken as R and used in Equation 9 to yield the uncorrected atom % abundance. This value was corrected with the appropriate ^{15}N phthalimide calibration curve for the response of the spectroscope (Figure 10). A second correction for the presence of blank nitrogen was then applied:

$$\text{at\%}_c \; {}^{15}N_t = [(PN_b/PN_s) \text{ x } (\text{at\%}_a - 0.366)] + (\text{at \%}_a) \qquad (10)$$

In equation 10 $at\%_c$ is the corrected ^{15}N enrichment used in all subsequent calculations. Figure 7 indicates the blank correction was of negligible importance when the sample nitrogen was large (PN_b/PN_s approaches 0); but was significant in samples containing little nitrogen, especially if these samples were moderately enriched.

A valuable addition to the described analytical set up was the development and use of a data acquisition system. The system used a Hewlett-Packard 85 microcomputer interfaced to the digital multimeter by a HP 82937A interface bus (IEEE Standard 488-1978). In addition to the inputs from the pressure gauge controls, the multimeter received the millivolt signal from the spectroscope strip chart pen. By manually selecting the input to the multimeter the computer would acquire data from the proper instrument.

A program was developed in BASIC to sample the emission spectrum from the spectroscope and measure the $^{14}N_2$ and $^{14}N^{15}N$ peak heights. The speed of sampling is limited by the slowest member in the communications group which in this case was the multimeter which was capable of sending a digital signal at a maximum rate of 4.7 sec^{-1}. Since the spectroscope produced smooth, rounded peaks this sampling frequency measured peak height more precisely than the manual measurements which were used previously. A "hard copy" of the spectroscope output was also kept.

Conditional tests were incorporated into the data acquisition program to monitor for unsmooth peaks or repetitive scans in which the $^{14}N_2$ / $^{14}N^{15}N$ ratio changed significantly. In this way error messages would signify which machine-read measurements should be rechecked. A flow chart for the measurements taken and the corrections applied is presented in Figure 13.

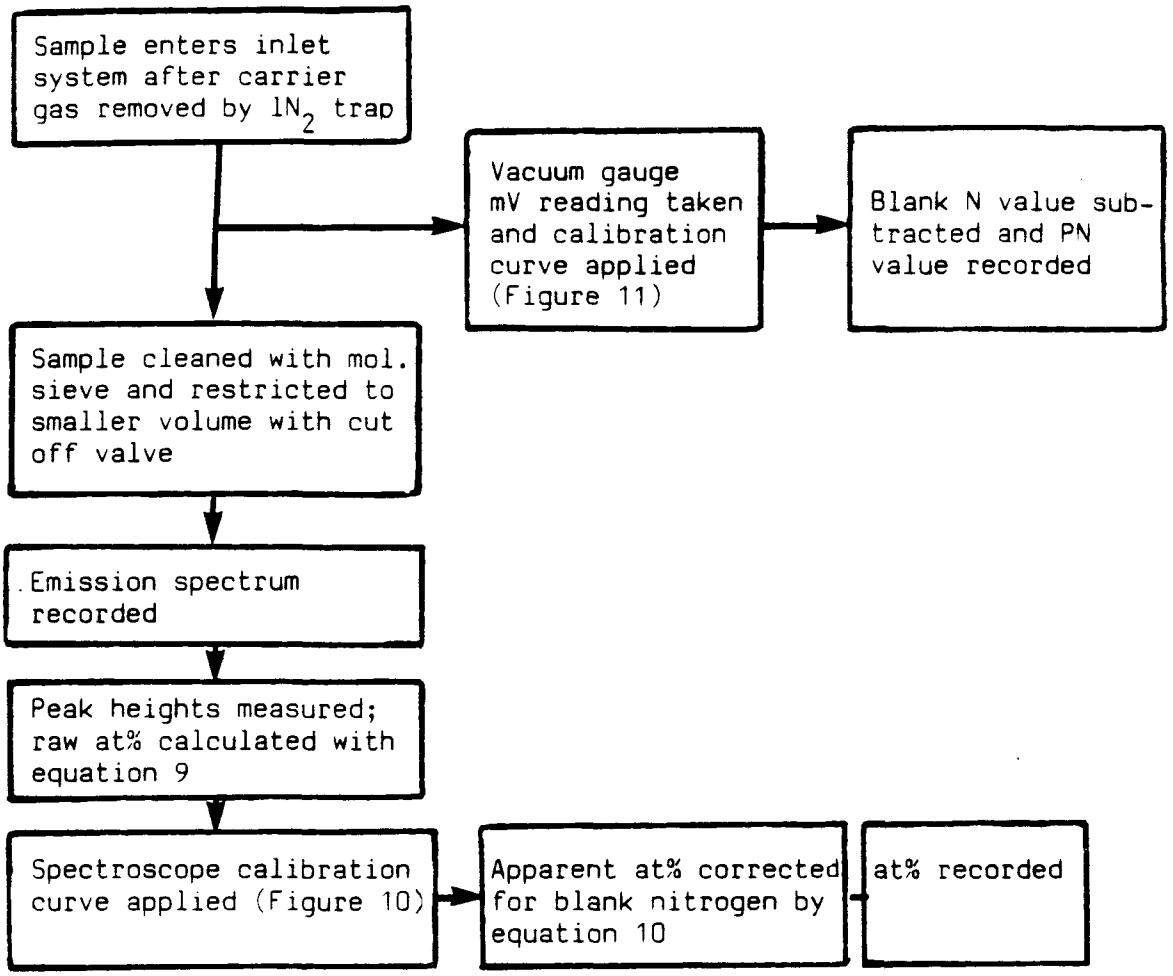

Figure 13.

Flow chart for data acquisition and calibration sequence during sample runs.

End of incubation specific growth rates (v_t, hr^{-1} were calculated using the measured excess at $\%^{15}N$, the incubation time, and the abundance ratio for the nitrogen species under consideration (Shepard, 1963):

$$v_t = [at\%_c - at\%_{t0}] / [at\%_{ep} \times \Delta T] \quad (11)$$

where $at\%_{t0}$ = zero time blank enrichment, $at\%_{ep}$ = external pool excess enrichment and ΔT = the incubation time in hours. An initial v (v_i) was estimated by subtracting $at\%_s$ from $at\%_{ep}$ in the denominator. The product of the proper specific uptake rate (v_t or v_i) and PN measurement (PN_t or PN_i) yields the absolute uptake for the particular nitrogen compound (ρ, mg-at m^{-3} hr^{-1}. The final sample nitrogen measurements (PN_t) were corrected for the increase in PN during the incubation by subtracting the ρ value. This correction made the PN value consistent with other initial biomass measurements (Chl a, PC, etc.).

Chapter 3

Relationships Among Vertical Mixing, Nitrate Uptake, and Growth During the Spring Bloom

3.1 Introduction

The interaction of wind induced vertical mixing with two fundamentally important influences on phytoplankton growth, light and nutrients, is evaluated in this chapter. The course of three high latitude continental shelf spring blooms has been followed using nitrate uptake as a developmental index. Developmental time series of nitrogen uptake have been attempted previously (Dugdale and Goering, 1970), and the central shelf area of the southeast Bering Sea presented itself as a useful area to further such studies in the context of a large, interdisciplinary, oceanographic research effort (PROBES - Processes and Resources of the Southeast Bering Sea).

Spring in high latitude shelf waters of moderate depth is characterized by the transition from deeply mixed surface layers to less turbulent, more

shallow layers. The suppression of vertical turbulence by a density discontinuity improves light conditions for the mixed layer phytoplankton community and ultimately restricts the exchange of properties between deeper water and the upper euphotic zone. This leads to conditions in which phytoplankton production can be limited by the availability of nutrients (Dugdale and Goering, 1967), among which nitrogen is generally in shortest supply relative to its utilization in the marine environment (Ryther and Dunston, 1971).

The assimilation of nitrate nitrogen is less energetically favorable for a plant cell than ammonium nitrogen assimilation, and it has been suggested that ammonium is the "preferred" nitrogen source (McCarthy, et al., 1977). Even so, nitrate accounts for over half the phytoplankton nitrogen supply during productive periods in coastal waters such as the west coast of Mexico (MacIssac and Dugdale, 1972), California (Eppley et al., 1978), and the southeast Bering Sea (Dagg, et al., 1982). A review of available measurements indicated that eutrophic areas are characterized by the use of nitrate as the dominant nitrogen source for plant growth (Eppley and Peterson, 1980).

During instances of high productivity in the ocean, diatoms are usually the dominant component of the plant community. They have been consistently found to dominate the phytoplankton during eutrophic conditions in coastal waters. Examples include Peru (Walsh et al., 1980), the New York Bight (Malone et al., 1977), and the southeast Bering Sea (Iverson, et al., 1979). Water column conditions in which diatoms are prevalent appear to be highly dependent on specific mixing conditions (Riley et al., 1950). Diatom prevalence can in fact be induced by artificially mixing previously stable

surface waters in both marine (Eppley et al., 1978) and freshwater (Lund, 1971) environments.

Specifically, it is hypothesized that in the Bering Sea middle shelf domain, the amount of mixing between the upper and lower strata of the water column assumes the dominant role in controlling the temporal development of the spring diatom bloom. Due to nitrate's simultaneous nutritive importance and dependence on vertical mixing processes to reach the trophogenic zone, rates of nitrate uptake should be a sensitive indicator of the physical - biological development taking place during the spring bloom period.

3.2 Results

Most of the data presented are from Station 12 (depth 77 m) located ca. 25 km inshore from the middle front on the main PROBES line (Figure 3). This station was occupied frequently during the 1979, 1980 and 1981 field seasons (17 April - 13 June 1979; 25 March - June 1980; and 14 April - 17 July 1981; T. G. Thompson cruises 138, 149 and 159 respectively). Extensive time series of physical, biological and chemical measurements have been compiled at this station and these form the basis of observations on the interaction between water column stability and the spring bloom production cycle presented in this communication.

For clarity the results of these time series are organized by developmental periods demarcated by the physical and biological conditions in the water column. Prebloom periods are considered those in which little or no vertical structure is present in the profiles of temperature, Chl *a*,

and nitrate. Peakbloom conditions are the relatively short lived periods which exhibit a surface (0-20 m) maximum in Chl *a*. The postbloom period follows the exhaustion of mixed layer nitrate.

3.2.1 The Prebloom Period

At the end of winter and throughout most of April, the mixed layer was relatively deep, often encompassing the entire water column which displayed little density structure (Figures 14c and f, 15 and 16d). The lack of upper water stability at this time was also reflected by the usually homogeneous vertical distribution in temperature, Chl *a*, and nitrate (Figures 14d, g and h, and 15 and 16c, e, and f). At times during April, a shallow mixed layer formed following a period of calm winds. These shallow layers were usually quickly deepened by subsequent wind mixing which destroyed most of the initial stability (e.g. - 25 April 1981, Figure 16 b and d).

In 1981, the observed maximum upper air wind flow coincided with the mean, keeping most low pressure out of the Bering Sea. In 1979 and 1980 the observed maximum upper air flow was approximately 1000 km farther north than the mean, driving some storms over the region. This resulted in generally greater wind speeds throughout the 1980 bloom period relative to the other years (compare Figures 14, 15, and 16 b).

Interannual variability was also recorded in April water temperatures. Mid April 1980 temperatures were significantly cooler than the other years (Figures 14 d, and 15 and 16 c). On a larger time and space scale, the May density structure variations observed here are related to short term (~years)

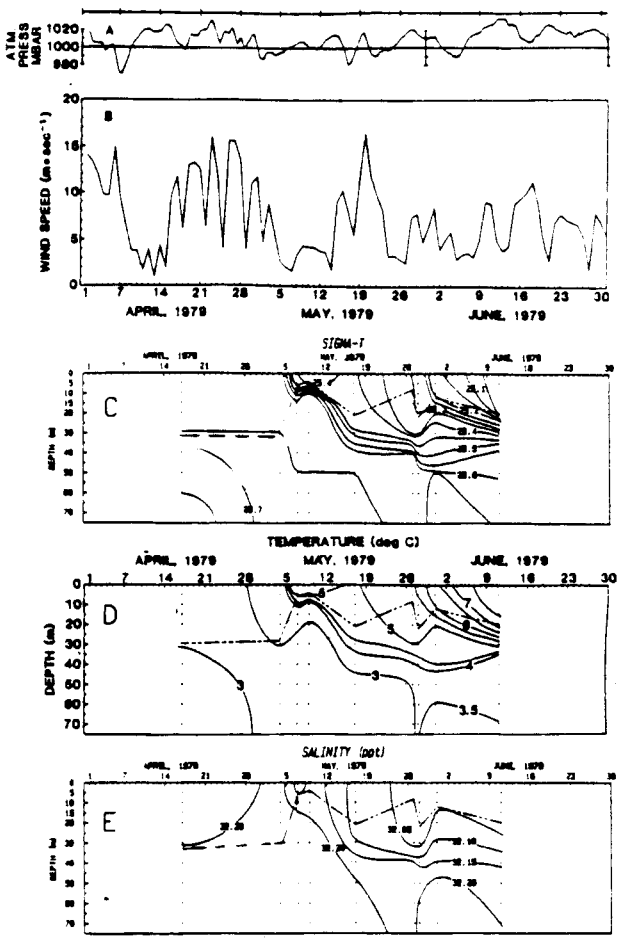

Figure 14.

Time series of selected parameters at Station 12 during April, May and June of 1979. The sampling days and depths are indicated by the vertical dots. Included on each time series are the mixed layer depths which are connected between stations by a broken line. A) Atmospheric pressure (mbarr), B) Calculated wind speed (m sec^{-1}), C) σ_t, D) Temperature (^{o}C), E) Salinity ($^{o}/oo$).

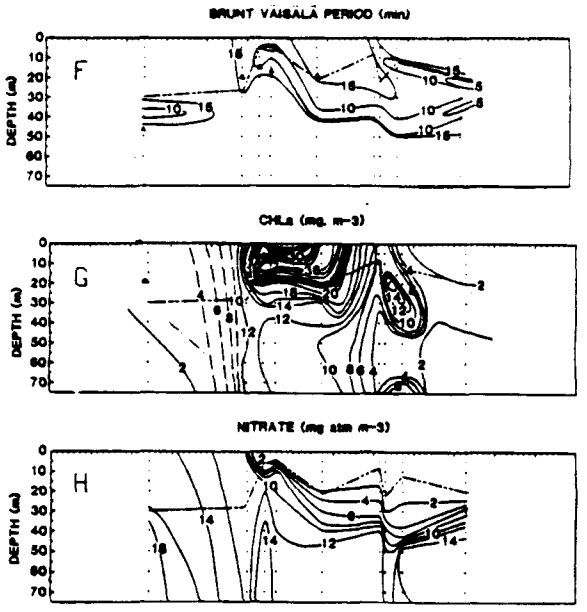

Figure 14 (continued).

F) Brunt - Vaisala period (min); included in this panel are the 0.1% light penetration depths (Δ), G) Chl *a* (mg $^{-3}$), H) Nitrate (mg-at m $^{-3}$).

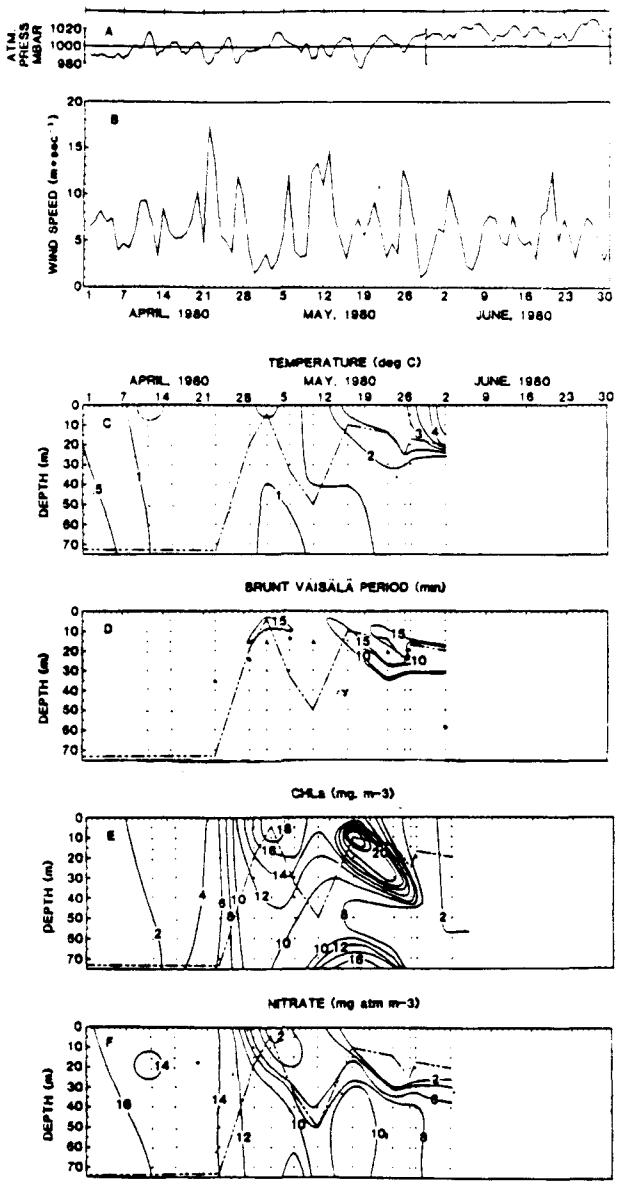

Figure 15.

Time series of selected parameters at station 12 in 1980. Presentation is like that of Figure 14 save for the exclusion of the σ_t and salinity panels.

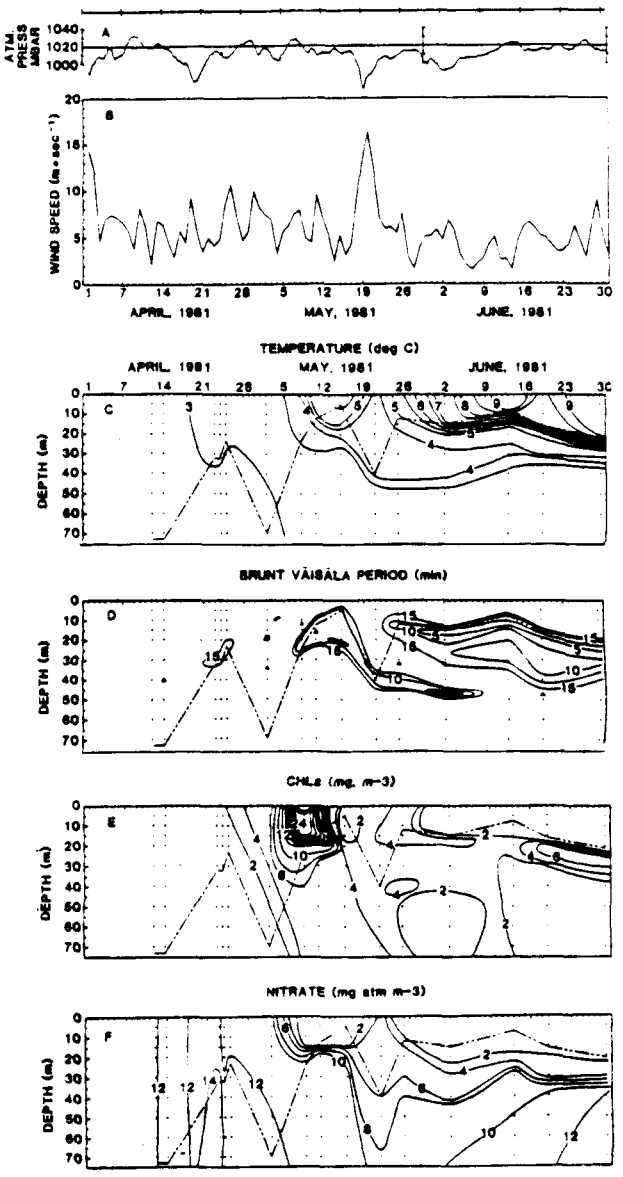

Figure 16.

Time series of selected parameters at station 12 in 1981. Presented as in Figure 15.

climatic fluctuations that strongly affect the eastern Bering Sea. May is the transition period during which the water column changes from homogeneous to strongly stratified.

Throughout the deeply mixed prebloom period nitrate uptake rates and phytoplankton standing crop remain low (Figures 17, 18 and 19 a and b). In Figure 17, 18, and 19 b, the prebloom period is characterized by the mixed layer containing more Chl a than (i.e. being deeper than) the euphotic zone. The water column was mixed to the bottom throughout most of April 1980 and doubling times for the mixed layer Chl a was correspondingly long (e.g. 14 days for the Chl a to increase from 2 mg m^{-3} on 7 April to 4 mg m^{-3} on 21 April (Figure 16c).

Sverdrup's (1953) mathematical model relating the mixed layer depth (Zm) to the critical depth (Zc) was followed through the three middle shelf time series as an index of the changing water column respirational losses experienced by the mixed layer phytoplankton community (Figure 20 a, b, and c iv.). The mixed layer depth criterion was given previously and the critical depth formula used is that of Sverdrup (1953):

$$Zc = \bar{I}_e / (k \times I_c) \qquad (12)$$

where in the present study k = PAR extinction coefficient (m^{-1}), $\bar{I}_e$ = the average hourly PAR entering the sea surface after allowing for reflectance losses (einsteins $m^{-2}hr^{-1}$), and I_c = the compensation point light level at which daily photosynthysis balances respiration. The I_c value used was that of Jenkin (1937) for Coscinodiscus (0.027 einsteins $m^{-2}hr^{-1}$). Based on a number of paired air and surface water PAR measurements made under a variety

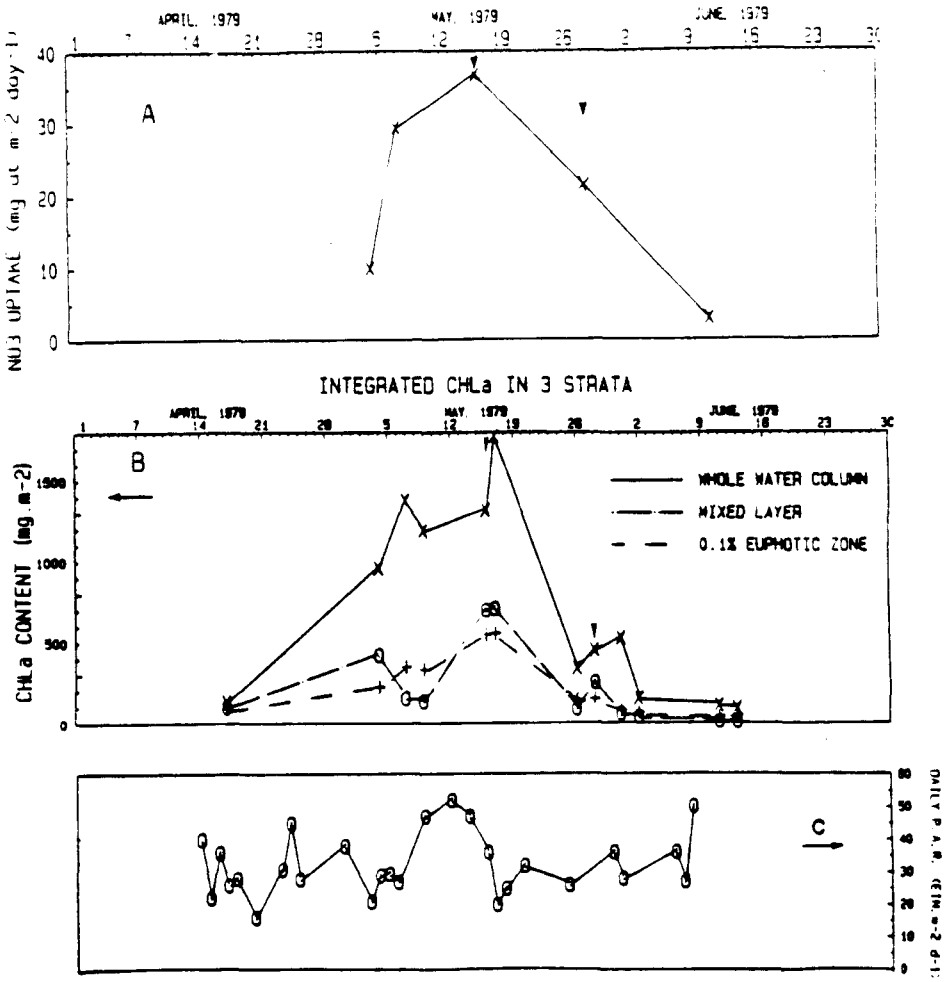

Figure 17.

Time series of nitrate uptake, standing crop, and daily light at station 12 in 1979. A) ρNO_3^- (mg-at m^{-2} day^{-1}), B) Chl *a* in selected water column strata (mg m^{-2}), C) daily P.A.R. measured at ship positions across the shelf (ein. m^{-2} day^{-1}). The solid arrowheads denote the arrival of postbloom storms.

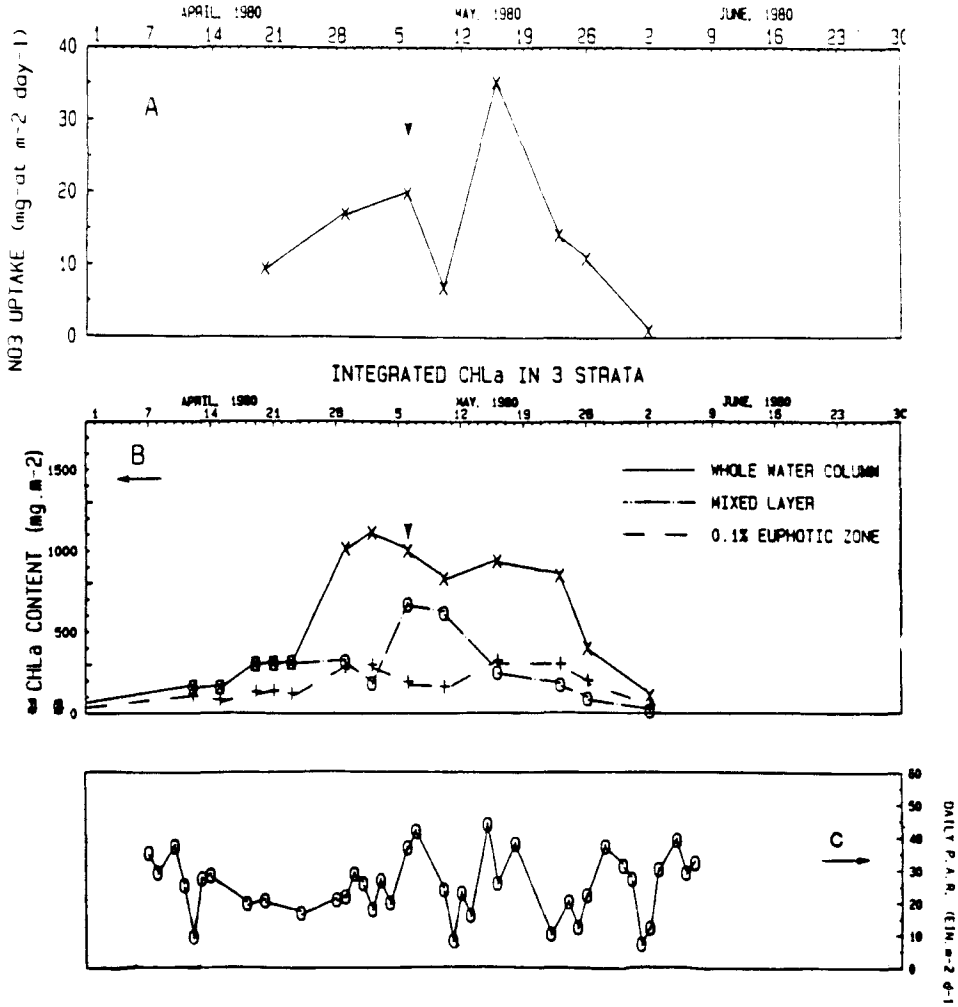

Figure 18.

As in Figure 17, but for 1980.

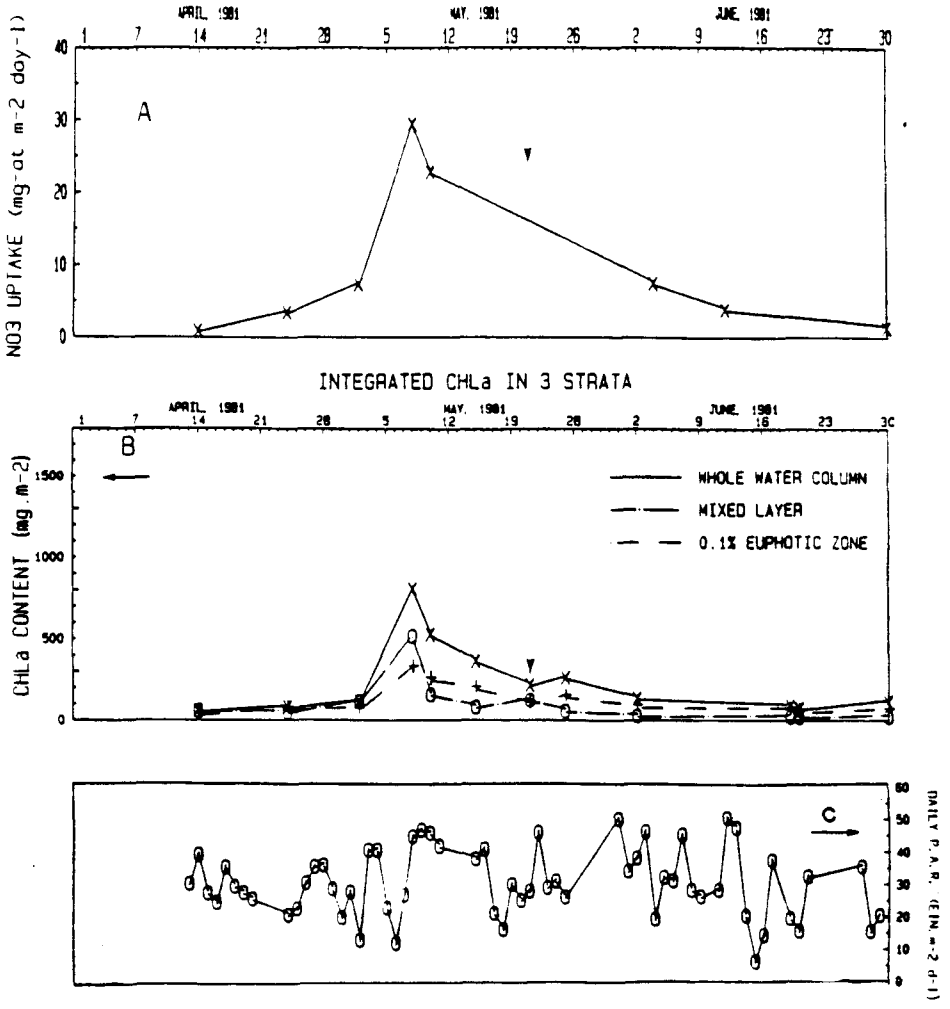

Figure 19.

As in Figures 17 and 18, but for 1981.

A - 1979

B - 1980

C - 1981

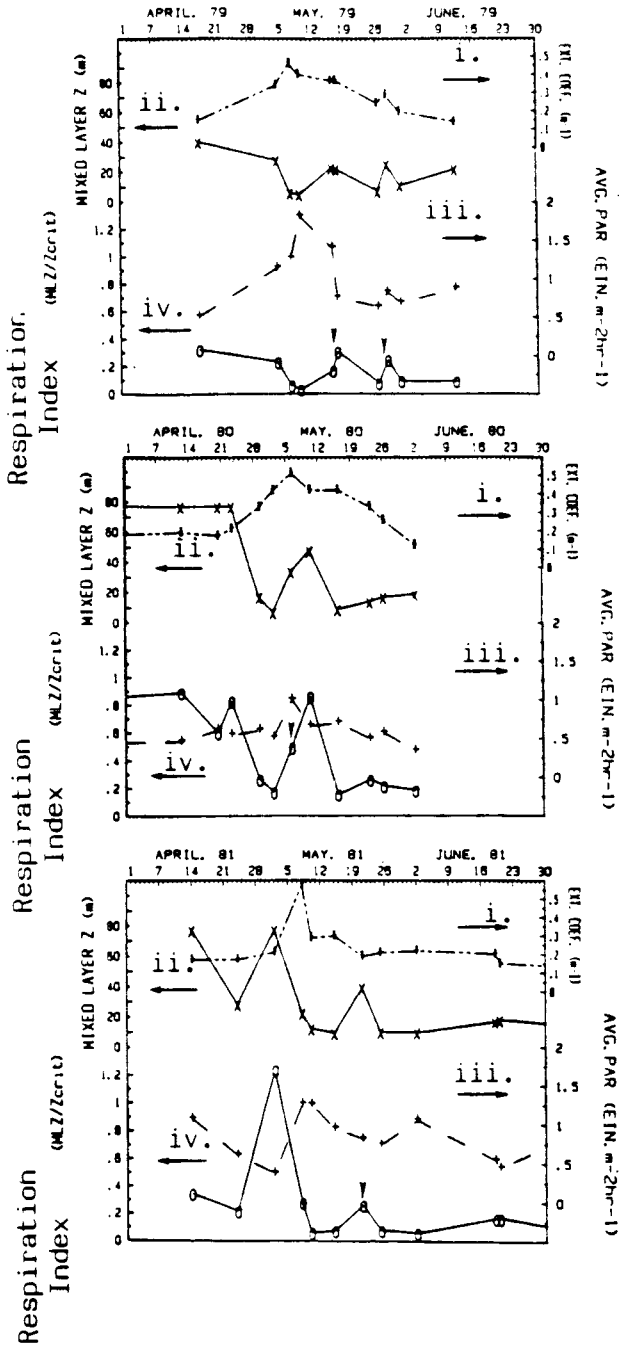

Figure 20.

Time series of the respiration index and its component variables at station 12 during A) 1979, B) 1980, and C) 1981.
The solid arrowheads denote the arrival of postbloom storms.

of sea surface conditions, 0.65 x deck integrated daily PAR was used to estimate $\bar{I}_e$.

The ratio Zm:Zc decreases along with the respirational losses of the phytoplankton as the plants spend an increasing proportion of the day under favorable light conditions for photosynthesis. This interaction between mixing depth and respirational losses has been an explicit concept in the systematic treatment of marine productivity for some time (Steele, 1966). Theoretically, net water column production begins when this "respirational index" becomes less than one, a development which preceeded middle shelf sampling in all three years. In ice free years at Station 12, a ratio of less than one is brought about by the deepening of the critical depth to more than 77 m (the water depth) and occurs in March when the daily incoming PAR first exceeds approximately 7 einsteins m^{-2} day^{-1}.

3.2.2 Peak bloom periods

Peak bloom conditions were observed on 4-7 and 16-17 May, 1979, 29 April - 2 May 1980, 14-17 May, 1980, and 2-10 May 1981 (Figures 14 g and h, and 15 and 16, f and g). Each of these periods was preceded by the shoaling of the mixed layer above the bottom of the euphotic zone (Figures 14 f, 15 and 16 d) and coincided with a doubling of the upper water Chl a concentrations to maximum bloom values of >20 mg m^{-3} (Figures 14 g, 15 and 16 e) and peak water column nitrate uptake and Chl a content (Figures 17, 18 and 19, a and b).

It is necessary in the following discussion to distinguish this high growth rate period from the preceding prebloom period in which net water column phytoplankton growth has taken place, but at a lower rate. Accelerated phytoplankton growth rates following mixed layer shallowing have been observed in the deeper areas of the Baltic (Kaiser and Schulz, 1978) and the North Sea (Williams and Lindley, 1980) and is consistent with generally held concepts of water column stability and light interactions in the sea (Ryther, 1963).

The specific timing of the phytoplankton bloom periods was controlled by a hiatus in wind mixing events associated with low pressure systems moving through the area such as 29 April - 2 May 1980 and 14 - 17 May 1980 (Figure 15 b and f). The meteorological conditions surrounding the development of the peakbloom period in early May of 1979 are shown in Figure 21. Initially, the winds associated with this low pressure system which moved into the Southeast Bering Sea from the western North Pacific were over 30 kts., but from about 2 May on, the low dissipated and winds dropped to 5-10 knots (Figure 14 b). The reduced cloudiness associated with this storm abatement resulted in the daily PAR flux more than doubling between 3 and 10 May and it remained at this level until about 14 May (Figure 20 a iii.).

The decreased winds and increased insolation resulted in rapid formation of stratification in the upper 10-20 m which was dependent more on an increase in temperature (Figure 14 d), than on a decrease in salinity (Figure 14 e). The temperature increase during these initial stabilizations always accounted for more of the density difference between the top and bottom layers than did the salinity change. The requirement of a sufficient heat flux to stabilize the surface water may also contribute (along with

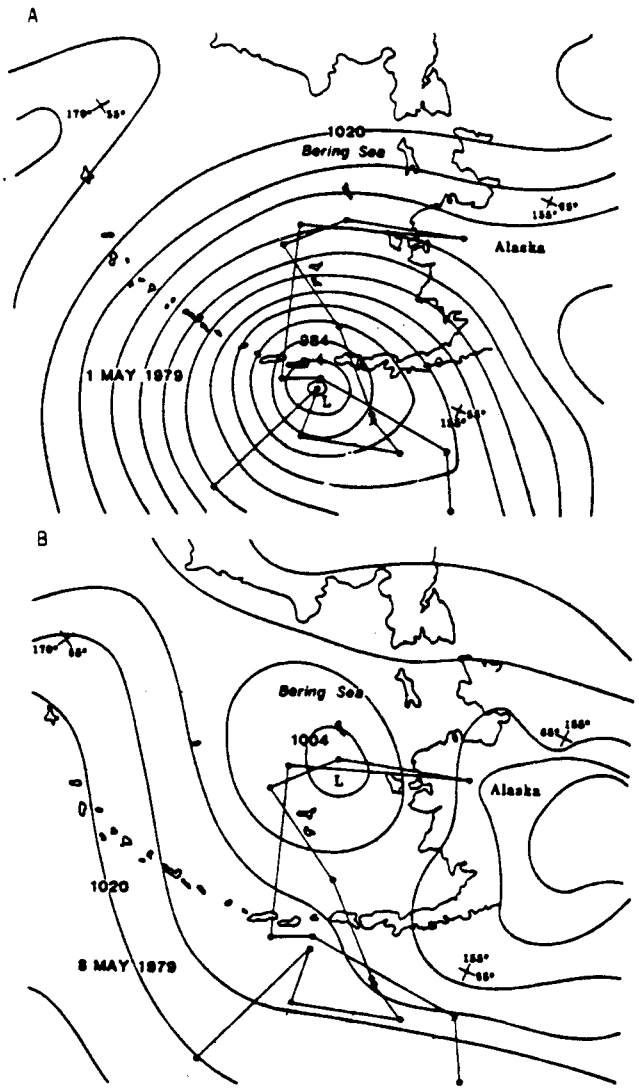

Figure 21.

Surface pressure map of low pressure system in the southeast Bering Sea area on A) 1 May 1979, and B) 8 May 1979. The solid circles represent the center of the system at daily intervals from 30 April to 14 May.

April wind mixing) to the observed absence of stable bloom conditions before late April.

Areal nitrate uptake rates increased significantly during the initial stabilizations. Peakbloom values of over 30 mg-at m^{-2} day^{-1} were consistently measured at these times (Figures 17, 18 and 19 a) and were accompanied by the depletion of nitrate from the mixed layer (Figures 14 h, 15 and 16 g). The shoaling of the mixed layer also coincided with a dramatic shortening of the mixed layer Chl A doubling times (e.g. in a 4 day period Chl A increased from 8 mg m^{-3} on 25 April 80 to more than 16 mg m^{-3} on 29 April 80 (Figure 15 f).

3.2.3 The Exhaustion of Mixed Layer Nitrate and the Occurrence of Postbloom Storms:

The end of May marked the transition to postbloom water column conditions and after 1 June, surface bloom conditions ceased. Chl A values returned to early April levels (Figures 17 and 18 and 19 a), and nitrate was not observed in the mixed layer after June (Figures 13h and 14 and 15 f). After nitrate is exhausted in the mixed layer during the peak bloom period, continued new productivity depends on the supply of nutrients from deeper water. This supply is hampered, however, by the intensifying pycnocline, a situation which develops by late May in the middle shelf area (Figures 14 f and 15 and 16 d). The mixed layer depths of June were comparable to peak bloom mixed layer depths (Figure 20 a-c i.), yet nitrate uptake rates and standing crop decreased dramatically due to nutrient limitation (Figures

18, and 19 a and b respectively). Also, coincident with the depletion of mixed layer nitrate, the bloom forming diatoms sank from the surface water.

The respirational index is not adequate to describe the constraints on productivity beyond this point in bloom development since the species composition changes during the peak bloom and Jenkin's (1937) compensation depth light intensity is no longer applicable. Because of this, the late May respirational indices, while apparently very favorable, are not directly comparable to the earlier values. Also during this time, the phytoplankton community is no longer homogeneously distributed throughout the upper water, an important assumption in Sverdrup's (1952) model.

The calmer 1981 conditions may have been responsible for the shallow nitrate nutricline found in early June. For example, the 2 mg-at m^{-3} isopleth in early June 1981 was at 18 m, while in 1979 and 1980 it was at 25 and 26 m respectively (Figures 14 h, 15 and 16 f). The favorable light level at which this 1981 middle shelf nitracline existed in 1981 may have played a role in the occurrence of a pronounced subsurface Chl a maximum found at 20 to 30 meters throughout June (Figure 16 e). A similar June Chl a layer was not found in postbloom 1980 stations although sampling was not continued as long as in 1981. The presence of such a structure was suggested by the last few stations occupied in June 1979 (Figure 14 b). The establishment of such a two layered system marks the first appearance in the spring bloom sequence of the situation often found in lower latitude waters, that is, a nutrient limited upper layer overlying a light limited deeper layer (Goering, et al., 1970).

A number of storms passed through the area during the spring bloom period which were considered postbloom if they arrived after the initial

establishment of surface peak bloom conditions. A 24 hour station occupied on the 16-17 May 1979 documented a wind mixing event caused by the 20 knot winds associated with this mid - May storm (Figure 14 b). This storm was neither long lived or extremely intense but wind mixing was sufficient to deepen the mixed layer to 23 meters on 17 May 1979. Importantly, this wind mixing occurred when many of the peakbloom forming diatoms (which had sunk from the euphotic zone during the previous week) remained in a subsurface Chl a maximum layer (Figure 14 g). This situation fostered the entrainment of these diatoms back into the mixed layer. Nitrate was also entrained into the deepened mixed layer, although the upper water ambient pool of NO_3^- did not increase beyond 2 mg-at m^{-3} (the concentration interval which was chosen for the isopleths in Figure 14 h). The mixing increased mixed layer respirational losses from the previously very favorable initial bloom conditions. The increase was mild, however, and the respirational index did not increase beyond 0.3 (Figure 20 a iv.).

During this entrainment event, the measured decreases in nitrate and ammonium content of the upper 25 m corresponded to the ^{15}N measured rates of uptake of these nitrogen compounds (ΔNO_3^- = 38.3 mg-at m^{-2} day^{-1}, ρNO_3^- = 36.4 mg-at m^{-2} day^{-1}, ΔNH_4^+ = 27.9 mg-at m^{-2} day^{-1}, ρNH_4^+ = 44.3 mg-at m^{-2} day^{-1}). Also, the total ^{15}N measured transport rates approach the observed 24 hour change in particulate nitrogen (90 mg-at m^{-2}), (Figure 22). The nitrate uptake rates measured at this time were the highest observed during 1979 (Figure 17 a). The stimulatory effect of this wind mixing on phytoplankton growth is also supported by the time series of integrated water column Chl a (Figure 17 b) which reached the highest amount recorded over the three year study period. In Figure 17 b the mixing event

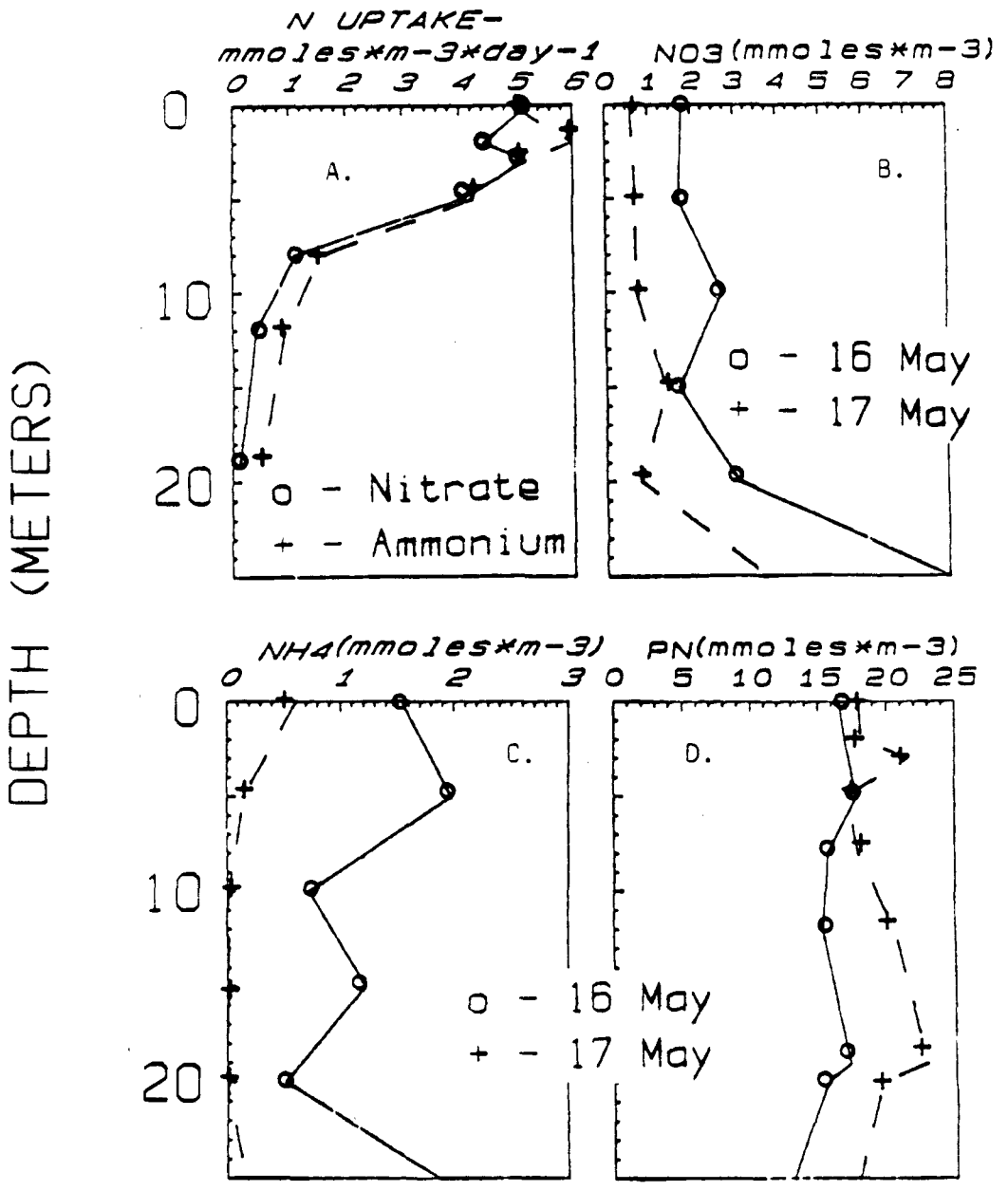

Figure 22

Nitrogen uptake and changes in dissolved and particulate nitrogen over a 24 hr. period during a storm event.

stands out as the point at which the mixed layer Chl *a* content surpassed that of the euphotic zone; a situation indicative of prebloom conditions.

Strong winds were also recorded on 19-23 May 1979 (Figure 14 b), a period which was not sampled. The deepened mixed layer found on 28 May 1979 suggests that a wind mixing event again produced the observed increase in water column Chl *a* since this increase also coincided with an increase of mixed layer Chl *a* over that in the euphotic zone (Figure 17 b). This mixing may have been responsible for the deepening of the nitrate nutricline (Figure 14 h) and ultimately the observed subsurface Chl *a* maxima during 28 - 31 May 1979 which subsequently sank from the upper water (Figure 14 g). Nitrate was exhausted at the surface and the subsurface Chl *a* layer found at approximately 20-35 m was coincident with the nutricline and located between a double pycnocline (Figure 14 f). This double pycnocline, which was much more evident in the Brunt Vaisala Period (Figure 14 f), than the density profiles (Figure 14 c) was formed when the initial wind induced deepening of the pycnocline in mid-May was followed by the surface formation of a second insolation generated pycnocline. These two pycnoclines appear to have gradually merged during June.

Bloom development after the initial surface Chl *a* appearance in early May 1980 was notably different than that in 1979 due to the timing of an early May storm. Before phytoplankton nitrate uptake rates reached peak 1979 values (Figures 17 and 18 a) and all of the NO_3^- was taken up from the surface mixed layer and maximum biomass had been produced (Figures 15 e and f), an intense low pressure system moved into the area from the west. By 10 May, under winds of approximately 30 knots, the mixed layer had deepened to almost 50 m (Figure 15 d). This wind mixing coincided with spring tidal

currents having estimated speeds of at least 20-25 cm/sec and the simultaneous presence of these two mixing forces in the water column destroyed most of the earlier water column stability.

By 10 May the mixed layer was several times deeper than the 0.1% euphotic zone (Figure 15 d), and this deep mixing greatly increased mixed layer respirational losses (Figure 20 b). During this time, nitrate uptake rates decreased (Figure 18 a). Also, Chl a was diluted in the surface waters (Figure 15 e) and the whole water column Chl a content declined (Figure 18 b). This Chl a loss suggests that some of the surface Chl a had been mixed into the bottom waters where it had settled to the bottom.

Winds calmed to 5-10 knots on 14-16 May 1980 (Figure 15 b) and the mixed layer depth again shoaled to approximately 10 m (Figure 20 b ii.). This quiescence marked the return of low water column respirational losses (Figure 20 b iv.) in the presence of increased nitrate concentrations recently brought into the mixed layer by the storm (Figure 15 f). The main spring phytoplankton bloom of 1980 then commenced with Chl a concentrations of >30 mg m^{-3} found at 10-15 m on 15-17 May (Figure 15 e). The nitrate uptake rates at this time were comparable to peak 1979 values (Figures 17 and 18 a) and surface nitrate during this growth period was exhausted by 15 May (Figure 15 f). During 1980, the early May storm apparently "reset" the hydrographic conditions on the middle shelf to prebloom conditions (e.g. high nutrient concentrations, relatively large respirational losses, low nitrate uptake and growth rates) which were followed by bloom conditions when the upper water column again stabilized.

From 16-20 May, 1981 low pressure associated strong winds deepened the pycnocline (Figure 16 b) and mixed nitrate rich water (>4 mg-at m^{-3}) into

the surface layer (Figure 16 f). An immediate response was not observed in either nitrate uptake or gwowth until several days later, as judged from Chl *a* concentrations (25 May 1981, Figure 16 e). Respirational losses experienced by mixed layer phytoplankton increased as a consequence of the deep mixing (Figure 20 c iv.). Other factors also contributed th the delay in growth response. Importantly, this wind mixing did not occur until a week after the peak bloom diatom community had sank from the surface water (Figure 16 e). Quantitatively, this left low concentrations of Chl *a* available for resuspension (<2 mg m^{-3}). Also, qualitatively the bloom forming phytoplankton themselves were not entrained by this storm event, and their absence was probably mainly responsible for the lack of an observed response in nitrate uptake.

3.3 Discussion

3.3.1 Water Column Stability and the Improvement of Growth Conditions Initiating the Bloom

Phytoplankton growth rates are temperature dependent (Eppley, 1972). Since the temperature of the surface water increased during spring, the data were examined to determine how much of the increase in Chl *a* doubling rates could be accounted for by temperature increase alone (Tables 3 and 4). The prebloom respirational index exhibited a relatively large range during this physically dynamic period. The prebloom respirational index average for the three years (0.54 $\pm$ 0.24), however, was significantly greater than the

Table 3.

Changes in Mixed Layer Chl *a* Doubling Rates, Temperature, and Respiration Index Between the Pre-Bloom and Peak-Bloom Periods. Between these two periods defined in the text, the respiration index decreased and the Chl *a* doubling rate increased; both changes were significant ($p = 0.95$ and 0.90, respectively).

Time Period	Average Chl *a* doubling rate (doublings/day)	Temperature °C	Average respiration index
Pre-bloom			
17 April-4 May 79	0.11	3.5°	0.28
12 April-19 April 80	0.04	0.8°	0.75
14 April-2 May 81	0.09	3.0°	0.58
	$\bar{x} = 0.08 \pm 0.04$		$\bar{x} = 0.54 \pm 0.24$
Peak-bloom			
4 May-7 May 79	0.49	5.0°	0.15
29 April-2 May 80	0.14	1.5°	0.22
2 May-8 May 81	0.25	5.0°	0.28
	$\bar{x} = 0.29 \pm 0.18$		$\bar{x} = 0.22 \pm 0.07$

Table 4.

Comparison of Observed Increases in Average Mixed Layer Chl a Doubling Rates Between Pre- and Peak-Bloom Periods with the Increases Predicted by Temperature Rise Alone Using the Relationship Given in Eppley, 1972. The doubling rate increases appear to be much more dependent on the decrease in respirational losses (see text).

Pre-bloom to peak-bloom periods in:	Observed % Increase in doubling rate	Predicted % Increase in doubling rate due to temperature rise
1979	447%	10%
1980	350%	5%
1981	275%	14%

average respirational index preceding peak bloom conditions, (0.22 $\pm$ 0.06; p=0.05; Table 3).

In each year the observed increase in doubling rates between the prebloom and peak bloom periods was greater than that predicted by temperature increase alone using Eppley's (1972) relationship (Table 4). A relationship between doubling rates and temperature can be derived from the data in Table 4, but the slope is 15 times steeper than that derived by Eppley (1972). Since the growth vs. temperature relationship derived by Eppley (1972) has proven robust in subsequent studies (e.g. Goldman and Carpender, 1974), the increase in temperature itself is not responsible for the accelerated growth. Instead, it is hypothesized that the increase in doubling rates was due mainly to the dimunition of water column respirational losses between the two periods brought about by the stabilization of the upper water column.

Each of the peak bloom periods recorded corresponded to a decrease of the respirational index to less than 0.3 such as on 8 May 1979, 2 May 1980, 16 May 1980, 10 May 1981 (Figure 20 a-c iv.). The relationship between the average mixed layer Chl *a* doubling rates and the average respirational index for the 6 cases from Table 3 is shown in Figure 23. The resulting model: μ (day^{-1}) = (0.46) x exp (-3.18 x Zm/Zc) fit the data reasonably well (r^2 = 0.75). Such a relationship suggests that during the early bloom stages, the ratio Zm:Zc encompasses the important factors in the environment to which prebloom phytoplankton growth responds. During this period, water column respirational losses controlled net production and surface bloom conditions deveveloped only in the presence of low mixed layer respirational losses.

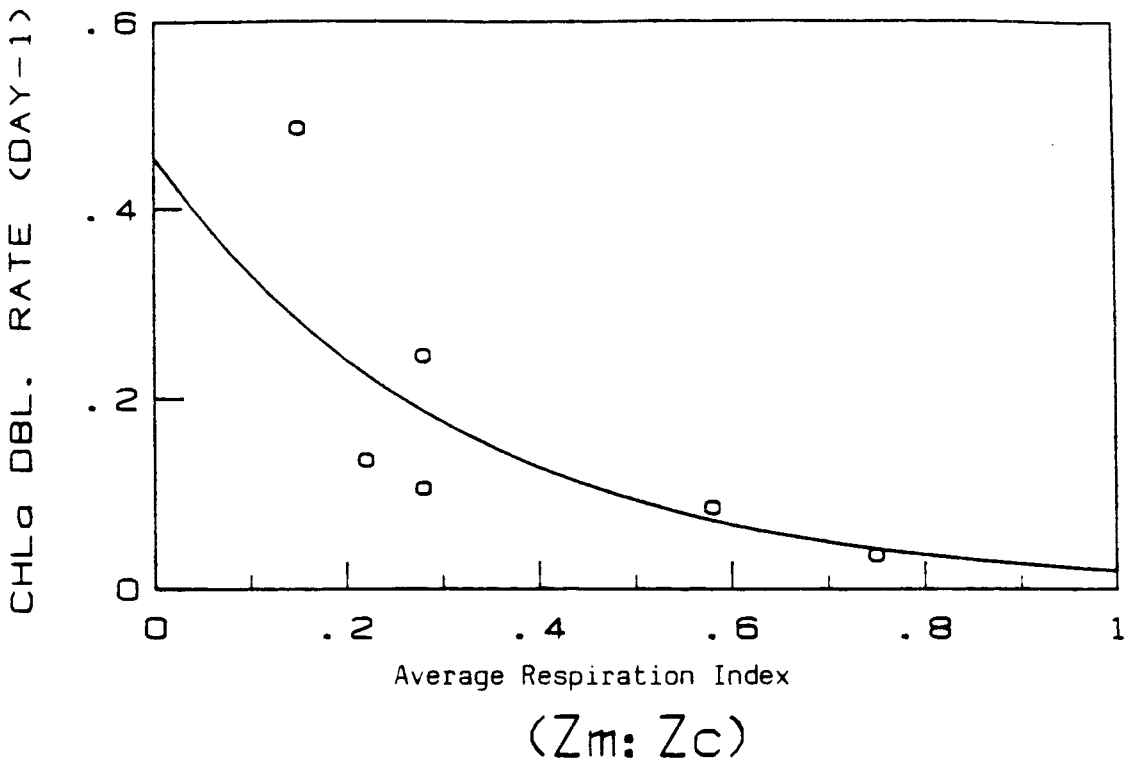

Figure 23

Relationship between Chl a doubling rate and respiration index during pre- and peak bloom periods.

Since Sverdrup's critical depth formula (equation 2) contains variables which are dependent on the phytoplankton community itself (k and $\bar{I}_c$), it is subject to biological feedback during bloom development. Light attenuation in the relatively shallow spring bloom euphotic zones is largely a function of the phytoplankton present (Lorenzen, 1972), and increases in the standing crop in the upper water column tend to decrease the critical depth. A more difficult phenomena to deal with is the species succession taking place throughout the bloom period, since compensation light intensities vary among species (Falkowski and Owens, 1978). Shipboard observations indicated that in each year the prebloom community was dominated by the diatoms Thalassiosira aestivalis and T. nordenskioldii. Under the more stable peakbloom conditions, large increases in Chaetoceros spp. (most notably C. debilis) were observed.

Comparisons such as Table 3 and Figure 23 were restricted largely to the prebloom period. The simplifying assumption that the average daily compensation depth light level was constant during this time was not unrealistic. Although phytoplankton are capable of adapting their photosynthetic efficiency to changing light regimes (Falkowski, 1980), such adaptation cannot compensate for the low winter - early spring light levels under which the phytoplankton present are largely dormant (Slagstad, 1982). There exists, therefore, a lower limit for the compensation depth light level. Although Falkowski and Owens (1978) did not give compensation depth light levels, this value was calculated from their Figure 3 for Skeletonema costatum. The resulting value of 0.025 einsteins m^{-2} $hr.^{-1}$ was very similar to the value of Jenkin (1937) which most likely represents a realistic early bloom, minimum compensation point light level. This value is also in the

range measured for temperate coastal phytoplankton by Platt and Jassby (1976) and Cote and Platt (1983).

As species composition changes, however, this value would increase as judged by the larger compensation depth light levels for the other phytoplankton species in the figure shown by Falkowski and Owens (1978). Therefore postbloom changes in the respiration index do not quantitatively reflect the growth conditions in which these later successional stage communities exist. Instead, the Zm:Zc ratio indicates changes in respiration conditions relative to the light requirements of the prebloom community. The 0.3 Zm:Zc ratio, however, is most likely an accurate value for the peakbloom trigger conditions.

An approach similar to the respiration index was taken by Packard (1979). In his study the ratio of the measured compensation depth and the mixed layer depth was used to compare the phytoplankton growth conditions of northwest Africa and the Peru upwelling region. Such field measurements would enable the compensation depth light level to be treated as an additional variable in the respiration index

Sverdrup's (1952) treatment of high latitude spring phytoplankton growth encompasses light variation due to latitude and season ($\bar{I}_o$) and also the variation caused by vertical mixing (Zm), both of which are influenced by meteorological conditions. The rather restrictive mixed layer depth definition used here was found to be the most sensitive in following biologically important water column dynamics during spring. These mixed layer depths coincided with discontinuities in important nutrients such as PO_3^{3-} and NO_3^- even when the pycnocline was weakly developed. This indicates that the mixed layer definition used reflects a valid boundary to

the mixed layer phytoplankton.

To partition the relative importance of the component variables in the respirational index more quantitatively, a multiple regression was carried out. A transformed model of the respirational index was used assuming that in this form the multiplicative model was intrinsically linear (Draper and Smith, 1981). The regression model itself, of course, is of little interest but the correlation matrix generated for the four variables based on stations over three years is informative (Table 5). The mixed layer depth was most highly correlated with the respirational index, and surface irradiance was also important

These findings are somewhat different than those of Cushing (1962), who partitioned the cause of the spring North Sea productivity increase more equitably between radiant energy and the decrease in the depth of mixing. Additionally, notable interaction exists among the independent variables themselves, in that k, for example, which is largely dependent on phytoplankton standing stock, increases as the mixed layer depth shoals and/or the light increases, while increases in light are also correlated with the shallowing of the mixed layer.

These results emphasize the conditional nature of bloom development during periods of large water column respirational loss due to the dependence of phytoplankton growth on upper water column stabilization in middle shelf and deeper water. In shallower inshore waters, the mixed layer is constrained by water depth to consistently more favorable Zm:Zc ratios. In such shallow areas, the mixed layer is invariant and the respirational index reduces to two variables: $\bar{I}_o$ and k. Increases in spring phytoplankton growth in these areas can be described simply as a function of

Table 5.

Correlation Matrix Derived From the Multiple Regression of the Respiration Index on the Three Independent Variables Indicated, N = 34. In 6 cases the extinction coefficient (k) was estimated from mixed layer Chl *a* concentrations. In 11 cases the average hourly PAR was interpolated from proximate stations where data were available.

	Respiration index Zm: Zc	Mixed layer depth	Extinction coefficient (k)	(Average hourly PAR)$^{-1}$
Respiration index	1.00			
Mixed layer depth	0.88	1.00		
Extinction coefficient (k)	-0.04	-0.33	1.00	
(Average hourly PAR)$^{-1}$	0.57	0.38	0.43	1.00

daily incident light (Hitchcock and Smayda, 1977). Chl a production and NO_3^- depletion were, in fact, always recorded at inner shelf stations (<50m) earlier in the year than at deeper, middle shelf stations.

3.3.2 Vertical Mixing During Bloom Development

An approach to following changing growth conditions during the bloom which avoids dealing with the species dependent variation in compensation light levels, is to simply compare the light levels at the base of the mixed layer. For this purpose the data from Figure 20 was segregated into pre-, peak, and postbloom categories and the resulting average values are shown in Table 6. Table 6 indicates that there is a marked increase in mixed layer light levels as the bloom progresses. The increase in light at the base of the shallower peakbloom mixed layers relative to prebloom conditions is restrained by the compensatory increase in the extinction coefficient during this time. After most of the production has sunk from the mixed layer in the postbloom period, however, the light deep in the mixed layer increases dramatically. Riley (1957) took a similar approach in comparing mixed layer light conditions.

Indexes such as I_{MLZ} and Zm:Zc can only reflect average mixed layer conditions. The average peak bloom mixed layer in Table 6 is 8 m deeper than the compensation depth, as judged by the value of Jenkin (1937) (I_{MLZ} < .027 einsteins m^{-2} hr^{-1}). Net phytoplankton growth is not dependent on continuous residency at photosynthetically saturating depths (Smayda, 1970). Time scales of light exposure are, therefore, dictated by vertical mixing

Table 6.

Average mixed layer light conditions during bloom developmental stages.

	MLZ(m)	$k(m^{-1})$	I_e (Einsteins m^{-2} day^{-1})	I_{MLZ}
Prebloom ($\bar{x}_5$)	54.0±25	0.17±0.01	14.8±6.2	0.002
Peak bloom ($\bar{x}_{11}$)	18.8±12	0.39±0.08	26.7±10.3	0.018
Postbloom ($\bar{x}_{12}$)	14.3±4.2	0.20±0.07	18.6±2.3	1.038

rates.

To examine this hypothesis the present data were analyzed by the use of a nitrate advection - diffusion model. The two dimensional model contained a biological consumption term for nitrate uptake with the assumption that no horizontal processes were taking place:

$$\frac{dNO_3^-}{dt} = -\rho NO_3^- - W_z \frac{dNO_3^-}{dZ} + K_n \frac{d^2NO_3^-}{dZ^2} \quad (13)$$

(Sverdrup, Johnson and Flemming, 1942). Equation 13 can be put in finite difference form and rearranged to yield:

$$\overline{\rho NO_3^-} = -\frac{\Delta N_t \times \overline{\Delta Z}}{\Delta t} + \frac{\overline{K_n}}{\overline{\Delta Z}} - \overline{W_z} \times \overline{\Delta N_z} \quad (14)$$

where in each interval:

$\overline{\rho NO_3^-}$ - average ^{15}N measured nitrate uptake in mixed layer (mg-at m^{-2} day^{-1})

$\overline{\Delta N_z}$ - average change in nitrate concentration between top and bottom layer (mg-at m^{-3})

ΔN_t - change in nitrate concentration of mixed layer from time t_1 to t_2 (mg-at m^{-3})

$\overline{\Delta Z}$ - average height of nitracline (m)

Δt - time interval between sampling (days)

$\overline{K_n}$ - average nitrate eddy diffusion coefficient in pycnocline (m^2 day^1)

$\overline{W_z}$ - average vertical velocity (m day^{-1})

Most of the parameters in equation 14 could be evaluated time centered between two successive sampling days from the hydrographic and productivity stations, and these results are shown in Table 7. The intervals indicative of peak bloom conditions were 4-7, 16-17, 26-28 May 1979, 20-29 April, 29 April - 6 May, 10-16 May 1980, and 2-8 May, 8-10 May 1981. The averages from these periods can be compared to those from the post bloom intervals 31 May - 12 June 1979, 26 May - 2 June 1980, and 2-19 June 1981. Nitrate productivity decreases drastically between the two periods and the mixed layer reaches steady state with respect to nitrate concentrations.

Equation 14 is in straight line form and the two dimensional model was used to estimate the intercept $[(\overline{K_n}\,\overline{\Delta N_z}/\overline{\Delta Z} - \overline{W_z}) \times \overline{\Delta N_z}]$, a parameterization of the combined vertical mixing in the pycnocline produced by the advective $(\overline{W_z})$ and diffusive $(\overline{K_n}\,\overline{\Delta N_z}/\overline{\Delta Z})$ components (Figure 24). The resulting intercept (13.2 mg-at m^{-2} day^{-1}) was based only on the 8 peak bloom intervals (open circles in Figure 24) since it was felt that the nitrate concentration changes and uptake measurements were best sampled in these periods. Inclusion of the other intervals which displayed a measurable change in mixed layer nitrate (x symbols in Figure 24) does not change the intercept significantly (13.5 mg-at m^{-2} day^{-1}), but it does reduce the percentage of variance explained by the model (r^2 decreases from 0.48 to 0.32).

This intercept can then be normalized to $\overline{\Delta N_z}$ to yield the vertical mixing rate. Such an estimate made using the average peak bloom $\overline{\Delta N_z}$ from Table 7, suggests that 2.1 ± 1 m day^{-1} is an optimal mixing rate for spring bloom diatom growth. Eppley et al., (1979) calculate a similar value for W_z during a winter diatom bloom in the southern

Table 7.

Sampling intervals and parameters for advection - diffusion model.

Date	Stn.#	$\sqrt{\rho}NO_3^-$	$(\bar{x})$	ΔN_t	ΔN_z	$(\bar{x})$	ΔZ	$(\bar{x})$	Δt	K_N	Rich#
4 May 1979	2012	9.00	NA	NA	1	NA	5	NA	NA	NA	19
7 May 1979	2031	29.20	19.50	-3.06	12.00	6.90	10	7.50	3	11.20	1923
16 May 1979	2077	36.40	10	1.70	5	6.70	6	0	9	9.20	247
17 May 1979	2090	NA	36.40	-1.30	9	7	21	13.50	1	12.50	267
26 May 1979	3012	NA	14	-0.00	3.70	6.40	14	10	9	37.60	1030
28 May 1979	3026	21.60	10	-1.20	7.50	5.60	14	14	2	5.00	6677
31 May 1979	3050	NA	12	-0.20	13.50	10.50	25	19.50	3	20.90	1102
12 June 1979	3140	2.00	4.70	0	13.50	12.90	0	21.10	12	7.70	007
28 April 1980	2079	9.40	NA	NA	0	NA	0	NA	NA	NA	0
29 April 1980	3014	16.90	13	-7.50	2.50	1.30	5	2.50	9	-2.20	60
6 May 1980	3057	19.00	10.30	-1.70	6	4.25	10	11.50	7	29.00	25
16 May 1980	3006	0.70	13.20	0.90	3	4.50	9	13.50	4	24	33
16 May 1980	3132	35	21	-5.80	7.20	5.10	20	14.50	6	35.80	377
23 May 1980	4012	14.10	20	-0.30	6	7.60	25	22.50	7	51	706
26 May 1980	4039	10.00	12.50	0	9	8.50	25	25	3	36.00	70
2 June 1980	4090	0.00	3	0	6.90	0	20	22.50	7	0.40	023
14 April 1981	1034	0.70	NA	NA	NA	NA	NA	NA	NA	NA	101
24 April 1981	1111	3.30	2	NA	1.50	NA	5	NA	10	NA	427
2 May 1981	2014	7.20	5.30	-1.80	1	1.30	9	7	0	-14	0
8 May 1981	2040	29.20	10.50	-0.40	5	3	10	9.50	6	-24	199
10 May 1981	2055	22.50	25.90	-1.60	11	0	7	0.50	2	17.30	630
25 May 1981	2116	7.30	14.90	2	10	7.25	35	21	15	47.60	350
2 June 1981	3016	3.30	5.50	-2.10	10.50	10.30	34	34.50	0	2.70	035
19 June 1981	3124	1.20	2.50	0	11.20	10.90	15	25	17	5.70	1771

Peak bloom interval averages:

$\bar{x}_{(8)}$	22.3	-0.9	6.4	10.2
S.D.	7.1	0.4	2.4	4.1

Post bloom interval averages:

$\bar{x}_{(3)}$	3.4	0	10.6	22.9
S.D.	1.2	-	3.4	2.0

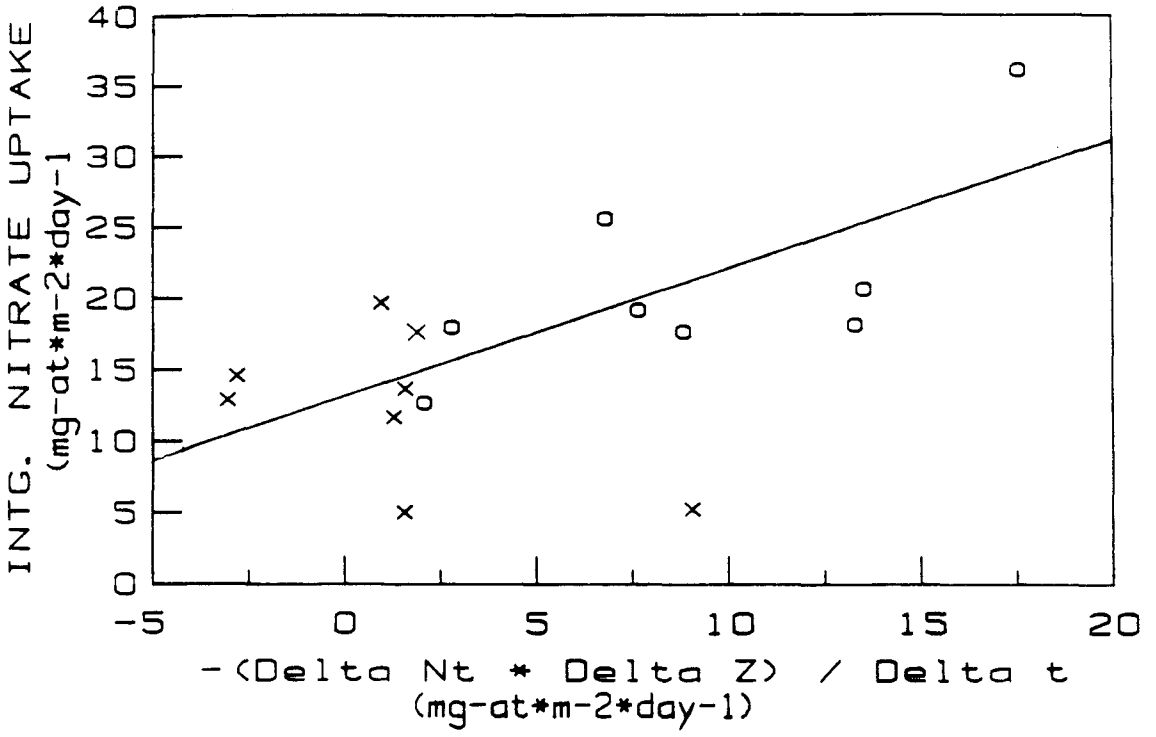

Figure 24.

Advection - diffusion model used to estimate combined vertical mixing term in the pycnocline.

California bight which they suggest is in the range of accepted upwelling rates.

This mixing can be parameterized completely as a diffusive flux by using the peak bloom interval average for ΔZ from Table 7. The resulting $\bar{K}_n$ of 21.4 m^2 day^{-1} (185 cm^2 sec^{-1}) represents the pycnocline mixing coefficient associated with peak bloom diatom growth. The mixed layer at this point averaged 18.8 m. In a numerical simulation, Slagstad (1982) suggested that phytoplankton were not capable of exhibiting a vertical structure in growth characteristics if the mixing coefficient was greater than 200 cm^2 sec^{-1} in a 100 m mixed layer. It follows that the mixing coefficient calculated here would be slightly smaller since it coincides with the initial development of vertical structure in phytoplankton growth.

An alternative estimate of the pycnocline $\bar{K}_n$ can be made from the Fickian diffusion model:

$$\bar{K}_n = NO_3^- \text{ Flux } / (\Delta N_z/\Delta Z) \qquad (15)$$

where the NO_3^- flux was calculated as the difference between the ^{15}N measured mixed layer nitrate uptake and the observed rate of change in mixed layer nitrate content. The values for $\bar{K}_n$ calculated in this manner are also shown in Table 7. For the peak bloom intervals the average value was 10.8 m^2 day^{-1}, suggesting that on average, the $K_n/\Delta Z$ term contributes half of the 2.1 m day^{-1} peak bloom mixing rate. The standard deviation for the calculated diffusive flux however, includes 0. These values must be considered maxima since some of the flux is actually due to the entrainment

of deeper water, especially for those intervals in which wind mixing was occurring, and cannot be attributed entirely to a diffusive flux.

Periods in which a negative K_n was calculated in Table 7 correspond to periods in which the estimated nitrate uptake was less than the observed loss. Accurately estimating the integrated nitrate loss from the mixed layer is difficult especially in late April and early May when the mixed layer depth is changing quickly. The negative K_n values all correspond to such physically dynamic periods.

King and Devol (1979) demonstrated a relationship between K_n and stability (E) at the bottom of the mixed layer. Their relationship was applied to the average stability at the base of the peakbloom southeast Bering Sea station mixed layers ($17.9 \times 10^{-6} \pm 13.7\ m^{-1}$). The resulting K_n of 53 $m^2\ day^{-1}$ was much larger than the maximal 10.8 $m^2\ day^{-1}$ average from Table 7. The stability at the base of these spring bloom mixed layers was smaller than the range of stability King and Devol (1979) based their relationship on and this may contribute to the lack of correspondence. Additionally, these authors assumed a constant vertical shear, which is related to the eddy diffusivity coefficient via:

$$K_n = K_0 \times [1 + B \times (N^2/(dU/dZ)^2)]^{-m} \qquad (16)$$

where K_0 = the value of K_n at neutral stability, B and m are constants, and the term $(N^2/(dU/dZ)^2$ is the Richardson number (Munk and Anderson, 1948). Equation 15 suggests the discrepancy between King and Devol's relationship and the results of the present study is due to the presence of less vertical shear near the pycnocline at these peakbloom, continental shelf stations

than exists in this water layer in the tropical oceanic area where King and Devol's relationship was derived.

The pycnocline mixing rate derived from the advection - diffusion model does not apply to the mixing velocity of the mixed layer itself, however. The entrainment velocity was employed as an index of this mixed layer property. An entrainment velocity (W_o) can be defined as a function of the Richardson number (Phillips, 1977):

$$W_o = U_* / \bar{R}_i \qquad (17)$$

where $\bar{R}_i$ = the bulk Richardson number and U_* = friction velocity in which:

$$U_* = (T / \rho_w)^{1/2} \qquad (18)$$

where ρ_w = the density of sea water (1.025 g cm^{-3}) and T = wind stress such that:

$$T = \rho_a \times C_D \times \bar{W}^2 \qquad (19)$$

where ρ_a = density of air (1.3 Kg m^{-3}), C_D = drag coefficient (a step function but here taken as a constant - 1.4×10^{-3}), and $\bar{W}$ = daily wind speed averaged from 6 hour values (m sec^{-1}). The constants can be collected so that:

$$U_* \text{ (m sec}^{-1}) = 1.333 \times 10^{-3} \times \bar{W} \qquad (20)$$

The bulk Richardson number ($\bar{R}_i$) may be defined as:

$$\bar{R}_i = (g \times \Delta\rho \times h) / (\rho \times U_*) \quad (21)$$

(Johnson, 1973) where g = acceleration of gravity (980 cm sec^{-2}), $\Delta\rho$ = the density difference between the top and bottom layers (g cm^{-3}), and h = height of mixed layer (m). After grouping the constants:

$$\bar{R}_i = 53.85 \times [(\Delta\rho \times 10^5) \times h] / \bar{W}^2 \quad (22)$$

A time series of the entrainment velocity was constructed for each year and these are shown in Figure 25 along with the $\bar{K}_n/\Delta Z$ term calculated from equation 15. The entrainment velocity appears to be a useful indicator of the interaction of wind and water column stability in regulating upper water mixing conditions which, in turn, control the time scales of phytoplankton light exposure. This velocity is large and dominates the diffusive term during the low stability, prebloom conditions as well as periodically later in the season when storm events occur (arrowheads in Figure 25). Conversely, it is low during nitrate depleted postbloom periods.

Using this range of mixing rates as an indicator of the vertical velocity suggests that peak bloom growth occurs when the cells are moving fairly slowly through the mixed layer, in comparison, for example, to possible values of Langmuir circulation (Ledbetter, 1979). The initiation of high nitrate productivity intervals are associated with relatively low entrainment velocities of between 1 and 5 m day^{-1}. This interval includes

A) 1979

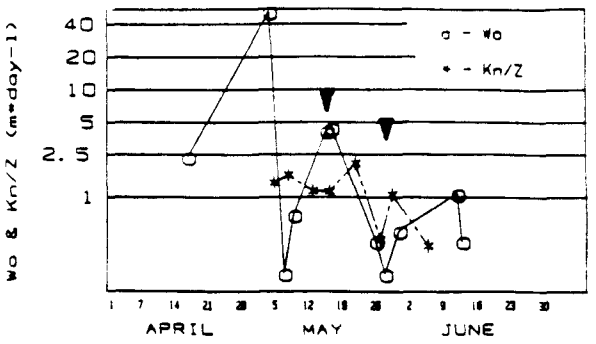

B) 1980

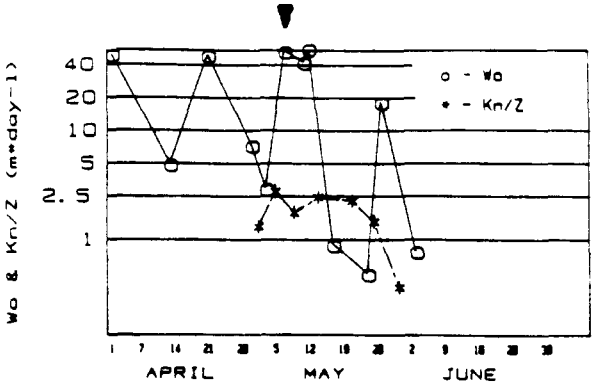

C) 1981

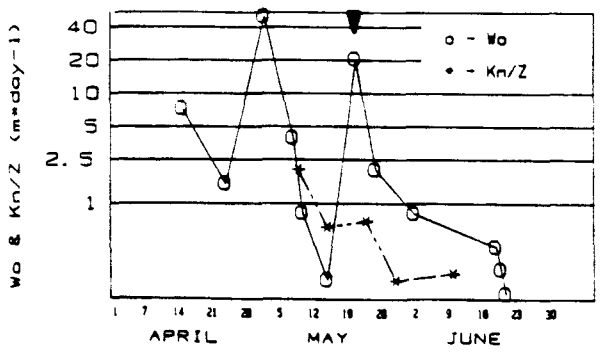

Figure 25.

Time series of the entrainment velocity (W_o - equation 17) and the $K_n/\Delta Z$ term from equation 15. The solid arrowheads denote the arrival of postbloom storms.

the peak bloom mixing rate derived from the advection - diffusion model (2.1 m day^{-1}).

Nitrate uptake light response experiments indicated that nitrate uptake became less light dependent as the mixed layer shallowed and growth rates increased (i.e. - 2-10 May 1981, Figure 26). This response is different from carbon uptake which has been shown to be more efficient in cells adapted to low light (Beardall and Morris, 1976). Packard, (1973), however, found that nitrate reductase decreased in cells in low light. Also, nitrate reductase activity appears to reflect the environmental history of the cells (Blasco, et al., 1983), which helps to explain the decreased light dependence of nitrate uptake as vertical mixing decreased.

Based on the peak bloom mixing rate (2.1 m day^{-1}), parameters from Table 6, and the light dependence of the peak bloom phytoplankton (Figure 26), it appears that the high growth rate intervals coincide with the cells remaining at very favorable light levels for nitrate uptake for a time approaching a full peak bloom doubling period (ca. 1-2 days). Apparently the nitrate uptake light dependence of the postbloom phytoplankton is not responsible for their exclusion from the prebloom period. A more important factor may be the inability of their photoadaptive processes to keep pace with the changing light regime under substantial vertical mixing rates.

A recent laboratory study demonstrated that the growth of Skeletonema costatum was dependent largely on the total light received regardless of the experimental light conditions which simulated the effects of vertical mixing (Cosper, 1982). Such a response would be expected from a phytoplankter which is typical of early bloom conditions in many areas. The growth response of later bloom species may not be as conservative when faced with a

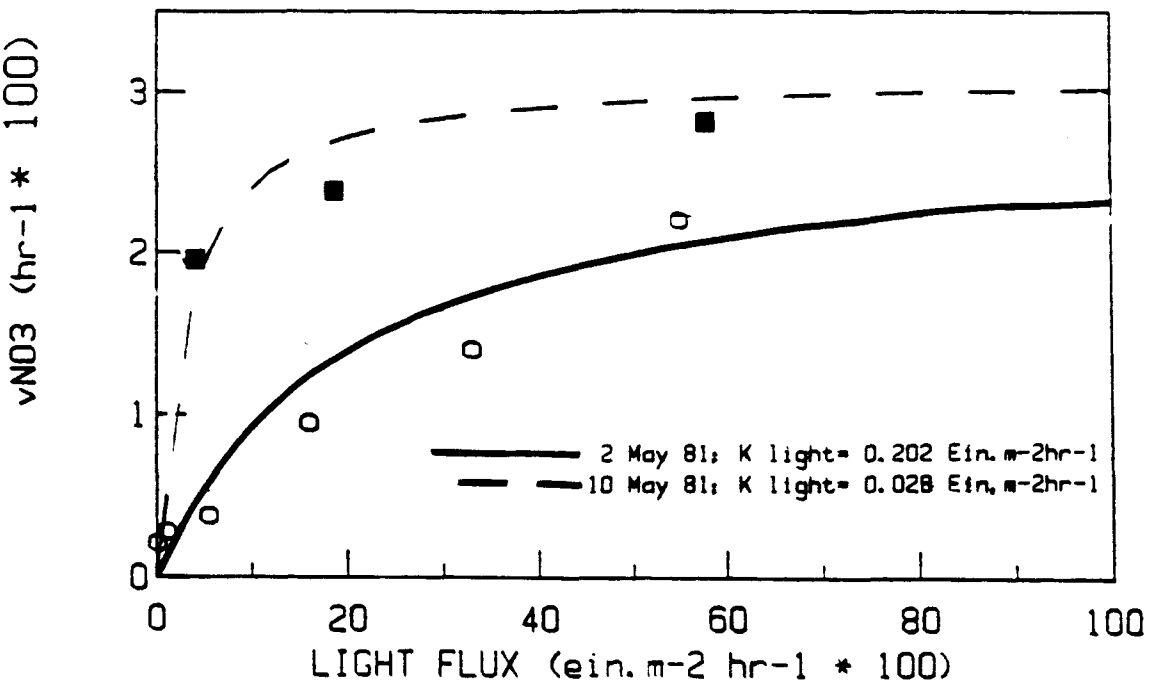

Figure 26.

Changes in the light response of nitrate uptake during period leading to peak bloom conditions in 1981. Each curve is based on 7 points, although only those less than 1 Ein. m^{-2} $hr.^{-1}$ are shown.

similar range of light exposure times scales. Further delineation of these characteristics in the ocean, however, awaits more accurate measurements of vertical mixing.

3.3.3 Nitrate Uptake as a Continuous Function of Upper Water Mixing

In all three years, nitrate uptake increased with decreased vertical mixing as indicated by either the advection diffusion model or the entrainment velocity. The associated growth response which followed is similar to the findings of Semina (1960) in the western Bering Sea in which phytoplankton biomass increased with upper water column stability. Also, Riley et al. (1949) constructed a theoretical model to deal with the interaction of vertical turbulence and production based on growth and sinking interactions. This model was limited to water columns containing a stable upper layer. There were two reasons for this, the first being the simplifying assumption of steady state conditions. In addition, the initial statement of the problem given by Riley et al. (1949) (their equation 2) did not consider the negative effect deep mixing and high respirational losses can have on phytoplankton growth. Such an effect has been incorporated into later mathematical models of production (Steele and Menzel, 1962).

The dependence of early bloom growth rates (i.e. Chl a doubling times) on the respiration index (Figure 23) was shown to be largely due to the shallowing of the mixed layer. A similar approach can be used to describe

the increase in nitrate uptake for the period prior to nitrate depletion (Figure 27). The independent variable used in Figure 27 is composed of $\Delta\rho$ - the density difference between the top and bottom layers adjusted for the estimated change in this difference during the previous 24 hours. Since $\Delta\rho$ is inversely proportional to the entrainment velocity (equations 17 and 21) it increases as vertical mixing decreases. The amount of mixing determines the exchange of salt and heat between the top and bottom water which is reflected in $\Delta\rho$.

The adjustment for the previous 24 hour change was estimated from the $\Delta\rho$ time series. This adjustment was necessitated by the rapid changes in surface buoyancy which were observed either during periods of very low wind and rapid surface warming (e.g. 4-7 May 79, Figure 14 b and d) or during periods of strong wind mixing and rapid $\Delta\rho$ decrease (e.g. 6-10 May 80, Figure 15 b and c). Under such conditions it appears that the light environment changed faster than the response rate of the biological community. The $\Delta\rho$ adjustment serves as a historical factor to account for the non - steady state character of the physical - biological system during these periods. The necessity for this adjustment suggests that the respirational history to which the cells have been exposed is very important in determining growth response to changing environmental conditions. Such developmental factors appear to dominate effects of the prevailing vertical mixing during the course of an incubation (Gallegos and Platt, 1982).

This "mixing index" was normalized to the coefficient of thermal expansion for the end of winter middle shelf water temperature. This normalization produced a better fit since for the cooler water temperature

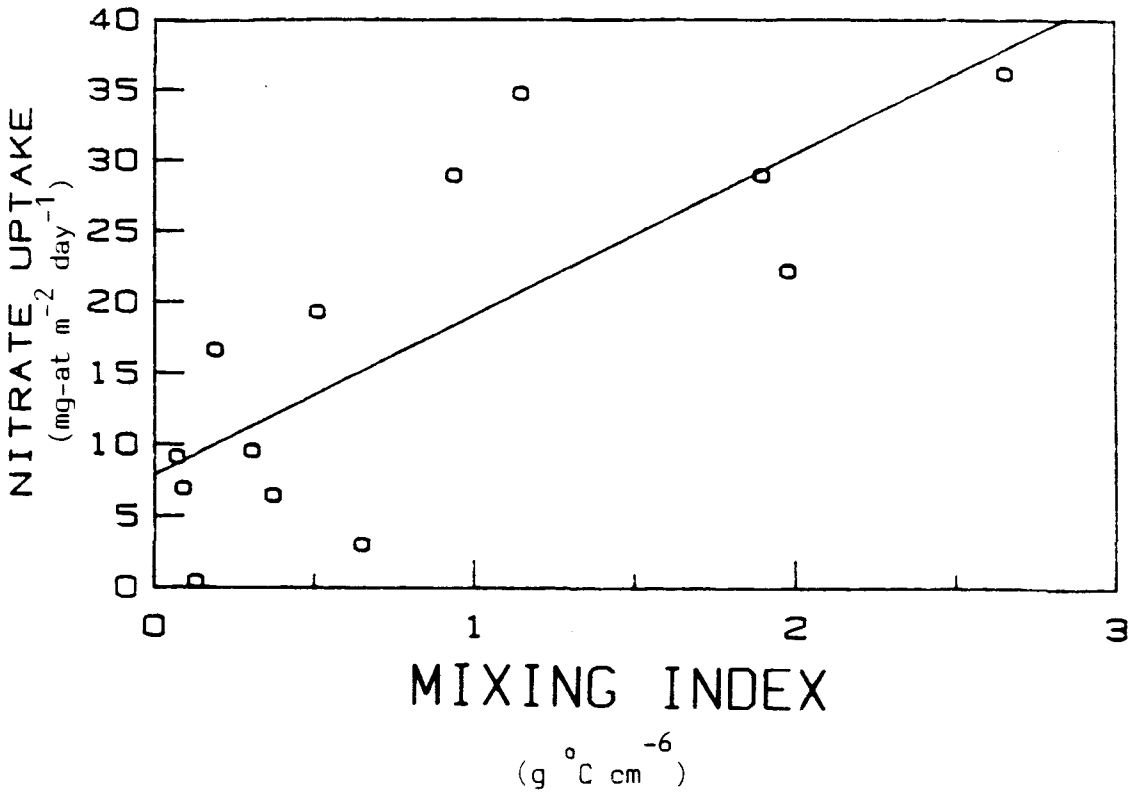

Figure 27.

Relationship between nitrate uptake and the mixing index during the pre- and peak bloom periods.

in early April, 1980 the expansion coefficient which was largely responsible for the $\Delta\rho$ was 25% less than during the other two years. This normalization yields a factor with units of g ^{o}C cm^{-6}.

Importantly, however, in Figure 27 the independent variable is based solely on an index of upper water mixing and is independent from the physiological characteristics of the population. This criterion alone accounts for 61% of the variability recorded in early bloom nitrate productivity. Also, even though incoming light and the extinction coefficient are not factors in the mixing index, it explains much of the variation in the respiration index (Figure 28, r^2 = 0.57).

Nutrient effects have been treated quantitatively using nutrient limitation factors in models of phytoplankton growth (Steele and Menzel, 1962), and the dependence of productivity on a diffusive nutrient flux in water columns containing a pronounced pycnocline has been investigated (Eppley et al., 1979). The latter approach was based on the stability of the upper water column. Diminished mixing not only minimizes respirational losses, but restricts nutrient supply. Nitrate uptake, therefore, should follow the development of upper water buoyancy from respiration limited through nutrient limited bloom phases.

A continuum of this sort is suggested by the relationship of all nitrate productivity stations to the mixing index (Figure 29 a-d). The nitrate uptake on mixing index figures all demonstrate the expected change in slope beyond an index of 1.5 to 2.3, as decreased mixing restricts the supply of nutrients to, and therefore the standing stock present in, the mixed layer. The post-bloom 1980 and 1981 series, (Figure 29 b and c) strongly suggest an exponential decay function that would be expected if

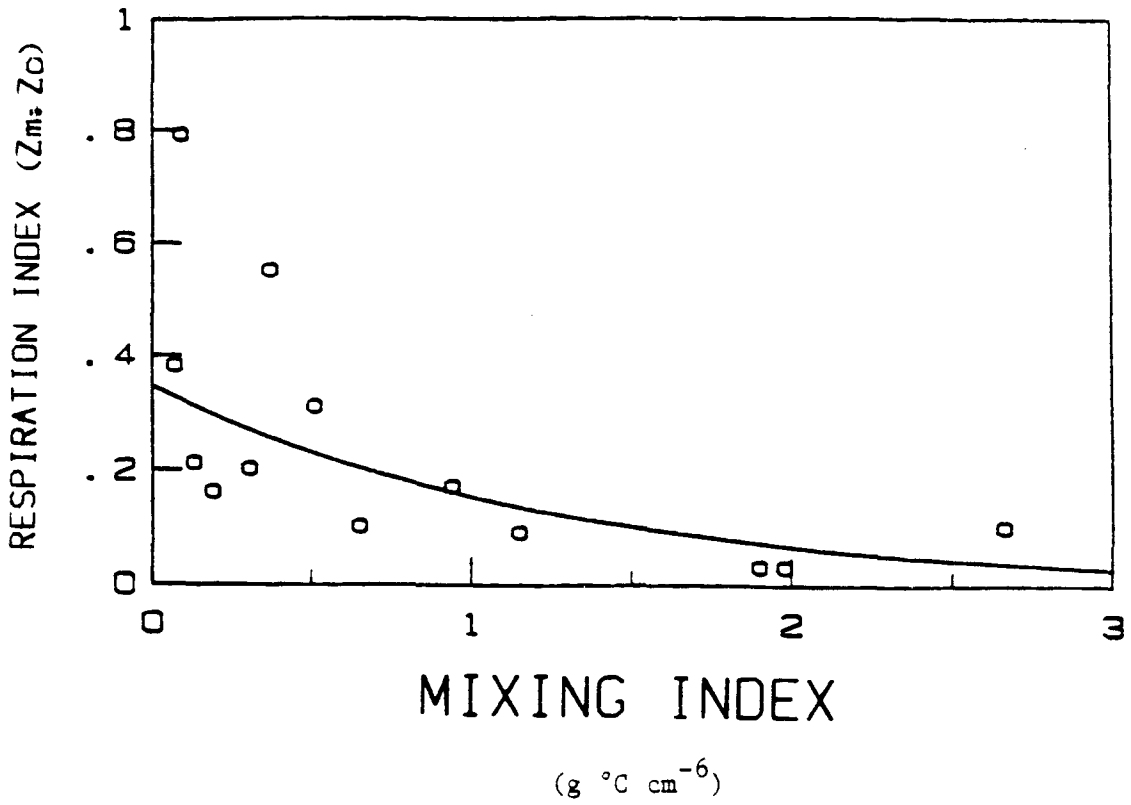

Figure 28.

Relationship between the respiration index and the mixing index.

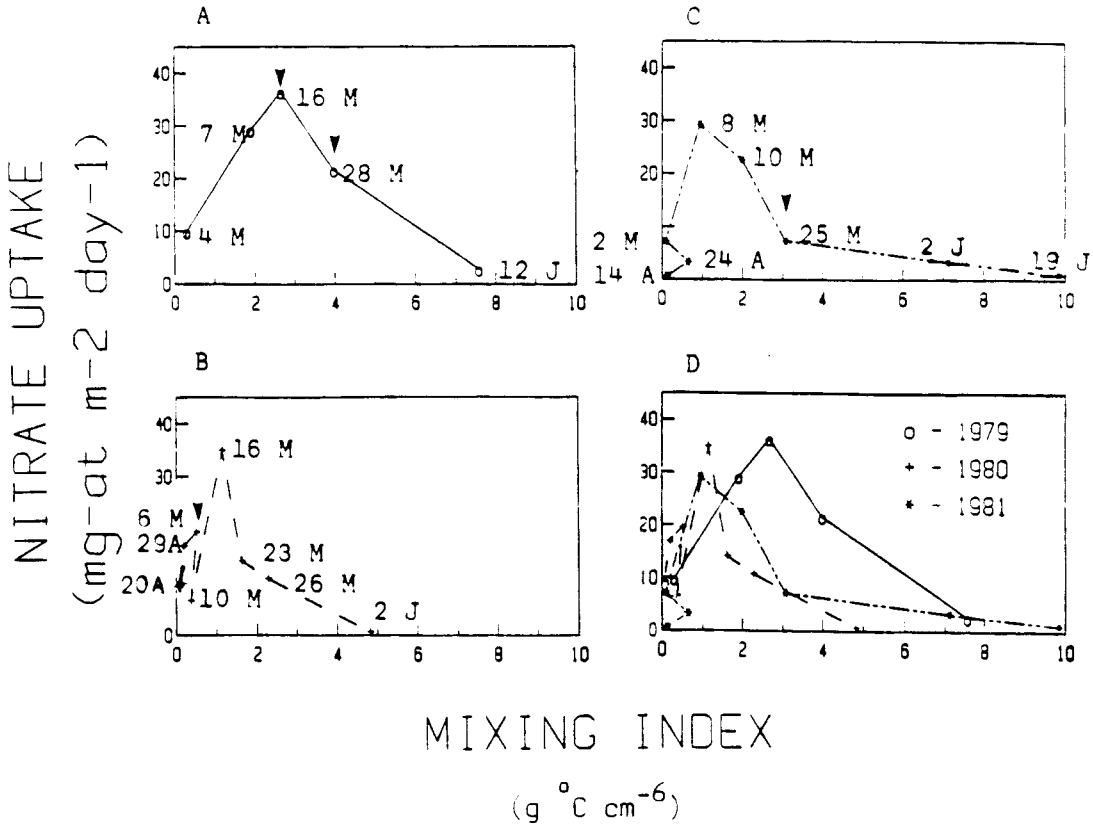

Figure 29.

The relationship between measured new productivity and the mixing index during three bloom periods.

nitrate uptake during this time was dependent on a diffusive flux across a pycnocline and this flux decreased as stratification intensified.

The fundamental importance of vertical mixing enables diatom growth dynamics to be interpreted either on the basis of nutrient limitation (Dugdale, 1967), or sinking losses (O'brien, 1974). Both of these factors are manifestations of the vertical mixing properties of the surface waters. Mixing defines a physical gradient which the successional dynamics of the spring bloom are closely associated with (Margalef, 1978).

This is not to say that mixing itself is responsible for changes in phytoplankton community composition and production with time, but rather that the environmental gradients which cause succession (which can be grouped broadly into light and nutrient categories) are themselves dependent on vertical turbulence (Ignatides, 1979). A succession of species following the transition from mixed to stratified water columns has been observed previously (Walsh, et al., 1974, Reynolds, 1976). These observations reinforce still earlier hypotheses pertaining to seasonal succession and the "interrelationship between turbulence and sinking speed" (Hutchinson, 1967).

The intensity of nitrate varies with a variety of physical indexes in addition to the accumulation of buoyancy. These include the Brunt - Vaisala frequency in various strata, the stability (E) at the nitracline, and the entrainment velocity. None of these indexes, however, exhibited as smooth a trend in nitrate uptake as the buoyancy. The entrainment velocity, for example, can undergo large variations due to its geometric dependency on wind velocity. The mixing index is much more conservative and has an implicit time dimension since it integrates heat flux to the surface water.

The time scale of buoyancy accumulation is similar to the time needed for a large standing crop to develop.

Conditions of peak productivity occur in a physically defined "window" between the large respirational losses which occur in the low stability, prebloom water column and the more stable nutrient limited conditions of the postbloom water column. The window restricts the bloom to a brief time period by the relatively rapid transition from a respiration limited to a nutrient limited water column. This restriction is the temporal analogue to the previously recognized restriction of phytoplankton production in postbloom or low latitude oligotrophic water columns to the interface between a nutrient limited mixed layer and light limited lower layer (Goering et al., 1970). Surface bloom conditions represent the temporal interface between these two types of limitation to growth, both of which are dependent on the degree of upper water column stability.

Steele (1962) observed that optimal primary production results from a very specific combination of hydrographic conditions. Some balance between the stability necessary for favorable light conditions and that necessary to allow for a supply of nutrients for growth must be present for maximum productivity. This point has been developed from critical depth considerations by Yentsch, (1981) and the concept of an "optimum diffusion rate" for water column production was identified at least as long ago as Riley, Stommel, and Bumpus, (1949).

A schematic interpretation of Figure 29 is shown in Figure 30. Nitrate uptake can be effected positively or negatively by increased mixing. For example, a mixing event during the respiration limited phase would decrease nitrate uptake (arrow A indicates the actual change during the early May

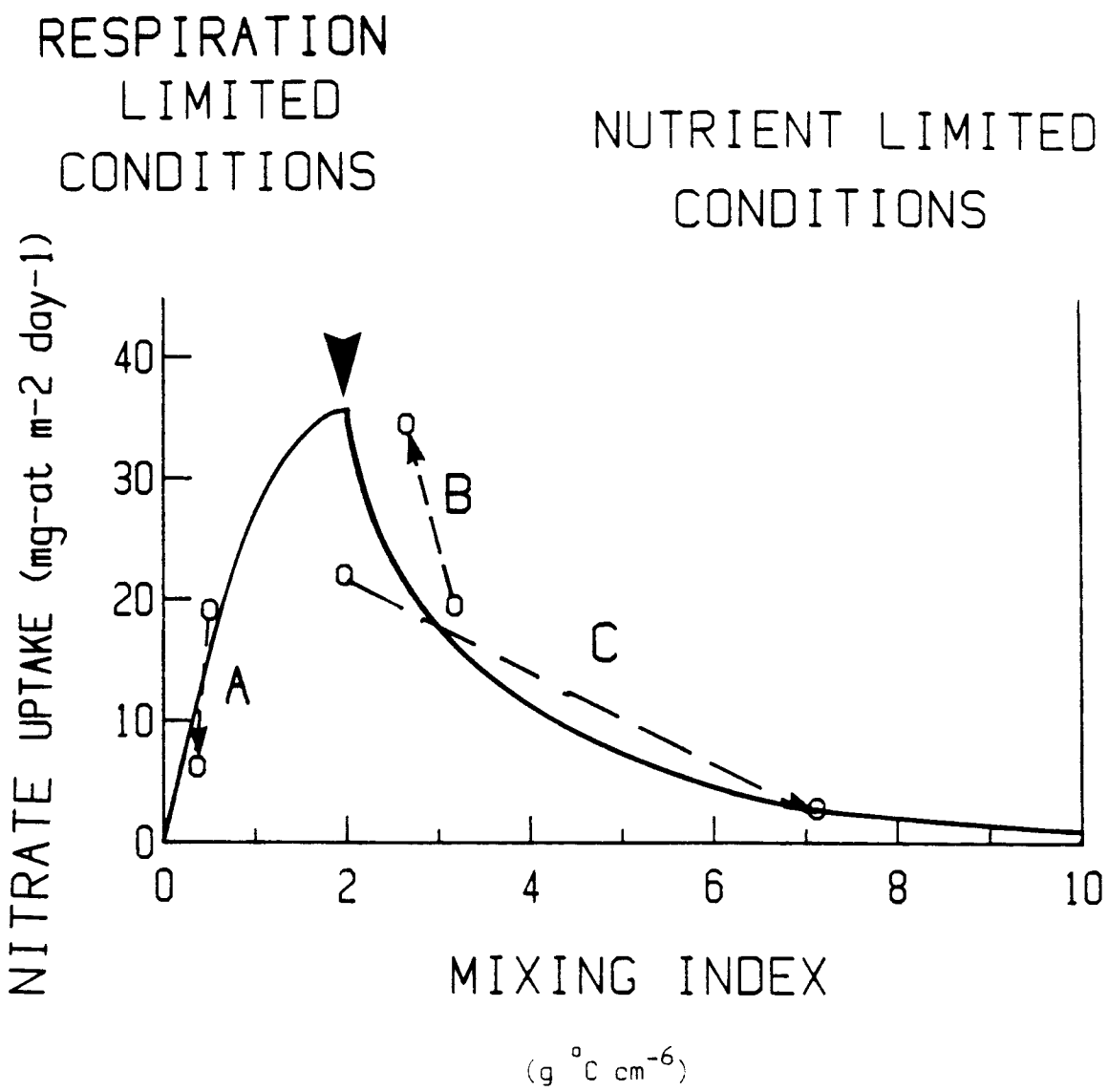

Figure 30.

Schematic interpretation of the developmental relationship between mixing and nitrate uptake.

1980 storm). Mixing during nutrient limitation, on the other hand, would restore higher nitrate uptake (arrow B indicates the estimated changes during the mid-May 1979 storm). The solid arrowhead indicates the point of nitrate depletion from the mixed layer which separates the respiration limited from the nutrient limited phases and marks the termination of peak bloom conditions. The postbloom restriction of nitrate uptake in the mixed layer is pictured as a an exponential decay function (arrow C indicates the net change from 10 May to 2 June 1981.)

3.3.4 Cross Shelf Pumping of Properties by Atmospheric Low Pressure Systems

Low frequency advective "events" were recorded during the study periods. These occurances are not causally associated with the surface phytoplankton bloom, but are of significance to the cross shelf distribution of properties. For example, net onshore nitrate fluxes were recorded in station 12 bottom water following storm systems which passed through the area such as on 7 and 31 May, 1979; 16 May 1980; and 23 April, 25 May, and 13 June, 1981 (Figures 14 h, 15 and 16 f). These events often followed by 3 - 6 days relative lows in atmospheric pressure such as on 1 - 4 May 1979, 20 April 1981, or 19 May 1981 (Figures 14 and 16 a).

Station 12 is just inshore (~25 km) of the middle front and this nitrate may have surged onshore from deeper shelf water in association with the passage of these low pressure systems. Although vector mean flows on the middle shelf are not significant (Coachman, 1982), a recent study based

on six years of moored current measurements across the shelf found that low frequency currents, thought to be associated with meteorological events, displayed maximum 5 day velocities of 4 to 8 cm sec^{-1} (Schumacher and Kinder, 1983). Based on progressive vector diagrams these authors suggest that middle shelf currents respond to the wind as rotating vectors. The alternating "appearance" and "disappearance" of the high nitrate values in deep Station 12 water following a storm passage would be the expected signal produced in the essentially Eulerian time series by a rotating current vector.

Spring tidal currents were present during the cross shelf water movement recorded on 16 May 1980. This does not appear to be a necessary condition for water movement, however, since the other events did not correspond to similar points in the neap - spring tidal cycle. The occurrence of relatively high Chl a concentrations in the near bottom water such as was found on 31 May 1979 and 16 May 1980 (Figures 14 g and 15 e), however, consistently appeared at the spring tide. It is likely that this Chl a originated in earlier surface production and was kept in suspension above the bottom by the strong tidal currents during these time periods.

The occurrence of high nitrate concentrations in bottom water following the shoreward passage of low pressure systems suggests that these storm systems play a role in the onshore "pumping" of nutrient-rich slope water onto the middle shelf. Nitrate sections taken before and after the passage of some of these storms allowed an estimate of cross shelf advection to be made for the deeper nitrate rich water which presumably was the source of the nitrate enrichment observed in Station 12 bottom waters. For example, the 14 mg-at m^{-3} isopleth which appeared in the Station 12 bottom water on 7

May 1979 (Figure 14 h) was 23 km farther offshore when a cross shelf transect was done on 3-4 May 1979, a movement which required an average flow of ca. 7.6 cm sec^{-1}. Also, during the 16 May 1980 event, considering only cross shelf advection, a net current of 2-4 cm/sec would have been necessary to increase Station 12 bottom water nitrate concentration to 11 mg-at m^{-3} between 10 and 16 May. A similar transient was observed in deep station 12 water during the 16 May 1980 event in measurements of total CO_2 (Codispoti et al., 1982).

The results of Schumacher and Kinder (1983) support the hypothesis that "storm pumping" was responsible for the observed episodic nitrate concentration increases in Station 12 bottom water for two reasons. The calculated current speeds necessary for the nitrate enrichment at station 12 is similar to the reported speeds of the low frequency pulses observed by these authors. Also, the alternating "appearance" and "disappearance" of the NO_3^- rich station 12 bottom water following a storm passage would be the expected signal produced in the essentially Eulerian time series (Figures 14 h, 15 and 16 f), by a rotating current vector.

Passage of these low pressure systems through the southeastern Bering Sea may represent an important mechanism for the supply of NO_3^- to the middle shelf. A deep slope water advective source for shelf nutrients has been identified on other shelves (Riley, 1967; Yoder et al., 1982). The low pressure system "pumping" described here, however, represents a separate mechanism from the previously recognized importance of tidal diffusion in the process of cross shelf nutrient transport (Coachman and Walsh, 1981) The net result of such pumping is to enhance the onshore diffusion of nutrients to the middle and inner shelves where it can fuel continued

productivity upon reaching the euphotic zone either by wind mixing or by upwelling at the inner front.

Storm pumping is not limited to actions against the cross shelf nitrate gradient, but would affect other cross shelf gradients in water column properties. One of the more significant affects of this pumping, may be its ability to transport particulate material from the middle shelf into deeper water. In the southern Bering Sea a cross shelf bottom water particle gradient occurs during the spring bloom. This takes place since much of the lightly grazed middle shelf phytoplankton production reaches the bottom virtually intact. Under circumstances such as those occurring around 16 May 1980, advective movement was recorded coincident with spring tidal currents capable of keeping particulate Chl a suspended off the bottom (Figure 15 e). This situation is potentially capable of transporting these particles into deeper water.

The winnowing of fines due to the roiling of shelf sediments by storms has previously been observed and is thought to occur frequently at depths of 80 to 90 meters (Lisitsyn, 1966). Based on estimated water particle velocities caused by storm activity Sharma et al. (1972) suggest that such sediment transport is responsible for the absence of fine and clay size material from water depths less than 80 meters in the southeast Bering Sea due to deposition of this material in deeper areas of lower turbulence. Additionally, Sancetta (1981) found the tests of neritic phytoplankton species such as Biddulphia aurita common in outer shelf surface sediments which may be due to their transport from shallower waters.

The bottom water Chl a values recorded on 16 May 1980 (Figure 15 c) were actually a conservative indicator of the suspended particulates

present. Particle volume measurements at this station indicated that there was significantly more particulate material in the bottom water than in the surface. This observation of suspended phytodetritus in the bottom mixed layer appears to be very similar to bottom nepheloid layers observed on other shelves (Pak and Zaneveld, 1977, Houghton, 1978)

Chapter 4

Changes in Particulate Matter Composition and Specific Uptake Rates

4.1 Introduction

In this chapter the examination of ship time series are continued. Additional time series from station 12 are presented which deal more qualitatively with the changes taking place in the phytoplankton community throughout the bloom. The PROBES data include a great deal of information on the composition of particulate material. Time series changes indicated distinct trends in composition which may be interpreted in light of the supporting data.

Specific ($hr.^{-1}$) nitrogen and carbon uptake rates were examined and interpreted relative to the mixing dynamics which were found to be of importance to growth and nitrate uptake. The data suggest the spring bloom phytoplankton are extremely plastic in composition and specific uptake

rates.

4.2 Results

4.2.1 Changes in Nitrogen Kinetic Parameters With Time

Bloom dynamics were closely related to the measured changes in $V_{max(NO_3^-)}$ (Figures 31 and 32) Especially significant are the increases or decreases associated with observed changes in upper water mixing. For example, the steady increase in $V_{max(NO_3^-)}$ in early May 1980 (Figure 32 a) corresponds to the stabilization of the water column at this time. The deep mixing which was recorded on 10 May 80 was associated with significant decrease in this rate as for $V_{max(NH_4^+)}$ (Figure 32 b). Conversely, the entrainment activity of the storm on 16 May 1979 resuspended diatoms which exhibited a very high $V_{max(NO_3^-)}$ (Figure 32 a).

There also were trends in the measured K_s values (Figures 33 and 34). The depletion of NO_3^- from the mixed layer in early May 1979 coincides with a decrease in $K_{s(NO_3^-)}$ during this time (Figure 33). During the deep mixing on 10 May 1980, $K_{s(NO_3^-)}$ increases over earlier, more stable periods, although $K_{s(NH_4^+)}$ is less sensitive to this effect (Figure 34 a and b). The 16 May 1979 entrainment also resulted in an increase in $K_{s(NO_3^-)}$ (Figure 33). In 1980, post bloom stations exhibited much lower K_s values for both NO_3^- and NH_4^+ (Figure 34).

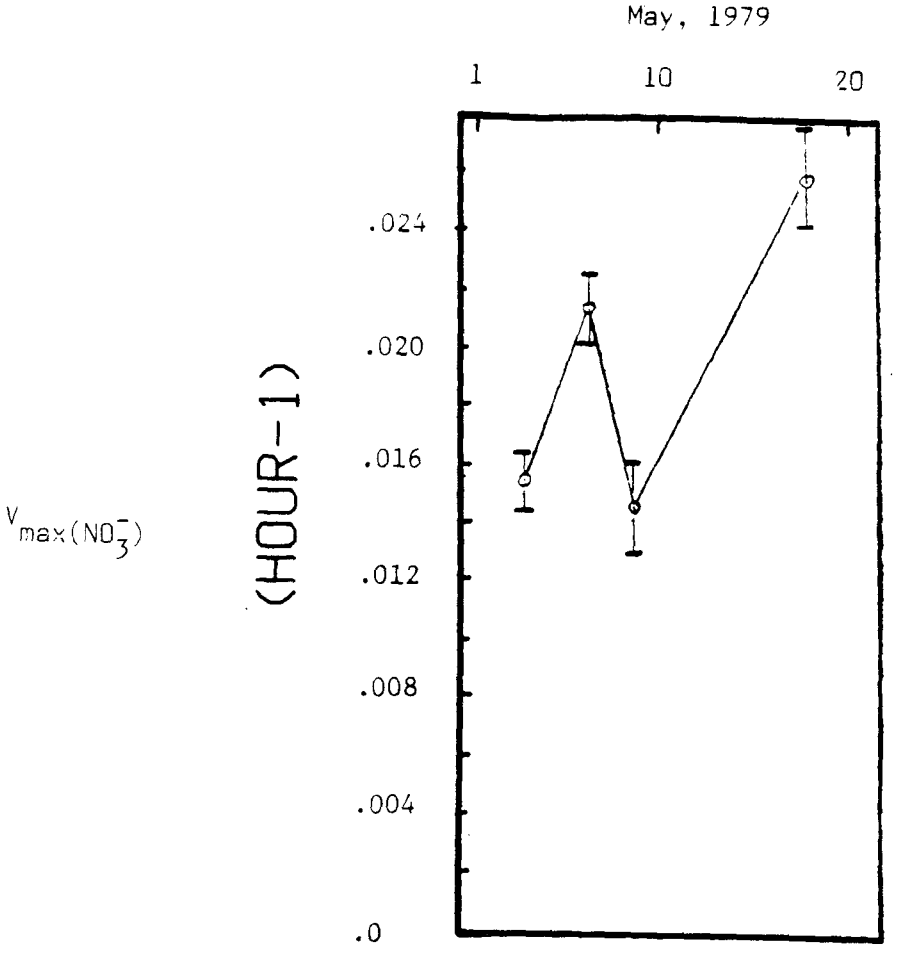

Figure 31.

Changes in $V_{max(NO_3^-)}$ at the 50% light depth with time at station 12 during 1979.

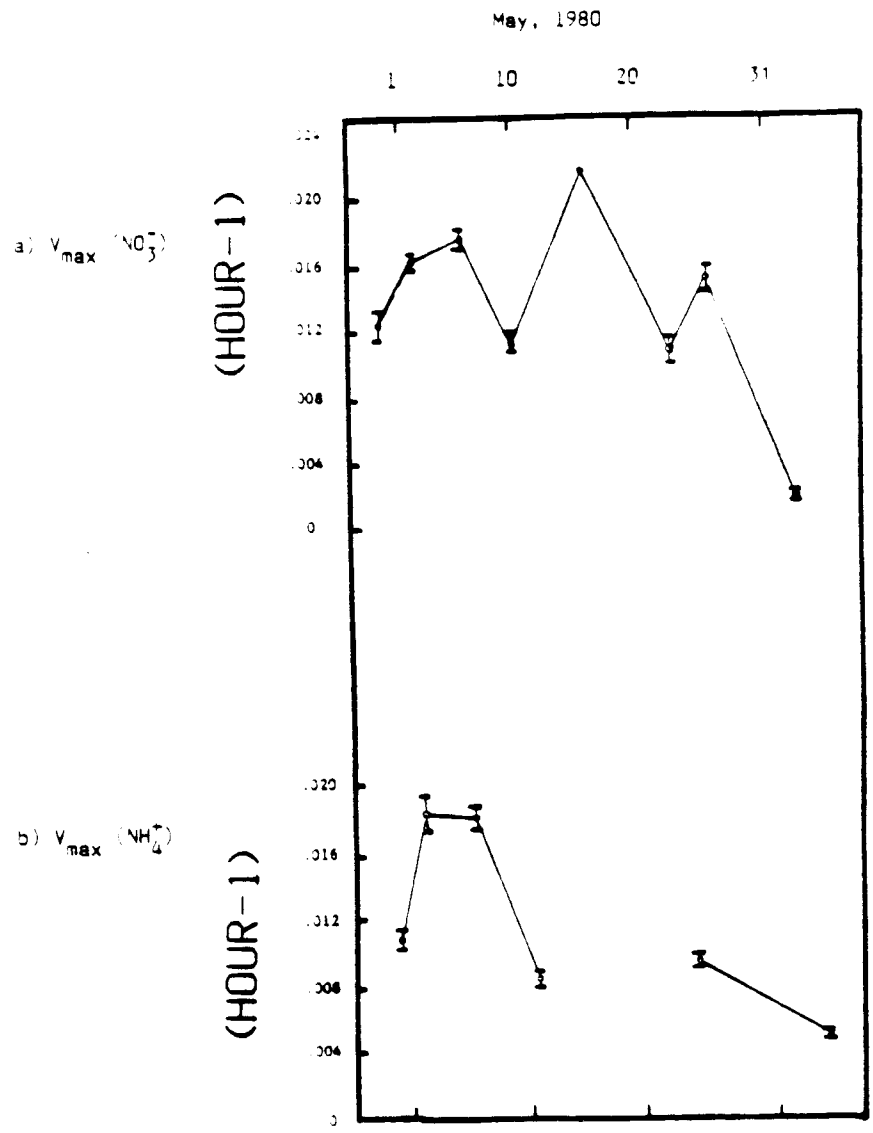

Figure 32.

Changes in A) $V_{max(NO_3^-)}$ and B) $V_{max(NH_4^+)}$ at the 50% light depth with time at station 12 during 1980.

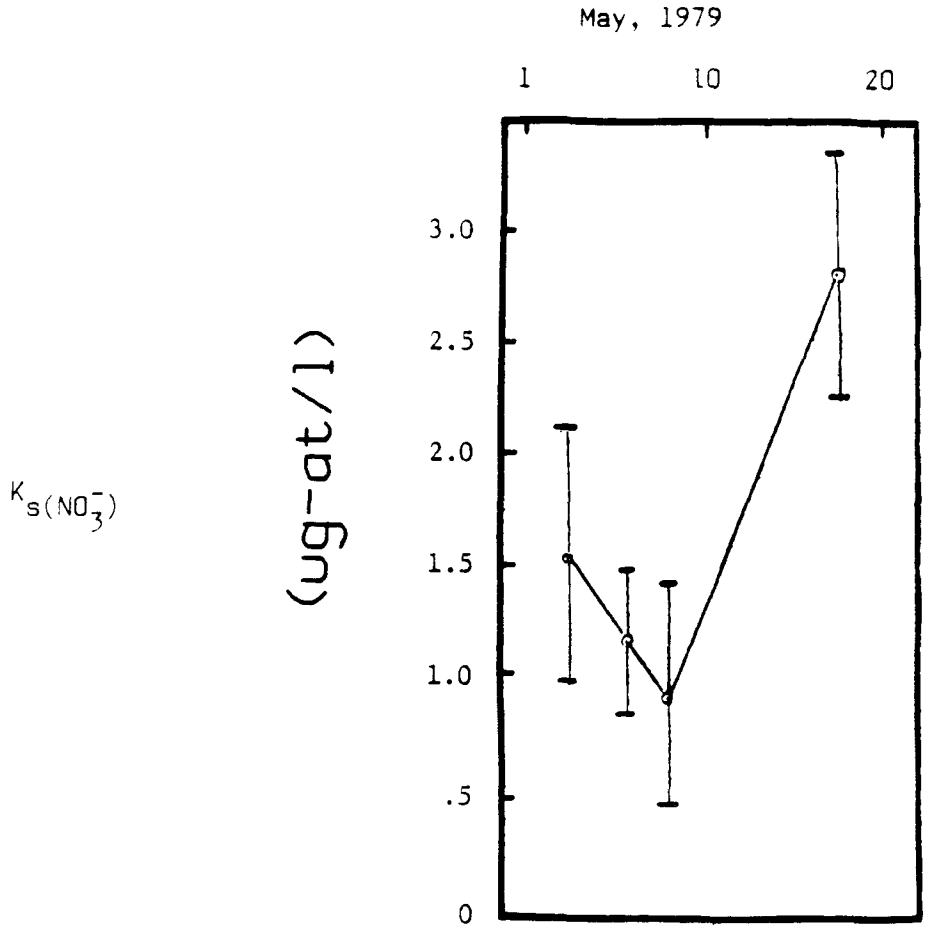

Figure 33.

Changes in $K_{s(NO_3^-)}$ at the 50% light depth with time at station 12 during 1979.

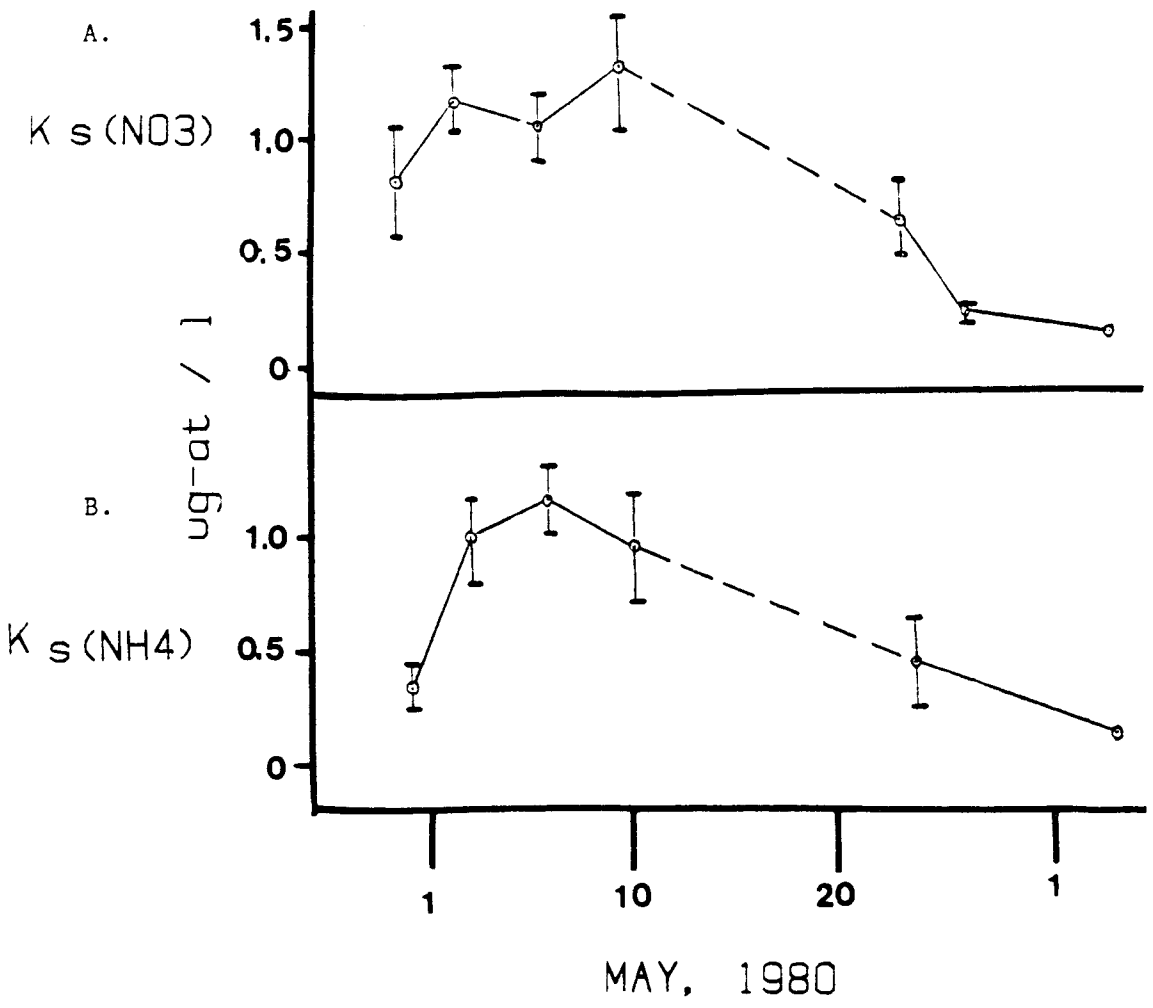

Figure 34.

Changes in A) $K_{s(NO_3^-)}$ and B) $K_{s(NH_4^+)}$ at the 50% light depth with time at station 12 during 1980.

4.2.2 Changes in Nitrogen Kinetic Parameters with Depth

It appears that the settled "pioneer" diatoms resuspended by the 16 May 1979 storm had very different nitrogen uptake characteristics than the mixed layer community before the storm. Such vertical structure in biological characteristics was frequently recorded at post bloom stations which exhibited sub mixed layer Chl *a* maxima (Figure 35). Nitrate kinetic experiments were carried out on water from the 50% and 0.1% light depths at this station and the results are shown in Figure 36. The deeper community from the Chl *a* maxima clearly had a much higher nitrate V_{max}. Such a capacity for nitrate uptake could have been put to use during a wind event strong enough to entrain this community into the mixed layer.

Conditions such as those sampled in Figure 36 were most likely also present before the 16 May 1979 entrainment event. When sampled during the calm conditions on 9 May 1979 station 12 exhibited a pronounced Chl *a* maxima (Figure 37). Only the nitrate V_{max} at the 50% light depth was measured on 9 May 1979. It is likely however, that plants deeper in the main Chl *a* layer would have exhibited a larger specific uptake rate similar to the situation depicted in Figure 36. An influx of such cells having a large nitrate V_{max} into the mixed layer would explain the rapid increase in the nitrate V_{max} measured at the 50% light level on 16 May relative to the earlier measurements in this time series (Figure 31).

Data on the nitrate uptake photoadaptive capabilities of the early bloom phytoplankton has previously been introduced (Figure 26) which indicated that the light efficiency of nitrate uptake increased as the water

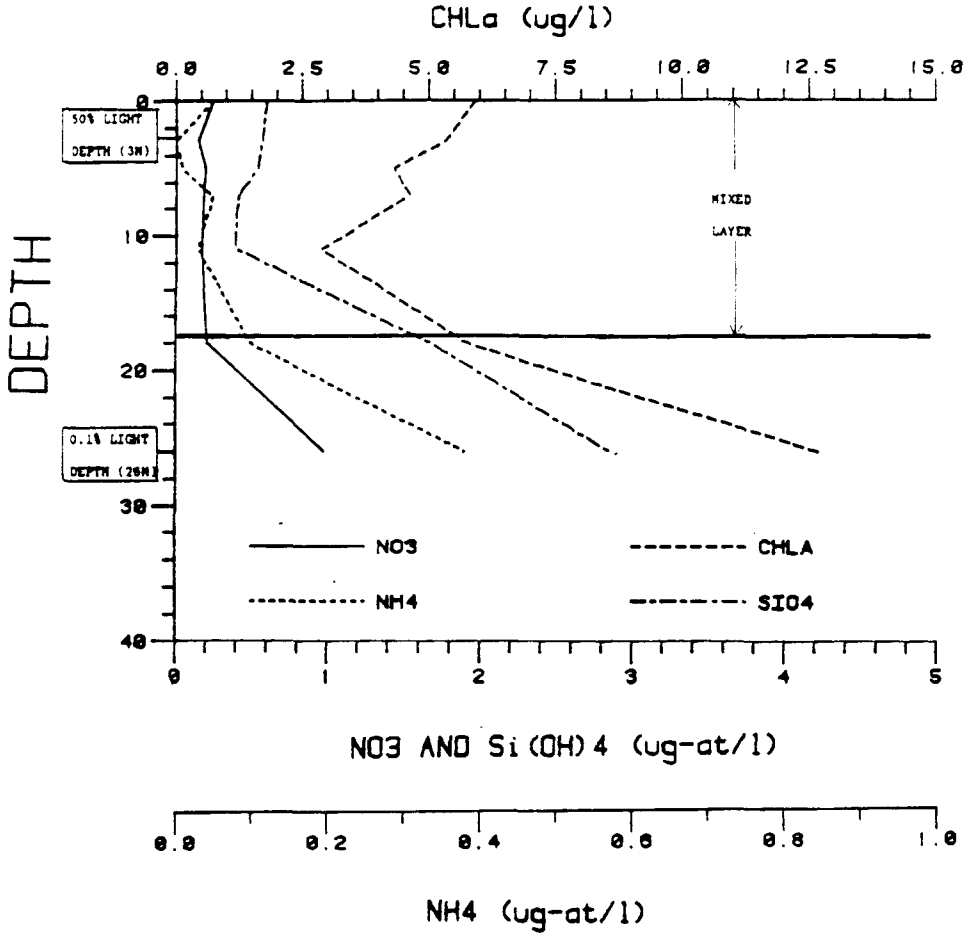

Figure 35.

Vertical structure of Chl a and nutrients at a postbloom station.

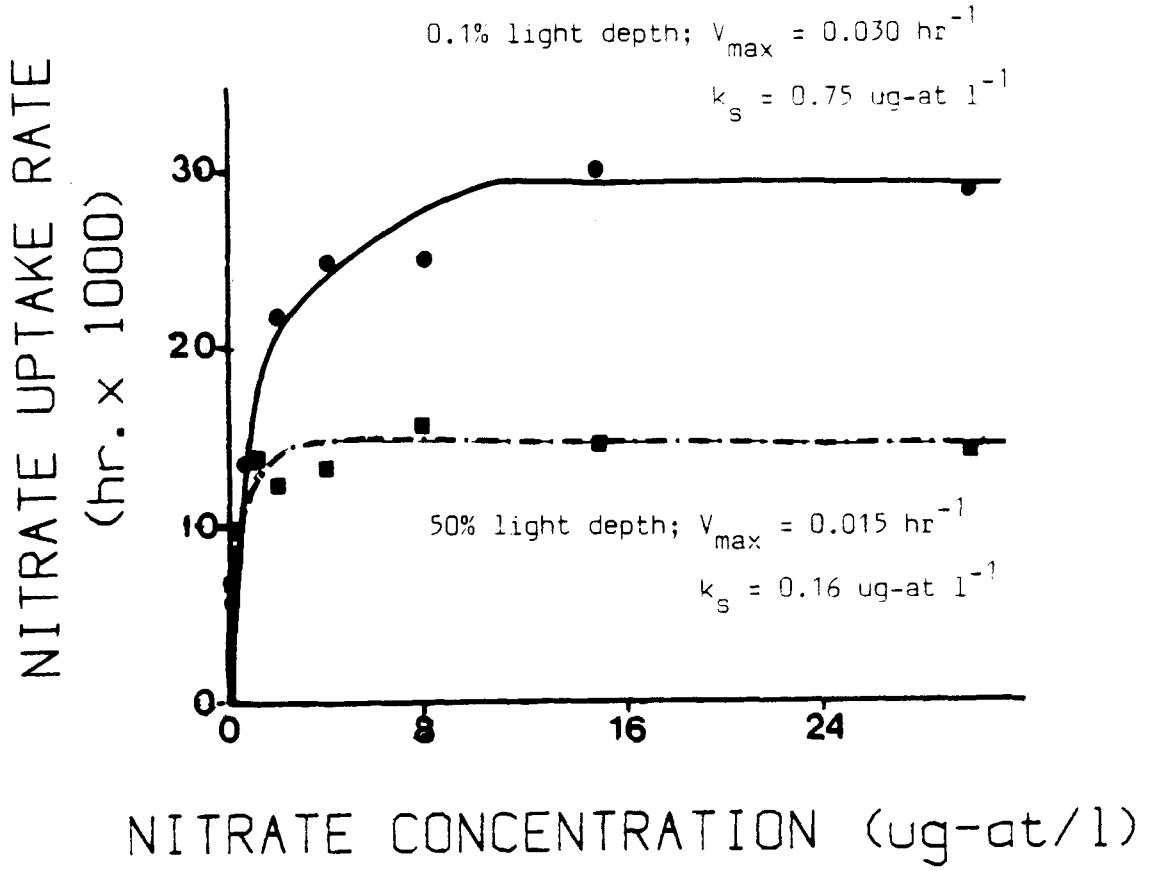

Figure 36.

Comparison of nitrate kinetics from two depths in the same water column.

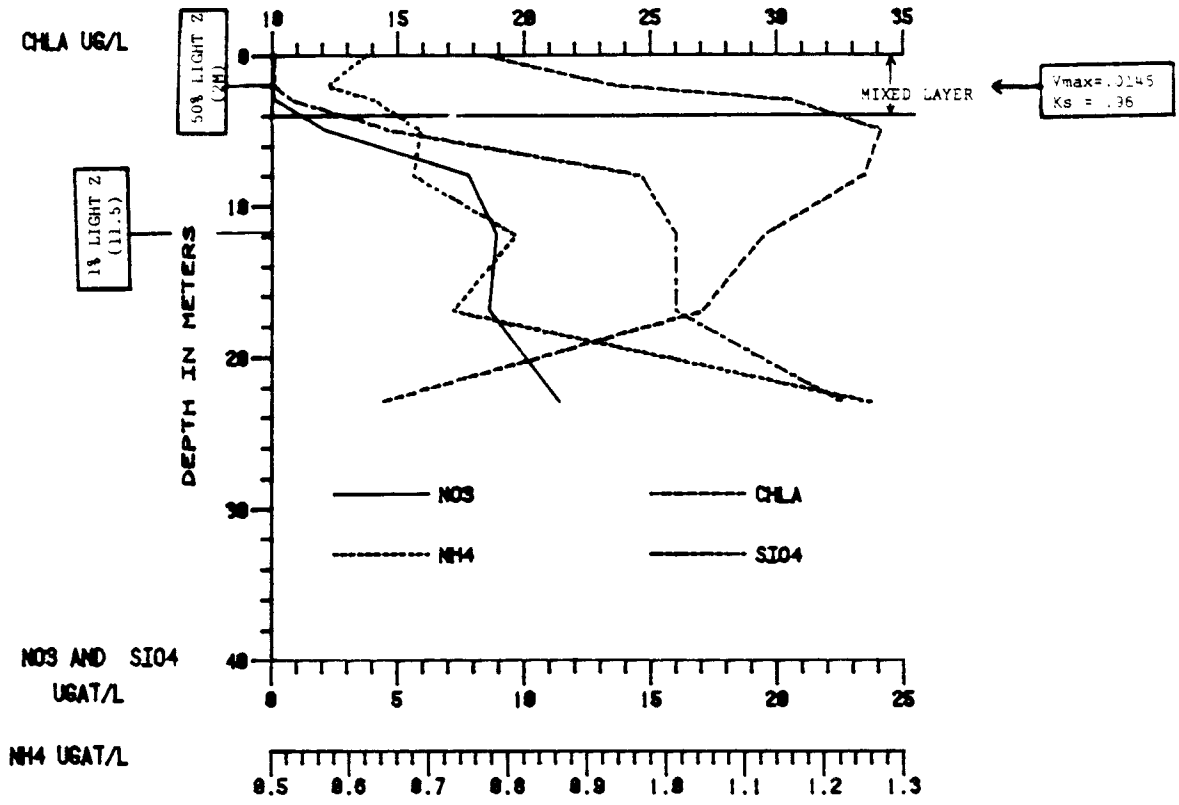

Figure 37.

Vertical structure in Chl a and nutrients at a post bloom station before a storm.

column stratified. On 10 May 81, at the point of NO_3^- exhaustion and the appearance of a sub-mixed layer Chl *a* maximum, K_{light} and $K_{s(NO_3^-)}$ kinetic experiments were done at the 50 and 1% light depths (Table 8). This station exhibited vertical structure in nitrate V_{max} just as was found at other stations (i.e. Figure 36). Importantly the data in Table 8 also indicate that there was vertical structure in the half saturation values for light and nitrate concentration.

Postbloom mixed layer communities did not continue the trend of the prebloom K_{light} values. The greater K_{light} value found in the 50% community relative to the 1% in Table 8, indicates postbloom mixed layers often contained communities which exhibited relatively "sun adapted" K_{light} values. For example, a post bloom community composed mainly of *Phaeocystis pouchetti* exhibited a K_{light} similar to the light conditions from which it was collected (Figure 38). This K_{light} was far greater than a typical diatom dominated Chl *a* layer which was adapted to much lower light levels (Figure 38).

4.2.3 Changes in the Bulk Composition of Particulate Matter During Bloom Development

The data permit an examination of the changes in particulate C/N ratios relative to the measured carbon and nitrogen (NO_3^- + NH_4^+) uptake rates (ρ) during bloom development (Figure 39, 40, and 41). These properties, as others to be introduced, were integrated in two distinct strata. The first was the mixed layer itself, and the other was the strata below the

Table 8.

Comparison of nitrate kinetic parameters with depth.

	V_{max} (hr^{-1})	K_{light} ($Ein.m^{-2}hr^{-1}$)	$K_{s(NO_3^-)}$ ($\mu g\text{-at } l^{-1}$)
50%	0.0258(±0.0074)	0.028(±0.015)	0.32(±0.09)
1%	0.0434(±0.0025)	0.016(±0.005)	1.09(±0.1)

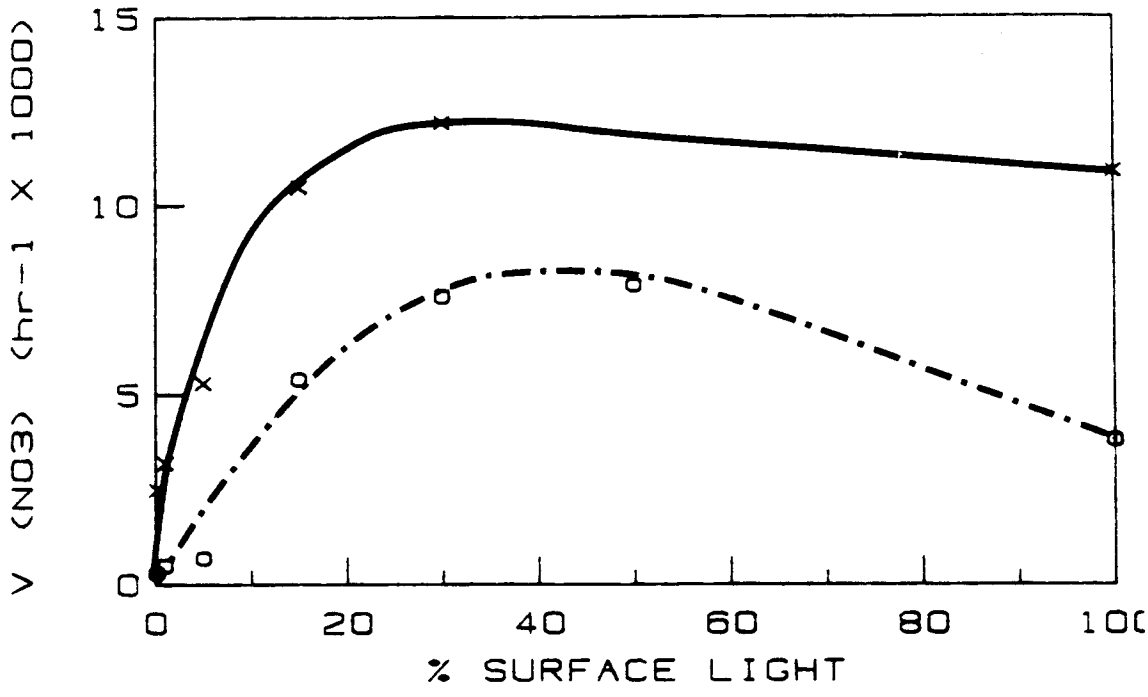

Diatoms; 0.01% light Z:
Vmax = 0.0121 hr.-1
K(light) = 3% of surface light

Phaeocystis; 15% light Z;
Vmax = 0.0085 hr.-1
K(light) = 11% of surface light

Figure 38.

Comparison of relative nitrate uptake light response of Phaeocystis and diatom dominated communities.

Figure 39.

1979

Figure 40.

1980

Figure 41.

1981

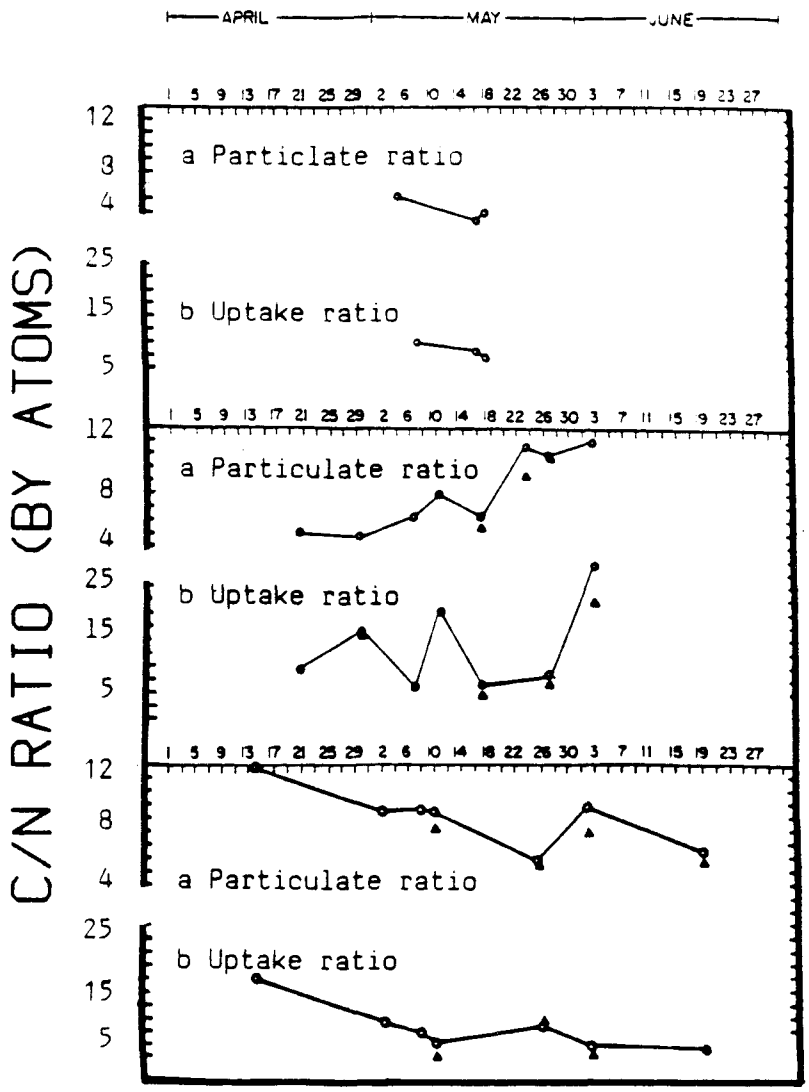

Figures 39, 40, and 41.

Changes in carbon to nitrogen ratios for particulate matter composition and for uptake with time during 1979, 1980 and 1981 respectively.

the mixed layer but above the 0.1% euphotic zone when such a layer existed.

The particulate C/N values were relatively high during April - early May 1981 (>9), while during the height of the bloom in 1979 and 1980 they were much lower. As observed in previous time series data (e.g. Antia et al., 1963), peaks in productivity take place in association with relative lows in the C/N ratios of particulate material. The C/N ratios of each peakbloom period were weighted on the basis of Chl *a* and averaged. The resulting "average" particulate C/N ratio for the spring bloom was approximately 6.5, quite similar to the "average" compositional value reported for marine phytoplankton (Redfield et al., 1963).

In the Southeast Bering Sea middle shelf area in 1980 the post bloom euphotic zone was characterized by significantly higher particulate C/N ratios than occurred during the rapidly growing peak bloom. The post bloom euphotic zone in 1981 did not display a similar increase in C/N ratios and may reflect the more favorable mixed layer nutrient conditions present in this year compared to 1980. The sub-mixed layer consistently displayed a lower C/N ratio when such a layer was encountered (Figures 40 and 41 a).

The C/N uptake ratios correspond at least qualitatively to the compositional ratios (Figures 39 - 41 b). The uptake ratios, as did the C/N compositional ratios, decreased as peak bloom conditions developed. Also, the deep mixing on 10 May 1980, is associated with a large increase in the uptake ratio (Figure 40 b), and a less dramatic although perceptible rise in C/N compositional ratio (Figure 40 a).

A variable proportion of the collected particulate material represents living phytoplankton. This can influence the measured particulate C/N ratios (Banse, 1974). For example, when normalized to Chl *a*, particulate

carbon and nitrogen consistently increased in post bloom stations (Figure 42, 43, and 44 a and b). At this nutrient limited stage in bloom development, the larger C/Chl *a* and N/Chl *a* ratios may indicate residual flocculent detrital material remaining after most of the new production has settled from the mixed layer. The very different nature of the postbloom matter is even more apparent when Chl *a* is normalized to particle volume (Figures 45, 46, and 47 c). In all three years the Chl *a*/P.V. ratio decreases during the post bloom interval. Much of the particulate material at this time, therefore, may not be living phytoplankton.

Differences were noted among peak bloom C/N ratios, (i.e. 5, 7 and 9.5 in 1979, 1980 and 1981 respectively). In these peakbloom stations, the particulate material was consistently "rich" in Chl *a*, when normalized to particle volume, nitrogen or carbon (Figure 45 - 47 c). This strongly suggests the peakboom particulate material was dominated by living phytoplankton Further, the species composition of the bloom was similar each year. On a volume basis the diatoms *Thalassiosira sp.*, *Chaetoceros sp.* (especially C. *debilis*), and *Corethron sp.* dominated the community (shipboard observations per Cupp, 1943). Taken together, these factors suggest that peak bloom phytoplankton elemental composition varied with prevailing environmental conditions.

Figure 42 - 1979.

Figure 43 - 1980.

Figure 44 - 1981.

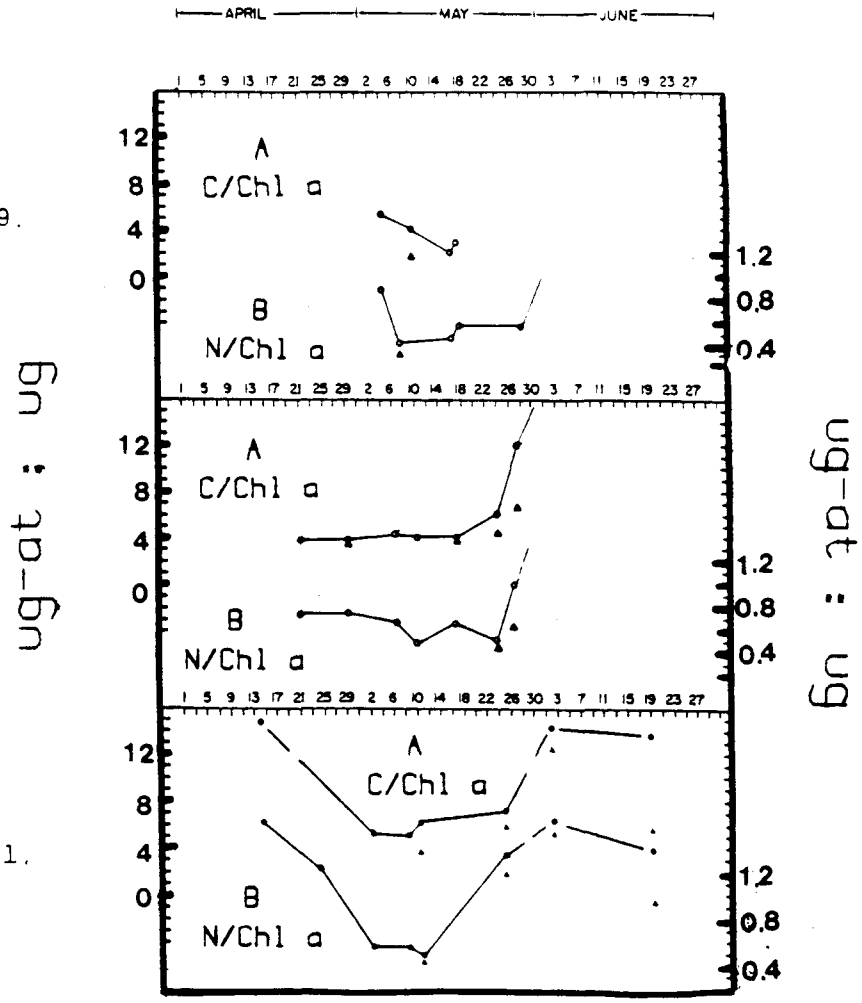

Figure 42, 43, and 44.

Changes in carbon/ Chl a and nitrogen/ Chl a ratios of particulate matter with time during 1979, 1980, and 1981 respectively.

Figure 45 - 1979.

Figure 46 - 1980.

Figure 47 - 1981.

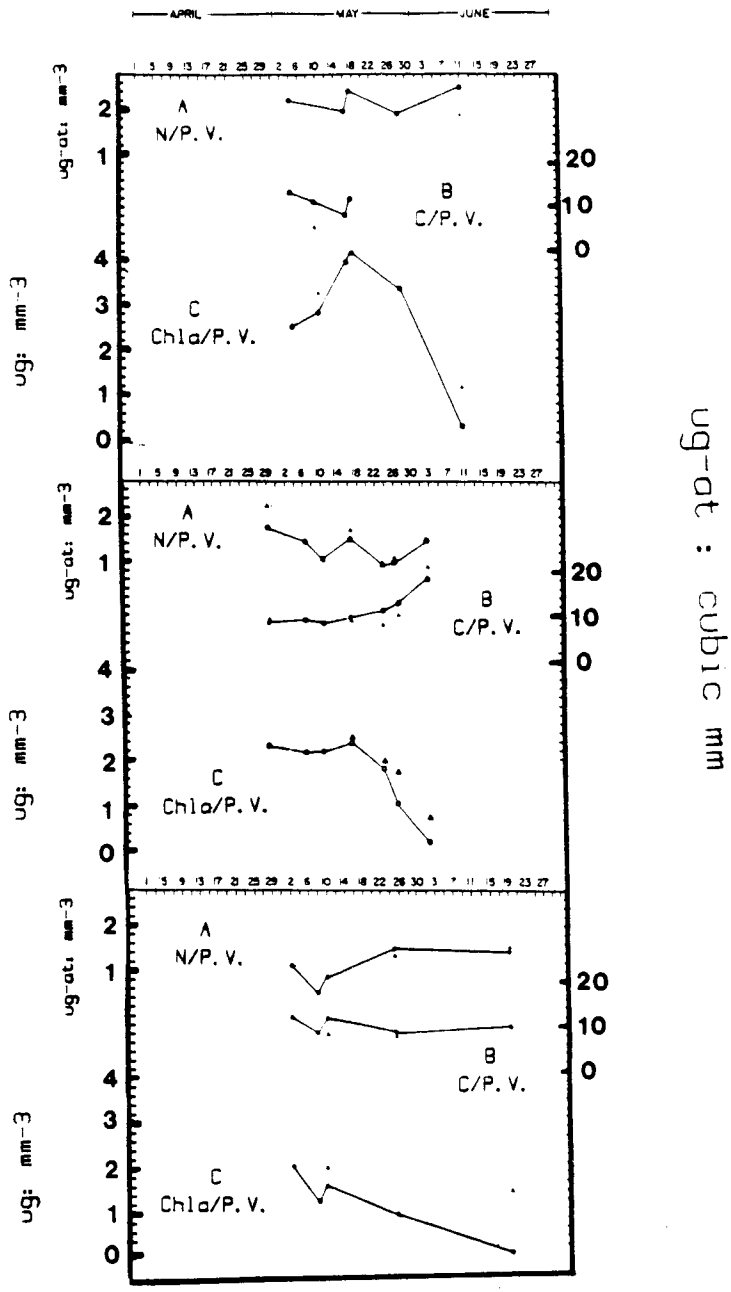

Figure 45, 46, and 47.

Changes in the ratios of particulate nitrogen, particulate carbon, and Chl a to particle volume with time during 1979, 1980, and 1981 respectively.

4.3 Discussion

4.3.1 The Regulation of Specific Uptake Rates by Vertical Mixing During Nutrient Sufficient Conditions

The effects of nutrient conditions can be removed as an independent variable to examine in isolation the effects of mixing on specific growth rates. This was done by considering only data from stations with an immediate history of ambient NO_3^- in the mixed layer from the larger data set covering the entire spring bloom period. These stations are the prebloom and peakbloom stations which preceded the summer disappearance of NO_3^- from the mixed layer.

Examination of mixed layer respirational losses immediately preceding the blooms (Figure 20 a-c iv) indicates that the respirational histories of the developing blooms differed among years. In 1979 very low respirational losses preceded the bloom, while in 1980 diminishing respirational losses at the beginning of May were interrupted by a storm event on 10 May which greatly augmented respirational losses. The 8 May 1981 bloom was preceded by very large respirational losses due to late April storm mixing. The hypothesis is made that the spread in peakbloom C/N ratios from just above that of pure protein (3.64; Holmquist, 1973) in 1979 to the high 1981 value is due to the difference in mixing conditions leading to the exhaustion of mixed layer nitrate. On a mechanistic basis, the assimilation rates of carbon and nitrogen must have a differential dependence on water column mixing conditions to produce the observed covariance of mixing and C/N

ratio.

The respiration indexes were used as an environmental independent variable for the phytoplankton rate measurements. The $V_{max(NO_3^-)}$ data from pre and peakbloom stations were examined relative to the respirational history derived from Figure 20 (Figure 48). The average respiration conditions during the three days preceding the station occupations were used as the independent variable. This "respiration history" parameter yielded a better fit of the data points than was obtained using only the light conditions on the day of the station occupation itself.

The relationship is weak, but suggests that high nitrate specific uptake rates occur only under low respirational losses. The maximum ammonium specific uptake rates varied with maximum nitrate specific rates which suggests nitrogen utilization by the phytoplankton is limited by respirational losses regardless of nitrogen form. It is probably protein synthesis therefore, which is sensitive to respirational losses, since the formation of this substance is the fate of most assimilated nitrogen (Ditullio and Laws, 1983). The large rates of nitrate uptake found at peakbloom stations are not merely due to the large biomass present, but also reflect the high specific rates of phytoplankton nitrogen utilization at these times. The association of these high specific rates with low respirational losses explains their confinement to stable, peakbloom periods.

Uptake and reduction of NO_3^- competes with other cellular processes requiring reducing power and ATP generated by photophosphorylation reactions (Collos and Slyawk, 1980). Also, changes in NO_3^- uptake have been shown to be associated with changes in patterns of cellular energy flow (Falkowski

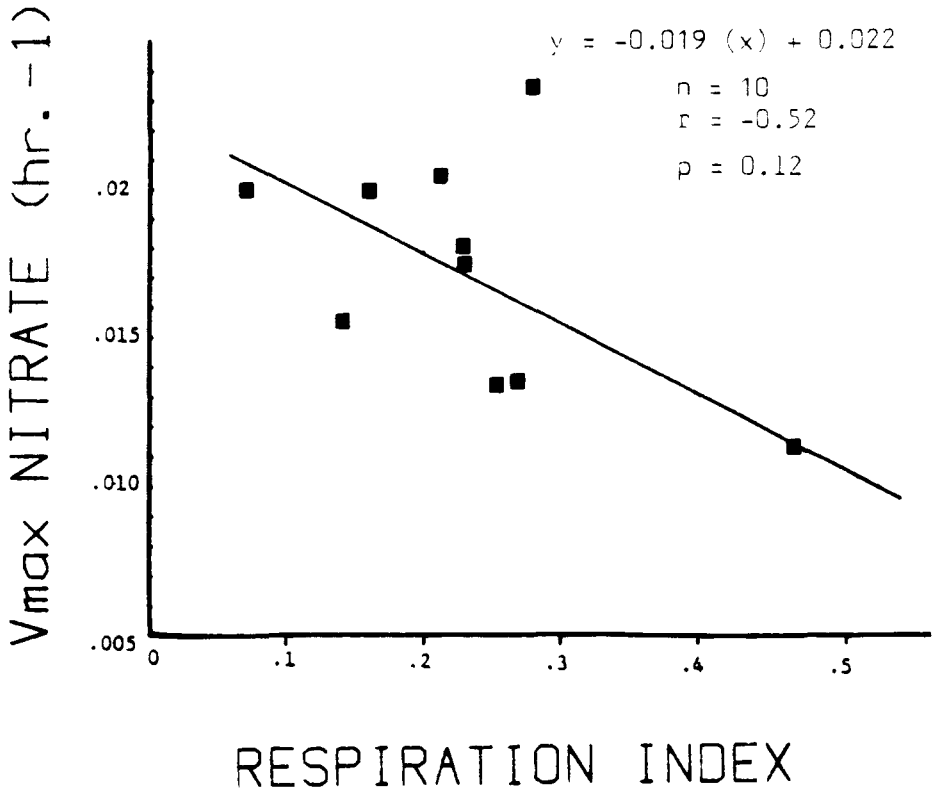

Figure 48.

Relationship between $V_{max(NO_3^-)}$ and the respiration index at nutrient sufficient stations.

and Stone, 1975). These findings suggest cellular energetics are sensitive to mixed layer respirational losses, explaining their usefulness for interpreting the changes observed in V_{max} NO_3^-.

Faced with a high respirational loss as on 10 May 1980 (Zm:Zcr = 0.57), these spring bloom diatoms apparently have the capacity to relatively quickly (within 2 days) regulate specific nitrogen uptake rates. These decreases in specific rates occurred despite relatively high nitrate concentrations (>6 mg-at m^{-3}), suggesting that cellular energetics and not nutrient limitation was the cause. When low respirational loss conditions returned on 16 May 1980, the maximum NO_3^- specific growth rate was almost double that found at the height of the storm.

Peaks in the V_{max} NO_3^- time series were not found to correspond to peaks in carbon specific uptake rates. This lack of correlation is similar to the observed variation in C/N uptake ratios (Figures 39 - 41 b). Further, there was an increase in carbon specific uptake rates during the poor light conditions on 10 May 1980. A linear regression analogous to Figure 48 was done using carbon specific uptake rates as the dependent variable for the same nine stations. The correlation was less significant ($r = 0.47$), but importantly the slope was positive, indicating that opposite to their effect on NO_3^- specific uptake rates, carbon specific uptake rates increase with net respirational losses. Diatoms are capable of regulating photorespiration in such a way as to maximize net photosynthesis (Harris and Piccinin, 1977). This suggests that there exists a priority for carbon uptake during periods of high water column respirational loss. A schematic representation of the proposed regulation of NO_3^- and carbon uptake rates by the accumulated net photosynthate is shown in Figure 49.

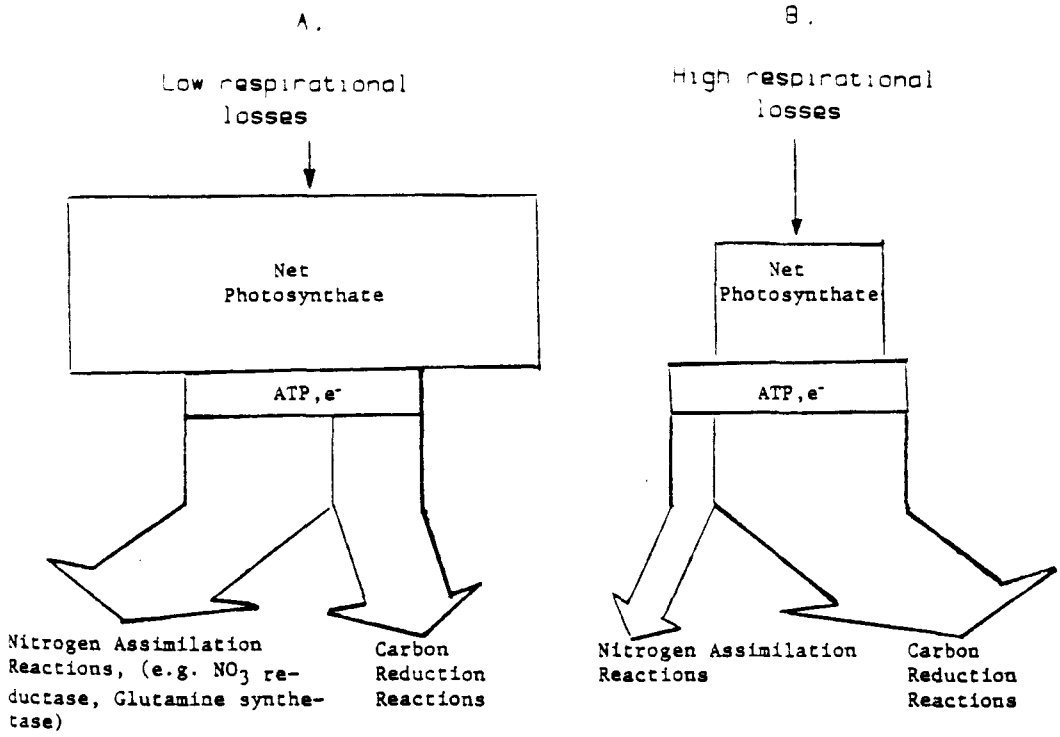

Figure 49.

Schematic of the proposed regulation of nitrogen and carbon uptake by respirational history.

This flow diagram depicts the suggested hierarchical control of nitrogen and carbon specific uptake rates (and ultimately N/C composition) during nitrogen sufficient, early bloom periods. Two situations are contrasted in the figure; that in which there has been low mixed layer respirational losses (i.e. Zm:Zcrit <.3) and that which follows a period of high respirational losses (i.e. Zm:Zcrit >.5). The photosynthesis : respiration (P/R) ratio can vary (Eppley and Sloan, 1965). Although both processes increase with growth rate, the increase in photosynthesis is relatively greater (Laws and Caperon, 1976). The respirational history parameter (Zm:Zcr) can be interpreted as an index of the ratio of respirational losses to total photosynthesis (R:Pt; Yentsch, 1981). It would control therefore, the net photosynthate which the mixed layer phytoplankton are able to maintain.

The net photosynthate of diatoms appears to be very susceptible to vagaries in light conditions unlike flagellates, for example, which maintain stored carbon pools for use in poor light conditions (Rivkin et al., 1982). More detailed and specific models of cellular energy and material flow associated with carbon and nitrogen metabolism have also been presented, (Solomonson, 1978, and Falkowski, 1978)

The relative lows in particulate C/N ratios which occurred during stable, peakbloom periods are due to the differential dependence of carbon and nitrogen assimilation on respirational losses. During these periods nitrogen assimilation rates are maximum while carbon assimilation rates are actually lower then they had been previously. The C/N composition of particulate material collected before stabilization has been found to be high (>10) in other areas as well (Landing and Freely, 1981). Also,

particulate material collected in interceptor traps during the spring bloom in the Baltic Sea (Smetacek et al. 1978) exhibited relatively low particulate C/N ratios coincident with the highest percentage of phytoplankton particulate carbon to total particulate carbon (i.e the sedimentation of the peak spring diatom bloom). Traps set after the peak bloom periods collected particulate material with higher C/N ratios. The time series of C/N particulate ratios for 1980 in the present study (Figure 40 a) most closely parallels Smetacek et al.'s (1978) bloom data.

V_{max} NO_3^- is not solely a function of Zm:Zcr, however, as the spread in the early bloom 1981 data in Figure 48 suggests. The maximum NO_3^- uptake rates measured on 2 and 8 May 1981 were anomalously large when compared to the other two years solely on the basis of recent respirational losses. Mixing rates were larger in late April, 1981 than previous to the other peak blooms (Figure 25 c). The high C/N compositional ratios found during the 1981 bloom may have been the result of this mixing analogous to the effect the 6 May 80 storm had on particulate C/N (Figures 41 and 40 a).

Investigators using laboratory chemostats have developed a model for phytoplankton growth based on the cell content of various important nutrients (Caperon and Meyer, 1972; Droop, 1974). In an attempt to couple growth and nutrient uptake Dugdale (1977) suggests that: $V_{max} = \rho m/Q$, where V_{max} here is a nutrient specific maximum uptake rate (hr^{-1}), ρm is the maximum transport rate ($pg\ at\ cell^{-1}$) and Q is the cell quota for the nutrient in question ($pg\ at\ cell^{-1}$). If ρm is assumed constant, V_{max} should vary inversely with the cell quota.

To explore the applicability of the internal pool model to the field data collected here the N/C compositional ratio was used as an indicator of

the cells internal nitrogen pool (Figure 50). The inverse relationship holds fairly well with the exception of 10 May 80 and 17 May 79, both of which are stations taken during a storm event. This supports the earlier suggestion that the uptake rates and compositional ratios are not in steady state due to the varying mixing conditions.

When the water column respiration parameter (Zm:Zcr) is combined with the N/C ratio, however, the spread of the data points for all the prebloom stations is reduced markedly (Figure 51). In this form, the model greatly resembles the relationship shown by Dugdale (1977) between Q and V_{max} from the chemostat data of Eppley and Renger (1974). During bloom development in the southeast Bering Sea, the largest $V_{max(NO_3^-)}$ were consistently observed in communities with low N/C particulate ratios and in water columns in which they experienced low respirational loss. This suggests that the N/C compositional ratio and the immediate respirational history from the field data define a parameter analogous to the cell quota during bloom development and in turn V_{max} NO_3^-.

Growth rates in nutrient limited chemostat culture work have consistently been shown to increase with increasing cell quota. Laws and Bannister (1980), however, present laboratory data which show that the N/C ratio of Thalassiosira in continuous culture decreases with increasing growth rate under light limited conditions. These results may be analogous to the observed depression of N/C ratio brought about by the large respirational losses on 6 May 1980 (Figure 40 a). Apparently, the basic priority under poor light conditions is to maintain optimal growth rates. Decreasing the cell quota for nitrogen allows the cells to maintain division rates without draining limited energy supplies for nitrogen assimilation.

Figure 50.

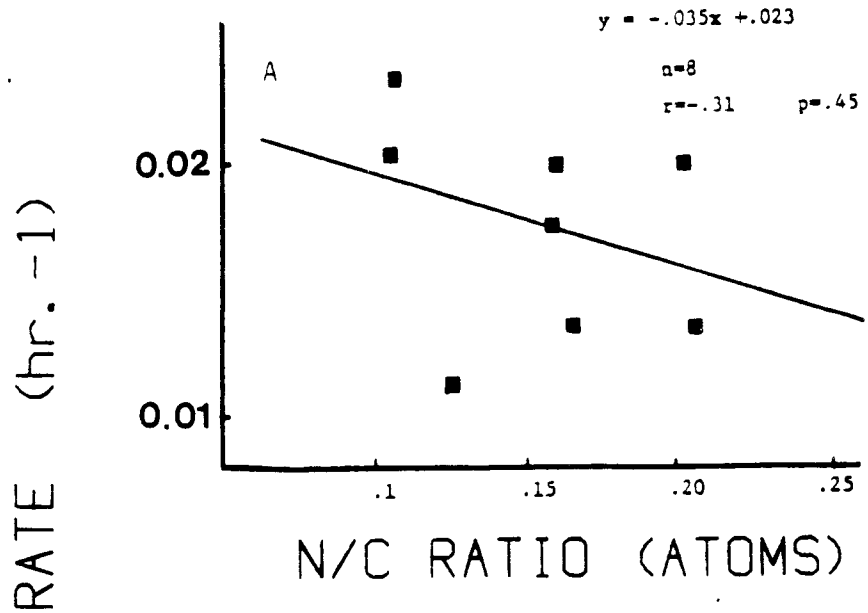

Figure 51.

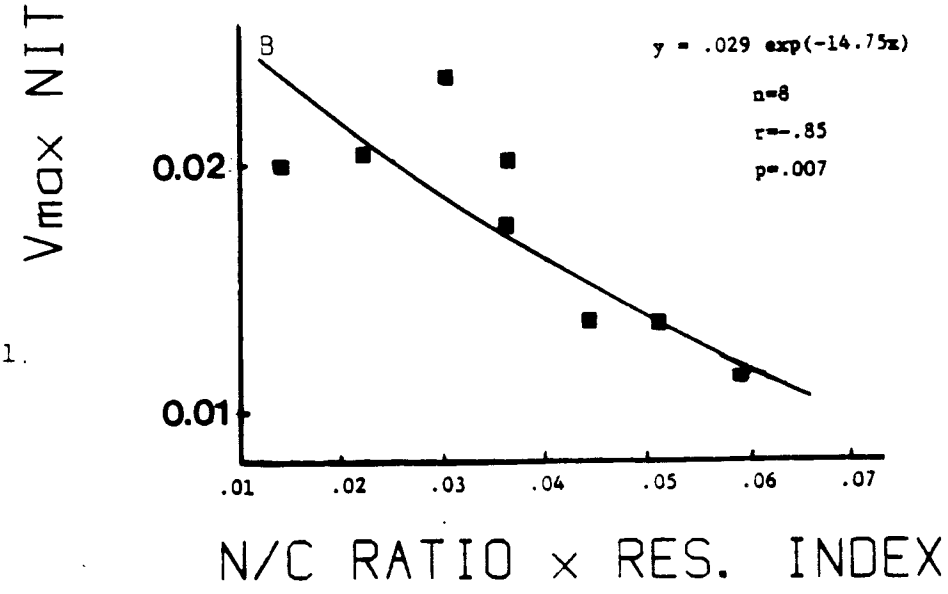

Figure 50.

Relationship between $V_{max(NO_3^-)}$ and the nitrogen to carbon compositional ratio of the particulate matter.

Figure 51.

Relationship between $V_{max(NO_3^-)}$ and a parameter composed of both internal and external influences on phytoplankton nitrogen uptake rates.

Cell composition would be expected to lag behind uptake ratios. Specific uptake rates are presumably under "real time" cellular regulation while cell composition integrates the assimilative rates of the last several doubling times. The 1980 bloom, then, is a good illustration of the non-steady state character of the spring bloom system since dynamic cellular rate processes responded quickly to changed mixing conditions, while the more static compositional properties had longer response times.

4.3.2 A Model of Nitrate Productivity Based on Changes in Specific Uptake Rates

These results are the first to quantify a relationship between the historical aspect of water column mixing, cell composition, and NO_3^- uptake. Specifically, it is suggested that during the early bloom period the diatoms net photosynthate controls V_{max} NO_3^- and carbon specific uptake rates. The V_{max} model can then be used, along with a suitable estimate of standing stock, to estimate rates of spring bloom new productivity.

Since light history data is less commonly available, a model of areal NO_3^- uptake was constructed using simply the C/N compositional ratios as an indicator of NO_3^- specific uptake rates. As a measure of standing crop, the integrated NO_3^- content of the 0.1% euphotic zone was used. The model of areal NO_3^- uptake based on these parameters is shown in Figure 52.

The depth of the euphotic zone is related to upper water column standing crop (due to the influence of the particulate material on the extinction coefficient - Lorenzen, 1976). The integrated NO_3^- content of the euphotic zone exhibits a minimum during peak bloom conditions and

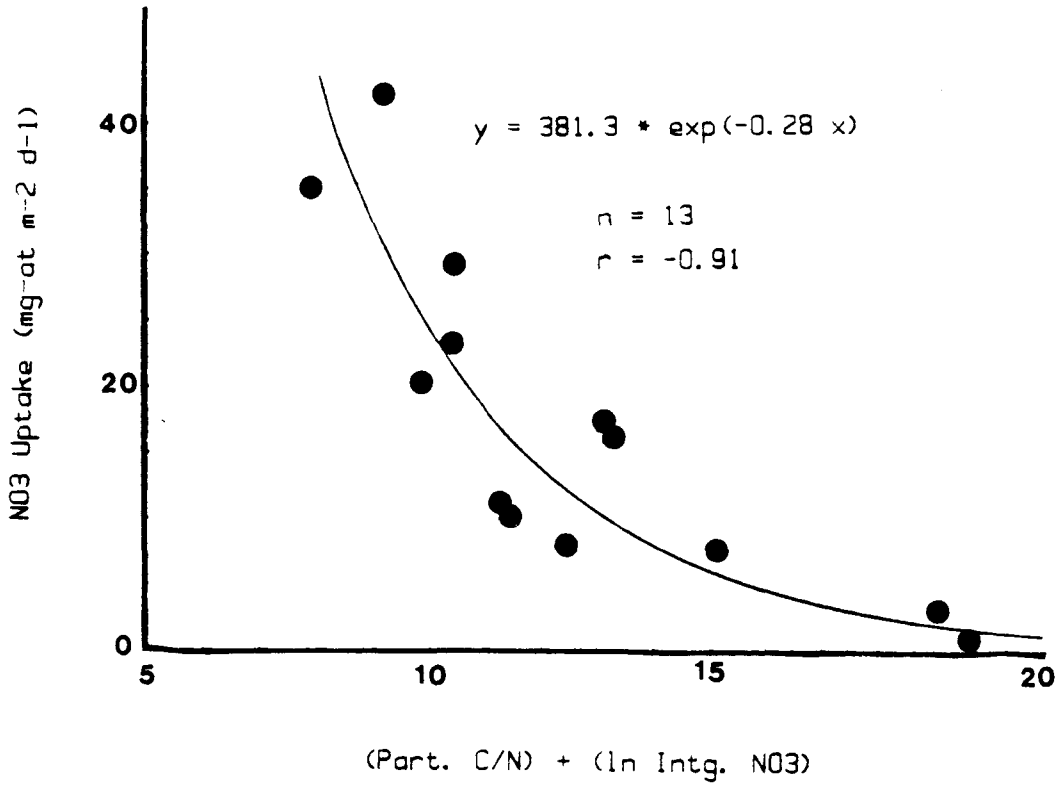

Figure 52.

A simple regression model for areal nitrate uptake.

increases in either pre- or post bloom water columns. These temporal changes are similar to the observed changes in C/N ratio. Although plant growth removed NO_3^- from the post bloom mixed layer, the sinking of most of the diatoms out of the euphotic zone decreased the PAR extinction coefficient and deepened the euphotic zone to include NO_3^- rich water.

The areal uptake rates were standardized to 4°C using Eppley's (1972) temperature growth relationship. The model in Figure 52 is also accurate for the post bloom 1980 stations. Only the late May 1981 stations and others which exhibit pronounced sub-mixed layer Chl *a* maxima fall significantly off this line. The late May 1980 stations do not have sub-mixed layer Chl *a* maxima and due to their high particulate C/N ratios fall on the same line as the pre- and peak bloom stations.

The areal rates of new productivity, like the growth rate, are correlated with the N/C ratio and coincide with the presence of the maximum standing crops in the mixed layer. The relatively high N/C ratios during the peak bloom stations do not promote the highest V_{max} although this is compensated for by the greatly increased biomass present and perhaps reduced light dependence of NO_3^- uptake.

There were differences in early May mixed layer temperatures in that 1979 was relatively warm (mixed layer temperatures of 3-5°C) and 1980 was cooler (temperatures - 1.5°C). Degens (1970) reports a positive relationship between phytoplankton protein content and temperature, and these two years follow this trend, although in 1981 water temperatures were again warm and the N/C composition of the main bloom was the lowest of the three years.

Most of the spring bloom biomass is associated with relative lows in the C/N ratios in each year (Figures 39 -41 a) as well as peaks in rates of areal new productivity. It follows that the main pulse of spring bloom diatoms sinking out of the surface waters over the middle shelf carry with them a relatively low (< 8) C/N signature. Walsh et al. (1981), have suggested that the C/N content of coastal sediments can be used as indicators of the historical new production regime of the overlying shelf waters, and the present data suggest the initial steps in such a proposed sequence certainly take place. Further information on the fate of this sinking material after it leaves the upper water column is necessary to complete the evaluation, however.

In its present form the model is a first order equation of the type that describes diffusion from a finite reservoir. It is interesting that Sharp and Church (1981) in the middle Atlantic Coastal region show a mathematically similar relationship between the difference in nitrogen concentration between surface and bottom waters and the preformed nitrogen calculated from the estimated amount of nitrogen of oxidative origin. Their two plotted parameters are not independent, however since both the under estimate of the preformed nitrogen and the vertical difference in nitrogen concentration are dependent on the intensity of nitrogen uptake in the surface waters. However, the fact that a first order diffusion type equation describes this intensity supports the form of our model as presented here.

In most of the ocean, low mixed layer respirational losses prevail (i.e. Zm/Zcr<0.3). In lower latitude non-coastal waters with characteristic low extinction coefficients and high daily PAR inputs such a situation is not difficult to envision. For example Yentsch (1981)

estimates the critical depth in clear Sargasso Sea waters at 700 m. The model as presented here was applied to the extensive data set collected in the Weddell Sea (El Sayed and Taguchi, 1981). At the relatively productive Station 14 between 75 and 76 degrees south our model predicts a temperature corrected NO_3^- uptake of 5.6 mg-at m^{-3} day^{-1} and for their lower productivity Station 4, 2.6 mg-at m^{-3} day^{-1}. Although there is little data on maximum growth rates at the Weddell Sea temperatures (below 0^oC) these estimates of NO_3^- uptake appear reasonable.

4.3.3 The Dependence of Vertical Kinetic Structure on Previous Mixed Layer Bloom Development

The deeper light depths consistently exhibited a lower light half saturation value than the upper water when these layers were dominated by the peak bloom diatoms. Such conditions can be attributed to light - shade adaptation, although this adaptation began while the cells were still in the mixed layer as mixing rates decreased (Figure 26). The $K_{s(NO_3^-)}$ values of the deeper postbloom light depth communities are similar to those of the prebloom mixed layer plants. For example, the 1% light depth $K_{s(NO_3^-)}$ value from Table 8 was three times that of the surface community and very similar to values recorded early in the 1979 and 1980 bloom (Figures 33 and 34). Apparently the nitrate uptake mechanisms of the early bloom diatoms do not show the same adaptability to low nitrate levels as they do to changing light, which may be a factor hastening their sinking from the mixed layer.

This lack of adaptability in $K_{s(NO_3^-)}$ was illustrated by the results of an on deck hold over experiment on water collected from the deeply mixed,

nitrate enriched station of 10 May 1980 (Table 9). During this three day holdover, K_s did not change significantly, although V_{max} increased. The V_{max} increase observed in this experiment was similar to the results from the 1980 $V_{max(NO_3^-)}$ time series when the wind mixing abated after 10 May (Figure 32 a) Apparently the holdovers simulated the effects of decreased mixing since the samples were held at an essentially constant and favorable light depth. The vertical structure observed in the rate parameters of post bloom stations, therefore, resulted from the interaction of diatom sinking with the bio-physical developmental changes taking place in the mixed layer. A similar interaction has been observed in the photoinhibition parameter of Chl a layers (Gallegos et al., 1983).

Table 9.

Changes in V_{max} and $K_{s(NO_3^-)}$ during 72 hour holdover experiment.

Holdover time	$V_{max(NO_3^-)}$ (hr^{-1})	$K_{s(NO_3^-)}$ ($\mu g\text{-at } l^{-1}$)
24 hr.	0.0109 ($\pm$0.0006)	1.30 ($\pm$0.30)
48 hr.	0.0136 ($\pm$0.0008)	1.34 ($\pm$0.30)
72 hr.	0.0156 ($\pm$0.0003)	1.02 ($\pm$0.08)

Chapter 5

Factors Influencing the Relative Utilization of Nitrate and Ammonium

5.1 Introduction

The relative utilization of nitrate and ammonium (commonly called the f factor) has been recognized as an important factor in marine trophodynamics (Dugdale and Goering, 1967). A commonly used index of nitrogen utilization patterns is the percentage of total production which is "new" (i.e. fueled by nitrate uptake). This index has been called the f factor (Eppley and Peterson, 1979) and in this study was defined as:

$$\frac{\rho\ NO_3^-}{\rho\ NO_3^- + \rho\ NH_4^+} \qquad (23)$$

Recently, this factor has been used to analyze carbon loss from surface waters (Eppley and Peterson, 1979; Eppley et al., 1983). This ratio is also indicative of the relative amount of nitrate reduction occurring

in association with primary productivity in various ocean areas.

Two approaches were taken to examine the influences on the forms of nitrogen utilized by the phytoplankton. Rate measurements were analyzed in the context of the bloom developmental cycle and its associated bio - physical changes. Also, an experimental approach to evaluate the effect of grazing on patterns of nitrogen utilization was carried out.

In seasonally productive waters such as the Bering Sea, ambient NH_4^+ concentrations rise in surface waters of certain areas following the onset of active phytoplankton growth. In the southeastern Bering Sea this NH_4^+ increase occurs predominantly in the outer shelf region and is associated with a relatively large concentration of ontogenetically migrating oceanic zooplankton. The grazing activity of macrozooplankton results in a reduction of total cell volume and, at times, the excretory products supplied by this activity can be an important source of nitrogen for algal growth (Eppley et al. 1973).

Several investigators have measured nitrogen excretion by various species of zooplankton In general, excretion rates vary with temperature, density of food particles, and are inversely related to the size of the animal. Few studies have addressed the interaction between ammonium excretion and its uptake by phytoplankton. In one of the few papers addressing this subject, Takahashi and Ikeda (1975) concluded that actual excretion rates may be underestimated due to the uptake of ammonium by phytoplankton when excretion measurements are made in unfiltered seawater. The present experiment considers this interaction more closely using a ^{15}N tracer technique.

5.2 Results

5.2.1 Middle Shelf f factor Changes

The proportion of total inorganic nitrogen (TIN) uptake due to nitrate is shown in Figure 53 for the three bloom periods at the middle shelf reference station 12. The connected circles represent the values derived from integration of the entire 0.1% euphotic zone. These f factors were always lower than those derived only from the uptake measurements in the upper light depths (100 - 15%; triangles in Figure 53) since ammonium uptake has been shown to be less light dependent than nitrate uptake and does not decrease as drastically as nitrate uptake in the lower light depths (Nelson and Conway, 1979). The whole euphotic zone f factors averaged 17% less than the respective light saturated values (S.D. = 11%, n = 17).

The greater light dependence of nitrate uptake relative to ammonium is even more apparent in the f factors from the sub - mixed layer euphotic strata, when these were encountered (+ symbols in Figure 53). Because of this differential light dependence the plant communities in such strata rely predominantly on ammonium even though nitrate is usually abundant at these depths. The effects of post bloom wind mixing is of interest, although only two events were sampled (16 May 1979 and 6 - 10 May 1980 in Figure 53). The effects of the 16 May storm have been discussed previously but are significant again in this context because the resuspended diatoms retained high nitrate uptake rates. These high rates of nitrate uptake were

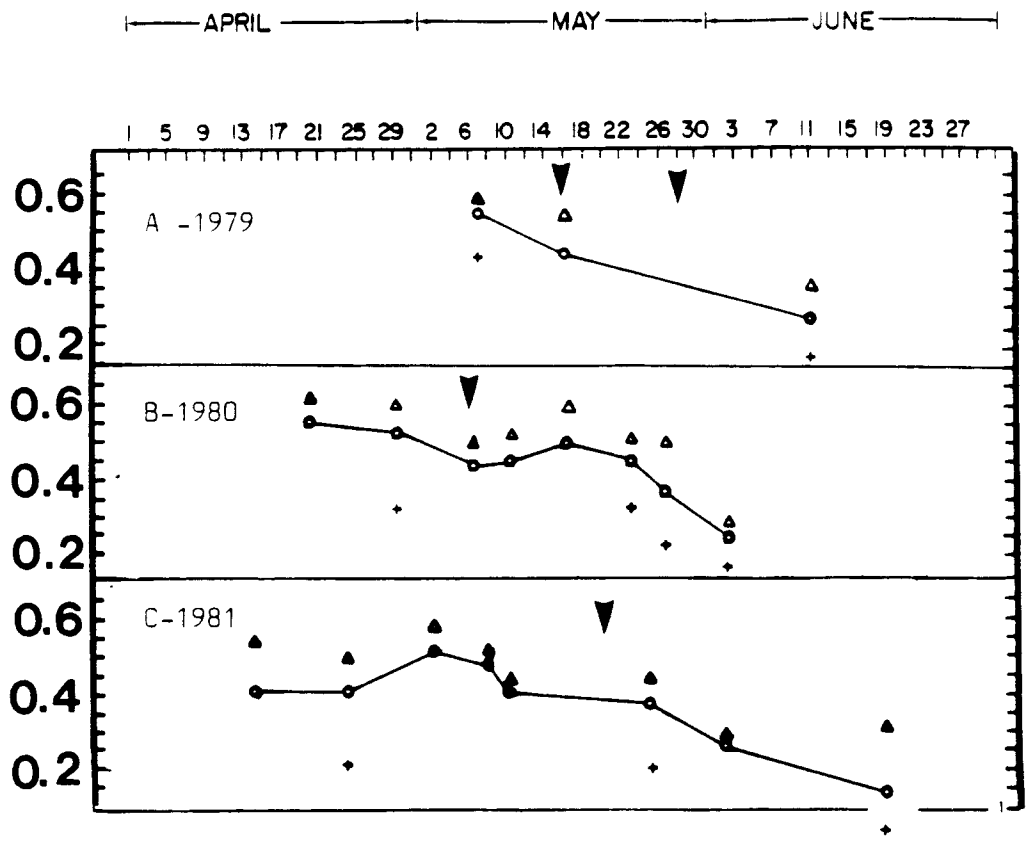

Figure 53.

Changes in the f factor with time during A) 1979, B) 1980, and C) 1981.

maintained despite the probable history of ammonium uptake in the deep euphotic zone Chl a layer (Figure 37) and the relatively high ammonium concentrations in the mixed layer at the beginning of the storm (ca. 1 mg-at m^{-3}, Figure 22).

Peak bloom periods were associated with the largest f factors and follow the observed dependence of nitrate uptake on upper water stability during the early bloom periods. In all three years the f factor decreases significantly after peak bloom periods and the nitrogen demands of the early June communities are met mainly by regenerated nitrogen. On 3 June 1981 a urea uptake profile was obtained and indicated that urea uptake was equal to that of the diminished nitrate uptake at this time (Figure 53 c). If this urea uptake is included in the denominator of equation 23, the f factor decreases by approximately 25% from the value calculated considering ammonium uptake alone. This is similar to the effect of urea uptake on nitrogen utilization patterns in summer stations in the California Bight (McCarthy, 1972). Unfortunately, no urea uptake data are available earlier in any of the blooms to evaluate the importance of urea as a nitrogen source in pre- or peakbloom periods.

5.2.2 Outer Shelf f factor Changes

The cross shelf time - space f factor patterns indicate that the f factor is much more patchy in the heavily grazed outer shelf than on the middle (Figure 54). In the middle shelf a smooth transition from high to low f factors parallels the decreasing isopleths for mixed layer nitrate concentration (Figure 55). In the outer shelf (stations 1 - 8), the f factors consistently decreased independently of the nitrate concentrations. Such nitrate independence was especially clear in the early June 1979 and 1980 outer shelf stations, in which the f factor isopleths are perpendicular to those for nitrate concentration (Figures 54 and 55).

5.2.3 Grazing Experiments

The experimental approach involved collecting high Chl a, low ammonium peak bloom middle shelf water and exposing it to net collected outer shelf zooplankton. The collected middle shelf diatom assemblage was dominated by *Chaetoceros spp.* (largely *C. debilis*), but included significant numbers of *Rhizosolenia*, *Thalassiosira*, and *Corethron spp.*. Before the experiment began, Guillard's nutrient media (f/50, Stein, 1973), which contained ammonium as the nitrogen source, was added to all carboys except the one destined for an ammonium kinetic experiment (which received the media minus any nitrogen source). The kinetic experiment indicated that the original

A. - 1979

B. - 1980

C. - 1981

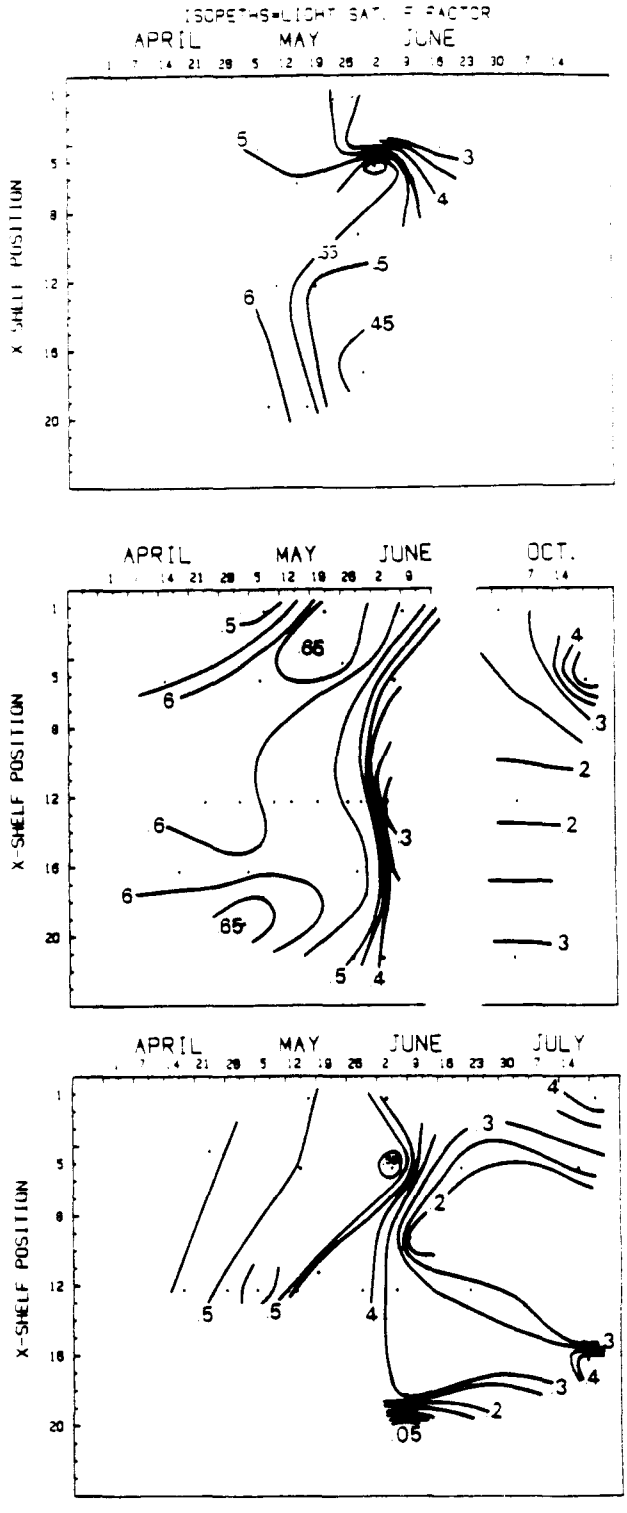

Figure 54.

Time - space changes in the f factor during A) 1979, B) 1980, and C) 1981.

A. - 1979

B. - 1980

C. - 1981

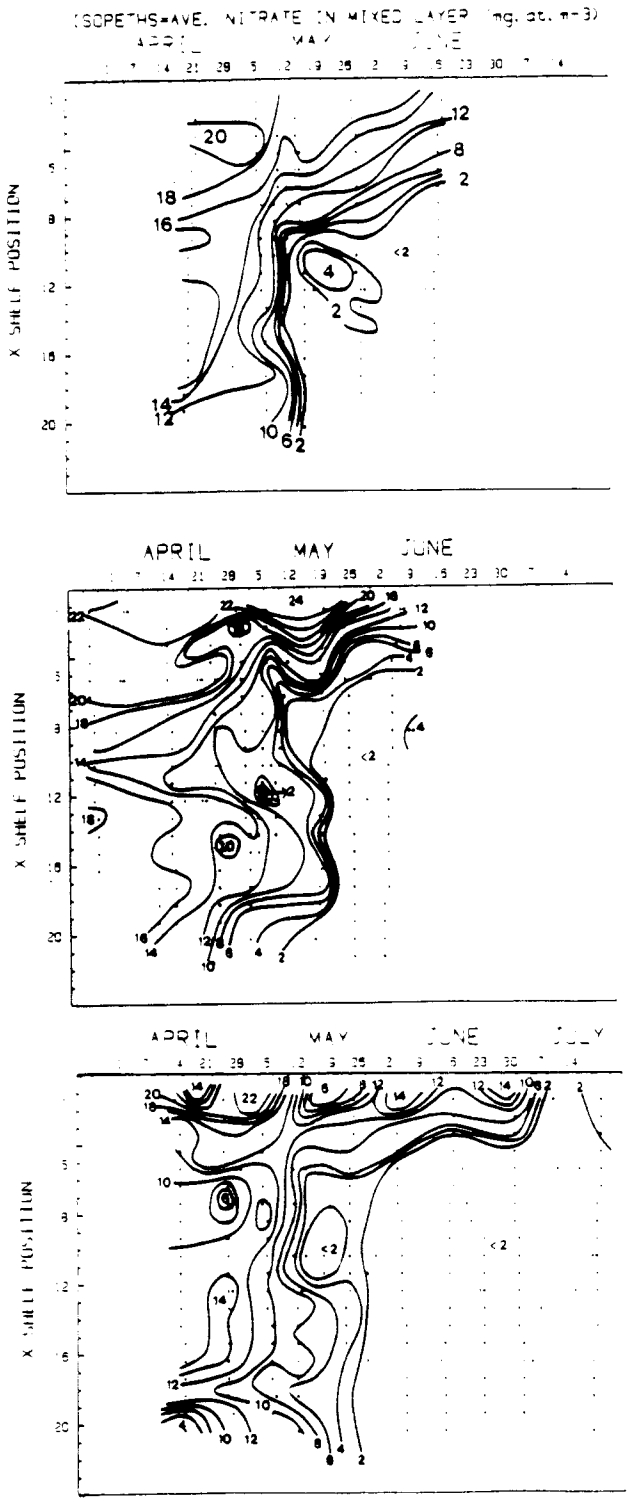

Figure 55.

Time - space changes in mixed layer nitrate during A) 1979, B) 1980, and C) 1981.

middle shelf community had a $K_{s(NH_4^+)}$ of 0.37 μg-at l^{-1} and a $V_{max(NH_4^+)}$ of 0.0143 $hr.^{-1}$.

Macrozooplankton were collected at an outer shelf station in an area of high secondary production. Ambient ammonium was high (ca. 2 μg-at ammonium) and Chl a low (ca. 2 mg m^{-3}) relative to the middle shelf station where the diatom community was obtained. Animals which appeared healthy were sorted from the catch, and varying numbers of them were added to three of the 20 l carboys containing diatoms. These containers will be referred to by the number of macrozooplankton added to each. Table 10 details the zooplankton composition of the experimental containers after the addition of the animals.

Metridia pacifica and NeoCalanus plumchrus were the most prevalent oceanic grazers added. Oithona similis and Pseudocalanus sp. were present initially in the water collected from Station 3097. Mortality of the added macrozooplankton was negligible during the course of the experiment. A fourth container with its original zooplankton population served as a control. After addition of animals all four containers were kept in constant motion in a rotating rack in a deck incubator cooled with running surface seawater and exposed to natural light approximately 30-50% of that incident on the sea surface.

The nutrient concentrations, particle volume, and Chl a in each of the experimental containers were similar preceding addition of macrozooplankton (Figures 56 and 57). After addition of nutrients and macrozooplankton from Station 3105, differences among the experimental treatments became apparent. The particle volume and Chl a in the 221 grazers/l container (Figure 57 a and b) exhibited the greatest decline during the three day period. In the

TABLE 10.

Macrozooplankton composition of experimental containers .

(animals / l).

	Control	11 Grazers/l	120 Grazers/l	221 Grazers/l
Neocalanus plumchrus	0	4	30	65
Metridia pacifica	0	7	90	156
Pseudocalanus sp	23	14	39	15
Oithona similis	7	4	6	3

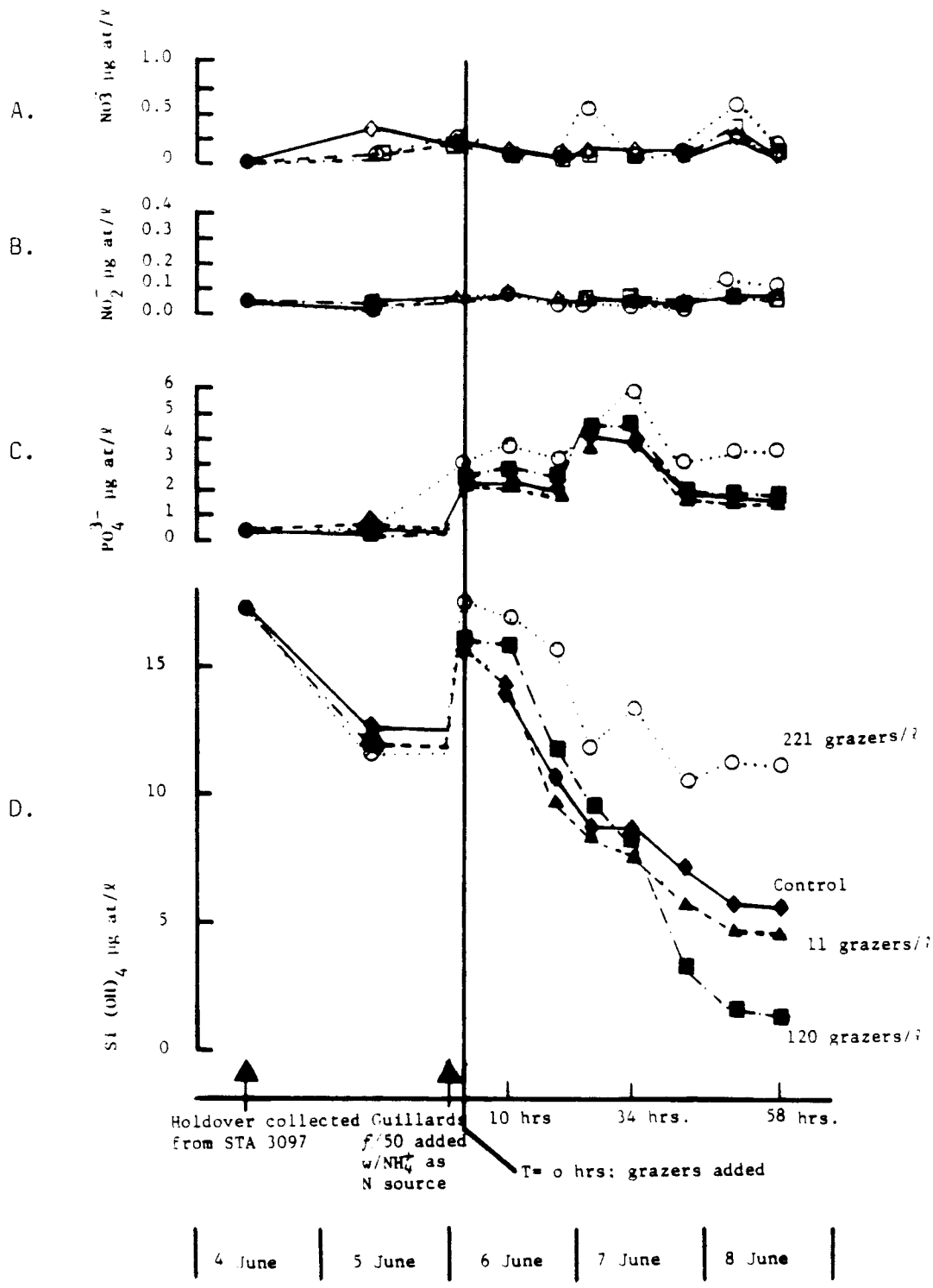

Figure 56.

Changes in nutrient concentrations with time in experimental containers for A) nitrate, B) nitrite, C) Phosphate, and D) Silicate.

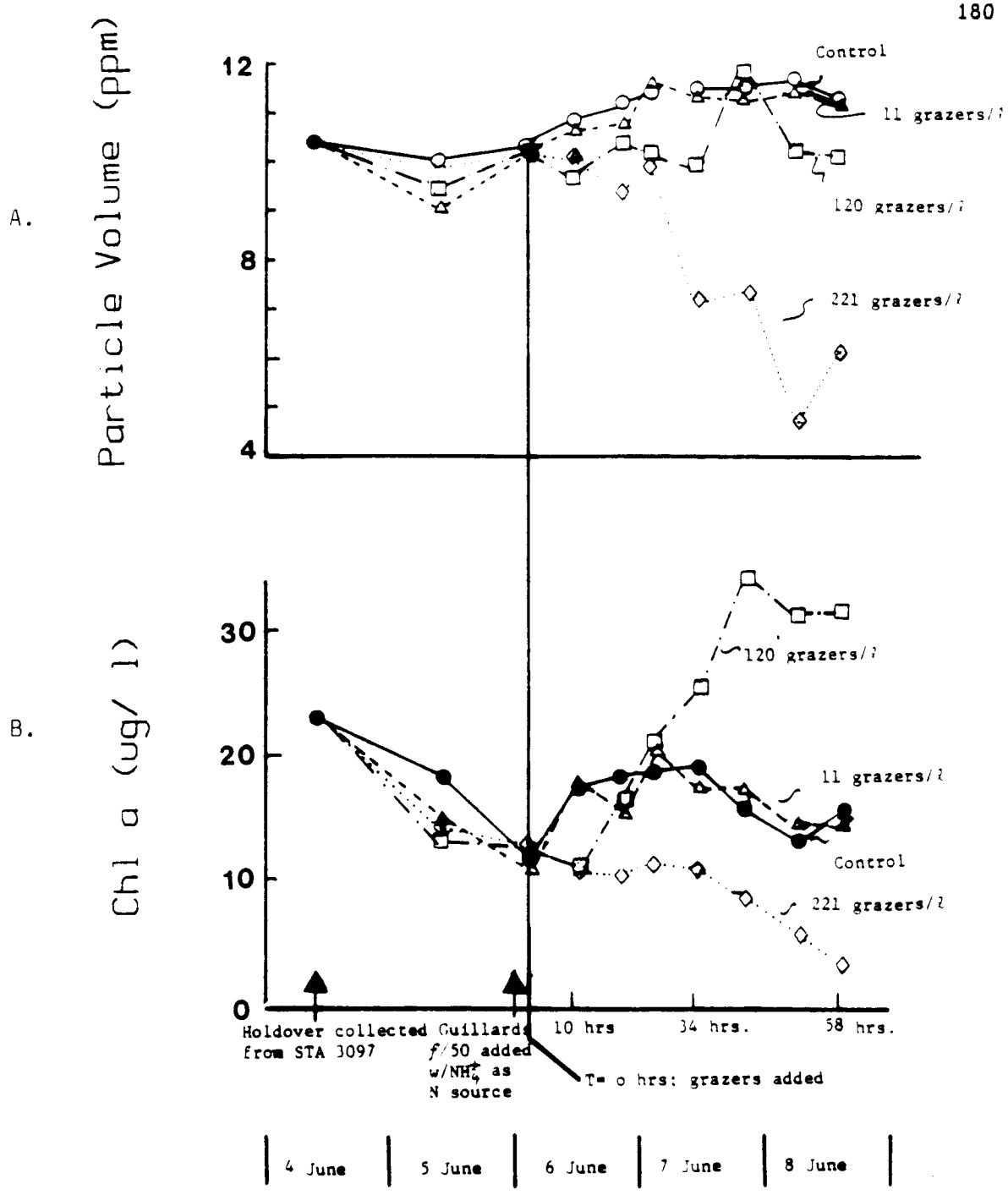

Figure 57.

Changes in A) particle volume and B) Chl a with time in experimental containers.

120 grazers/l container an initial decrease in particle volume occurred after which it remained nearly constant. Chl *a* levels in the 120 grazers/l container ultimately exhibited the highest value measured during the course of the experiment. The Chl *a* rise in this container corresponded to a peak in particle volume as well as to a sharp decline in ambient $Si(OH)_4$ concentrations (Figures 57 a and b, and 56 d).

The 11 grazers/l container displayed the least detectable change in nutrients, particle volume and Chl *a* relative to the control among the group, although there were slight changes in particle volume and $Si(OH)_4$ concentrations over time as compared to the experimental control. All three containers to which macrozooplankton were added displayed an initial increase in $Si(OH)_4$ above the control. In the 11 grazers/l container $Si(OH)_4$ by 20 hours had declined below the control; in the 120 grazers/l container it declined after the rapid rise in Chl *a*; and in the 221 grazers/l container it consistently remained at concentrations greater than those in the control. The ambient $Si(OH)_4$ concentration in the control, after an initial rise due to the nutrient addition, declined at a rate similar to the depletion rate it displayed before the macrozooplankton were added.

Changes in ammonium concentration associated with the numbers of added macrozooplankton are shown in Figure 58. Large increases in ammonium concentration above that added with Guillard's medium (ca. 2 μg-at NH_4^+ /l) were displayed in the 120 and 221 grazers/l containers. No increase in ammonium levels in the 11 grazers/l treatment relative to the control were observed. In fact, the concentrations may be lower than those in the control. After two days the 120 grazers/l container displayed

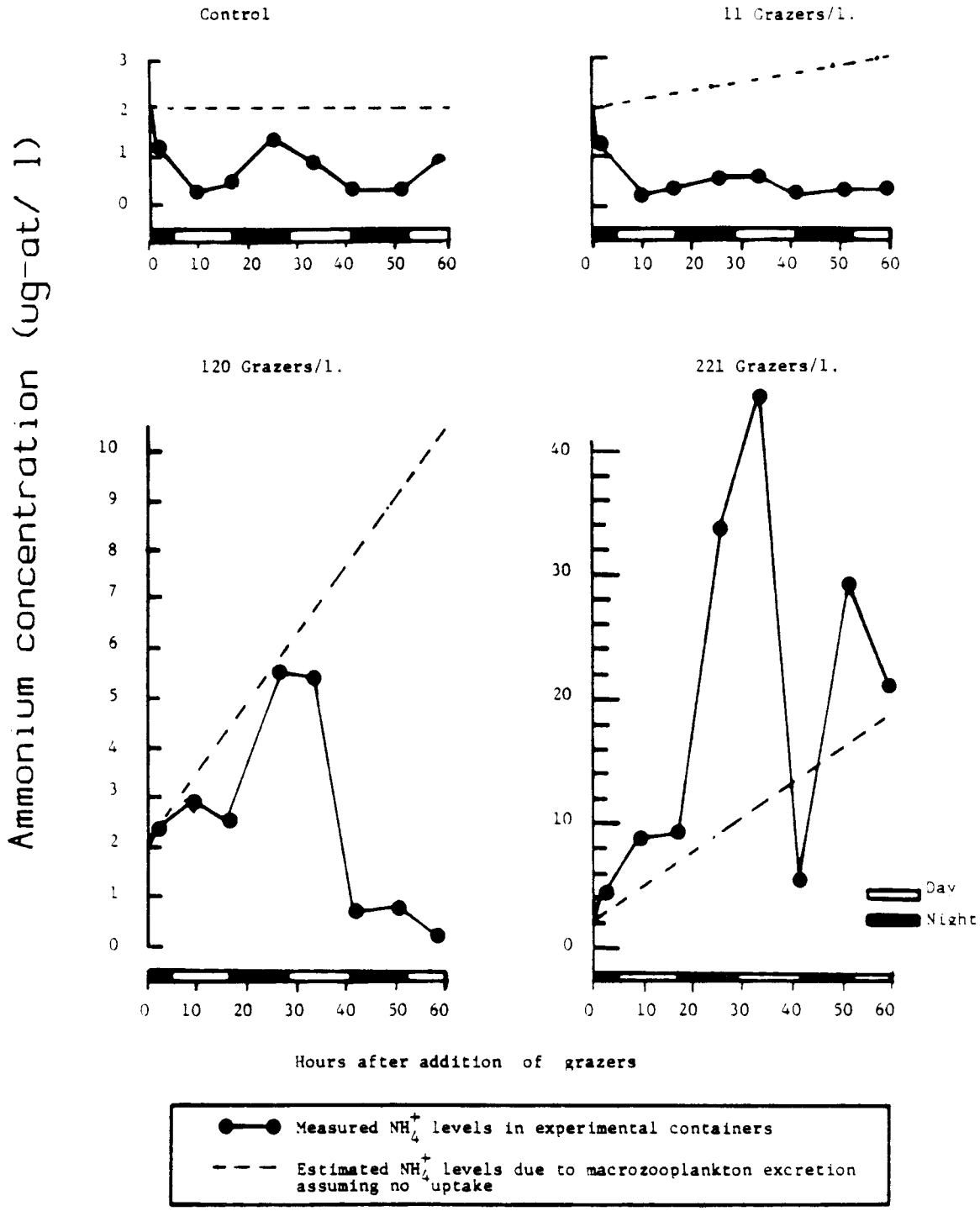

Figure 58.

Changes in NH_4^+ concentrations with time in the four experimental containers.

ammonium concentrations similar to those in the control and an increase in Chl *a* and particle volume. At 30 hours the ammonium concentrations in the 221 grazers/l container reached a maximum and then began to decline, although they never reached the low levels of those in the other experimental containers.

Phosphate also displayed a consistent pattern in the experimental containers (Figure 56 c). Phosphate concentrations were consistently higher in the 221 grazers/l container than in the less grazed containers. Apparently under heavily grazed conditions, phytoplankton have a continual supply of $Si(OH)_4$ and PO_3^{3-} as well as NH_4^+ made available to them.

5.3 Discussion

5.3.1 Species Succession and the Changing f factors During the Bloom

Several different approaches were taken in an attempt to build a predictive model for the proportion of new productivity to total nitrogen productivity in the middle shelf area. A graph of f factors on average mixed layer nitrate, for example, resembles a rectangular hyperbola with an asymptote of approximately 0.5 above nitrate concentrations of 3 μg-at l^{-1}. There is little resolution among the low f factors however, and an estimate of the initial slope by such a method is not possible. This situation is greatly improved when both the average particulate nitrogen and nitrate concentrations of the mixed layer are considered together as the

independent variable (Figure 59 a and b).

Early in the bloom sequence the particulate nitrogen (PN) pool increases compensate for the declining ambient nitrate pool and the f factor remains high ()0.5). It is not until the exhaustion of nitrate from the mixed layer and the consequent settling of the pioneer diatoms from the mixed layer that the total (PN + nitrate) index falls appreciably and with it the measured f factors. The exponents found for the relationships shown in Figure 59 are probably applicable to lightly grazed spring bloom development in general. The constant, however, would vary among oceanic regimes and depends on the nitrate levels available in the "end of winter" (i.e. pre - biological uptake) water column.

The success of this model suggests the f factor is closely associated with successional dynamics during the spring bloom. The species composition of the mixed layer changed dramatically after the exhaustion of nitrate. This change was brought about mainly by the loss of the early bloom, pioneer diatoms from the water column. Apparently the high utilization rate of nitrate is an attribute of these particular species. This explains the precipitous decline in f factors after the peakbloom community sinks from the surface layer.

Laboratory studies suggest ammonium assimilation inhibits nitrate uptake, (Cresswell and Syrett, 1979) and it has been suggested that such a mechanism occurs in marine environments (Glibert, et al., 1982). The peak bloom diatom community examined here however, appears to be rather insensitive to such inhibition over the time period studied. The poor water column respirational conditions surrounding the 6 - 10 May 1980 storm were associated with a lowered f factor (Figure 53 b). In this instance the

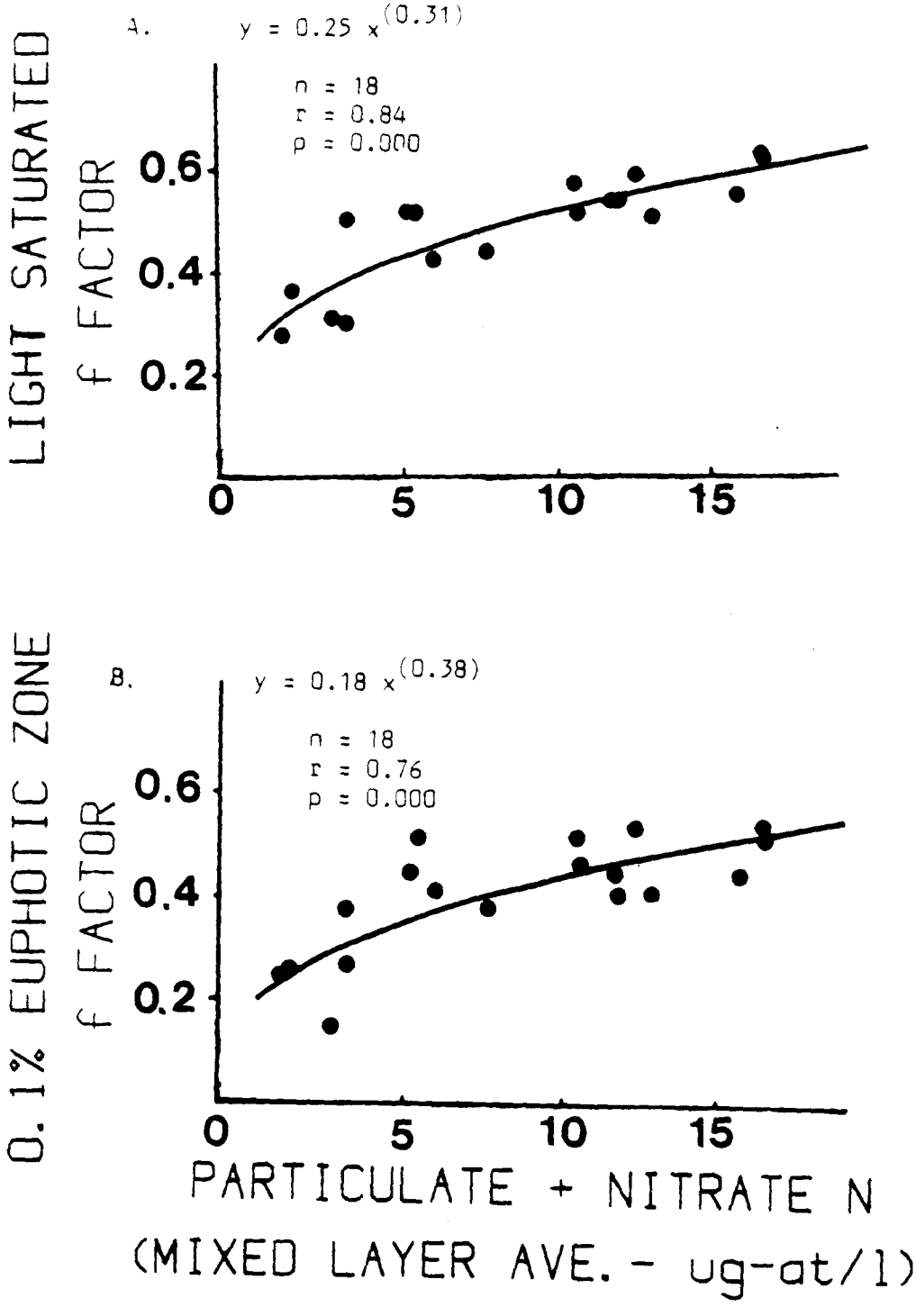

Figure 59.

Relationship between A) light saturated (>15% light depth) f factors and B) integrated 0.1% euphotic zone f factors and the particulate + nitrate nitrogen in the mixed layer of the middle shelf.

sensitivity of nitrate uptake to respirational losses is most likely mainly responsible for the decline.

The f factor is relatively high during the deeply mixed prebloom period in April of 1980. Chl a doubling rates, however, during this period (Table 3) are far below that predicted by the model of Sharp et al., (1980), in which: [μ (day^{-1}) = 0.97(F) + 0.11]. This model does yield realistic results for peak and post bloom stations, however. The large respirational losses of the prebloom period may be responsible for the less than predicted growth rates in April, 1980. Growth rates at this time, in fact, were less than predicted from ^{14}C measurements also. For example, based on ^{14}C uptake rates and particulate carbon data, doubling rates can be estimated by assuming cell carbon quotas are constant and the relationship $\mu = V / \ln 2$ is valid. Based on these calculations the estimated doubling rates should be approximately 0.7 day^{-1}. Observed Chl a doubling rates during this period, however were only 0.16 day^{-1}).

The f factors based only on the 100 - 15% light depths (the light saturated f factors; Figure 53 - open triangles) yielded a better fit than those based on integrated nitrogen uptake in the whole euphotic zone (Figure 53 - open circles). The greater spread in the euphotic zone figure is largely due to the variable presence of sub - mixed layer Chl a maxima in the lower euphotic zone. Such layers can influence euphotic zone nitrogen utilization patterns.

A useful comparison to the present data can be made from recent nitrogen uptake measurements reported from similar latitudes in the Antarctic Scotia Sea (Olson, 1980). The austral station dates correspond to late March - early April in the southeast Bering Sea although most of the

Antarctic stations are at the shelf break or deeper. The reported nitrogen uptake rates are similar to those measured in the present study in mid April 1981. Also similarities exist in the high ambient nitrate levels, deep euphotic zones, and April f factors.

On the Bering Sea middle shelf, however, no correlation of f factor with mixed layer ammonium concentrations could be discerned as in the Antarctic stations. In fact mixed layer ammonium concentrations are lower in the postbloom, low f factor stations ($\bar{x}$ = 0.39 μM NH_4^+), than they are in pre- and peakbloom stations where the f factor was relatively high ($\bar{x}$ = 0.62 μM NH_4^+), (Figure 60).

On the outer shelf, an examination of f factors reveals that the (PN + nitrate) model which worked well for the middle shelf stations, (Figure 59 a) explains much less of the variance in f factors in this more heavily grazed area (Figure 61). As in the middle shelf, however, the variation in f factors cannot be explained by mixed layer ammonium concentrations in the outer shelf (Figure 62). Instead, the hypothesis is made that the abrupt changes in the nitrogen utilization patterns observed in the outer shelf area were due to the filtering effects of large outer shelf grazers.

Such filtering would remove the pioneer spring bloom diatoms from the water and leave a community enriched in smaller plants with smaller effective cross sectional diameters. Electivity of this sort has been demonstrated in postbloom periods (Chervin, 1978). Also, an opportunistic feeding response by the large outer shelf grazers N. cristatus and N. plumchrus has been documented (Frost, et al., 1983). These relatively rapid feeding responses may be the cause of the temporal patchiness observed in the patterns of outer shelf nitrogen utilization. This line of reasoning

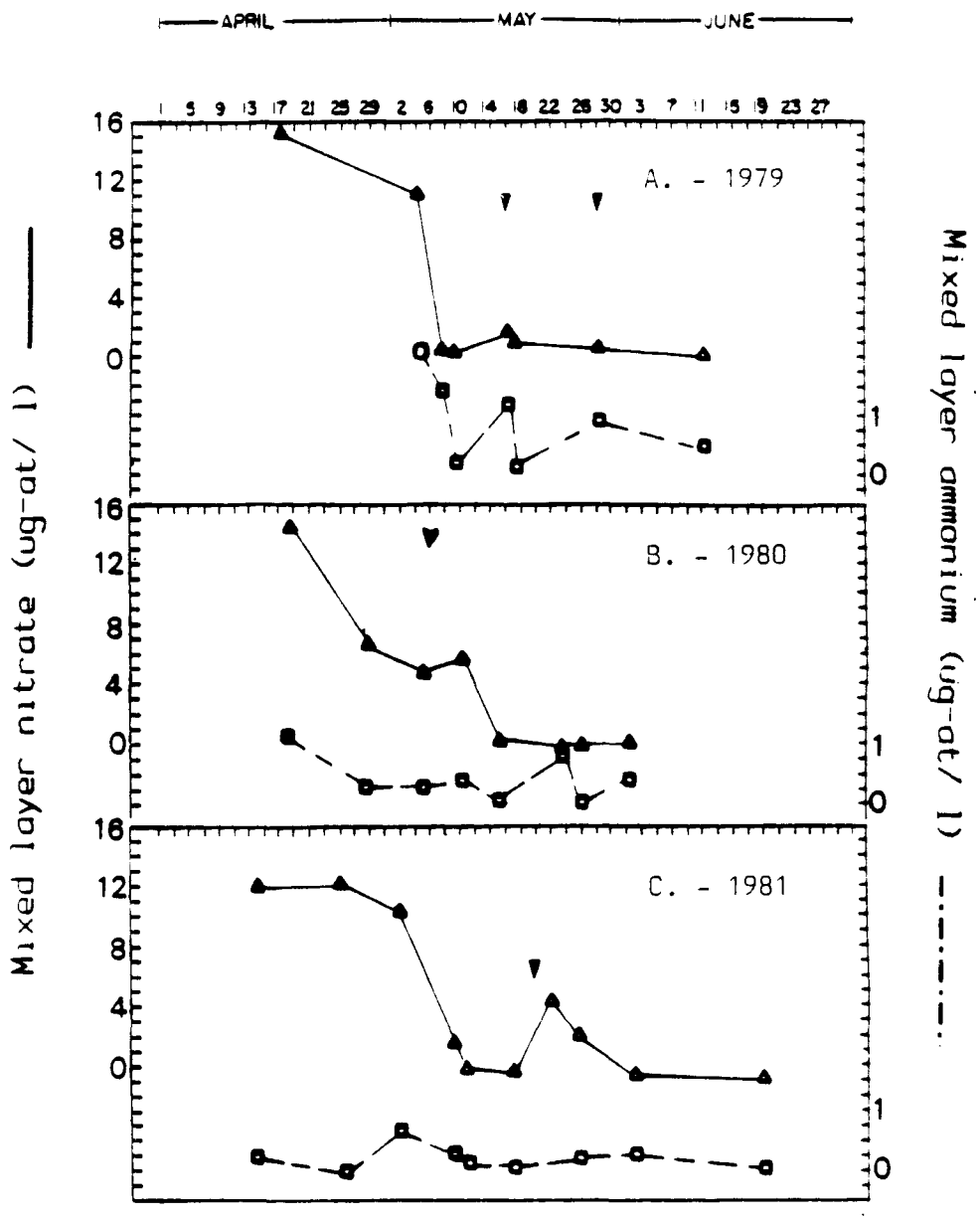

Figure 60.

Changes in mixed layer nitrate and ammonium with time during A) 1979, B) 1980, and C) 1981.

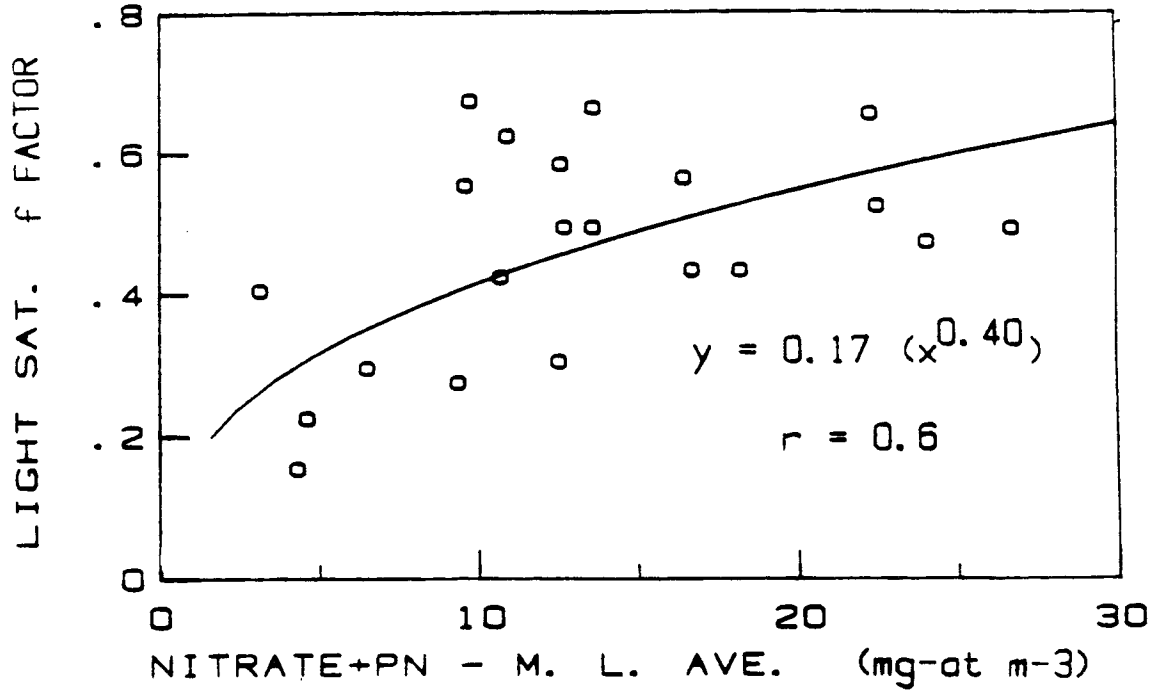

Figure 61.

Relationship between the outer shelf light saturated f factors and the particulate + nitrate nitrogen in the mixed layer.

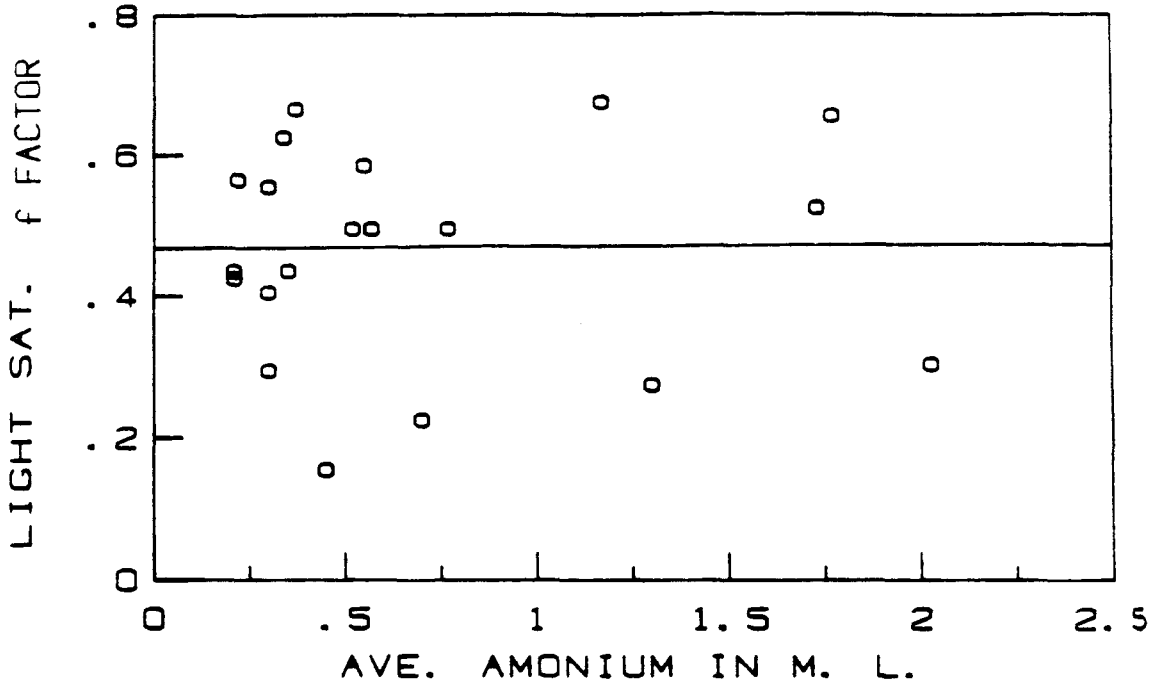

Figure 62.

Relationship between the outer shelf light saturated f factors and the ammonium concentration of the mixed layer.

suggests the post grazing residual nanoplankton community has a much lower dependence on nitrate as a nitrogen source.

Such a grazing induced species change may also be largely responsible for the reported f factor dependence on ambient ammonium concentrations. Ammonium concentration in this view only reflects the extent of destruction of the initial net plankton diatom community by grazing. Outer shelf grazing effects bring about a species change similar to that caused by lack of turbulence on the middle shelf. Importantly, however, this outer shelf species change is not necessarily associated with nitrate depletion as it is in the middle shelf.

5.3.2 Simulation of Outer Shelf f factor Changes in Experimental Containers

The specific uptake rate (V) is underestimated if the ammonium concentration increases during the incubation period and dilutes the added ^{15}N nitrogen source. Also, in the 20 l experimental containers, the problem of detrital build up increases with time as zooplankton fecal material and non-viable cells accumulate. This detrital material dilutes the living material which in turn causes V to be underestimated. However, the effect of detrital material cancels when absolute transport rates (ρ) of ammonium are computed (Figure 63).

The ρ values in the 120 grazers/l container during the first two days and in the 221 grazers/l container on the last day were clearly greater than those observed in the control. These absolute uptake rates, however,

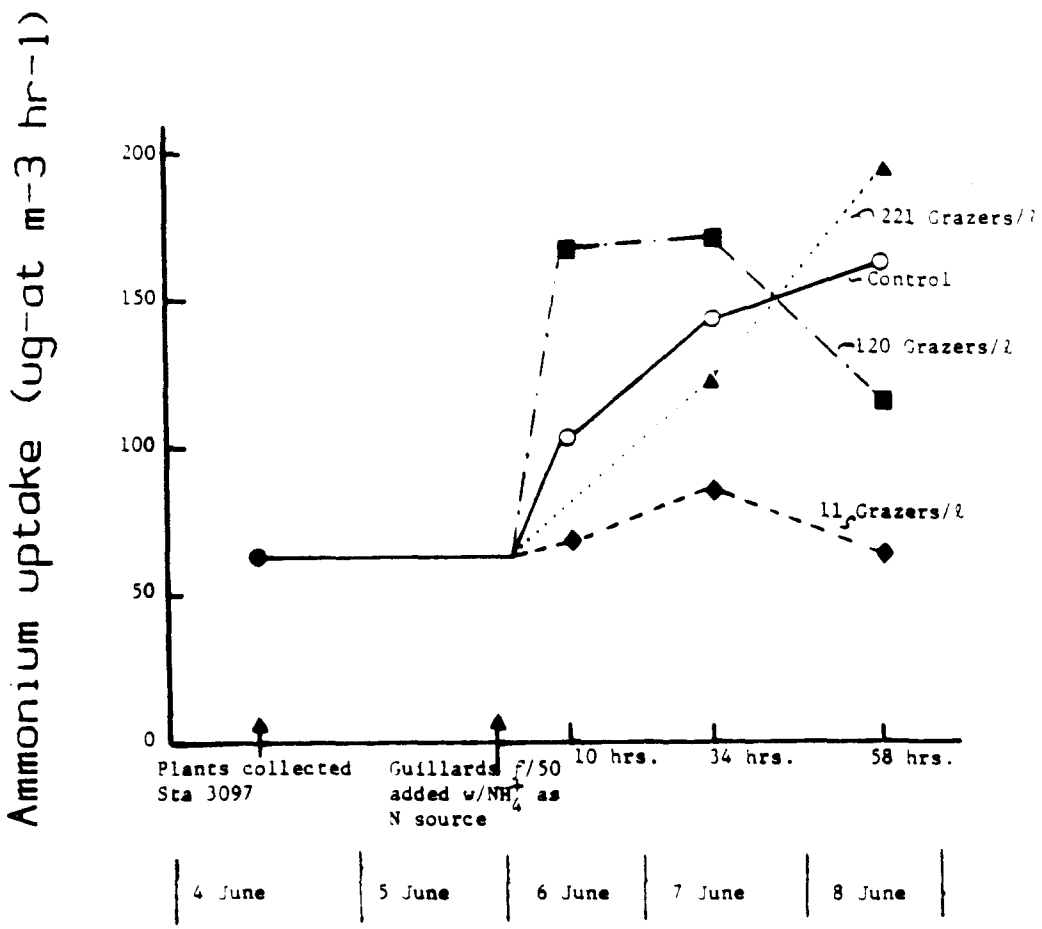

Figure 63.

Changes in ammonium transport rates with time in experimental containers.

are strongly influenced by ambient ammonium concentration since they have been calculated using an external pool model of nutrient uptake. Low ambient ammonium concentrations are reflected in the ρ values measured during the final day in the 120 grazers/l container and throughout the experiment in the 29 grazers/l container.

Apparently, the removal of many of the larger diatoms by grazing accounted for the observed decline in particle volume in the 16-32 μm size range (Table 11). The effect of the macrozooplankton in the two most populated containers was to graze down the initial diatom population. As expected, this grazing rate appeared proportional to the number of macrozooplankton present.

The gross ammonium regenerated in the experimental containers was estimated from previous measurements of macrozooplankton ammonium excretion (Corner and Newell, 1967; Szyper et al., 1976; Takahashi and Ikeda, 1975). Based on these literature values for the ammonium excretion of M. pacifica and N. plumchrus, at the temperature and Chl a levels in the experimental containers, ammonium concentrations were estimated assuming no nutrient uptake occurred (dashed lines in Figure 58). These values are conservative estimates of the total ammonium regeneration occurring in the containers since they do not include the contributions of the original zooplankton or micro- or nanoplankton. Due to their disproportionately large concentration, however, the added macrozooplankton would be expected to contribute most of the regenerated ammonium.

The diurnal pattern exhibited in the measured ammonium concentrations (Figure 58) probably resulted from increased excretion by the zooplankton at night and greater ammonium uptake during the day. The containers with the

TABLE 11.

Comparison among *Cheatoceros spp.* populations at the end of the grazing experiment.

	Control	11 Grazers/l	120 Grazers/l	221 Grazers/l
cells/l	35,870	37,830	17,600	200
Average # of cells / *Chaetoceros* chain	5.6	4.8	1.8	1.5

added macrozooplankton exhibited three different patterns. In the 11 grazers/l container the amount of estimated excreted ammonium was never reflected in the ambient ammonium levels. Apparently, the original diatom population was able to remove ammonium at a rate surpassing the regeneration rate in this container. On the contrary, in the 221 grazers/l container, ammonium removal by the phytoplankton never kept pace with the amount regenerated. The ambient levels here exceeded the concentrations predicted by the excretion estimates at several points although the final values are close to those predicted.

One estimate of the net ammonium uptake can be made from the difference between the estimated minimum amount of ammonium regenerated after 58 hours by excretion alone (in addition to the 2 μg-at NH_4^+ /l added initially) and the ambient ammonium concentrations measured at the end of the experiment. This estimate is compared to the values obtained from the integration of <u>in situ</u> ammonium uptake over the 58 hours of the experiment (Table 12). Both estimates predict the moderately grazed 120 grazers / l container had the highest ammonium utilization Apparently ammonium cycling between the plants and grazers was limited by excretion rates in the control and 11 grazers / l container. In the 221 grazers / l container, however, the destruction of plant biomass limited phytoplankton uptake. There exists therefore, some optimal level of grazing at which regenerated production is maximal.

Such grazing experiments can accurately reproduce several differences observed between the middle and outer shelf phytoplankton community. Importantly, grazing creates qualitative as well as quantitative changes during the removal of edible species. Models based on the inhibition of

Table 12.

Comparison of Two Methods of Estimating NH_4^+ Uptake in Experimental Containers Over 58-Hour Period.

	Uptake derived from gross excretion-ambient NH_4^+ concentration at T=58 hours (µg-at NH_4^+ ℓ^{-1})	Uptake derived from *in situ* transport rates integrated over 58 hours (µg-at NH_4^+ ℓ^{-1})
Control	1.2	7.35
11 grazers/ℓ	2.7	4.17
120 grazers/ℓ	10.0	8.49
221 grazers/ℓ	-3.0	6.78

nitrate uptake by ammonium uptake, while apparently accurate, (Olson, 1980), may over simplify the more complex interactions taking place between zooplankton and phytoplankton.

Chapter 6

Mass Balance Approach to Carbon Loss from Surface Waters Based on Nitrogen Productivity

6.1 Introduction

Since measurements of important parameters in the inorganic carbon system were made by the PROBES group in 1980 and 1981, a unique opportunity existed to compare the instantaneous rate measurements with a budget of inorganic carbon. Such an approach offered a method of analyzing the interaction between the carbon and nitrogen cycles on this shelf. Also, the comparison can be used as a cross check on the productivity measurements. This is especially important in the case of the NH_4^+ uptake measurements since these cannot be compared to observed losses as can the NO_3^- uptake rates.

6.2 Results

6.2.1 *Nitrate and Carbon Utilization in the Mixed Layer*

The pCO_2 component of CO_2 system was routinely analyzed during 1980 and 1981 in the PROBES program (Codispoti et al. 1982). The pCO_2 values prior to the bloom period were in equilibrium or slightly above atmospheric pressure. Upon the initiation of phytoplankton growth, pCO_2 of the surface water became undersaturated in proportion to the decrease in NO_3^- and ΣCO_2 (Hood, 1981). The prebloom concentrations of ΣCO_2 and NO_3^- were taken as the concentration found in the water column before pCO_2 had been depressed below atmospheric pressure (Table 13). Likewise, it was found that the end of the bloom was best described as the time when pCO_2 was at a minimum. The reason for this choice was that NO_3^- depletion occurred before pCO_2 had reached its minimum. Conversely, the ΣCO_2 minimum is difficult to detect because of the large reserve of this component always present in the water column.

During the period 24 March - 3 June 1980 and 12 April - 20 July 1981, the changes in ΣCO_2 and NO_3^- in the water column at 20 stations on the PROBES lines (Figure 3) were monitored at approximately two week intervals. The average concentrations for ΣCO_2 and NO_3^- found in the mixed layer for four representative stations (5, 8, 12, and 16) are shown in Figures 64 and 65, respectively. The bottom water column is the strata from the bottom of the upper mixed layer to the bottom as determined acoustically. The data for the bottom layer are shown in Figures 66 and 67.

Table 13.

Pre-Bloom Concentrations of Total Carbon Dioxide Components (ΣCO_2, pCO_2) and Nitrate on the Southeast Bering Sea Shelf as Sampled at the PROBES Line.

Year	Station	Day	ΣCO_2 ($M \times 10^{-3}$) Top	ΣCO_2 ($M \times 10^{-3}$) Bottom	NO_3^- ($\mu gA/\ell$) Top	NO_3^- ($\mu gA/\ell$) Bottom	pCO_2 (ppm) Top
1980	5	April 11-15	2021	2057	21.4	25.0	369
	8	March 30-April 12	2023	2031	16.2	17.5	328
	12	March 25-April 14	2026	2061	16.2	16.0	348
	16	April 13	1999	1999	16.4	16.4	333
1981	5	April 11-15	2073	2083	14.3	18.4	346
	8	March 30-April 12	2045	2075	10.1	13.7	-
	12	March 25-April 14	2016	2027	11.8	11.8	-
	16	April 13	2056	2056	11.7	11.7	335

Top = Average concentration in water above maximum density gradient

Bottom = Average concentration in water below maximum density gradient

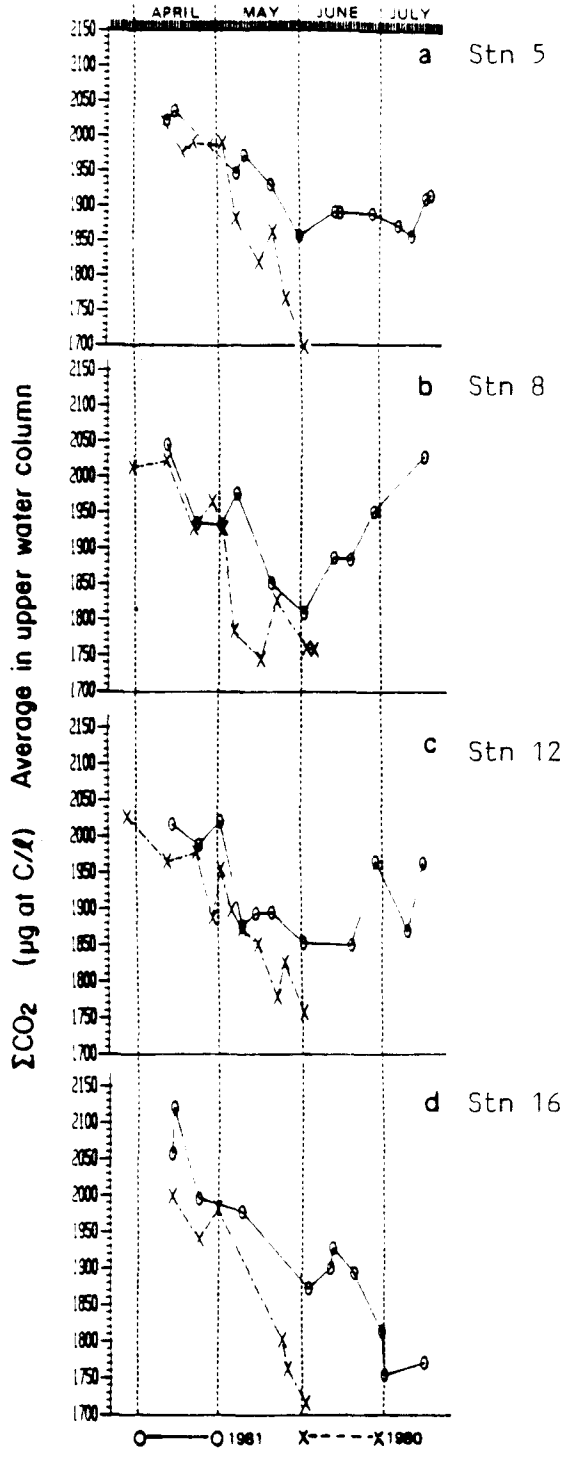

Figure 64.

Changes in mixed layer ΣCO_2 with time across the shelf during 1980 and 1981.

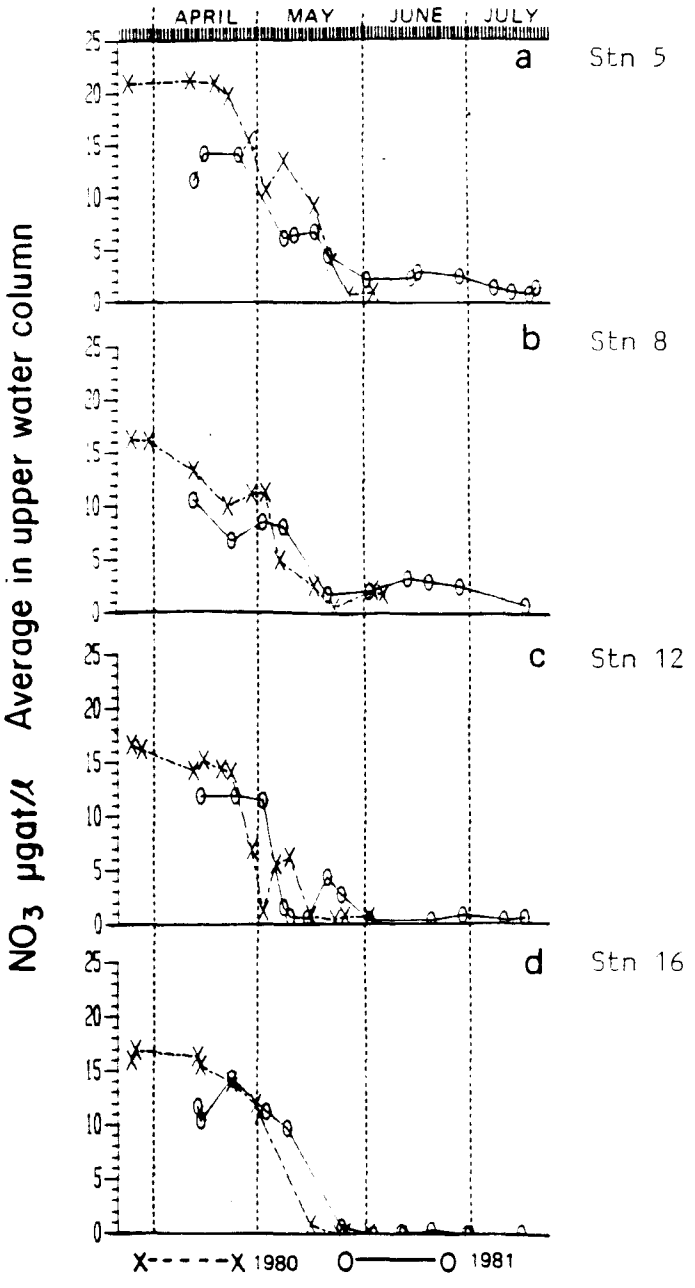

Figure 65.

Changes in mixed layer nitrate with time across the shelf during 1980 and 1981.

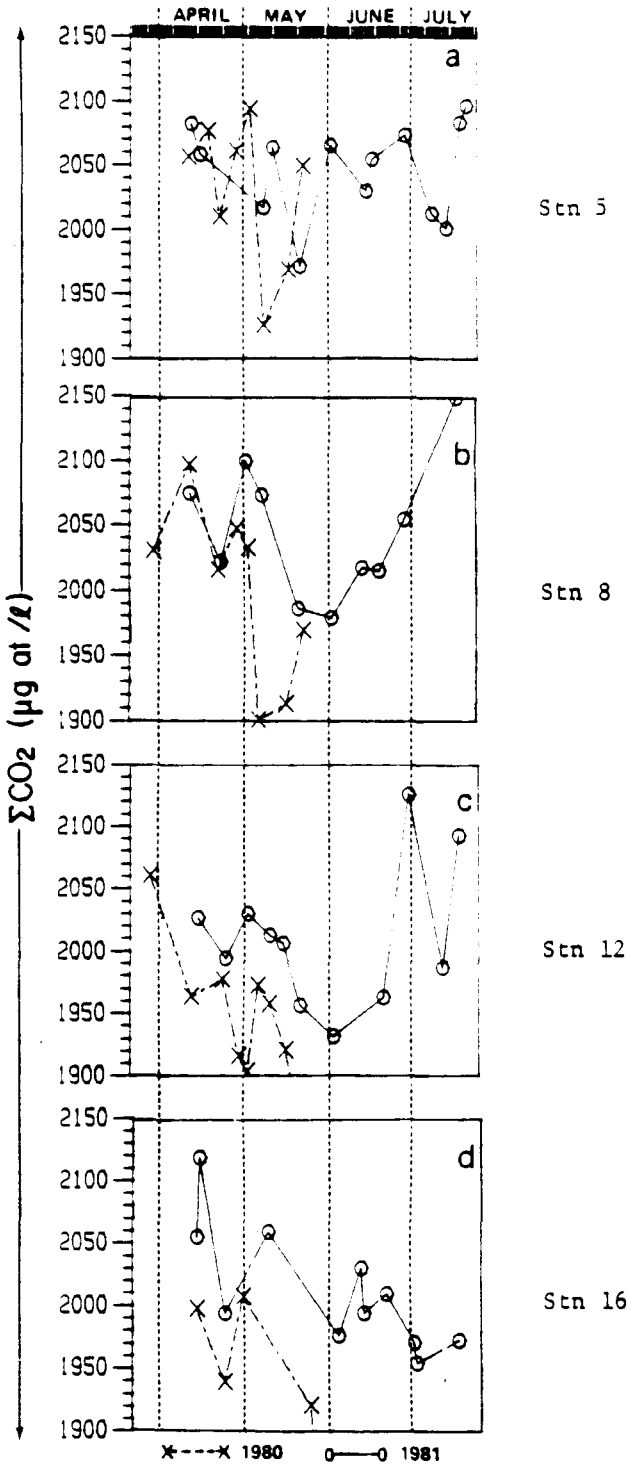

Figure 66.

Changes in bottom layer ΣCO_2 with time across the shelf during 1980 and 1981.

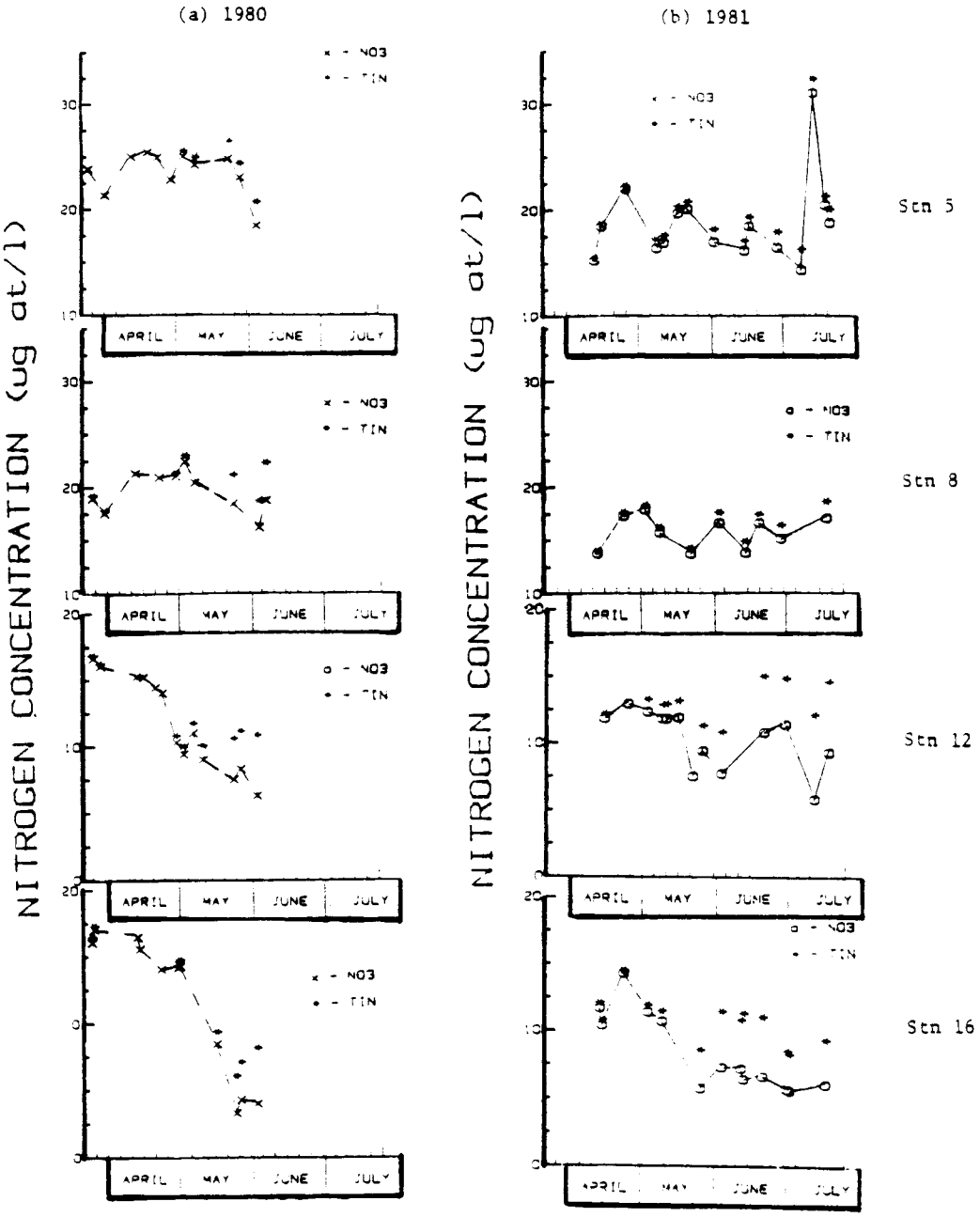

Figure 67.

Changes in bottom layer nitrate and TIN with time at the four cross shelf staions indicated during A) 1980 and B) 1981 .

The mixed layer ΣCO_2 concentrations (Figure 64) and NO_3^- concentrations (Figure 65) for stations 5, 8, and 12 had reached minimum values by June 1 - 3. At station 16, however, the concentrations remained low through the last sampling at 16-18 July. The ΣCO_2 and NO_3^- utilization data for each station in 1980 and 1981 during the spring bloom period are listed in Table 14. The values shown represent differences in mixed layer average concentrations. While variations occur between stations and years, there is reasonable uniformity of utilization rates across the shelf to give an average C/N utilization ratio of 15.5 ± 6.6.

6.2.2 Whole Water Column Nitrate and Carbon Changes

The time series of whole water column total dissolved inorganic carbon content (ΣCO_2; Figure 68) and of water column NO_3^- and total inorganic nitrogen (TIN) content (Figure 69) also exhibited changes which are consequences of the spring bloom cycle. In particular, with the exception of Station 5, there is a clear decrease in water column ΣCO_2 content across the shelf commencing in early May (Figure 68), coincident with the first appearance of large standing crops of phytoplankton in these areas.

In 1981 the carbon content at Stations 12 and 8 decreased to a minimum at approximately 1 June by which time 108 and 132 g C m^{-2}, respectively, had been lost from the ΣCO_2 pool. June and July sampling at these stations revealed the recovery of water column carbon content to levels equal to, or above, those found at the early April stations. The

Table 14.

Ratio of C/NO_3 Utilization During Bloom in Upper Layer.

Station	Year	Δt (days)	$\Delta\overline{\Sigma CO_2}$ (µg at/ℓ)	$\Delta\overline{NO_3}$ (µg at/ℓ)	$\frac{\Delta\overline{\Sigma CO_2}}{\Delta\overline{NO_3}}$
5	1981	50	166	11.9	13.9
	1980	48	139	7.7	18.1
8	1981	51	235	7.9	29.7
	1980	54	185	15.5	11.9
12	1981	49	165	11.5	14.3
	1980	54	248	15.8	15.7
16	1981	51	183	11.7	15.6
	1980	41	196	16.4	12.0
Average ± S.D.			189.6 ±36.4	12.3 ±3.4	15.5 ±6.6

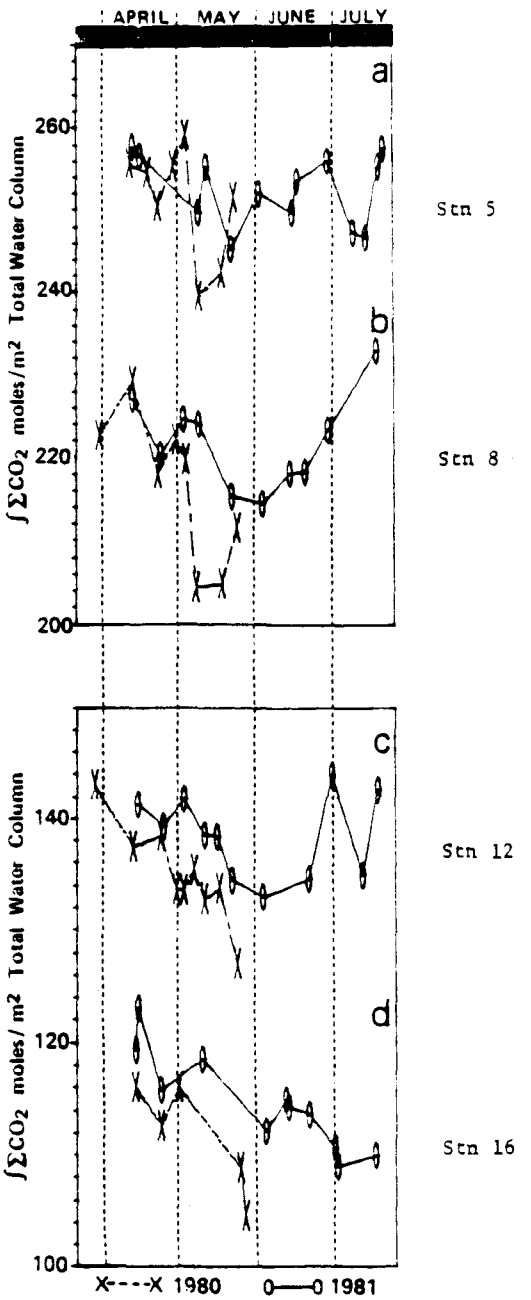

Figure 68.

Changes in whole water column ΣCO_2 with time at the four cross shelf stations indicated during 1980 and 1981.

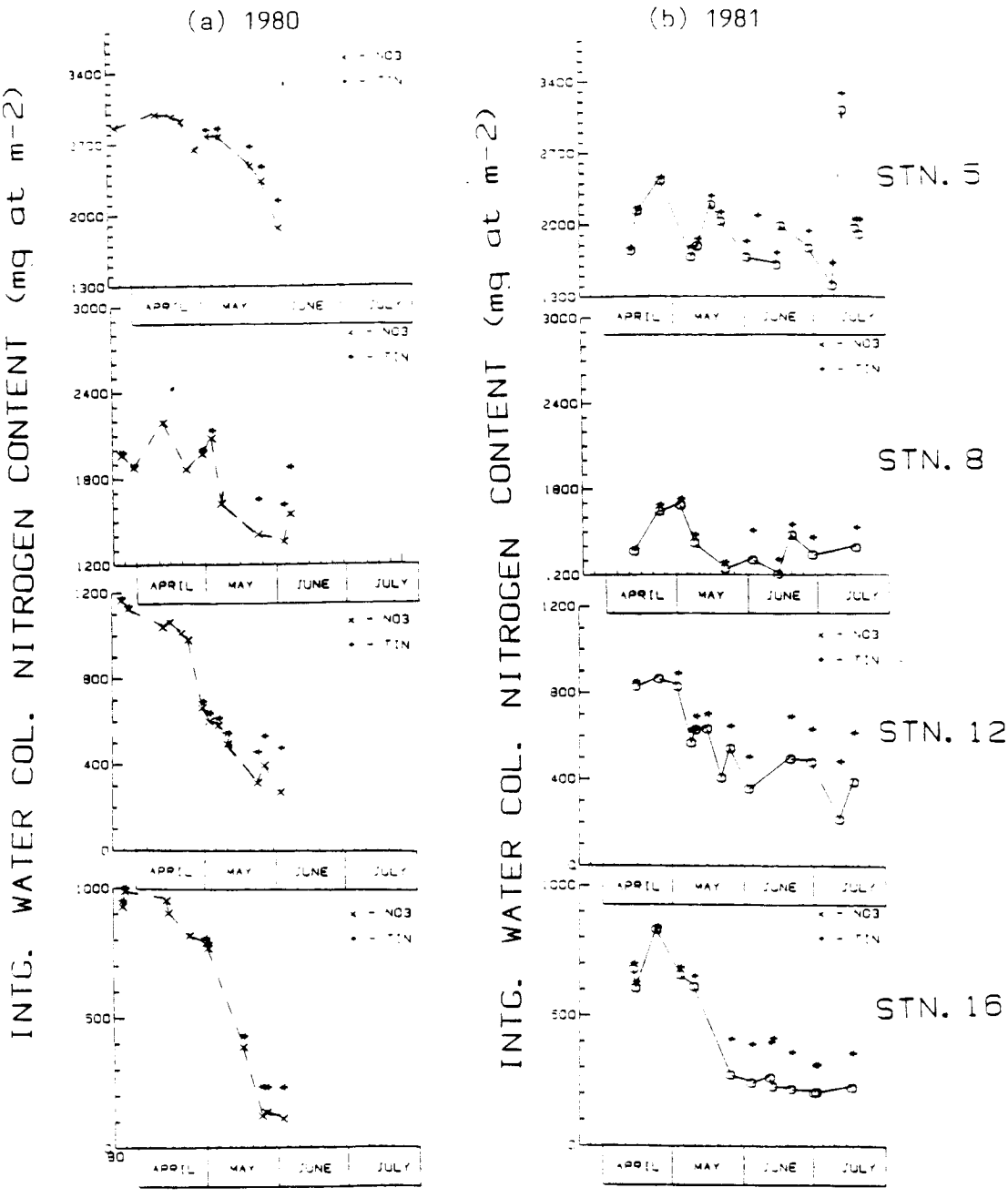

Figure 69.

Changes in whole water column nitrate and TIN with time at the four cross shelf stations indicated during A) 1980 and B) 1981.

recovery is apparent in both the upper and lower water column concentrations of TDIC (Figures 64 and 66). The bottom water increase, however, contributes relatively more to the increase observed in the whole water column due to both the higher concentrations attained in this layer and its greater thickness.

The recovery period coincides with the cessation of high ^{14}C and ^{15}N uptake rates measured during May. This indicates that the supply rates of carbon to the dissolved inorganic pool from sources such as respiratory processes in the bottom water and invasion of atmospheric CO_2 to the surface water exceeded the loss rate of dissolved inorganic carbon.

The time series of water column ΣCO_2 content at Stations 8 and 12 during 1980 is qualitatively similar to that in 1981 during the length of time sampled. The initial loss of ΣCO_2 is greater at Station 12 during 1980 however (Figure 68). Also, Station 8 exhibits an abrupt drop in carbon content in 1980 coincident with a similar decrease observed at Station 5 in 1980. In both these cases, the decrease in bottom water ΣCO_2 concentration is largely responsible.

At the most inshore station presented in Figure 68 (Station 16) the ΣCO_2 content of the water column never exhibited any indication of recovery back to end of winter values during the study period. In contrast, the outer shelf station 5 never reflected any significant sustained, depression in ΣCO_2 content. Several factors contribute to the greatly diminished spring bloom signal in the $\Sigma CO2$ content of the outer shelf station 5. Chiefly, the depth of integration (ca. 125 m) produces a carbon content large enough to obscure even a 10 mole change in ΣCO_2 content. Also in 1981 a large phytoplankton standing crop was not observed until the

final July occupation at the outer shelf station indicating that the bloom here was delayed and out of phase with the more inshore stations.

The changes in water column TIN content at these cross shelf stations (Figure 69) also reflect the dramatic influence of spring phytoplankton growth and subsequent remineralization processes. At all early April stations most of the nitrogen was in the form of NO_3^-. Following the onset of vigorous phytoplankton growth, the water column displayed an increase in NH_4^+ content which occurred almost exclusively in the bottom water (Figures 67). Because of continued phytoplankton uptake, NH_4^+ concentrations never reached comparable levels in the upper waters.

At the two innermost stations (12 and 16), it appears that much of the NO_3^- photosynthetically reduced in the upper water is remineralized in the bottom water after the intervening particle flux. At Station 12 during 1981, however, there is a net loss of approximately a third of the initial TIN from the water column which does not recover (as ΣCO_2 did here) by mid July (Figure 69). Biological consumption in middle shelf surface waters is probably not the reason since ^{15}N measurements indicated that total nitrogen uptake was low after May in this area.

This net loss is even greater (> 50%) from the Station 16 water column from April to July 1981. It appears that the growth of phytoplankton in the inner front area continues to act as a sink for TIN well into the summer. This view is supported by the observation of a dense growth of dinoflagellates in the inner front area throughout June and early July. Their appearance here is very similar to their appearance in the tidally mixed front around the English channel during the summer months (Pingree et al., 1975). ^{15}N uptake experiments in the Bering Sea revealed that these

dinoflagellates were heavily dependent on NH_4^+ as a nitrogen source, which is perhaps a consequence of the TIN pool composition to which these phytoplankton have access. Thiz prolonged inshore growth appears to draw upon the shoreward diffusive flux of TIN from middle shelf bottom waters which would account for the lack of recovery in the TIN content at Station 12. This also accounts for the discrepancy between the recovery of ΣCO_2 and TIN content at Station 12 since unlike TIN, $\Sigma O2$ has an atmospheric source.

At the deeper stations (8 and 5), bloom induced changes in water column TIN content were not as dramatic as those at the more inshore stations. Although the NH_4^+ content of the water column increased at these outer stations after the bloom, a clear decrease in water column TIN content was not observed. The reasons for the lack of a clear signal in TIN content at Station 5 are similar to those given during the discussion of the ΣCO_2 water column content at this station. These reasons are less persuasive in explaining the lack of a water column TIN decrease at Station 8, however. There was an observed decrease in water column $\Sigma CO2$ at this station. This discrepancy is largely due to processes occurring in the bottom water (Figures 66 and 67).

6.3 Discussion

6.3.1 Mass Balance Approach to the Net Carbon loss from Surface Water

The following equation is used in analyzing the present data:

$$\Delta\Sigma CO_2 - \Delta(PC + DOC) = S_G + CO^{=}_{3(ppt)} \pm F_{sedi.} \pm F_{atmos.} - R \qquad (24)$$

Equation 24 is a modification of earlier equations dealing with carbon fluxes, most notably that of Hood (1981). Importantly, Equation 24 recognizes the consumption of ΣCO_2 by chemosynthetic as well as photosynthetic processes since both are encountered in dealing with the entire water column. The units are g C m^{-2} day^{-1} and its components are defined as follows:

$\Delta\Sigma CO_2$	the net change in ΣCO2
$\Delta(PC + DOC)$	adjustment for the in situ change in particulate and dissolved organic carbon
R	the contributions to ΣCO_2 from respiratory processes.

F_{atmos} — the flux of atmospheric CO_2 across the sea surface. This can be a positive or negative term depending on partial pressure of CO_2 in water and atmosphere.

S_G — the loss of ΣCO_2 to synthetic processes, both photosynthetic and chemosynthetic.

$CO_{3(ppt)}^{=}$ — the loss of ΣCO_2 to carbonate precipitation.

$F_{sedi.}$ — the net flux of ΣCO_2 to (or from) the sediments.

Equation 24 incorporates the major processes acting on the ΣCO_2 pool in the whole water column and contains a variety of unknowns. This situation is greatly improved, however, by assuming that the photosynthetic and chemosynthetic processes are segregated vertically in the water column. Using the previously defined upper and lower water layers to represent the strata of photosynthesis and chemosynthesis respectively, equation 24 becomes tractable within the present data set.

In many cases during the spring bloom on the southeast Bering Sea, the bottom of the euphotic zone is very near that of the discontinuity density layer separating the upper and lower water columns. This effectively prevents photosynthetic processes from having a substantial direct

impact on bottom water chemistry. Chemosynthesis is probably not zero in the upper water column. The assumption that the utilization of carbon by photosynthesis overwhelms other autotrophic processes in this layer is valid, however, especially for the spring bloom period when plant growth is at its peak.

In the upper water column several terms in Equation 24 can be simplified. Only the gross photosynthesis component of S_G is considered and chemosynthesis is set to zero. Ambient NH_4^+ levels remain low in the upper waters during the early bloom period which allows the accumulation of regeneration products such as NH_4^+ to be neglected in the upper water. The surface waters are considered isolated from the bottom fluxes so that $F_{sedi.}$ is also neglected. Equation 24 then reduces to:

$$\Delta \Sigma CO_2 - \Delta(PC + DOC) = (P_G - R) + CO_{3(ppt)}^{=} - F_{atoms.} \qquad (25)$$

Equation 25 is analogous to Hood's (1981) equation 2 in which P_G is gross photosynthesis. The term $(P_G - R)$ represents the net carbon loss from the upper water (P_N). The components of equation 25 are depicted schematically in Figure 70.

Alkalinity changes recorded in the shelf surface water indicated the precipitation of $CO_3^=$ from surface waters was approximately 25% of net productivity (L. Codispoti, personal communication). This value is similar to the estimate of $CaCO_3^=$ precipitation made by Broecker and Peng, (1982). Presumably these alkalinity changes are produced in the formation of calcium carbonate plates by coccolithophorids. The total biogenic carbon loss from

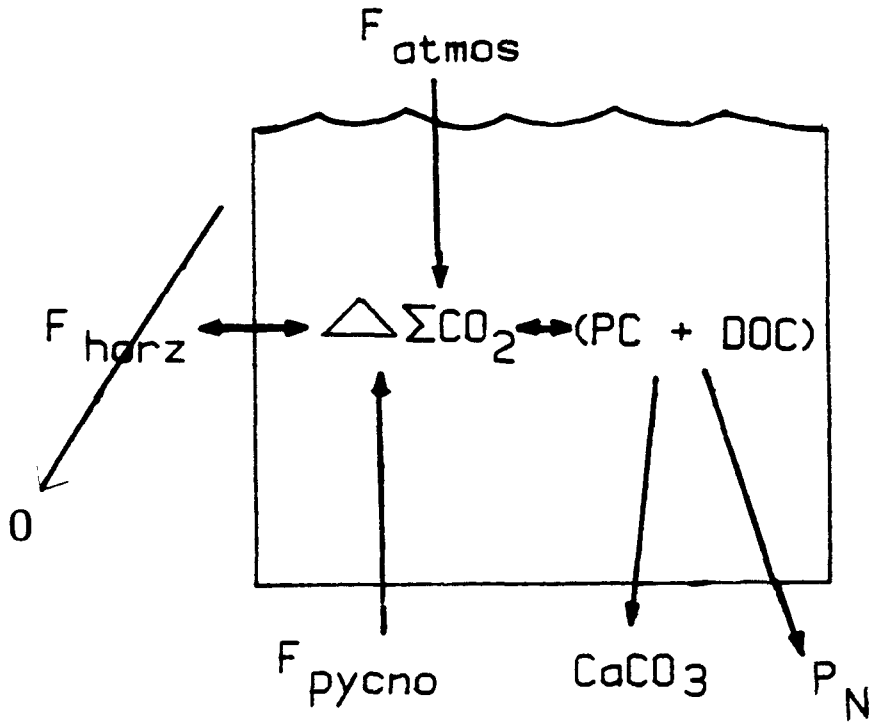

Figure 70.

Components of the carbon mass balance model for the mixed layer.

surface waters, therefore was estimated as 1.25 x P_N.

The $F_{atmos.}$ term was estimated from a stagnant film model (Broecker and Peng, 1974), such that:

$$F_{atmos.} = D_{CO_2} [(pCO_2 - ap) / F.T.] \quad (26)$$

where D_{CO_2} = temperature dependent molecular diffusivity of CO_2, pCO_2 = CO_2 partial pressure in surface water, a = temperature dependent solubility of CO_2, p = partial pressure of CO_2 in air, and F.T. = film thickness of the stagnant boundary layer. Actual film thickness measurements were made in the PROBES area using a Radon technique. Thicknesses varied widely depending on surface conditions, but an average value of 26 μm (D. Glover, personal communication) was used in equation 26. This value is similar to the average warm water figure reported by Broecker and Peng (1974).

An important factor influencing mixed layer ΣCO_2 concentrations which is not considered in equation 25 is the flux of bottom water ΣCO_2 through the pycnocline. This was estimated by the difference between the measured $\int \rho NO_3^-$ uptake rates and the observed change of NO_3^- concentrations in the mixed layer such that:

$$F_{pycno.} = [(\Sigma CO_{2(b)} - \Sigma CO_{2(U)}) \times (\rho NO_3^- - \Delta NO_3^-) / (NO_{3(b)}^- - NO_{3(u)}^-)] \quad (27)$$

In equation 27, (b) and (a) indicate the bottom and top water, respectively. This last factor was incorporated into a carbon mass balance equation to estimate the net loss of ΣCO_2 from the surface water. This loss is

defined as net production (P_N) which can be calculated for intervals between station sampling such that:

$$P_N\ (CB) = [\Delta \Sigma CO_2 - \Delta(PC + DOC) + F_{atmos.} + F_{pycno.}] \times 0.8 \qquad (28)$$

This method for estimating net productivity can then be compared to the instantaneous rate measurements:

$$P_N\ (^{15}N) = (C/N)_C \times (\rho NO_3^- + \rho NH_4^+) \qquad (29)$$

$$P_N\ (^{14}C) = \rho C \qquad (30)$$

These three models were calculated between station occupations at station 12 in 1980 and 1981 and the results are shown in Figures 71 and 72. In these calculation intervals the $\Delta(PC + DOC)$ term was not considered. In 1980 (Figure 71), the carbon budget model displays large excursions which are due to the difficulties of estimating F_{pycno} during periods in which the mixed layer is changing rapidly. The ^{14}C estimates of productivity, however, are larger than the ^{15}N estimates in the deeply mixed late April - early May period. During the calmer 1981 bloom the carbon budget approach follows the ^{15}N measurements fairly closely (Figure 72). The ^{14}C rates, however, are lower than either method during most of May. These directional differences supports the hypothesis that the uptake of these nutrients exhibit a differential dependence on respirational history.

The same approach can be taken in the outer shelf (Figures 73 and 74). The carbon budget again exhibits negative values due to errors in the

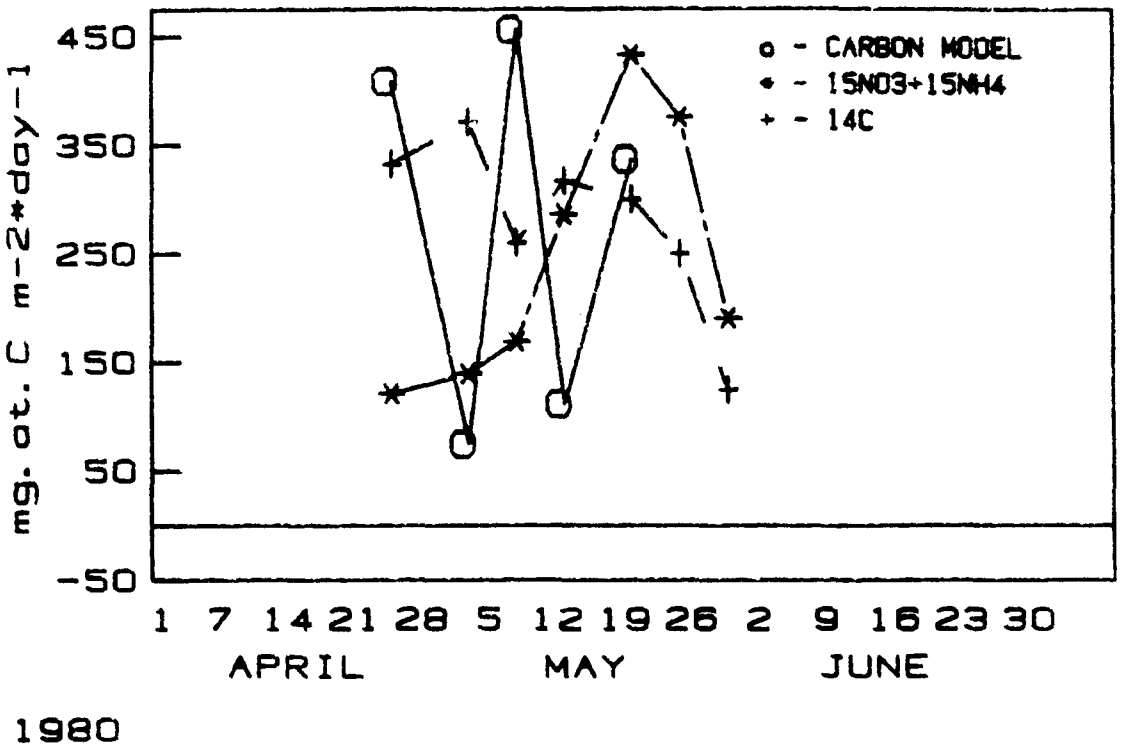

Figure 71.

Comparison among the three indicated methods of estimating carbon productivity in the middle shelf during 1980.

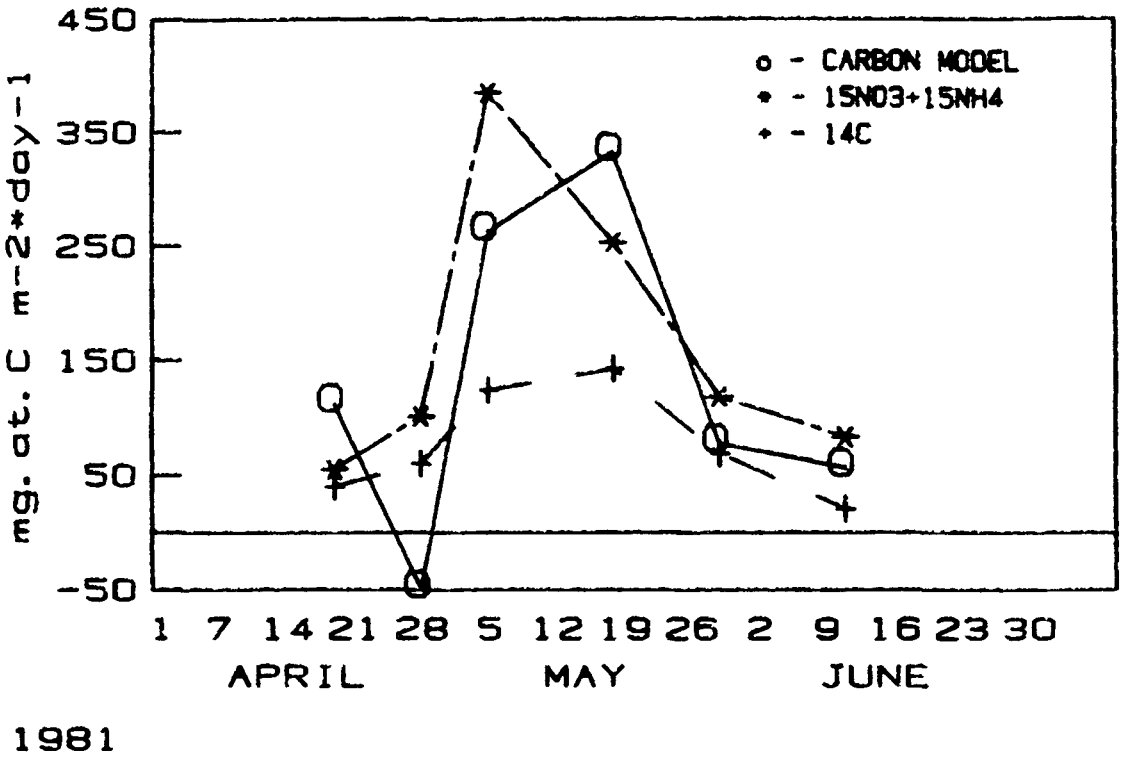

Figure 72.

Comparison among the three indicated methods of estimating carbon productivity in the middle shelf during 1981.

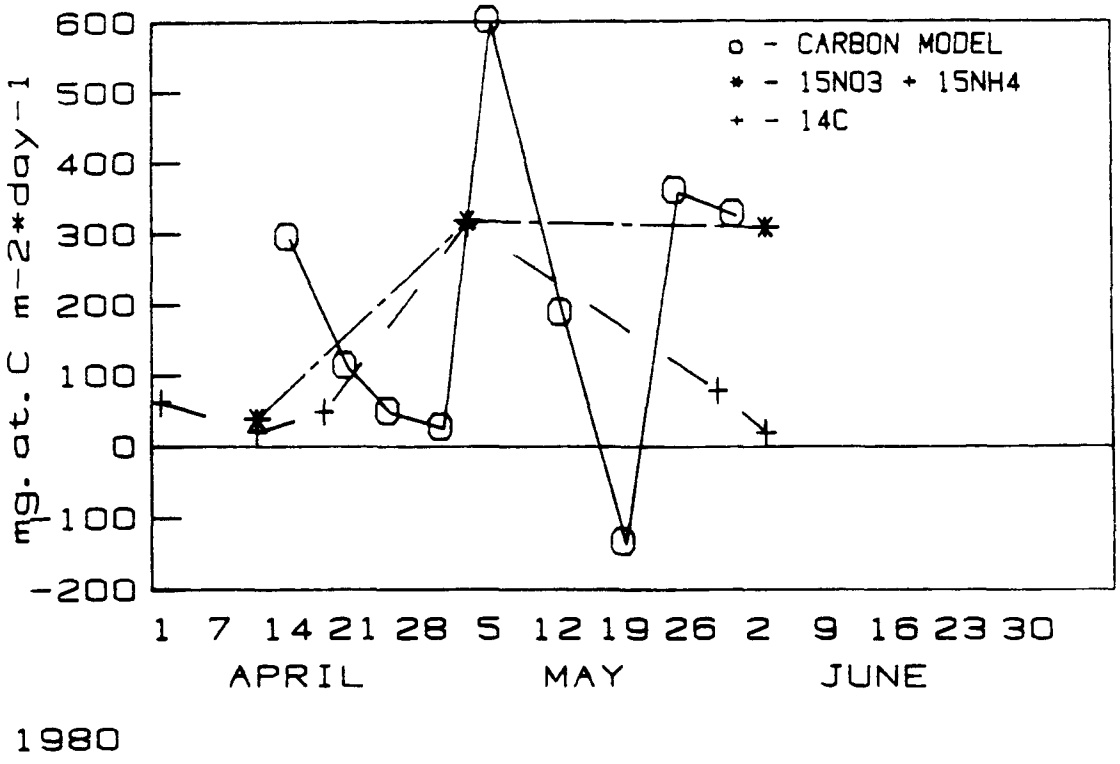

Figure 73.

Comparison among the three indicated methods of estimating carbon productivity in the outer shelf during 1980.

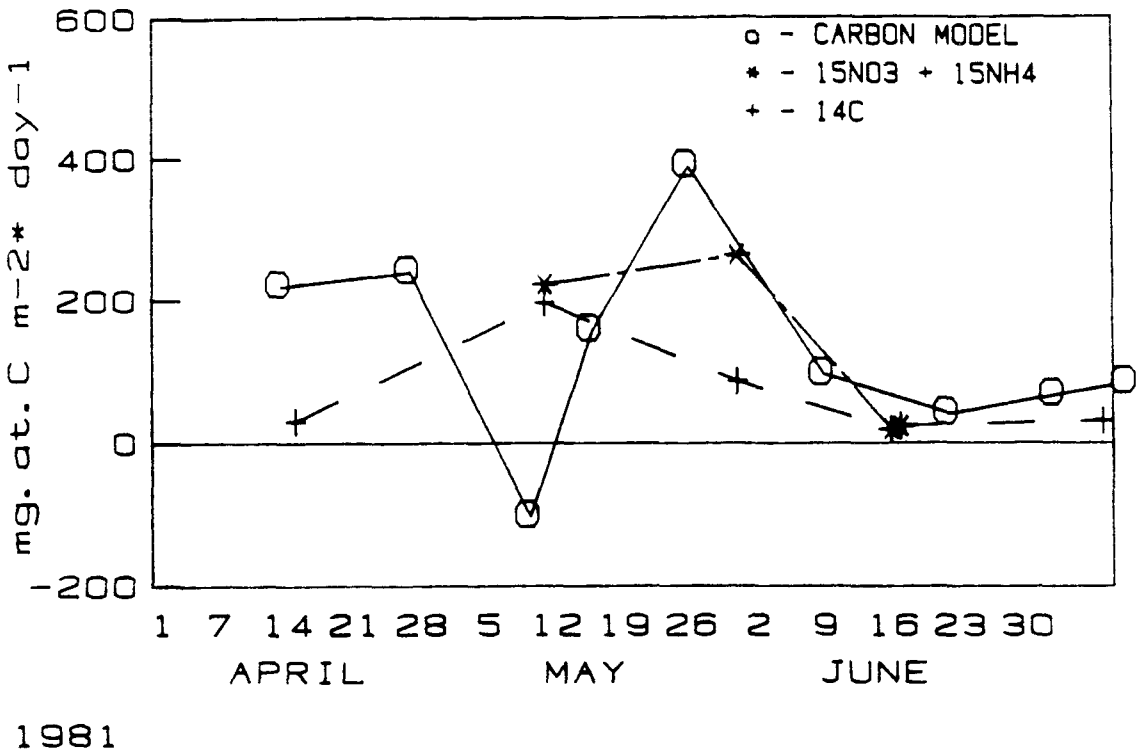

Figure 74.

Comparison among the three indicated methods of estimating carbon productivity in the outer shelf during 1981.

estimation of F_{pycno}. Also, in the outer shelf, the instantaneous rate measurements are not as well distributed throughout the sampling period as on the middle shelf time series. An additional problem in such an approach at station 5 is the greater advection in the outer shelf, and this signal most likely also contributed to the "noise" in Figure 73 and 74. It appears, however, that high values of productivity persist longer in the outer shelf (eg. early June 1980, Figure 73 and early July 1981, Figure 74). This also is probably a result of the greater advection in this area which results in a larger effective diffusivities of nutrients into the upper water.

Recently, nitrate uptake has been used to estimate the carbon loss from the surface water (Eppley et al., 1983). Such an approach, however, implicitly assumes that the remineralization rate of POC is the same as PON. These rates may not be the same. In fact, available evidence suggests that PON remineralization rates are faster (Degens, 1970). Also this discrepancy can be inferred from the increase in particulate C/N ratio which occurs with depth (Honjo, 1980), and with distance offshelf (Handa and Tanoue, 1981).

The predicted carbon loss from equation 28 can be compared to the amount of new carbon production associated with nitrate uptake (calculated as $\rho\ NO_3^- \times C/N_{(p)}$) (Table 15). The values in Table 15 represent the net changes over the period from late April to early June at station 12 in the middle shelf. Unlike the calculations made above for Figures 71 - 74, the Δ(PC + DOC) adjustment was evaluated in Table 15. Although measurements of DOC were not available, it was estimated from data presented by Loder (1971). Based on Loder's (1971) measurements during productive periods in Bering Strait, the relationship (PC + DOC) = 0.88 + 1.9 x POC

Table 15.

Comparison of carbon loss from surface waters predicted from carbon mass balance (equation 25) and nitrate productivity.*

Year	$\Delta\Sigma CO_2$	Δ(PC+DOC)	F_{Atmos}	F_{Pycno}	$CO_{3(ppt)}^{=}$	P_n	$\propto NO_3^- xC/N_{(p)}$
1980	4.96	2.4	0.94	7.68	2.24	8.94	5.25
1981	2.97	2.0	0.94	5.57	1.50	5.98	4.40

*Calculations based on 6 week bloom period (late April through early June). (units are moles carbon m^{-2})

(r^2 = 0.88) was used to estimate the quantity Δ(PC + DOC) in Table 15.

The data in Table 15 indicates new production cannot account for all of the carbon leaving the mixed layer (P_n). The disparity is even greater if the loss of carbon due to $CaCO_3$ precipitation is considered. The f factor therefore may only be a qualitative index of carbon loss from surface waters. In circumstances such as the high latitude spring diatom bloom in the southeast Bering Sea, the f factor is a conservative estimator of surface carbon loss.

A discrepancy between the C/N uptake ($C/N_{(u)}$) and regeneration ($C/N_{(r)}$) ratios is suggested by the underestimate of surface carbon loss by ΔNO_3^- x $C/N_{(u)}$. If the two C/N ratios were equal, the two estimates of carbon loss would also be similar. The ratio of the carbon budget to nitrate productivity in Table 16 suggests $C/N_{(u)}$ is 1.5 - 1.9 times as large as $C/N_{(r)}$ in the surface water depending on wether or not $CO_{3(ppt)}^{=}$ is considered.

The observed ratio of ΣCO_2 / NO_3^- utilization during the bloom (Table 14) indicates that ca. 15 atoms of C are removed from the surface water for every atom of NO_3^--N . The fact that the average particulate C/N compositional ratio observed at these same stations was approximately 7 also suggests $C/N_{(u)}$ is larger than $C/N_{(r)}$. This comparison does not consider the fluxes across the sea surface or pycnocline, however. The discrepancy between C/N ratios is also supported by laboratory measurements of recycling as well as other estimates of C and N recycling in the upper waters. If these results apply to other ocean areas, significantly more carbon is lost from surface waters than can be accounted for by nitrate

productivity alone.

6.3.2 Mass Balance in the Whole Water Column: Effects of Regeneration and Chemosynthesis in Bottom Water

When the net change in water column ΣCO_2 to NO_3^- are compared over the course of the bloom (Table 16) the ratios are significantly larger than those observed in the upper water column (Table 14). This suggests that processes in addition to upper water column consumption are acting on these constituents. The precipitation of $CaCO_3$ by the benthic community for example, is one such process.

Differential regeneration of carbon and nitrogen in the bottom water may also account for the large $\Delta/\Sigma CO_2/\Delta/TIN$ ratios observed (Table 16) These water column ratios are almost double the loss ratios observed in the upper water. This discrepancy suggests that some part of this regenerated nitrogen is being nitrified in the bottom waters and masking some of the net water column nitrate change.

Ammonium values increase in the deeper water of the middle and outer shelves after early May, after the spring bloom biomass sinks from the upper water. The observed rates of bottom water increase in NH_4^+ and ΣCO_2 concentrations is shown in Table 17 (columns 2 and 4). Assuming carbon and nitrogen are regenerated in the Redfield ratio from the particulate material, bottom water ammonium accumulation rates did not keep pace with those of ΣCO_2. This disparity is presented as the "NH_4^+ deficit" in Table 17. Actually this deficit is conservative since the ratio of C/N

Table 16.

Ratio of $C/\overline{NO_3}$ and C/TIN Net Change During Bloom in Whole Water Column for Time Periods Indicated in Table 14.

Station	Year	Initial NO_3	Initial TIN	Final NO_3	Final TIN	$\Delta\int NO_3$ mg·at/m^2	$\Delta\int$TIN mg·at/m^2	$\frac{\Delta\int \Sigma CO_2}{\Delta\int NO_3}$	$\frac{\Delta\int \Sigma CO_2}{\Delta\int TIN}$
5	1980	2985	2995	2625	2710	360	285	44.4	56.1
	1981	2100	2105	2000	2070	102	35	120.9	352.4
8	1980	2150	2160	1410	1640	740	520	23.4	33.33
	1981	1600	1620	1220	1310	380	310	32.7	40.1
12	1980	1120	1122	315	450	805	672	19.7	23.6
	1981	830	845	355	495	475	350	18.9	25.7
16	1980	950	960	135	220	815	740	14.1	15.5
	1981	685	700	240	380	445	320	24.7	34.4

Table 17.

NH_4^+ and ΣCO_2 Increases in Cross Shelf Bottom Water and NH_4^+ Deficit Based on Difference Between Them.

		gC m^{-2} d^{-1}		mgat·m^{-2} d^{-1}
Station #	May NH_4^+ generation[a] (mgat·m^{-2} d^{-1})	Regenerative ΣCO_2 increase[b]	Observed ΣCO_2 increase June 81	NH_4^+ deficit[c]
5			0.86	4.0
8	6.7	0.53	2.70	26.9
12			2.21	20.8
16			-0.84	-17.1

[a] based on observed NH_4^+ accumulation in bottom water.

[b] May NH_4^+ generation x $\frac{C}{N}$.

[c] [ΣCO_2 increase ÷ $\frac{C}{N}$] - observed NH_4^+ generation.

regeneration is probably lower than the Redfield ratio.

The NH_4^+ deficit is apparent across the shelf during June, 1981 except at the most inshore station (16) The net consumption of both carbon and nitrogen at the most inshore station (16) was probably due to extensive growth of the dinoflagellate Gonyaulax sp. observed well into July in this area. The observed rate of carbon respiration is greatest in the middle front area between stations 12 and 8. This is the same shelf depth associated with high microbial activity by Griffiths, et al., (1983). These workers noted that the relatively low temperatures were no great deterrent to substantial microbial activity.

Another contributory factor to these NH_4^+ deficits may be ammonium oxidation occurring in the bottom water. In North Sea sediments, integrated nitrification measurements of 4 - 9 mg-at m^{-2} $dy.^{-1}$ have been reported which are dependent on the organic carbon content of the sediments (Billen, 1978). The range of organic content Billen reported are comparable to the organic content of southeast Bering Sea sediments (Walsh, 1983). The actual net flux of nitrate from the sediments, however, is more likely less than 0.7 mg-at m^{-2} $dy.^{-1}$ (Henriksen, et al., 1981.). Some of the difference is due to the denitrification of recently oxidized combined nitrogen as it diffuses from surface sediments into deeper anoxic layers.

The amount of denitrification occurring in the southeast Bering Sea is not known. It has been reported to be quite active by some investigators (Koike and Hattori, 1979) and not measurable by others (Griffiths et al., 1983). Measurements of nitrification in the water column are fairly rare although a ^{15}N technique has been applied, (Olson, 1981), and new methods are available (Vincent and Downes, 1981).

The net cross shelf change in water column ΣCO_2 and total inorganic nitrogen (TIN = NO_3^- + NO_2^- + NH_4^+) during the bloom period both display a transition from on shore deficits to outer shelf excesses in the middle front region (Figure 75). This transition is especially evident for TIN (Figure 75 b). A possible explanation for the observed cross shelf patterns is the off shelf movement of particulate or dissolved organic carbon and nitrogen which is undergoing remineralization enroute. Regardless of the exact sequence of events producing such cross shelf patterns, the spring phytoplankton bloom is the driving force behind the subsequent biogeochemical transformations taking place.

A.

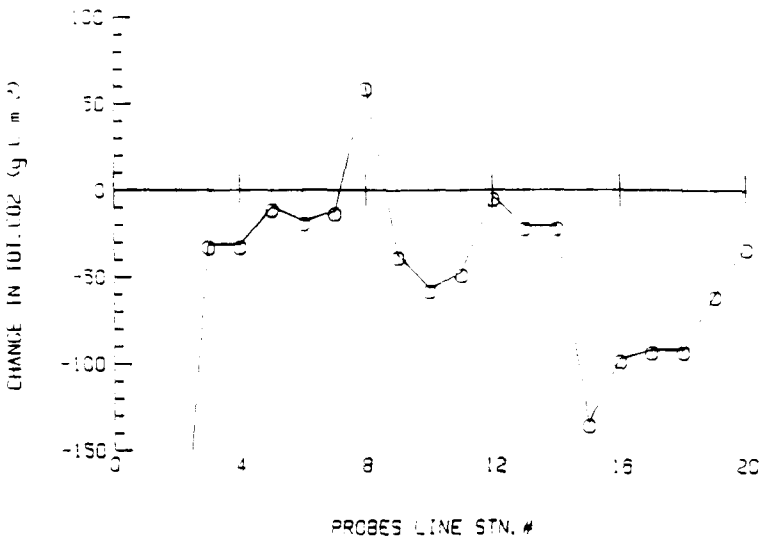

WATER COL. TOT. CO2 CHANGE FROM APRIL TO JULY 1981

B.

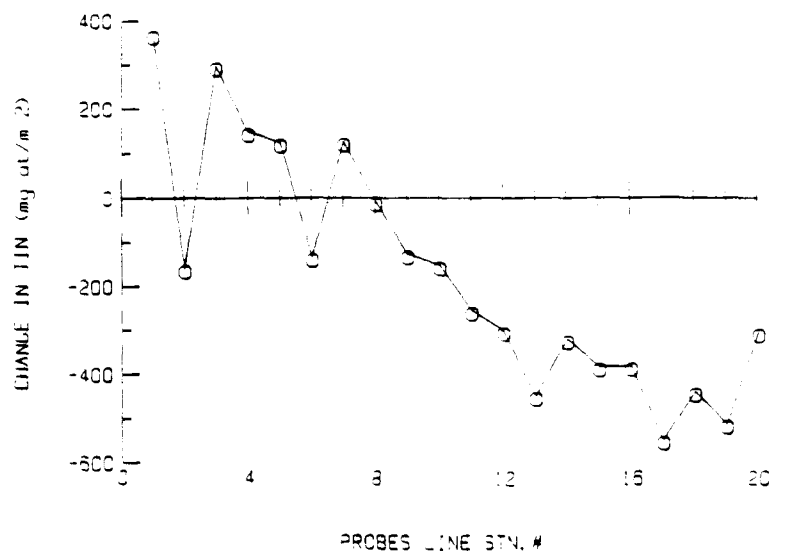

WATER COL. TIN CHANGE FROM APRIL TO JULY 1981

Figure 75.

Net water column change in ΣCO_2 and TIN from April to July, 1981 across the southeast Bering Sea shelf.

Chapter 7

Summary of Productivity Measurements and Observations of Interannual Variability

7.1 Seasonal and Yearly Estimates of Nitrogen Productivity and Associated Processes

Table 18 organizes the various methods used to estimate primary productivity during this study by shelf domain, station 12 representing the middle domain and station 5 the outer. Nitrate productivity is estimated from the time and depth integrated $\rho\,{}^{15}NO_3^-$ measurements and the net water column change in nitrate content. Carbon productivity is derived from the three methods discussed in chapter 6.3.1 (equations 28, 29, and 30).

The two estimates of nitrate productivity agree closely in each year on the middle shelf (station 12) and the difference between them is never more than 11%. These data indicate 690 mg-at m^{-2} is the average nitrate consumption during the spring bloom period on the middle shelf. This value is substantially lower than the estimate used by Coachman and Walsh, (1981)

Table 18.

Comparison Among Years and Methods of Measuring Productivity in the Middle and Outer Shelves during the Spring Bloom*

Station	Year	$\int \rho\, {}^{15}NO_3^-$	$\Delta \int NO_3^-$	Ave. $\frac{C}{N}$	Estimated Net Production (P_N) g C m^{-2}		
		mg at m^{-2}			Carbon budget	^{15}N	^{14}C
12	1979	920	830	5	-	109.8	74.9
	1980	670	710	7	98.7	105.8	134.2
	1981	484	500	8.8	83.2	105.6	48.2
$\bar{X}$ ± S.D.		691±219	680±167		91±11	107±2	86±44
5	1979	-	600	6.6**	-	91†	-
	1980	-	990	10.6	89	250†	99
	1981	-	390	6.7	91	71†	73
$\bar{X}$ ± S.D.			660±304		90±1	137±48	86±18

*All estimates applied to 25 April-2 June of each year.
**Assumed.
†Based on $\Delta \int NO_3^-$.

in their diffusive model of southeast Bering Sea cross shelf nitrate flux (1400 mg-at m^{-2}). The water column nitrate change in (Table 18) represents the local change plus the diffusive flux in the model of Coachman and Walsh (1981). Since $\Delta\sqrt{}\ NO_3^-$ is only slightly smaller than biological nitrate uptake, the remaining diffusive model component - cross shelf horizontal flux, which is the difference between these two, must be rather small. The diffusive supply of nutrient rich slope water to the middle shelf, therefore, may not be as great as previously thought. This suggests in situ regenerative processes play a significant role in the yearly supply of nutrients to the middle shelf.

Also at station 12, the three year average for the three estimates of net carbon productivity (equations 28 - 30), yield similar results when integrated over the entire bloom period. Although total nitrogen (NO_3^- + NH_4^+) uptake varied from 14 to 25 g m^{-2} among years, carbon productivity derived from this uptake does not. This is largely do to the compensatory changes in the particulate C/N ratio measured in the various years. The carbon budget estimates were similar in 1980 and 1981 although were lower in the calmer 1981. The time integrated ^{14}C estimates of spring bloom production display the greatest interannual variability.

During the spring bloom period, there is an average carbon productivity of 100 g. (R. Iverson, personal communication). Nitrate uptake alone can account for approximately 55% of this productivity. The three ^{15}N time series, however, yield an average f factor of 0.47. This disparity is most likely due to the overestimate of ammonium uptake by the ^{15}N technique employed which would make the f factor based on these measurements small. Assuming the f factor from the ^{14}C comparison is correct, suggests that the

ρNH_4^+ measurements are 32% larger than actual regenerated nitrogen uptake.

The course temporal sampling at the outer shelf station 5 may be largely responsible for the greater spread in the productivity estimates here (Table 18). The frequency of productivity estimates at station 5, for example, averaged 19 days, compared to 5 days at station 12 (Figure 76). It is better to judge cross shelf patterns in nitrate uptake, therefore, from changes in mixed layer nitrate concentrations which were more frequently sampled (Figure 55). Based on these measurements, there is no significant difference between middle and outer shelf productivity during the spring bloom period.

October productivity data are available in 1980, (Figures 54 and 76) and chemical and Chl a data exist from N.O.A.A. cruises at other times of the year. Estimates of yearly production can therefore also be made. Nitrogen productivity data was extrapolated from the June postbloom conditions on the middle shelf to the cessation of phytoplankton activity in November. This exercise suggests an annual nitrate uptake of 950 mg-at m^{-2} and an annual f factor of 0.40. The Redfield ratio was used to convert these values to carbon. The resulting estimate (188 g C m^{-2} $yr.^{-1}$), is in good agreement with the ^{14}C derived estimate of 166 g C m^{-2} $yr.^{-1}$ (R. Iverson, personal communication). Judging from observed cross shelf and temporal patterns of productivity, these yearly productivity values are applicable from approximately the 60 m depth out to 130 m, or almost 60% of the shelf area.

The amount of nitrification occurring on this shelf can also be estimated. This process may strongly influence N_2O production. The

A. - 1979

B. - 1980

C. - 1981

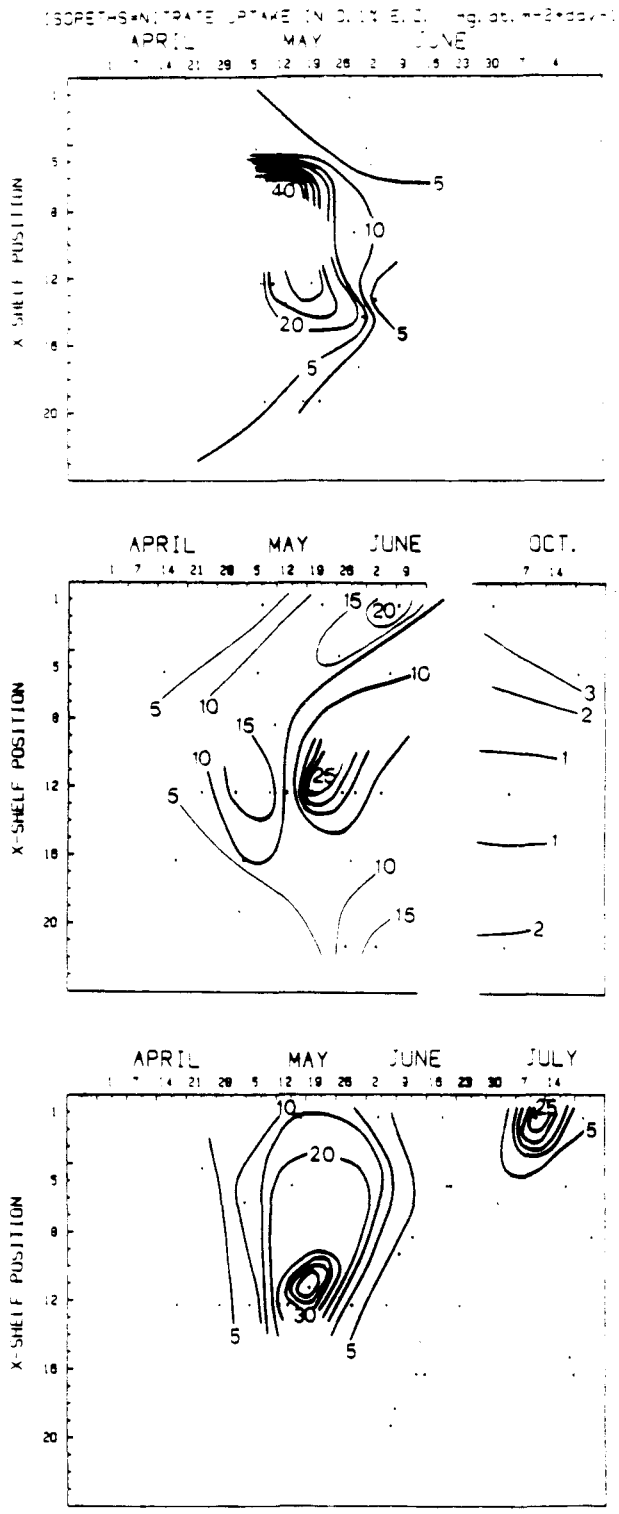

Figure 76.

Time - space changes in nitrate uptake during A) 1979, B) 1980, and C) 1981.

production of N_2O as a by product of nitrification is estimated to be between 0.01% to 0.30% of the amount of NO_3^- produced (Broecker and Peng, 1982 and Liu, 1979, respectively). In the process of nitrate photoassimilation each year, 1 g-at of NO_3^- is reduced to NH_4^+. To estimate N_2O production, therefore, the following assumptions were made. Of the total organic nitrogen produced from nitrate, 10% (liberally) is buried and 25% is denitrified after ammonification and diffusion from nitrifying to anoxic sediments. Additionally, 5% is left at the start of spring growth. After these quantities are removed, 60% of the original new production remains available for nitrification after first being ammonified.

Applying an average N_2O : NO_3^- production ratio of 0.0015 (atom : atom) to this remainder yields a potential N_2O production rate of 0.019 g N_2O m^{-2} $yr.^{-1}$. This value was extrapolated to the area of the world continental shelves and suggests a total shelf N_2O production of 1 Tg. This is less than 1% of the total ocean content of N_2O (Table 2), but may be of importance as an atmospheric source since shelf water is shallow and easily ventilated. Also, 1 Tg may represent a significant proportion of the estimated loss of N_2O from the ocean to the atmosphere. This loss is poorly known but suggested to be in the range of 4 to 10 Tg by Liu, (1979) and from 12 to 120 Tg by Hahn, (1981).

The nitrogen productivity data from the southeast Bering Sea follow the trend identified by Eppley and Peterson (1979) between new and total production (Figure 77). The f factor for the southeast Bering Sea is a minimum value since the measured $\rho\,^{15}NH_4^+$ values were used and the actual f factor may be as high as 0.45. The ratios of Eppley and Peterson (1979) may also be conservative due to their assumptions regarding the amount of

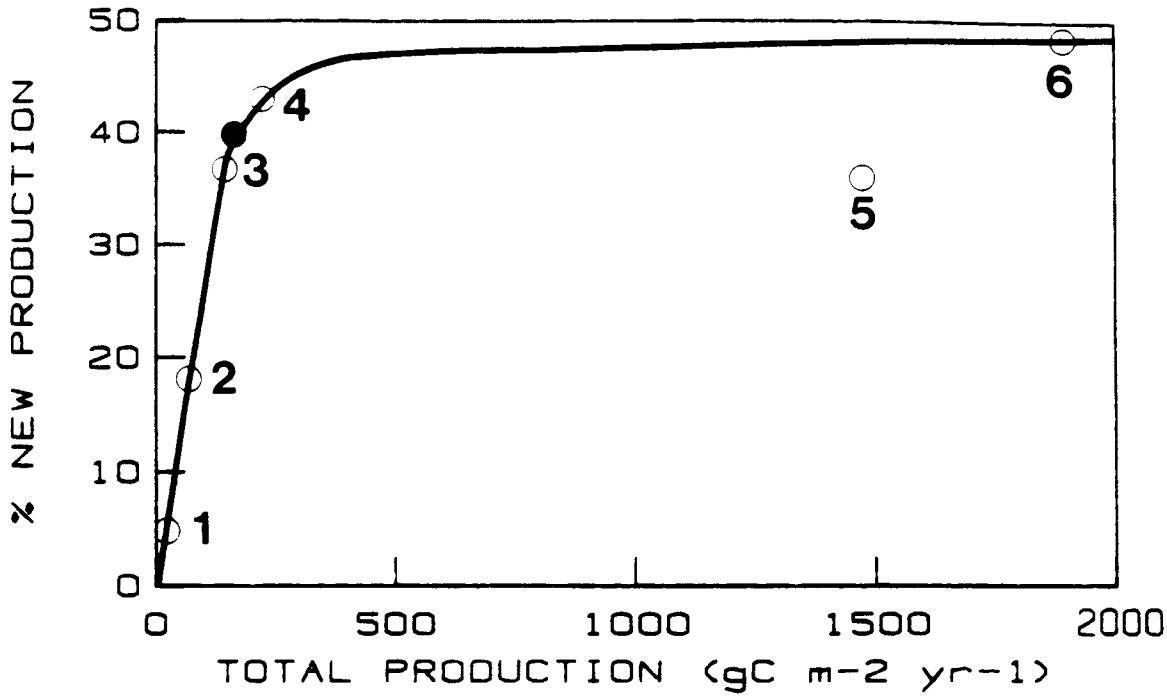

Figure 77.

The relationship between new and total production (modified from Eppley and Peterson, 1979). The open circles 1 - 6 are the original data given in Eppley and Peterson; the solid circle is the southeast Bering Sea based on data from the present study.

urea taken up. The results here support their contention that continental shelf waters are the site of almost 50% of the new production in the ocean.

7.2 Interannual Variability of Nitrogen Productivity and its Implications

Interannual variability in phytoplankton production has been documented in coastal areas where high productivity depends on specific physical phenomena such as the upwelling of nutrient rich sub-surface water (Cowles et al., 1977, Peterson and Miller, 1975). Meteorological influences are usually important in such low frequency biological variability. In the very productive Peru coastal area, for example, phytoplankton productivity decreases sharply during periods of warm equatorial water intrusion, and can impact the anchovy fishery (Cushing, 1981). The southern oscillation - El Niño events are associated with large scale (hemispheric) meteorological changes (Wyrtki, 1975). On the broad, high latitude southeast Bering Sea shelf, processes such as coastal upwelling or sharp gradients in horizontal advection are not available to supply surface nutrients for plant growth. Deep water nutrients, therefore are largely dependent on vertical mixing due to local wind activity to reach surface waters (Coachman and Walsh, 1981).

Since the supply of nitrate to the surface water is mediated by the mixing in this layer, biological nitrate uptake is a sensitive indicator of the physical changes effecting phytoplankton growth during the spring bloom. In the middle shelf domain and deeper (stations #'s less than 16) the nitrate concentration decreases only when the water column is stable and

favorable light conditions prevail, and increases when wind mixing deepens the pycnocline to nitrate rich depths. At inshore depths <50m such as at station 20 favorable light conditions do not depend on stratification and nitrate concentrations in this area are among the first to decrease (e.g. early April 1981, Figure 55 c).

Storms moving through the area were seen to have a significant impact on mixed layer nitrate concentrations across the shelf, this interaction being especially clear during the 6 - 10 May 1980 storm. Early May wind mixing returned nitrate concentrations to over 13 mg-at m^{-3} in the outer shelf surface water. This nitrate increase set the stage for a second period of rapid nitrate uptake during the latter part of May, which corresponds to the bimodal character of nitrate uptake observed at Station 12 during 1980 (Figure 18 a).

Estimates of spring bloom nitrate uptake indicate that nitrate uptake in 1981 was far less than during May 1980 in both the middle and outer shelf reference stations (Table 18). A similar discrepancy between 1980 and 1981 exists in the cross shelf intensity and persistence of the phytoplankton standing crop. The only shelf area in 1981 which exhibited higher nitrate uptake during the bloom period than in previous years was the oceanic area. The oceanic region during 1981 exhibited a consistent pattern of nitrate utilization and replenishment over a three month period (Figure 55 c). Station 1 nitrate increases corresponded to storm events which were recorded on 4 May 1981 and 26 May 1981 at inshore stations. However, it is also possible that yearly oceanic nitrate patterns are regulated by interannual differences in the amount of lateral advection. Unlike much of the rest of the study area the shelf break region is an area of strong advection. If

advection is responsible for the mixed layer nitrate pattern at station 1 during 1981, the intrusion of new water in to the oceanic area had a periodicity of approximately 21 days.

For the large area of the shelf delineated in section 7.1, however, it appears that differences in the amount of wind generated entrainment during May are responsible for the interannual variability in shelf nitrogen productivity. The mixed conditions in May 1980 were also associated with much higher ^{14}C productivities than were the calmer 1981 conditions. This was not reflected in the station 12 particulate C/N ratios, however. The ratios given in Table 18 are weighted by biomass and most of the spring bloom biomass in 1981 at station 12 occurred during a period of vigorous mixing in early May. At station 5 in 1980, the particulate C/N ratios were, as expected, larger in the more wind mixed 1980. The larger C/N ratios in 1980 correspond to the greater ^{14}C productivities in 1980 and support the hypothesis that there is a differential dependence of carbon and nitrogen specific uptake rates on upper water mixing.

Interannual differences in the ΣCO_2 / NO_3^- ratio in station 5 bottom water between 1980 and 1981 were also observed (Figure 78). Most of this difference is due to the smaller cross shelf NO_3^- concentrations encountered in April, 1981 (Table 13). A possible explanation lies in the association of storm events and cross shelf transport of water properties (section 3.3.4). The greater than average number of storms in 1980 may have removed a greater than average amount of organic nitrogen from the area. This removal would have decreased total nitrification, reducing the contribution of this on shelf process to the nitrate pool for the following spring.

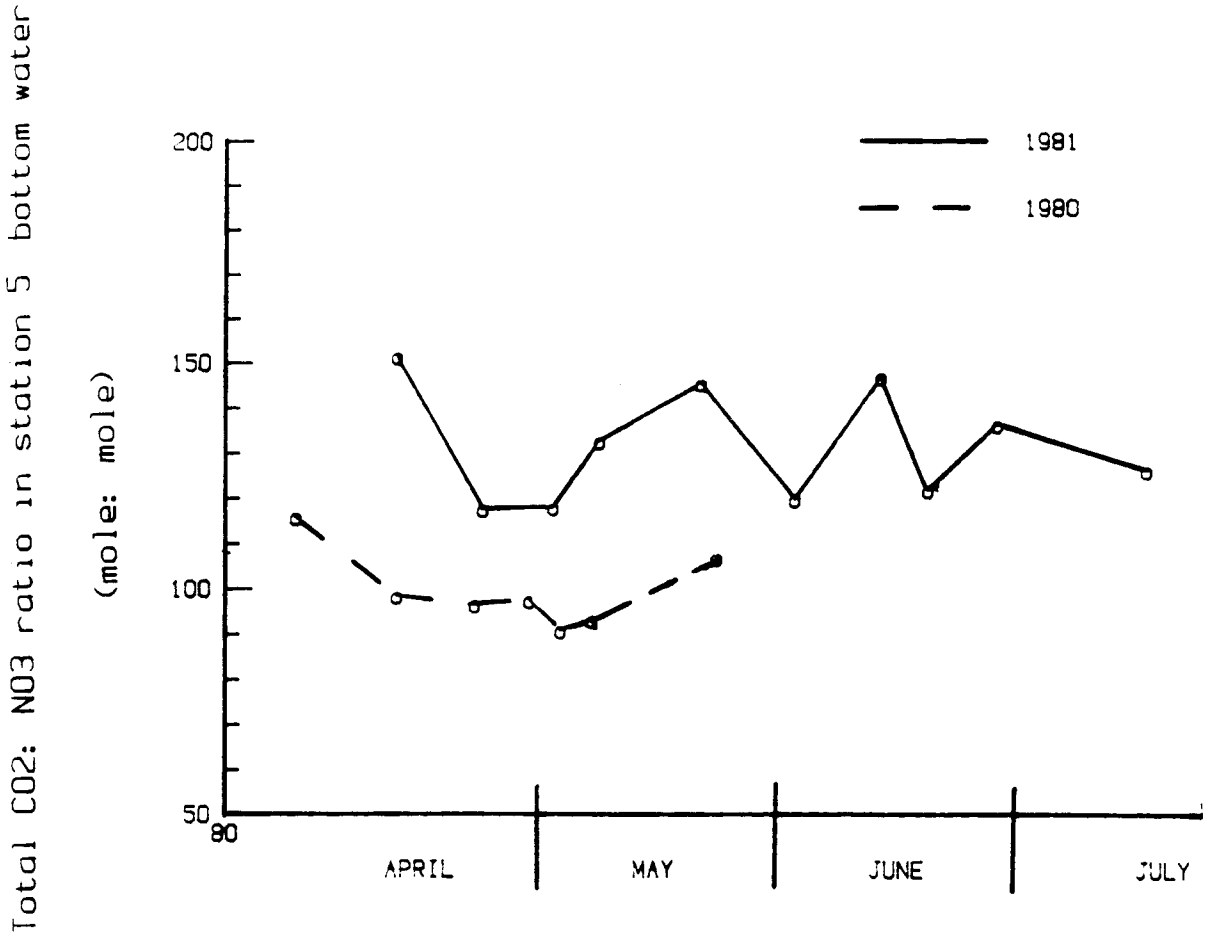

Figure 78.

Comparison of the $\Sigma CO_2 / NO_3^-$ ratio in station 5 (outer shelf) bottom water in 1980 and 1981.

The extensive zooplankton data collected by the PROBES project also reveals interannual variation, Dagg et al., (1982), Smith and Vidal (submitted), and Vidal and Smith (submitted). Selected zooplankton distributions presented by Smith and Vidal (submitted) appear to be closely associated with the bio - physical relationships observed in the cross-shelf patterns of primary production. For example, the mean abundance and growth rate of the larger outer shelf taxa such as Neocalanus plumchrus and Neocalanus cristatus was greater in 1980 than in 1981. Interannual temperature variations probably are not responsible since water temperatures were actually slightly cooler in 1980 and this would slow growth rates. However, food abundance and/or food quality may have played an important role in regulating population size and growth.

The larger standing crops supported by the more extensive wind mixing and nitrate resupply in 1980 may have provided a greater abundance of food for the rapacious outer shelf herbivores. This is a possible explanation for the greater growth rates observed in 1980. Also, higher concentrations of phaeophytin were observed in outer domain waters during May of 1980 than in 1981. This suggests an interannual difference in zooplankton food processing since phaeopigments have been shown to be a useful index of zooplankton grazing activity (Therriault and Platt, 1978).

Additionally, differences in species composition were observed between the May 1980 and 1981 phytoplankton communities in the outer shelf (R. Iverson, personal communication). During mid - May of 1980 Thalassiosira aestivalis and T. nordenskioldii dominated the diatom population, while in 1981 Chaetoceros curvisetus and C. debilis were most abundant. T. aestivalis and T. nordenskioldii compose the early successional stages of

the spring bloom and flourish in vigorously mixed water columns with high nitrate concentrations. These 1980 - 1981 differences indicate that the prolonged wind mixing in 1980 effected trophic levels in addition to the primary producers.

The amount of primary production reaching the benthos would similarly be dependent on prolonged mixing. In any year much of the primary production on this shelf reaches the bottom. The amount of organic matter reaching the benthos, therefore, varies among years in direct proportion to surface production. Caution, however, must be used in the generalization of the above relationships. For example, the mean abundance of Pseudocalanus spp. during spring and summer was on average much greater over the middle shelf domain stations 12 and 16 in 1981 than 1980. The difference in abundance was particularly large for copepodid stages II + III which were present in much higher numbers during the calm 1981 conditions.

This interannual difference may be due to the association of Pseudocalanus spp. with the subsurface Chl a layers which were much more pronounced and extensive in 1981 then they were in 1980 (Figure 79). Such layers (or the production maxima just above them) are commonly associated with relative maxima in zooplankton abundance as well (Herman, 1983). In the southeast Bering Sea, these layers appear to be the basis for an extremely active layer of pelagic trophic transfer which includes the larvae of the walleye pollock (Nishiyama et al., 1982). The dependence of larval fish survival with such layers has been documented in other areas as well (Lasker, 1975).

Interannual differences in wind mixing, therefore, may impact selected food chains in quite different ways. Years in which frequent storms pass

A.

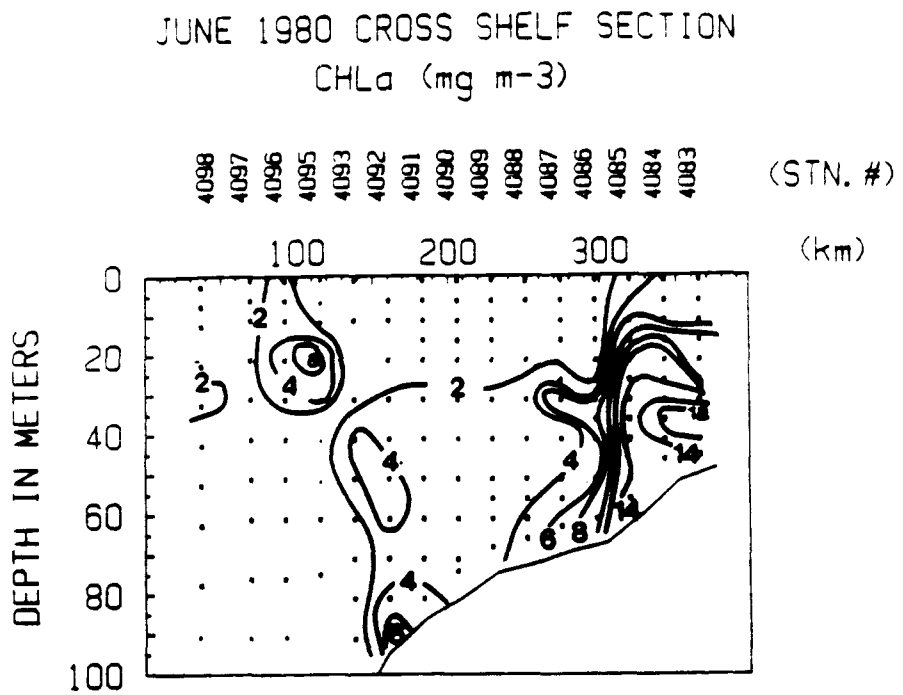

B.

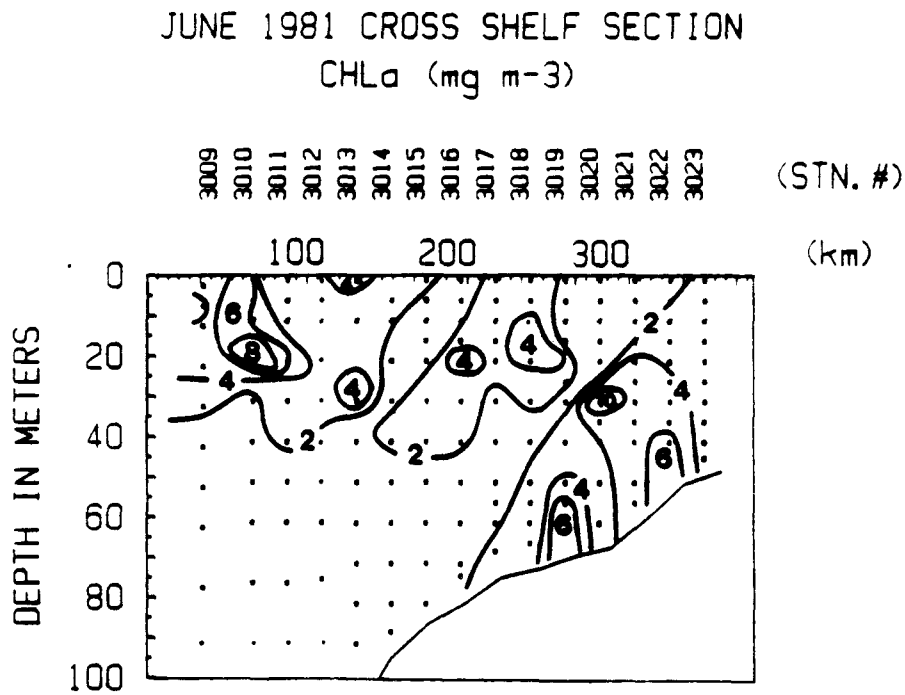

Figure 79.

Comparison of early June cross shelf Chl a in A) 1980 and B) 1981.

over the southeast Bering Sea in May and June, such as in 1980, generate relatively high production and may increase the total organic matter flux to the benthos and the growth rates of water column grazers such as *N. plumchrus*. In the absence of these storms, as in 1981, calm conditions promote the development of sub - surface Chl *a* layers and their associated food chains as typified by *Pseudocalanus spp*.. The intensity and spatial and temporal extent of these layers in turn, may influence the survival of pollock larvae. These results suggest that biological production on this high latitude shelf responds to large scale (e.g. North Pacific) climatic variations, and that these interannual variations may effect food chains of interest to man.

8. Conclusions

8.1 Phytoplankton Growth

The measurement of nitrogen uptake rates through a spring bloom developmental sequence is a powerful tool with which to examine mechanisms influencing phytoplankton growth. Major established depth and time dependent models of phytoplankton growth work well at selected bloom stages. This suggests models based on such apparently diverse approaches as vertical turbulence or nutrient limitation are actually manifestations of a common developmental continuum. The complex community succession involved in this development is closely associated with upper water mixing.

Specifically:

1) Maxima in both absolute (mg-at m^{-2} day^{-1}) and specific ($hr.^{-1}$) nitrogen uptake rates coincided with peak bloom conditions. Maximum rates depended on small mixed layer respirational losses and these conditions occurred between 25 April - 8 May when the mixed layer became shallower than the euphotic zone.

2) A pycnocline mixing rate of 2.1 m day^{-1} in an 18 m mixed layer separated respiration limited from nutrient limited mixed layer growth stages and was associated with maximum phytoplankton growth. In the middle shelf and deeper, upper water mixing conditions are controlled by wind stress.

3) The respiration limited bloom stage has not been rigorously addressed in previous studies. During this deeply mixed stage, the early bloom diatoms displayed measurable variation in their carbon to nitrogen uptake ratios and ultimately in their compositional ratios. These ratios qualitatively reflect the influence of mixing, but due to the aperiodic nature of wind mixing, steady state between instantaneous uptake and particulate composition is seldom achieved during the early bloom.

4) During stable water column, nutrient limited conditions, rate changes can be considered a result of the succession of stenotopic and physiologically distinct species. Large proportions of new to total productivity were associated with the presence of large bloom forming diatoms. In the middle shelf these species were removed from the mixed layer by a lack of turbulence and f factors decreased along with particulate and nitrate nitrogen in the mixed layer. On the outer shelf, grazers filter this community from the mixed layer, and the residual phytoplankton exhibited a relatively greater dependence on regenerated nitrogen.

8.2 Shelf Phytoplankton Growth and the Biogeochemistry of Carbon and Nitrogen

In addition to its trophodynamic importance, new production also influences the interaction between the marine carbon and nitrogen cycles. The f factor appears to be a conservative indicator of carbon loss from surface waters, which suggests $C/N_{(p)} > C/N_{(r)}$. Additionally, the change in nitrogen oxidative state associated with nitrate assimilation is a critical step in a nutrient cycle which includes N_2O as an intermediate. The participation of continental shelf production regimes in carbon and nitrogen cycling is a fruitful area for continuing study.

Specifically:

1) Nitrate uptake averaged 700 mg-at m^{-2} during the bloom and was estimated to be 1 g-at m^{-2} for the year. The yearly f factor over much of the shelf is 0.40 and total production estimated from nitrogen productivity and C/N particulate ratios is 188 g C m^{-2} $yr.^{-1}$. This production is lower than earlier estimates for the area. The relationship between the f factor and total production is similar to that previously reported.

2) The middle shelf $^{15}NO_3^-$ uptake measurements agree with observed changes in water column nitrate. The lack of a discrepancy between these two measurements suggests:

i. the saturation methodology used does not overestimate biological nitrate utilization during the bloom

ii. the diffusive supply of nitrate to the middle shelf is slow. Onshelf nitrogen recycling and oxidation therefore, may be a more significant factor in yearly shelf nutrient supply than previously thought.

3) Nitrification appears to be most intense near the middle front area and such environments may be a substantial source of marine N_2O.

8.3 Interannual Variability in Intensity and Patterns of Primary Production

Total bloom nitrogen production at a middle shelf location and cross shelf patterns of nitrate utilization differed among years by $\pm$ 50%. Interannual variability in bloom nitrogen production was proportional to the amount of deeper water entrained into the mixed layer by wind mixing during May. The intensity of production in turn, may also influence the amount of nutrients of regenerative origin present on the shelf the following spring. Postbloom Chl *a* layers were more robust and extensive when calm May conditions allowed nitrate to remain near the surface. Such interannual differences may be related to larger scale climatic variability. Much longer series of atmospheric - oceanic interaction are needed for such process studies.

9. Appendix

The complete set of standard nitrogen uptake measurements made during this study is contained in PROBES data report #82-009. Inquiries as to availability can be made to:

Institute of Marine Science

University of Alaska

Fairbanks, Alaska 99701

REFERENCES

Alexander, V. and H. J. Niebauer. 1981. Oceanography at the eastern Bering Sea ice-edge zone in spring. Limnology and Oceanography 26(6): 1111-1125.

Alexander, V. 1976. Relationships between turnover rates in the biological nitrogen cycle and algal productivity. Proceedings Industrial Waste Conference, Purdue University 25: 1-7

Antia, N. J., C. D. McAllister, T. R. Parsons, K. Stephens and J. D. J. Strickland. 1963. Further measurements of primary production using a large volume plastic sphere. Limnology and Oceanography. 8(2): 166-183.

Atkins, W. G. R. 1923. Seasonal changes in the phosphate content of seawater in relation to the growth of the algal population. Journal of the Marine Biological Association, U. K. 13: 119-150.

Azam, F. and R. E. Hodson, 1977. Size distribution and activity of marine microheterotrophs. Limnology and Oceanography 22(3): 492-501.

Bakala, R. G. 1981. Population characteristics and ecology of yellow fin sole In: Hood, D. W. and J. H. Calder (eds.). The Eastern Bering Sea Shelf: Oceanography and Resources. Seattle: Univ. of Washington.

Bakun, A., J. Beyer, D. Pauly, J. G. Pope, and G. D. Sharp. 1982. Ocean sciences in relation to living resources. Journal of Fisheries Research Board of Canada. 39: 1059-1070.

Bakun, A. 1973. Coastal upwelling indices, west coast of North America. 1946-1971. NOAA Tech. Rept. NMFS SSRF-671: 103 pp.

Banse, K. 1974. On the interpretation of data for the carbon to nitrogen ratio of phytoplankton. Limnology and Oceanography. 19: 695-699.

Barsdate R. J., R. C. Dugdale. 1965. Rapid conversion of organic nitrogen to N_2 for mass spectrometry: An automated Dumas procedure. Analalytical Biochemistry. 13: 1-5.

Beardall, J., and I. Morris. 1976. The concept of light intensity adaptation in marine phytoplankton: some experiments with Phaeodactylum tricornutum. Marine Biology 37: 377-388.

Becht, G. 1974. Systems theory, the key to holism and reductionism. Bioscience 24(10): 569-579.

Bienfang, P.K. 1981a. Sinking rate dynamics of Cricophaera carterae II: scenesence response to various laboratory substrates in non steady state populations. Journal of Experimental Marine Biology and Ecology 49: 235-244.

Bienfang, P.K. 1981b. Sinking rates of heterogenous, temperate phytoplankton populations. Journal of Plankton Research 3(2): 235-253.

Billen, G. 1978. A budget of nitrogen recycling in North Sea sediments off the Belgian coast. Esturine and Coastal Marine Science 7: 127-146.

Blackburn, T. H. 1979. Method for measuring rates of NH_4^+ turnover in anoxic marine sediments using a ^{15}-NH_4^+ technique. Applied and Environmental Microbiology. 37: 760-765.

Boardman, N. K. 1977. Comparative photosynthesis of sun and shade plants. Annual Review of Plant Physiology 28: 355-377.

Bolin, B. 1979. On the role of the atmosphere in biogeochemical cycles. Quaterly Journal of the Royal Meteorological Society. 105: 25-42.

Bolin, B. and E. Arrehnius. 1977. Nitrogen: an essential life factor and a growing environmental hazard. Ambio. 6: 96-105.

Brezinek, P. L. and G. F. Lee. 1968. Denitrification as a nitrogen sink in Lake Mendota. Wisconsin Environmental Science Technology. 2: 120-125.

Broecker, W. S. and T.H. Peng. 1982. Tracers in the Sea. Palisades, N.Y.: Columbia Univ.

Broecker, W. S. and T. H. Peng. 1974. Gas exchange rates between air and sea. Tellus 26(1): 21-35.

Broeker, W. S. 1971. A kinetic model for the chemical composition of seawater. Quarternary Research. 1: 188-207.

Brower, W. A., Jr., H. F. Diaz, A. J. Prechtel, H. W. Searby and J. L. Wise. 1977. Climatic atlas of the outer continental shelf waters and coastal regions of alaska. Vol. II. Bering Sea. NOAA, 443 p.

Bunt, J. S. 1975. Primary productivity of marine ecosystems. In: Lieth, H. and R. W. Wittaker (eds.). Primary Productivity of the Biosphere. New York: Springer- Verlag.

Caperon J. and J. Meyer. 1972. Nitrogen - limited growth of marine phytoplankton. II. Uptake kinetics and their role in nutrient limited growth of phytoplankton. Deep Sea Research. 19: 619-632.

Caperon, J., D. Schell, J. Hirota, and E. Laws, 1979. Ammonium excretion rates in Kaneohe Bay, Hawaii, Measured by a ^{15}N isotope dilution technique. Marine Biology 54: 33-40.

Carlucci, A. F. and P. M. McNally. 1969. Nitrification by marine bacteria in low concentrations of substrate and oxygen. Limnology and Oceanography. 14: 736-739.

Chatfield, C. 1980. The Analysis of Time Series: An Introduction. London: Chapman and Hall. 268 pp.

Chervin, M. 1978. Assimilation of particulate organic carbon by esturine and coastal copepods. Marine Biology. 49: 265-275.

Cleland, W. W. 1967. The statistical analysis of enzyme kinetic data. Advances in Enzymology. 29: 1-32.

Coachman, L. K. 1982. Flow convergence over a broad flat continental shelf. Continental Shelf Research. 1(1): 1-14.

Coachman, L. K. and J. J. Walsh. 1981. A diffusion model of cross-shelf exchange of nutrients in the southeastern Bering Sea. Deep Sea Research 28A: 819-846.

Coachman, L. K., T. H. Kinder, J. D. Schumacher, and R. B. Tripp. 1980. Frontal systems of the southeastern Bering Sea Shelf. pp. 917-933 in: Stratified Flows; Second IAHR Symposium Trondheim, June, 1980, Trondheim: Tapir.

Coachman, L. K. and R. L. Charnell. 1979. On lateral water mass interaction - A case study, Bristol Bay, Alaska. Journal of Physical Oceanography 9: 278-297.

Codispoti, L. A., G. E. Friederich, R. L. Iverson, and D. W. Hood. 1982. Temporal changes in the inorganic carbon system of the southeastern Bering Sea during spring 1980. Nature 296: 242-245.

Codispoti, L. A. and F. A. Richards. 1976. An analysis of the horizontal region of denitrification in the eastern tropical North Pacific. Limnology and Oceanography. 21: 379-388.

Cohen, Y. and L. I. Gordon. 1978. Nitrous oxide production in the ocean. Journal of Geophysical Research 84(C1): 347-353.

Collos, Y. and G. Slawyk. 1980. Nitrogen uptake and assimilation by marine phytoplankton. In P. G. Falkowski [ed.], Primary Productivity in the Sea. Plenum Press, New York.

Cooney, R. T., T. S. English and T. Nishiyama. 1978. Upper trophic level ecology with emphasis on juvenile Alaska pollock in the southeast Bering Sea, PROBES Phase I. Progress Report 1977-78. p. 251.

Cooney, R. T. and K. O. Coyle. 1982. Trophic implications of cross-shelf copepod distributions in the southeastern Bering Sea. Marine Biology 70: 187-196.

Cooper, L. H. N. 1937a. On the ratio of nitrogen to phosphorous in the Sea. Journal of the Marine Biological Association, U. K. 22: 177-182.

Cooper, L. H. N. 1937b. The marine nitrogen cycle. Journal of the Marine Biological Association, U. K. 22: 183-204.

Cooper, L. H. N. 1933. Chemical Constituents of Biological importance in the English Channel, November, 1930 to January, 1932. Part 1: Phosphate, Silicate, nitrate, nitrite and ammonia. Journal of the Marine Biological Association, U. K. 28: 677-728.

Corner, E. D. S. and Newell. 1967. On the nutrition and metabolism of zooplankton IV. The forms of nitrogen excreted by Calanus. Journal of the Marine Biological Association, U.K. 47: 113-120.

Corner, E. D. S. and A. G. Davies, 1971. Plankton in nitrogen and Phosphorous cycles. Advances in Marine Biology. Vol. 9: 101.

Corner, E. D. S., R. N. Head and C. C. Kilvington. 1972. On the nutrition and metabolism of zooplankton VIII. The grazing of Biddulphia cells by Calanus helgolandicus. Journal of the Marine Biological Association U. K. 52: 847.

Cosper, E. 1982. Effects of diurnal fluctuations in light intensity on the efficiency of growth of Skeletonema costatum in a cyclostat. Journal of Experimental Marine Biology and Ecology. 65: 229-239.

Cote, B., and T. Platt. 1983. Day to Day variations in the spring - summer photosynthetic parameters of coastal marine phytoplankton. Limnology and Oceanography 28(2): 320-344.

Cowles, T. J., R. T. Barber and O. O'Guillen. 1977. Biological consequences of the 1975 El Nino. Science 195: 285-287.

Craig, H. 1969. Abyssal carbon and radiocarbon in the Pacific. Journal of Geophysical Research. 74: 5491-5506.

Cresswell, R. C. and P. J. Syrett. 1979. Ammonium inhibition of nitrate uptake by the diatom Phaeodactylum tricornutum. Plant Science Letters. 14: 321-325.

Crutzen, P. J. 1974. Estimates of possible variations in total ozone due to natural causes and human activities. Ambio. 3: 201-210.

Cuhel, R. L., C. D. Taylor and A. W. Jannasch. 1981. Assimilatory sulfur matabolism in marine microorganisms: sulfur metabolism, protein synthesis, and growth of Pseudomonas halogurans and Alteromonas luteoviolaceus during unperturbed batch growth. Archives of Microbiology. 130: 813.

Cupp,E. A. 1943. Marine Plankton Diatoms of the West Coast of North America. Berkeley: University of CaliforniaPress.

Cushing, D. H. 1962. An alternative method of estimating the critical depth. Journal du Conseil, Conseil International pour l'Exploration de la Mer 27: 131.

Cushing, D. H. 1975. Marine Ecology and Fisheries. Cambridge: Cambridge University Press.

Cushing, D. H. 1981. The effect of El Nino upon the Peruvian anchoveta stock. In F. A. Richards (ed.), Coastal Upwelling. Washington: American Geophysical Union.

Dagg, J. J., J. Vidal, T. E. Whitledge, R. L. Iverson, and J. J. Goering. 1982. The feeding, respiration, and excretion of zooplankton in the Bering Sea during a spring bloom. Deep Sea Research 29(1A): 45-63.

Deason, E. E. and Smayda. 1982. Ctenophore - zooplankton phytoplankton interactions in Narragansett Bay, Rhode Island, USA from 1972 - 1977. Journal of Plankton Research 4(2): 203-217.

Degens, E. T. 1970. Molecular nature of nitrogenous compounds in sea water and recent marine sediments. In D. W. Hood (ed.), Organic Matter in Natural Waters. University of Alaska, Fairbanks. 77-106.

Delwiche, C. C. and B. A. Bryan. 1976. Denitrification. Annual Review of Microbiology 30: 241-262.

Denman, K. L. and A. E. Gargett. (1983) Time and space scales of vertical mixing and advection of phytoplankton in the upper ocean. Limnology and Oceanography, 28(5): 801-815.

DeVooys, C. G. N. 1979. Primary production in aquatic environments. In: Bolin, B., E. T. Degens, S. Kempe, and P. Ketner (eds.). The Global Carbon Cycle. New York: Wiley 491 pp.

Ditullio, G. R. and E. A. Laws. 1983. Estimates of phytoplankton nitrogen uptake based on $^{14}CO_2$ incorporation into protein. Limnology and Oceanography. 28: 177-185.

Draper, N. R. and H. Smith. 1981. Applied Regression Analysis. 2nd ed. 709 p. New York: John Wiley & Sons, Inc.

Droop, M. R. 1974. The nutrient status of algal cells in continuous culture. Journal of the Marine Biological Association. U.K. 55: 825.

Dugdale, R. C. 1977. Modeling. In: Goldberg, McCove, O'Brien and Steele (eds.). The Sea, Vol. VI. New York: Wiley Interscience.

Dugdale, R. C., J. J. Goering, R. T. Barber, R. L. Smith and T. T. Packad. 1977. Denitrification and hydrogen sulfide in the Peru upwelling region during 1976. Deep Sea Research. 24: 601-608.

Dugdale, R. C. and J. J. Goering. 1970. Nutrient limitation and the path of nitrogen in Peru current production. In: Chin, E. (ed.). Scientific Results of the Southeast Pacific Expedition. pp. 53-58. College Station: Texas A&M University Press.

Dugdale, R. C. and J. J. Goering. 1967. Uptake of new and regenerated forms of nitrogen in primary productivity. Limnology and Oceanography. 12: 196-206.

Dugdale, R. C. 1967. Nutrient limitation in the sea: Dynamics, Identification and significance. Limnology and Oceanography. 12: 685-695.

Dugdale, V. A., J. J. Goering and J. H. Ryther. 1964. High nitrogen fixation rates in the Sargasso Sea and the Arabian Sea. Limnology and Oceanography. 9: 507-510.

Ehrlich, P. R., A. H. Ehrlich and J. P. Holdren. 1977. Ecoscience: Population, Resources, Environment. Freemon: San Francisco. 1053 pp.

El Sayed, S. Z. and S. Taguchi. 1981. Primary production and standing crop of phytoplankton along the ice edge in the Weddel Sea. Deep Sea Research. 28A(9): 1017.

El Sayed, S. Z. and J. T. Turner. 1977. Productivity of the antarctic and subtropical regions: A comparative study. In: Dunbar, M. (ed.). Polar Oceans. pp 463-504. Proceedings of SCOR/SCAR Polar Oceans Workshop. Montreal.

Eppley, R. W., E. H. Renger and P. R. Betzer. 1983. The residence time of particulate organic carbon in the surface layer of the ocean. Deep Sea Research. 30(3A): 311-323.

Eppley, R. W., E. H. Renger, and W. G. Harrison. 1979. Nitrate and phytoplankton production in southern California coastal water. Limnology and Oceanography. 29(3): 483-494.

Eppley, R. W. and B. J. Peterson. 1979. Particulate organic matter flux and planktonic new production in the deep ocean. Nature 282: 677-680.

Eppley, R. W., P. Koeller, and G. T. Wallace. (1978) Stirring influences the phytoplankton composition within enclosed columns of coastal sea water. Journal of Experimental Marine Biology and Ecology. 32: 219-239.

Eppley, R. W., J. H. Sharp, E. H. Renger, M. J. Perry, and W. G. Harrison. 1977. Nitrogen assimilation by phytoplankton and other microorganisms in the surface water of the central north Pacific. Marine Biology 39: 111-120.

Eppley, R. W., and E. M. Renger. 1974. Nitrogen assimilation of an oceanic diatom in nitrogen limited continuous culture. Journal of Phycology. 10: 15-23.

Eppley, R. W., F. H. Renger, E. L. Venrick and M. M. Mullin. 1973. A study of plankton dynamics and nutrient cycling in the central gyre of the North Pacific Ocean. Limnology and Oceanography. 18(4): 534.

Eppley, R. W. 1972. Temperature and phytoplankton growth in the sea. Fisheries Bulletin. 70: 1963-1985.

Eppley, R. W., J. L. Coatsworth, and L. Solarzano. 1969. Studies of nitrate reduction in marine phytoplankton. Limnology and Oceanography. 14: 194-205.

Eppley, R. W. and W. H. Thomas. 1969. Comparison of half saturation constants for growth and nitrate uptake of marine phytoplankton. Journal of Phycology. 5: 375- 379.

Eppley, R. W. and P. R. Sloan. 1965. Carbon balance experiments with marine phytoplankton. Journal of the Fisheries Research Board of Canada. 22: 1083-1097.

Falkowski, P. G. and C. D. Wirick. 1981. A simulation model of the effects of vertical mixing on primary production. Marine Biology. 65: 69-75.

Falkowski, P. G. 1980. Light shade adaptation in marine phytoplankton. in: P. J. Falkowski (ed.). Primary Productivity in the Sea. New York:Plenum.

Falkowski, P. G. 1978. In D. R. Nielson and J. McDonald [eds.] Nitrogen in the Environment. Vol. 2. New York: Academic Press.

Falkowski, P. G. and T. Owens. 1978. Effects of light intensity on photosynthesis and dark respiration in six species of marine phytoplankton. Marine Biology. 45: 289-295.

Falkowski, P. G. and D. P. Stone. 1975. Nitrate uptake in marine phytoplankton: Energy sources and the interaction with carbon fixation. Marine Biology. 32: 77.

Fiedler, R. and G. Proksch, 1975. The determination of Nitrogen 15 by emmission and mass spectrometry in biochemical analysis: A review. Analytica Chimica Acta. 78: 1-62.

Fitzwater, S. E., G. A. Knauer, and J. H. Martin. 1982. Metal contamination and its effects on primary production measurements. Limnology and Oceanography. 27: 544-551.

Frost, B. W., M. R. Landry and R. P. Hosset. 1983. Feeding behavior of large calinoid copepods Neocalonus cristatus and Neocalonus plumchrus from the subarctic Pacific Ocean. Deep Sea Research. 30(1): 1-13.

Gallegos, C. L. and T. Platt. 1982. Phytoplankton production and water motion in surface mixed layers. Deep Sea Research 29(1A): 65-76.

Gersberg, R., K. Krohn, N. Peck and C. R. Goldman. 1976. Denitrificatioon studies with ^{15}N labeled nitrate. Science 192: 1229-1231.

Gieskes, W. W. C., G. W. Kraay, and M. A. Barrs. 1979. Current ^{14}C Methods for measuring primary production: gross underestimates in oceanic waters. Netherlands Journal of Sea Research. 13(1): 58-78.

Glibert, P. M., F. Lipshultz, J. J. McCarthy and M. A. Altabet. 1982a. Isotope dilution models of uptake and remineralization of Ammonium by marine plankton. Limnology and Oceanography. 27(4): 639-650.

Glibert, P. M., D. C. Biggs and J. J. McCarthy. 1982b. Utilization of NH_4^+ and NO_3^- during Austral summer in the Scotia Sea. Deep Sea Research. (In Press).

Glover, H. E. 1982. Methylamine: an inhibitor of NH_4^+ oxidation and chemoautotrophic growth in the marine nitrifying bacterium Nitromonas. Archives of Microbiology. 132: 37-40.

Goering, J. J., R. C. Dugdale and D. W. Menzel. 1964. Cyclic diurnal variations in the uptake of ammonium and nitrate by photosynthetic organisms in the Sargasso Sea. Limnology and Oceanography. 9(3): 448-451.

Goering, J. J. and C. P. McRoy. 1981. A synopsis of PROBES. EOS 62: 730-731.

Goering, J. J. and R. L. Iverson. 1979. Phytoplankton distributions on the southeast Bering Sea shelf. In: D. W. Hood and J. A. Calder (eds.), The Eastern Bering Sea Shelf: Oceanography and Resources Vol. 2. 714 p. Seattle: University of Washington Press.

Goering, J. J. 1978. Denitrification in Marine Systems. In Schlessinger, D. [ed.]. Microbiology, 1978. Washington, D. C.: American Society for Microbiology.

Goering, J. J., F. A. Richards, L. A. Codispoti, and R. C. Dugdale. 1973. Nitrogen fixation and denitrification in the ocean: biogeochemical budgets. In: Ingerson, E. [ed.]. International Symposium on Hydrogeochemistry and Biogeochemistry. (Vol II). Washington, D. C.: The Clarke Co.

Goering, J. J., D. D. Wallen and R. M. Nauman. 1970. Nitrogen uptake by phytoplankton in the discontinuity layer of the eastern subtropical Pacific Ocean. Limnology and Oceanography. 15: 789-796.

Goering, J. J. and V. A. Dugdale. 1966. Estimates of rates of denitrification in a subarctic lake. Limnology and Oceanography. 11: 113-117.

Goldman, J. C., J. J. McCarthy and D. G. Peavy, 1979. Growth rate influence on the chemical composition of phytoplankton in oceanic waters. Nature. 279: 210-215.

Goldman, J. C. and E. J. Carpenter. 1974. A kinetic approach to the effect of temperature on algal growth. Limnology and Oceanography. 19(5): 756-766.

Goreau, T. J., W. A. Kaplan, S. C. Wofsey, M. B. McElroy, F. W. Valois and S. W. Watson. 1980. Production of NO_2^- and N_2O by nitrifying bacteria at reduced concentrations of oxygen. Applied and Environmental Microbiology. 40: 526-532.

Gran, H. H. and T. Braarud. 1935. A quantitative study of the phytoplankton in the Bay of Fundy and Gulf of Maine. Journal of the Biological Board of Canada. 1: 279-467.

Griffith, R. P., B. A. Caldwell, W. A. Broich and R. Y. Morita. 1983. Microbial processes relating to carbon cycling in Southeastern Bering Sea sediments. Marine Ecology Progress Series. 10: 265-275.

Hahn, J. 1981. Nitrous oxides in the oceans. In: Delwiche, C. C. [ed.]. Denitrification, Nitrification and Atmospheric Nitrous Oxide. New York: John Wiley & Sons.

Handa, N. and E. Tanoue. 1981. Organic matter in the Bering Sea and adjacent areas. In: D. W. Hood and J. H. Calder [eds.]. The Eastern Bering Sea Shelf: Oceanography and Resources. Vol. 1, p. 347-358.

Hansen, J., D. Johnson, A. Lacis, S. Lebedeff, P. Lee, D. Rind, and G. Russel. 1981. Climatic impact of increasing carbon dioxide. Science. 213: 957-966.

Harris, G. P. and B. B. Piccinin. 1977. Photosynthesis by natural phytoplankton populations. Archiv fuer Hydrobiologie. 80: 405-457.

Harrison, W. G. 1980. Nutrient regeneration and primary production in the sea. In: Falkowski, P.G. [ed.]. Primary Productivity in the Sea. New York: Plenum. 531 pp.

Harrison, W. G. 1978. Experimental measurements of Nitrogen Remineralization in Coastal Waters. Limnology and Oceanography. 23(4): 684-691.

Hauck, R. D. 1973. Nitrogen tracers in the nitrogen cycle studies; Past use and future needs. Journal of Environmental Quality. 2: 317-327.

Henriksen, K., J. I. Hansen and T. H. Blackburn. 1981. Rates of nitrification, distribution of nitrifying bacteria and nitrate fluxes in different types of sediment from Danish waters. Marine Biology. 61: 299-304.

Herman, A. W. 1983. Vertical distribution patterns of copepods, chlorophyll and production in northeastern Baffin Bay. Limnology and Oceanography 28(4): 709-719

Hitchcock, G.L. and T. J. Smayda. 1977. The importance of light in the initiation of the 1972-1973 winter - spring diatom bloom in Narragansett Bay. Limnology and Oceanography. 22(1): 126-131

Holligan, P. M. and D. S. Harbour. 1977. The vertical distribution and succession of phytoplankton in the western English Channel in 1975 and 1976. Journal of the Marine Biological Association, U. K. 57: 1075-1093.

Holmquist, R. 1978. Evaluation of compositional nonrandomness in proteins. Journal of Molecular Evolution. 11: 349-360.

Honjo, S. 1980. Material fluxes and modes of sedimentation in the mesopelagic and bathypelagic zones. Journal of Marine Research. 38: 53-91.

Hood, D. W. 1983. The Bering Sea. In: Ketchum, B. H. [ed.]. Estuaries and Enclosed Seas. Vol. 26, in Ecosystems of the World. CSIRO. New York: Elsevier.

Hood, D. W. 1981. Preliminary observations of the carbon budget of the eastern Bering Sea shelf. In: Hood, D. W. and J. A. Caulder [eds.]. The Eastern Bering Sea Shelf: Oceanography and Resources. Vol. I p. 347-358. Seattle: Univ. of Washington. 1339 pp.

Hood, D. W. and J. H. Calder [eds.]. 1981. The Eastern Bering Sea Shelf: Oceanography and Resources. Vol I and II. Seattle: Univ. of Washington 1339 pp.

Hood, D. W. and W. S. Reeburgh. 1974. Chemistry of the Bering Sea: an overview. In: Hood, D. W. and E. J. Kelly [eds.]. Oceanography of the Bering Sea. Occ. Publ. #2. IMS Fairbanks: Univ. of Alaska.

Horrigan, S. G. and J. J. McCarthy. 1982. Phytoplankton uptake of ammonium and urea during growth on oxidized forms of nitrogen. Journal of Plankton Research. 4(2): 379-387.

Hunkins, K. L. (1965) Tide and storm surge observations in the Chukchi Sea. Limnology and Oceanography. 10: 29-39.

Ignatiades, L.. 1979. The influence of water stability on vertical structure of a phytoplankton community. Marine Biology. 52: 97-104.

Iverson, R. L., L. K. Coachman, R. T. Cooney, T. S. English, J. J. Goering, G. L. Hunt, Jr., M. C. Mcauley, C. P. McRoy, W. S. Reeburgh and T. E. Whitledge. 1979a. Ecological significance of fronts in the southeastern Bering Sea. In: Livingston, R. J. [ed.]. Ecological Processes in Coastal and Marine Systems. New York: Plenum Press.

Iverson, R. L., T. E. Whitledge and J. J. Goering. 1979b. Chlorophyll and nitrate fine structure in the southeastern Bering Sea shelf break front Nature. 281: 664-666.

Iverson, R. L., H. F. Bittaker, and V. B. Meyers. 1976. Loss of radiocarbon in direct use of aquasol for liquid scintillation counting of solutions containing ^{14}C-$NaHCO_3$. Limnology and Oceanography. 21: 756-766.

Iverson, R. L., H. C. Curl, Jr., H. B. O'Connors, Jr., D. Kirk and K. Zakar. 1974. Summer phytoplankton blooms in Auk Bay, Alaska, driven by wind mixing of the water column. Limnology and Oceanography. 19: 271-278.

Jawed, M., 1973. Ammonia excretion by zooplankton and its significance to primary productivity during the summer. Marine Biology. 23: 115-120.

Jenkin, P. M. 1937. Oxygen production by the diatom Cosinodiscus excentricus (Ehr.) in relation to submarine illumination in the English Channel. Journal of the Marine Biological Association. U. K. 22: 301-342.

Johannes, R. E. 1968. Nutrient regeneration in lakes and oceans. In: Droop, M. R. and E. J. F. Wood [eds.]. Advances in Microbiology of the Sea. New York: Academic. 239 pp.

Johannes, R. E. 1964. Phosphorous Excretion and Body Size in Marine Animals; Microzooplankton and Nutrient Regeneration. Science. 146: 923-926.

Johnson, D. R. 1973. The Seasonal Density Structure and Circulation on the Continental Shelf. Ph.D. dissertation. Coral Gabels: U. of Miami 88p.

Johnson, P. W. and J. McN. Sieburth. 1979. Chroococcoid cyanobacteria in the sea: a ubiquitous and diverse autotrophic biomass. Limnology and Oceanography. 24: 929-934.

Junk, G. and H. J. Svek. 1958. The absolute abundance of the nitrogen isotopes in the atmosphere and compressed gas from various sources. Geochimica et Cosmochimica Acta. 14: 234-243.

Kaiser, W. and S. Schulz. 1978. On the causes for the differences in space and time in the commencement of the phytoplankton bloom in the Baltic. Kieler Meeresforschungen. 4: 161-170.

Kiefer, D. A. and J. N. Kremer. 1981. Origins of vertical patterns of phytoplankton and nutrients in the temperate, open ocean: a stratigraphic hypothesis. Deep Sea Research. 28A (10): 1087-1105.

Kinder, T. H. and J. D. Schumacher. 1981. Circulation over the continental shelf of the southeast Bering Sea. In: Hood, D. W. and J. A. Caulder [eds.]. The Eastern Bering Sea Shelf: Oceanography and Resources, Vol. 1. 625 pp. Seattle: University of Washington Press.

King, F. D. and A. H. Devol. 1979. Estimates of vertical eddy diffusion through the thermocline from phytoplankton nitrate uptake rates in the mixed layer of the eastern tropical Pacific. Limnology and Oceanography. 29 (4): 645-651.

Koblentz - Mishke, O. J., V. V. Volkovinsky, and J. G. Kabanova. 1970. Plankton primary production of the world ocean. In: Wooster, W. S. [ed.]. Scientific Exploration of the South Pacific. Washington: N.A.S.

Kocur, C. 1982. Phytoplankton Distribution in Southeastern Bering Sea Shelf Water During Spring. Master's Thesis. Florida State University: Tallahassee.

Koike, I. and A. Hattori. 1979. Estimates of denitrification in sediments of the Bering Sea Shelf. Deep Sea Research. 26(A): 409-415.

Koike, I. and A. Hattori. 1977. Simultaneous determination of nitrification and nitrate reduction in coastal sediments by a ^{15}N dilution technique. Applied and Environmental Microbiology. 35(5): 853-857.

Laevastu, T. and F. Favorite. 1977. Ecosystem model estimations of the distributions of biomass and predation with age for five species in the eastern Bering Sea. Proc. Rept. NMFS. Seattle: N.W.A.F.C.

Laitinen, H. A. and W. E. Harris. 1975. Chemical Analysis. New York: McGraw-Hill. 611 pp.

Landing, W. M. and R. A. Freely. 1981. The chemistry and vertical flux of particles in the Northwest Gulf of Alaska. Deep Sea Research. 28: 19-38.

Lasker, R. 1975. Field criteria for survival of anchovy larvae: the relation between inshore chlorophyll maximum layers and successful first feeding. Fisheries Bulletin. U. S. 73: 453-463.

Laws, E. A. and T. T. Bannister. 1980. Nutrient and light limited growth of Thalassiosira fluveatilis in continous culture, with implications for phytoplankton growth in the ocean. Limnology and Oceanography. 25(3): 457.

Laws, E. A. and J. Caperon. 1976. Carbon and nitrogen metabolism by Monochrysis lutheri: measurements of growth rate dependent respiration rates. Marine Biology. 36: 85-97.

Ledbetter, M. 1979. Langmuir circulation and plankton patchiness. Ecological Modelling 7: 289-310.

Legendre, L. 1980. Hydrodynamic control of marine phytoplankton production: the paradox of stability. In Ecohychodnamics. ed. J. C. J. Nihoul, 359- . New York:Elsevier Scientific Publishing Co.

Legendre, L., R. G. Ingram, and M. Poulin. 1981. Physical control of phytoplankton production under sea ice. Canadian Journal of Fisheries and Aquatic Science. 38: 1385-1392.

Lehninger, A. L. 1970. Biochemistry. New York: Worth. 833 pp.

Liebig, J. 1840. Chemistry and its Application to Agriculture and Physiology. London: Taylor and Walton. 401 pp.

Lisitsyn, A. P. 1966. Recent sedimentation in the Bering Sea (in Russian). 584 p. Moscow:Izdatel'stvo Nauka. (translation available from: National Technical Information Service, Springfield, Virginia; TT 68-50315.)

Liu, K.-K. 1979. Geochemistry of Inorganic Nitrogen Compounds in Two Marine Environments: The Santa Barbara Basin and the Ocean off Peru. Ph.D. Dissertation. Los Angeles: Univ. of California.

Loder, T. C. 1971. Distribution of Dissolved and Particulate Organic Carbon in Alaskan Polar, Subpolar, and Esturine Waters. Ph.D. Dissertation. IMS. Fairbanks: Univ. of Alaska. 236 pp.

Lorenzen, C. J. 1972. Extinction of light in the ocean by phytoplankton. Journal de Conseil, Conseil International pour l'Exploration de la Mer. 34: 262-267.

Lorenzen, C. J. 1976. Primary production in the sea. Chapter 8. In: Cushing, D. J. and J. J. Walsh [eds.], The Ecology of the Seas. W. B. Saunders Co., Philadelphia.

Lund, J. W. G. 1971. An artificial alteration of the seasonal cycle of the plankton diatom Melosira italica subs. subarctica in an English lake. Journal of Ecology. 59: 521-533.

MacIssac, J. J. and R. C. Dugdale. 1972. The interactions of light and inorganic nitrogen in controlling nitrogen uptake in the sea. Deep Sea Research. 19: 209-232.

MacIssac, J. J. and R. C. Dugdale. 1968. The kinetics of nitrate and ammonium uptake by natural populations of marine phytoplankton. Deep Sea Research. 16: 415-422.

MacKenzie, F. T. and R. M. Gorrels. 1966. Chemical mass balance between rivers and oceans. American Journal of Science. 264: 507-525.

Malone, T. C., P. G. Falkowski, T. S. Hopkins, G. T. Rowe and T. E. Whitledge. (1983) Mesoscale response of diatom populations to a wind event in the plume of the Hudson River. Deep Sea Research. 30(2A): 149-170

Mandelli, E. F., P. R. Burkholder, T. E. Doheny and R. Brody. 1970. Studies of primary productivity in coastal waters of southern Long Island, New York. Marine Biology. 7: 153-160.

Margelef, R. 1978. Life forms of phytoplankton as survival alternatives in an unstable environment. Oceanologia Acta 1: 493-509.

Martinez, L., M. W. Silver, J. M. King and A. L. Alldredge. 1983. Nitrogen fixation by floating diatom mats: a source of new nitrogen to oligotrophic ocean waters. Science. 221: 152-154.

Marra, J. Phytoplankton photosynthetic response to vertical movement in a mixed layer. Marine Biology 46: 203-208.

Marra, J. 1980. Vertical mixing and primary production. In: P. G. Falkowski, P. G. [ed.]. Primary Productivity in the Sea. New York: Plenum Press 531pp.

Martin, J. H. 1968. Phytoplankton - zooplankton relationships in Narragansett Bay III: seasonal changes in zooplankton excretion in relation to phytoplankton abundance. Limnology and Oceanography 13: 63.

McCarthy, J. J. and J. C. Goldman. 1979. Nitrogenous nutrition of marine phytoplankton in nutrient depleted waters. Science. 203: 670-672.

McCarthy, J. J., W. Rowland Taylor, and J. L. Taft. (1977) Nitrogenous nutrition of the plankton in Chesapeake Bay. 1. Nutrient availability and phytoplankton preferences. Limnology and Oceanography. 22: 996-1011.

McCarthy, J. J. 1972. The uptake of urea by natural populations of marine phytoplankton. Limnology and Oceanography 17(5): 738

McCarthy, J. J. and T. E. Whitledge. 1972. Nitrogen excretion by anchovy (Engraulis mordox and E. ringens) and Jack Mackerel (Trachurus symmetricus). Fishery Bulletin 70(2): 395

McCarthy, J. J. and R. W. Eppley. 1972. A comparison of chemical, isotopic, and enzymatic methods for measuring nitrogen assimilation of marine phytoplankton. Limnology and Oceanography. 17(3): 371-382.

McElroy, M. B., J. W. Elkins, S. C. Wofsy, C. E. Kolb, A. P. Durim and W. A. Kaplan. 1978. Production and release of N_2O from the Potomac Estuary. Limnology and Oceanography. 23: 1168-1182.

McRoy, C. P. and J. J. Goering. 1976. Annual budget of primary production in the Bering Sea. Marine Science Communications. 2: 255-267.

McRoy, C. P., J. J. Goering, and W. S. Shields. 1972. Studies of primary productivity in the eastern Bering Sea. In: Takenouti, A. Y. [ed.]. Biological Oceanography of the Northern North Pacific Ocean. pp. 199-216. Tokyo: Idemitsu Shoten.

Morris, I., A. E. Smith, and H. E. Glover, 1981. Products of photosynthesis in phytoplankton off the Orinoco river and in the Caribean Sea Limnology and Oceanography. 26(6): 1034-1044.

Morris, I., H. E. Glover and C. S. Yentsch. 1979. Products of photosynthesis by marine phytoplankton: the effect of environmental factors on the relative rates of protein synthesis. Marine Biology. 27: 1-9.

Mullin, M. M., M. J. Perry, E. H. Renger and P. M. Evans, 1975. Nutrient regeneration of oceanic zooplankton: a comparison of methods, Marine Science Communications 1(1): 1-13

Munk, W. H. and E. R. Anderson. 1948. Notes on a theory of the thermocline. Journal of Marine Research 7: 276-295.

Murphy, T. P. 1980. Ammonia and nitrate uptakee in the lower Great Lakes. Canadian Journal of Fisheries and Aquatic Sciences. 37: 1365-1372.

Neess, J. C., R. C. Dugdale, V. A. Alexander, and J. J. Goering. 1962. Nitrogen metabolism in lakes: 1. Measurements of nitrogen fixation with ^{15}N. Limnology and Oceanography. 7: 163-169.

Neuman, G. and W. J. Pierson. 1966. Principles of Physical Oceanography 545 p. Englewood Cliffs, N.J.: Prentice-Hall, Inc.

Niebauer, H. J. 1980. Sea ice and temperature fluctuations in the eastern Bering sea and the relationship to meteorological fluctuations. Journal of Geophysical Research 85: 7507-7515.

Niebauer, H. J. 1983. Multiyear sea ice variability in the eastern Bering Sea: and update. Journal of Geophysical Research 88: 2733-2742.

Nimmo, I. A. and G. L. Atlas. 1979. The statistical analysis of non-normal (real?) data. TIBS. October, 1979. 236-239.

Nishiyama, T., K. Hirano, and T. Haryu. 1982. Nursery layer of the walleye pollock (Theragra chalcograma) larvae. Transactions of the American Geophysical Union, Eos 63: 943

Odum, E. P., 1971. Fundementals of Ecology, 3rd ed. Philadelphia: W. B. Saunders 514 pp.

Okubo, A. 1974. Diffusion induced instability in model ecosystems: another possible explanation of patchiness. Tech. Rep. No. 86. 17 pp. Chesapeake Bay Institute: The John Hopkins University.

Olson, R. J. 1981. ^{15}N tracer studies of the primary nitrite maxima. Journal of Marine Research. 39: 203-226.

Olson, R. J. 1980. Nitrate and ammonium uptake in Antarctic waters. Limnology and Oceanography. 25(6): 1064-1074

Otto, R. S. 1981. Eastern Bering Sea crab fisheries. In: Hood, D. W. and J. H. Calder (eds.). The Eastern Bering Sea Shelf: Oceanography and Resources. Seattle: Univ. of Washington.

Packard, T. T. 1979. Respiration and respiatory electron transport activity in plankton from the northwest African upwelling area. Journal of Marine Research. 37(4): 711-742.

Packard, T. T. and D. Blasco. (1974) Nitrate reductase activity in upwelling regions. 2. Ammonium and light dependence. Tethys, 6(1-2): 269-280.

Packard, T. T., D. Blasco, J. J. MacIssac, and R. C. Dugdale. 1971. Variations of marine nitrate reductase activity in marine phytoplankton. Investigaciones Pesqueras. 35: 209-220.

Pak, H. and R. V. Zaneveld. 1977. Bottom nepheloid layers and bottom mixed layers observed on the continental shelf off Oregon. Journal of Geophysical Research. 82(27): 3921-3931

Patton, B. C. 1963. Plankton optimum diversity structure of a summer community. Science. 140: 894-898.

Peterson, W. T. and C. B. Miller. 1975. Year to year variations in the planktonology of the Oregon upwelling zone. Fishery Bulletin. 73: 642-853.

Phillips, O. M. 1977. The Dynamics of the Upper Ocean (2^{nd} ed.). Cambridge: Cambridge U. Press. 336 pp.

Pierotti, D. and R. A. Rasmussen. 1980. Nitrous oxide measurements in the eastern tropical Pacific Ocean. Tellus. 32: 56-72

Pingree, R. D., P. M. Holligan and G. T. Mardell. 1978. The effects of vertical stability on phytoplankton distributions in summer on the northwest European shelf. Deep Sea Research. 25: 1011-1028.

Pingree, R. D., P. R. Pugh, P. M. Holligan, and G. R. Forrester. 1975. Summer phytoplankton blooms and red tides along tidal fronts in the approaches to the English Channel. Nature. 258: 627-677.

Platt, T., and A. D. Jassby. 1976. The relationship between photosynthesis and light for natural assembeges of coastal marine phytoplankton. Journal of Phycology. 12: 421-430.

Platt, T. 1972. Local phytoplankton abundance and turbulence. Deep Sea Research. 19: 183-187.

Pomeroy, L. R. 1970. The stategy of mineral cycling. Annual Review of Ecology and Systematics. 1: 171-190.

Pratt, D. M. 1965. The winter - spring diatom flowering in Narragansett Bay. Limnology and Oceanography. 10(2): 173-184.

Prezlin, B. B. and A. C. Ley. 1980. Photosynthesis and chlorophyll a florescence rhythms of marine plankton. Marine Biology. 55: 295-307.

Quinby - Hunt, M. S. and K. K. Turekian. 1983. Distribution of elements in seawater. EOS. 64(14): 130-131.

Redfield, A. C., B. H. Ketchum and F. A. Richards, 1963. The influence of organisms on the composition of sea water. In: Hill, M. N. [ed.], The Sea, Vol 2 New York: Wiley Interscience.

Reynolds, C. S. 1973. Succesion and vertical distribution of phytoplankton in response to thermal stratification with special reference to nutrient availability. Journal of Ecology. 64: 529-550.

Riley, G. A. 1942. The relationship of vertical turbulence and spring diatom flowerings. Journal of Marine Research 5: 67-87.

Riley, G. A., H. Stommel and D. F. Bumpus. 1949. Quantitative ecology of the plankton of the western North Atlantic. Bulletin of the Bingham Oceanography Collection. 13 (3): 1-169.

Riley, G. A. 1956. Oceanography of Long Island Sound 1952-1954. Bulletin Bingham Oceanography Collection. 15: 1-46.

Riley, G. A. 1957. Phytoplankton of the north central Sargasso Sea 1950 - 1952. Limnology and Oceanography 2: 252-270.

Riley, G. A. 1967. Mathematical model of nutrient conditions in coastal water. Bulletin of the Bingham Oceanography Collection. 19: 72-80.

Rivkin, R. B., M. A. Voytek, and H. N. Seliger. 1982. Phytoplankton division rates and light limited environments; two adaptations. Science 215: 1123-1125.

Robinson, G. A. (1970) Continuous plankton records: variations in the seasonal cycles of phytoplankton in the north Atlantic. Bulletin of Marine Ecology 6: 333-345.

Roswall, T. 1981. The biogeochemical nitrogen cycle. In: Likens, G. E. [ed.]. Some Perspectives of the Major Biogeochemical Cycles. Chichester: John Wiley & Sons. 175 pp.

Rowe, G. T., C. H. Clifford, and K. L. Smith, 1977. Nutrient Regeneration in Sediments off Cape Blanc, Spanish Sahara, Deep Sea Research 24: 56-63.

Ryther, J. H. 1963. Geographic variation in productivity. In The Sea. Vol. II, ed. M.N. Hill, 347-438. New York: Interscience Publ.

Ryther, J. H. 1969. Photosynthesis and fish production in the sea. Science. 166: 72-76.

Ryther, J. H. and W. M. Dunston. 1971. Nitrogen, phosphorous and eutrophication in the coastal marine environment. Science. 171: 1008-1013.

Sancetta, C. 1981. Oceanographic and ecological significance of diatoms in surface sediments of the Bering and Okhotsk seas. Deep Sea Research 28: 789-817.

Schandelmeier, L. and V. Alexander. 1981. An analysis of the influence of ice on spring phytoplakton population structure in the southeast Bering Sea. Limnology and Oceanography. 26: 935-943.

Schell, D. M. 1974. Uptake and regeneration of free amino acids in marine waters of southeast Alaska. Limnology and Oceanography. 19: 260-270.

Schumacher, J. D., T. H. Kinder, D. J. Pashinski and R. L. Charnell. 1979. A structural front over the continental shelf of the eastern Bering Sea. Journal of Physical Oceanography. 9: 79-87.

Schumacher, J. D. and T. H. Kinder. (in press). Low frequency current regimes over the Bering Sea shelf. Journal of Physical Oceanography.

Seeliger, H. H., K. R. McKinley, W. H. Biggley, R. B. Rivkin and K. R. H. Aspden. 1981. Phytoplankton patchiness and frontal regions. Marine Biology. 61: 119-131.

Semina, H. J. 1960. The influence of vertical circulation on the phytoplankton in the Bering Sea. Internationale Revue der Gesamten Hydrobiologie. 45(1): 1-10

Sharma, G. D., A. S. Naidu and D. W. Hood. 1972. Bristol Bay: Model contemporary graded shelf. American Association of Petroleum Geologists Bulletin. 56 (10): 2000-2012.

Sharp, J. H. and T. M. Church. 1981. Biochemical modeling in coastal waters of the middle Atlantic states. Limnology and Oceanography 26(5): 843-854.

Sharp, J. H., M. J. Perry, E. H. Renger, and R. W. Eppley. 1980. Phytoplankton rate processes in oligotrophic waters of the central north Pacific Ocean. Journal of Plankton Research. 2: 335-353.

Shepard, C. W. 1963. Basic Principles of the Tracer Method. New York: Wiley.

Sinclair, M. 1978. Summer photoplankton variability in the lower St. Lawrence estuary. Journal of the Fisheries Research Board of Canada. 35: 1171-1185.

Sillen, L. G. 1967. The ocean as a chemical system. Science. 156: 1189-1197.

Slagstad, D. 1982. A model of phytoplankton growth-effects of vertical mixing and adaptation to light. Modeling, Identification and Control. 3: 111-130.

Smayda, T. J. 1975. Phased cell division in natural populations of the marine diatom Ditylum brightwelli and the potential significance of diel phytoplankton behavior in the sea. Deep Sea Research. 22: 151-165

Smayda, T. J. (1973) The growth of Skeletonema costatum during a winter - spring bloom in Narragansett Bay. Norwegian Journal of Botany. 20: 219-247.

Smetacek, V., K. von Brockel, B. Zietzschel, and W. Zenk. 1978. Sedimentation of particulate matter during a phytoplankton spring bloom in relation to the hydrographic regime. Marine Biology 47: 211-226.

Smith, G. B. 1981. The biology of walleye pollock. In: Hood, D. W. and J. H. Calder [eds.]. The Eastern Bering Sea Shelf: Oceanography and Resources. Seattle: Univ. of Washington.

Smith, S. and L. Codispoti. 1980. Monsoon of 1979: chemical and biological response off Solmali. Science 209: 597-599.

Smith, S. L. and J. Vidal. (submitted). Spatial and temporal effects of salinity, temperature, and shlorophyll on the communities of zooplankton in the southeastern Bering Sea. Journal of Marine Research

Soederlund, R. and B. H. Svensson. 1976. The global nitrogen cycle. In: Svensson, B. H. and R. Soederlund [eds.]. Nitrogen, Phosphorus, and Sulfur - Global Cycles. SCOPE Rept. 7. Ecological Bulletin (Stockholm) 22: 23-73.

Solomonson, L. P. 1978. Algal reduction of nitrate. In: Schlessinger, D. [ed.]. Microbiology, 1978. Washington: American Society for Microbiology.

Steele, J. H. 1978. Some comments on plankton patches. In: Steele, J. H. [ed.]. Spatial Patterns in Plankton Communities. Proceedings of a NATO conference. New York: Plenum Press.

Steele, J. H. 1962. The environmental control of photosynthesis. Limnology and Oceanography. 7(2): 137-150.

Steele, J. H. and D. W. Menzel. 1962. Conditions for maximum primary production in the mixed layer. Deep Sea Research. 9: 39-49.

Steele, J. H. 1966. Notes on some theoretical problems in production ecology. In C. R. Goldman [ed.], Primary Productivity in Aquatic Environments. Mem. Ins. Ital. Idrobiol., 18 Suppl. Berkely: Univ. of California Press.

Steele, J. H. and B. W. Frost. 1977. The structure of plankton communities. Philosophical Transactions of the Royal Society of London. 280: 485-534.

Steemen - Nielsen, E. 1958. A survey of recent Danish measurements of the organic productivity in the sea. Rapports Proces- Verbaux Reunion Conseil International pour l'Exploration de la Mer. 144: 92-95.

Stein, J. R. 1973. Handbook of Phycological Methods. Cambridge: Cambridge Univ. Press.

Stoker, S. (1981) Benthic invertebrate macrofauna of the eastern Bering/ Chukchi continental shelf. In: Hood, D. W. and J. A. Caulder [eds.] The Eastern Bering Sea Shelf: Oceanography and Resources. Vol II. 710 pp. Seattle: Univ. of Washington.

Stommel, H. 1963. Varieties of Oceanographic Experience. Science 139: 572-576.

Strickland, J. D. H. and T. R. Parsons. 1972. A Practical Handbook of Sea Water Analysis. 2nd Ed. Bulletin 167. Ottawa: Fisheries Research Board of Canada.

Sverdrup, H. U., M. W. Johnson, and R. H. Flemming. 1942. The Oceans. Englewood Cliffs: Prentice Hall.

Sverdrup, H. U. 1953. On conditions for the vernal blooming of phytoplankton. Journal du Conseil, Conseil International pour l'Exploration de la Mer. 18: 287-295.

Syrett, P. J. 1981. Nitrogen metabolism of microalgae. In: Platt, T. [ed.] Physiological Basis of Phytoplankton Ecology. Bulletin 210 of Canadian Bulletin of Fisheries and Aquatic Science. 346 pp.

Syrett, P. J. and I Morris. 1963. The inhibition of nitrate assimilation by ammonium in Chlorella. Biochimica et Biophysica Acta. 67: 566-575.

Szyper, J. P., J. Hirota, J. Caperon and D. A. Ziemann. 1976. Nutrient regeration by the larger net zooplankton in the southern basin of Kaneohe Bay, Oahu, Hawaiian Islands. Pacific Science 30(4): 363-372.

Takahashi, M. and T. Ikeda. 1975. Excretion of ammonia and inorganic phosphorous by Euphasia pacifica and Metridia pacifica at different concentrations of phytoplankton. Journal ofthe Fisheries Research Board of Canada. 32:2189-2195.

Therriault, J. C. and T. Platt. 1978. Spatial heterogeneity of phytoplankton biomass and related factors in the near surface waters of an exposed coastal embayment. Limnology and Oceanography. 23:888-889.

Thomas, W. H. 1970. On nitrogen deficiency in tropical Pacific Oceanic phytoplankton: photosynthetic parameters in poor and rich water. Limnology and Oceanography. 15(3): 380- 385.

Vaccaro, R. F. 1965. Inorganic nitrogen in seawater. In: Riley, J. P. and G. Skirrow [eds.]. Chemical Oceanography. Vol. 1. London: Academic Press. 712 pp.*

Vedernikov, V. I. and A. A. Solov'yena. 1972. Primary production and chlorophyll in the coastal waters of the Barents Sea. Oceanology. 12: 559-565.

Venrick, E. L., Beers, J. R., and J. F. Heinbokel. 1977. Possible consequences of containing microplankton for physiological rate measurements. Journal of Experimental Mararine Biology and Ecology. 26: 55-76.

Vidal, J. and S. L. Smith. (submitted). Biomass, growth, and development of populationnnnns of herbivore zooplankton in the southeastern Bering Sea during spring. Deep Sea Research.

Vincent, W. F. and M. T. Downes. 1981. Nitrate accumulation in anerobic hypolimnia: relative importance of benthic and planktonic nitrifiers in an oligotrophic lake. Applied and Environmental Miocrobiology. 42: 565-573

Walsh, J. J. 1983. Death in the sea: enigmatic phytoplankton losses. Progress in Oceanography 12: 1-86.

Walsh, J. J., G. T. Rowe, R. L. Iverson, and C. P. McRoy. 1981. Biological export of shelf carbon is a neglected sink of the global CO_2 cycle. Nature. 291: 196-201.

Walsh J. J., E. T. Premuzic, and T. E. Whitledge. 1981b. Fate of nutrient enrichment on continental shelves as indicated by the C/N content of bottom sediments. In: Nihoul, J. C. J. [ed.], Ecohydrodynamics. Amsterdam: Elsevier.

Walsh, J. J. 1980. Shelf sea ecosystems. In: Longhurst, A. R. [ed.], Analysis of Marine Ecosystems. New York: Academic Press.

Walsh J. J. 1978. The biological consequences of interactions of the climatic el Nio and event scales of variability in the eastern tropical Pacific. Rapports Proces-Verbaux Reunion Conseil International pour l'Exploration de la Mer 173(113): 182-192.

Walsh, J. J., T. E. Whitledge, F. W. Barvonik, C. D. Wirick and S. O. Howe. 1978. Wind events and food chain dynamics within the New York Bight. Limnology and Oceanography. 23(4): 659-683.

Walsh, J. J. 1976. Herbivory as a factor in patterns of nutrient utilization in the sea. Limnology and Oceanography. 21: 1-13.

Walsh, J. J. 1972. Implications of a systems approach to oceanography. Science. 176: 969-975.

Walsh, J. J. and R. C. Dugdale. 1971. A simulation model of the nitrogen flow in the Peruvian upwelling system. Investigaciones Pesqueras. 35(1): 309-330.

Ward, B. B., R. J. Olson, and M. J. Perry. 1982. Microbial nitrification rates in the primary nitrate maximum off southern California. Deep Sea Research. 29: 247-255.

Whitledge, T. E., 1978. Regeneration of Nitrogen by Zooplankton and Fish in the Northwest Africa Upwelling Ecosystem, In: Boje, R. and M. Tomczak (eds.). Upwelling Ecosystems. New York: Springer - Verlag.

Whitledge, T. E., S. C. Malloy, C. J. Patton and C. D. Wirick. 1981. Automated Nutrient Analysis in Seawater. Brookhaven National Laboratory #51398 UC-11. Springfield, Va.: National Technical Information Service U. S. Dept. of Commerce

Williams, P. J. LeB., 1970. Heterotrophic Utilization of Dissolved Organic Compounds in the Sea. 1. Size Distribution of Population and Relationship between Respiration and Incorporation of Growth Substances,. Journal of the Marine Biological Association U. K. 50: 859-870.

Williams, R. and J. A. Lindley. 1980. Plankton of the Fladen ground during FLEX 76; spring development of the phytoplankton community. Marine Biology. 57: 73-78.

Winter, D. F., K. Banse and G. C. Anderson. 1975. The dynamics of phytoplankton blooms in Puget Sound, a fjord in the northwestern United States. Marine Biology. 29: 139-176.

Wofsy, S. C. 1981. Exchange of trace gases between hydrosphere and atmosphere. Paper presented at Gordon Research Conference in Chemical Oceanography. 3-7 August, 1981. Plymouth, New Hampshire.

Wollast, R. 1981. Interactions between major biogeochemical cycles in marine ecosystems. In: Lichens, G. E. (ed.). Some Perspectives on the Major Biogeochemical Cycles. SCOPE 17. Chichester: John Wiley & Sons. p 125.

Wooster, W. S., A. Bakun, and D. R. Mclain. 1976. Seasonal upwelling along eastern boundry of north Atlantic. Journal of Marine Research 34: 131-141.

Wooster, W. S. and O. Cullen. 1974. Characteristics of El Niño in 1972. Journal of Marine Research 32: 387-403.

Wright, R. T., 1974. Mineralization of Organic Solutes by Heterotrophic Bacteria, In:R. R. Colwell and R. Y. Morita (ed.) Effect of the Ocean Environment on Microbial Activities. University Park Press.

Wyrtki, K. 1975. El Nino: The dynamic response of the equatorial Pacific Ocean to atmospheric forcing. Journal of Physical Oceanography 5: 572-584.

Yentsch, C. S. 1981. Vertical mixing, a constraint to primary production: An extension of the concept of an optimal mixing zone. In: Nihoul, J. C. J. [ed.]. Ecohydrodynamics. New York: Elsevier Ocn. Series 32.

Yentsch, C. S. 1974. The influence of geostrophy on primary production. Tethys. 6(1-2): 111-118.

Yoder, J.A., L. P. Atkinson, T. N. Lee, H. H. Kim and C. R. McClain. 1982. Role of Gulf Stream frontal eddies in forming phytoplankton patches on the outer southeastern shelf. Limnology and Oceanography. 26: 1103-1110.

Zobell, C. E. and C. B. Feltham, 1935. The Occurrence of Urea Splitting Bacteria in the Sea, Science 81: 234-236.